

The role of homeobox factors Barx2 and Pax7 in Wnt signalling in muscle stem cells

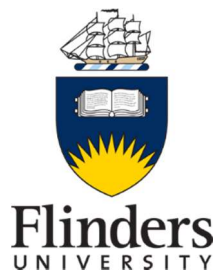
Julie-Ann Hulin

BMedSci, BSc (Hons)

Department of Clinical Pharmacology

Faculty of Medicine, Nursing and Health Sciences

Flinders University



A thesis submitted in fulfilment of the requirements for the degree of

Doctor of Philosophy

August 2016

Table of contents

LIST OF FIGURES.....	V
LIST OF TABLES	VIII
SUMMARY	IX
DECLARATION.....	XII
ACKNOWLEDGEMENTS	XIII
PUBLICATIONS ARISING DIRECTLY FROM THIS THESIS	XV
ADDITIONAL PUBLICATIONS RELATED TO THIS THESIS.....	XV
CONFERENCE PROCEEDINGS	XV
AWARDS IN SUPPORT OF THIS THESIS	XVII
ABBREVIATIONS	XVIII
CHAPTER 1 REVIEW OF THE LITERATURE	1
1.1 SKELETAL MUSCLE: A BRIEF OVERVIEW.....	2
1.1.1 <i>Formation of skeletal muscle</i>	4
1.2 MUSCLE STEM CELLS: THE SATELLITE CELL.....	4
1.3 MUSCULAR DYSTROPHY	7
1.3.1 <i>Mdx mice: a DMD model</i>	10
1.4 MOLECULAR REGULATION OF MYOGENESIS.....	11
1.4.1 <i>Myogenic Regulatory Factors</i>	12
1.4.2 <i>Myocyte Enhancer Factors</i>	15
1.4.3 <i>The Pax family</i>	17
1.5 THE BARX2 HOMEBOX PROTEIN	20
1.5.1 <i>Barx2 expression and a role in myogenesis</i>	21
1.5.2 <i>Barx2 null mice show skeletal muscle dysfunction and defective muscle repair</i>	23
1.5.3 <i>Functional domains and gene targets of Barx2</i>	26
1.5.4 <i>Regulation of Barx2</i>	30
1.6 ADULT SKELETAL MUSCLE REGENERATION.....	31
1.7 THE CANONICAL WNT SIGNALLING PATHWAY	33
1.7.1 <i>Wnt signalling in myogenesis</i>	36
1.8 POTENTIAL RELATIONSHIP BETWEEN BARX2, PAX7 AND WNT SIGNALLING.....	39
1.9 EXPERIMENTAL AIMS.....	41
CHAPTER 2 METHODS AND MATERIALS.....	44
2.1 CHEMICALS AND REAGENTS	45
2.2 GENERAL BUFFERS	45
2.3 MICE	45
2.4 EUKARYOTIC AND PROKARYOTIC CELL LINES.....	46
2.5 MAMMALIAN REPORTER AND EXPRESSION VECTORS.....	46
2.6 OLIGONUCLEOTIDES.....	47
2.6.1 <i>Polyacrylamide Gel (PAGE) purification of site directed mutagenesis oligonucleotides</i>	47
2.7 POLYMERASE CHAIN REACTION (PCR) AMPLIFICATION	48
2.7.1 <i>Equipment</i>	48
2.7.2 <i>PCR for cloning</i>	48
2.7.3 <i>PCR for genotyping or screening</i>	49
2.7.4 <i>Site-directed mutagenesis</i>	49
2.7.5 <i>Quantitative real-time PCR</i>	49
2.8 EXTRACTION OF TOTAL RNA.....	50
2.8.1 <i>Extraction of RNA from monolayer cells</i>	50
2.8.2 <i>Extraction of RNA from primary tissue</i>	50
2.9 GENERATION OF CDNA.....	51

2.10	CO-IMMUNOPRECIPITATION (CO-IP)	51
2.11	CHROMATIN IMMUNOPRECIPITATION (CHIP)	52
2.12	WESTERN BLOTTING	54
2.12.1	<i>Preparation of lysates</i>	54
2.12.2	<i>Protein concentration determination</i>	55
2.12.3	<i>Polyacrylamide gel electrophoresis (PAGE)</i>	55
2.13	PREPARATION OF PRIMARY MYOBLASTS	56
2.13.1	<i>Antibody labelling of myoblasts for fluorescence activated cell sorting (FACS)</i>	57
2.13.2	<i>FACS</i>	57
2.14	MOUSE TAIL TIP/EAR NOTCH GENOMIC DNA ISOLATION	57
2.15	MAINTENANCE OF MAMMALIAN CELL LINES.....	58
2.16	MAINTENANCE OF MOUSE PRIMARY MYOBLAST CULTURES.....	59
2.17	FROZEN CELL STOCKS.....	60
2.18	GENERATION OF L-CELL CONTROL AND WNT3A CONDITIONED MEDIA.....	60
2.18.1	<i>Testing activity of Wnt3a conditioned media</i>	60
2.19	BACTERIAL CULTURE	61
2.20	RESTRICTION DIGESTS.....	61
2.21	LIGATIONS AND TRANSFORMATIONS.....	61
2.22	PREPARATION OF COMPETENT CELLS	62
2.23	PLASMID PREPARATIONS.....	62
2.24	GEL ELECTROPHORESIS AND QUANTIFICATION OF DNA/RNA	64
2.25	DNA PURIFICATION.....	65
2.26	SEQUENCING	65
2.27	TRANSIENT TRANSFECTIONS.....	65
2.28	LUCIFERASE ASSAYS	66
2.29	IMMUNOFLUORESCENCE MICROSCOPY.....	67
2.29.1	<i>Antibody labelling</i>	68
2.29.2	<i>Mounting coverslips to slides</i>	68
2.29.3	<i>Imaging</i>	69
2.30	STATISTICS	69
CHAPTER 3 ANALYSIS OF BARX2-MEDIATED REGULATION OF THE WNT REPORTER TOPFLASH		70
3.1	INTRODUCTION	71
3.1.1	<i>The TOPflash reporter</i>	71
3.1.2	<i>Mechanisms of activation and repression by Barx2</i>	73
3.1.3	<i>The role of Pax7 in regulation of Wnt target genes</i>	76
3.1.4	<i>Aims</i>	77
3.2	METHODS.....	78
3.2.1	<i>Expression plasmids</i>	78
3.2.2	<i>In vitro transcription/translation of Barx2, β-catenin and TCF4</i>	79
3.2.3	<i>Immunofluorescence labelling</i>	80
3.2.4	<i>Pax7 siRNA design and transfection</i>	80
3.2.5	<i>Primers</i>	81
3.3	RESULTS	82
3.3.1	<i>The homeodomain is essential for Barx2-mediated activation of TOPflash</i>	82
3.3.2	<i>Barx2 synergistically activates TOPflash with MyoD and other MRFs</i>	85
3.3.3	<i>Barx2 may synergise with Wnt3a/β-catenin to activate TOPflash</i>	87
3.3.4	<i>Pax7 antagonises Barx2, β-catenin and Wnt3a-mediated activation of TOPflash activity</i>	90
3.3.5	<i>Delineation of the functional domains of Pax7 repression</i>	95
3.3.6	<i>Barx2 and Pax7 interact physically with β-catenin and TCF family members</i>	96
3.3.7	<i>Disruption of a phosphorylation site within Barx2 renders the protein inactive</i>	100
3.3.8	<i>Barx2 binds to the TOPflash promoter and promotes recruitment of β-catenin</i>	102
3.3.9	<i>Over-expression of Barx2 leads to accumulation of β-catenin in the nucleus</i>	105
3.4	DISCUSSION	109
CHAPTER 4 ANALYSIS OF THE EFFECT OF BARX2 LOSS-OF-FUNCTION ON WNT AND NOTCH SIGNALLING IN MYOBLASTS AND <i>IN VIVO</i>		116

4.1	INTRODUCTION	117
4.1.1	<i>Transgenic TCF/LEF reporters</i>	117
4.1.2	<i>The Notch signalling pathway</i>	119
4.1.3	<i>Aims</i>	122
4.2	METHODS.....	123
4.2.1	<i>Maintenance of mice</i>	123
4.2.2	<i>Genotyping for GFP</i>	123
4.2.3	<i>ChIP in whole muscle</i>	123
4.2.4	<i>RNA-Seq and PCR Pathway arrays</i>	124
4.2.5	<i>RNA analysis of whole muscle</i>	125
4.2.6	<i>Lentiviral packaging and transduction</i>	125
4.2.7	<i>Primers</i>	126
4.3	RESULTS	128
4.3.1	<i>Barx2 regulates known Wnt target genes, and genes within both the Wnt and Notch signalling pathways</i>	128
4.3.2	<i>Analysis of Wnt targets in whole muscle from Barx2 wildtype and null mice</i>	131
4.3.3	<i>Genotyping of TOPEGFP mice: A method for analysis of single-copy versus double-copy GFP allele</i>	132
4.3.4	<i>Generation of a Barx2-TOPEGFP mouse line (BAR-TOP)</i>	132
4.3.5	<i>Initial phenotypic analysis of BAR-TOP transgenic model</i>	135
4.3.6	<i>Ins-TOPEGFP mice are found to be TP1-Venus, a transgenic Notch reporter mouse strain</i>	135
4.3.7	<i>Canonical Wnt signalling promotes differentiation of myoblasts and expression of Barx2</i>	140
4.3.8	<i>Wnt3a-mediated regulation of Barx2 expression is indirect and does not involve MyoD binding to the proximal promoter</i>	143
4.3.9	<i>Barx2 protein may be regulated proteolytically in primary myoblasts</i>	148
4.4	DISCUSSION	151
CHAPTER 5 IDENTIFICATION OF DIRECT BARX2 TARGET GENES IN MYOBLASTS.....		159
5.1	INTRODUCTION	160
5.1.1	<i>Tet systems</i>	161
5.1.2	<i>Aims</i>	163
5.2	METHODS.....	163
5.2.1	<i>Expression plasmids</i>	163
5.2.2	<i>Development of double-stable C2C12 Barx2-TetON cell lines</i>	164
5.3	RESULTS	167
5.3.1	<i>Selection of suitable C2C12 pTet-ON stable lines</i>	167
5.3.2	<i>Identifying appropriate double-stable C2C12 mCherry/2A/mBarx2 Tet-ON lines</i>	170
5.3.3	<i>TOPflash is activated in the Barx2 Tet-ON stable lines</i>	175
5.3.4	<i>Identification of Barx2 targets from C2C12 Barx2 Tet-ON lines</i>	177
5.3.5	<i>The Axin2 and cyclinD1 promoters are regulated by Barx2</i>	181
5.3.6	<i>The role of TCF/LEF variants in regulation of Wnt-target promoters</i>	183
5.4	DISCUSSION	191
CHAPTER 6 REGULATION OF THE AXIN2 GENE BY BARX2, PAX7 AND WNT SIGNALLING IN MYOBLASTS		200
6.1	INTRODUCTION	201
6.1.1	<i>Regulation of the Axin2 gene by Wnt signals</i>	201
6.1.2	<i>Co-factors and epigenetic mechanisms involved in the transcriptional response to Wnt signalling</i>	202
6.1.3	<i>Aims</i>	204
6.2	METHODS.....	204
6.2.1	<i>Expression plasmids</i>	204
6.2.2	<i>Electrophoretic mobility shift assay</i>	206
6.3	RESULTS	210
6.3.1	<i>Barx2-mediated activation of Axin2 and cyclinD1 is regulated through TCF/LEF motifs</i>	210
6.3.2	<i>The C-terminal activation domain and homeodomain of Barx2 are required for Axin2 and cyclinD1 promoter regulation</i>	214

6.3.3	<i>Barx2 binds to the Axin2 T3-5 intronic region and promotes recruitment of β-catenin.....</i>	217
6.3.4	<i>Barx2 cannot bind to oligonucleotide probes containing TCF/LEF motifs in vitro</i>	220
6.3.5	<i>Pax7 partially antagonizes Barx2- and β-catenin-mediated induction of Axin2 promoter activity</i>	224
6.3.6	<i>Pax7 is recruited to the Axin2 T3 region</i>	227
6.3.7	<i>Barx2 and Wnt signalling alter histone modifications of the Axin2 promoter region</i>	228
6.3.8	<i>The histone acetyltransferase GRIP-1 synergizes with Barx2 in regulation of Axin2 promoter activity and is actively recruited to TCF/LEF elements.....</i>	234
6.3.9	<i>Pax7 associates with the histone deacetylase HDAC1.....</i>	238
6.4	DISCUSSION	243
CHAPTER 7 GENERAL DISCUSSION AND CONCLUSIONS.....		254
APPENDICES		267
REFERENCES.....		279

List of figures

FIGURE 1.1: STRUCTURE OF SKELETAL MUSCLE	7
FIGURE 1.2: SEQUENCE AND SCHEMATIC OF BARX2 PROTEIN	27
FIGURE 1.3: HIERARCHY OF TRANSCRIPTION FACTORS IN MYOGENESIS	33
FIGURE 1.4: THE CANONICAL WNT SIGNALLING PATHWAY	36
FIGURE 1.5: REGULATORY INTERACTIONS BETWEEN BARX2, B-CATENIN, MRFS AND PAX7	43
FIGURE 3.1: ANALYSIS OF NEW BARX2 DELETION CONSTRUCTS.....	84
FIGURE 3.2: MSX HOMEODOMAIN PROTEINS CAN ACTIVATE TOPFLASH.....	85
FIGURE 3.3: BARX2 REGULATES THE TOPFLASH REPORTER GENE SYNERGISTICALLY WITH MRFS IN C2C12 CELLS	87
FIGURE 3.4: BARX2 AND B-CATENIN MAY SYNERGISE TO ACTIVATE TOPFLASH WHILST MYOD REPRESSES B-CATENIN ACTIVATION	89
FIGURE 3.5: PAX7 ANTAGONISES THE ACTIVATING EFFECT OF BARX2 ON TOPFLASH ACTIVITY	90
FIGURE 3.6: EFFICACY OF PAX7 SIRNA KNOCKDOWN IN C2C12 CELLS	92
FIGURE 3.7: KNOCKDOWN OF PAX7 INCREASES THE ABILITY OF BARX2 AND MYOD TO ACTIVATE TOPFLASH	93
FIGURE 3.8: PAX7 ANTAGONISES THE ACTIVATING EFFECT OF B-CATENIN AND WNT3A ON TOPFLASH	94
FIGURE 3.9: THE PAX7 HOMEODOMAIN IS IMPORTANT FOR REPRESSION OF TOPFLASH ACTIVITY.....	96
FIGURE 3.10: BARX2 INTERACTS WITH B-CATENIN AND TCF4 <i>IN VITRO</i>	98
FIGURE 3.11: BARX2, B-CATENIN AND TCF4 PROTEINS DO NOT DIRECTLY INTERACT.....	99
FIGURE 3.12: PHOSPHORYLATION PREDICTION OF BARX2	100
FIGURE 3.13: ANALYSIS OF BARX2 PHOSPHORYLATION MUTANTS ON TOPFLASH ACTIVITY	102
FIGURE 3.14: BARX2 IS RECRUITED TO THE TOPFLASH PROMOTER IN C2C12 CELLS AND PROMOTES RECRUITMENT OF B- CATENIN.....	105
FIGURE 3.15: WNT3A STIMULATES NUCLEAR LOCALISATION OF B-CATENIN IN C2C12 CELLS.....	107
FIGURE 3.16: BARX2 OVER-EXPRESSION LEADS TO B-CATENIN ACCUMULATION IN THE NUCLEUS.....	108
FIGURE 4.1: A REPRESENTATIVE SET OF WNT AND NOTCH GENES FROM RNA-SEQ ANALYSIS OF BARX2 WILDTYPE AND NULL MYOBLASTS	130
FIGURE 4.2: WHOLE MUSCLE GENE EXPRESSION ANALYSIS.....	131
FIGURE 4.3: GENERATION OF THE BAR-TOP DOUBLE-TRANSGENIC MOUSE MODEL	134

FIGURE 4.4: ANALYSIS OF TOTAL BODY WEIGHT OF MALE BAR-TOP PUPS AT P21	135
FIGURE 4.5: BARX2 MRNA EXPRESSION IN WHOLE MUSCLE	136
FIGURE 4.6: SEQUENCING RESULT OF INS-TOPEGFP TRANSGENE	138
FIGURE 4.7: THE CANONICAL WNT3A PROMOTES DIFFERENTIATION OF C2C12 MYOBLASTS	141
FIGURE 4.8: MRNA EXPRESSION OF PRIMARY MYOBLASTS FOLLOWING 48 HOURS WNT3A STIMULATION	142
FIGURE 4.9: MRNA EXPRESSION OF FIBROBLASTS FOLLOWING 48 HOURS WNT3A STIMULATION.....	143
FIGURE 4.10: INDIRECT BARX2 MRNA INDUCTION BY WNT3A	145
FIGURE 4.11: MYOD IS NOT INDUCED OR RECRUITED TO THE BARX2 PROXIMAL PROMOTER FOLLOWING TREATMENT WITH WNT3A	147
FIGURE 4.12: THE PROXIMAL BARX2 PROMOTER IS NOT ACTIVATED BY B-CATENIN/WNT SIGNALLING.....	148
FIGURE 4.13: STIMULATION BY WNT3A INDUCES BARX2 PROTEIN EXPRESSION IN PRIMARY MYOBLASTS	149
FIGURE 4.14: BARX2 PROTEIN IS REGULATED PROTEOLYTICALLY IN PRIMARY MYOBLASTS.....	151
FIGURE 5.1: INITIAL SCREEN OF STABLE C2C12 pTET-ON CLONES	168
FIGURE 5.2: SECOND SCREEN OF STABLE C2C12 pTET-ON CLONES	169
FIGURE 5.3: C2C12 pTET-ON STABLE CLONES RESPOND TO WNT3A	170
FIGURE 5.4: IMMUNOFLUORESCENCE SCREENING OF DOUBLE-TRANSGENIC C2C12 BARX2 TET-ON CLONES	173
FIGURE 5.5: WESTERN BARX2 TET-ON LINES.....	172
FIGURE 5.6: INITIAL MRNA SCREEN OF STABLE C2C12 BARX2 TET-ON LINES	175
FIGURE 5.7: TOPFLASH IS ACTIVATED IN THE BARX2 TET-ON STABLE LINES.....	176
FIGURE 5.8: TARGET GENES NOT REGULATED BY DOX-INDUCED BARX2 EXPRESSION.....	178
FIGURE 5.9: TARGET GENES REGULATED BY DOX-INDUCED BARX2 EXPRESSION	180
FIGURE 5.10: PARENTAL RTTA-EXPRESSING CELL LINES DO NOT SHOW INDUCTION OF CYCLIND1 OR AXIN2 IN RESPONSE TO DOX.....	181
FIGURE 5.11: BARX2 REGULATES THE AXIN2 AND CYCLIND1 PROMOTERS.....	183
FIGURE 5.12: TCF/LEF MRNA EXPRESSION IN C2C12 CELLS AND PRIMARY MYOBLASTS	184
FIGURE 5.13: SIMPLIFIED SCHEMATIC OF EXON STRUCTURE OF Tcf4 VARIANTS CLONED FROM MYOBLASTS.....	187
FIGURE 5.14: TCF/LEF FAMILY MEMBERS DIFFERENTIALLY REGULATE BARX2+MYOD AND B-CATENIN-MEDIATED ACTIVATION OF TOPFLASH.....	188
FIGURE 5.15: LEF1 AND Tcf3 DIFFERENTIALLY REGULATE BARX2 AND B-CATENIN-MEDIATED ACTIVATION OF AXIN2-LUC	

.....	189
FIGURE 5.16: TCF4 VARIANTS DIFFERENTIALLY REGULATE BARX2 AND B-CATENIN-MEDIATED ACTIVATION OF AXIN2-LUC	
.....	190
FIGURE 6.1: BARX2-MEDIATED REGULATION OF CYCLIND1 IS REGULATED THROUGH A TCF/LEF MOTIF	212
FIGURE 6.2: BARX2-MEDIATED REGULATION OF AXIN2 IS REGULATED THROUGH TCF/LEF MOTIFS.....	214
FIGURE 6.3: ACTIVATION OF AXIN2 AND CYCLIND1 PROMOTER CONSTRUCTS BY BARX2 DOMAINS.....	216
FIGURE 6.4: CHIP ANALYSIS OF BARX2 RECRUITMENT TO THE AXIN2 PROMOTER AFTER HETEROLOGOUS OVEREXPRESSION	
.....	218
FIGURE 6.5: CHIP ANALYSIS OF BARX2 AND B-CATENIN RECRUITMENT AFTER WNT3A STIMULATION IN PRIMARY	
MYOBLASTS.....	219
FIGURE 6.6: CHIP ANALYSIS OF BARX2 AND B-CATENIN RECRUITMENT TO DISTAL AXIN2 TCF MOTIFS.....	220
FIGURE 6.7: GEL SHIFT ASSAYS WITH C2C12 NUCLEAR EXTRACTS	222
FIGURE 6.8: GEL SHIFT ASSAY WITH HEK293T NUCLEAR EXTRACTS.....	223
FIGURE 6.9: PAX7 ANTAGONISES THE ACTIVATING EFFECT OF BARX2 AND B-CATENIN ON THE AXIN2 PROMOTER.....	225
FIGURE 6.10: THE EFFECT OF CHIMERIC BARX2/PAX7 FACTORS ON AXIN2 PROMOTER ACTIVITY	227
FIGURE 6.11: PAX7 IS RECRUITED TO AXIN2 AND TOPFLASH PROMOTER DNA	228
FIGURE 6.12: BASAL CHROMATIN SIGNATURE OF TOPFLASH AND AXIN2 T3	230
FIGURE 6.13: CHROMATIN SIGNATURE OF AXIN2 FOLLOWING WNT3A STIMULATION.....	231
FIGURE 6.14: CHROMATIN SIGNATURE OF AXIN2 AND TOPFLASH FOLLOWING BARX2 OR B-CATENIN TRANSFECTION .	233
FIGURE 6.15: SCREENING OF POTENTIAL BARX2 CO-ACTIVATORS IN LUCIFERASE ASSAYS.....	235
FIGURE 6.16: GRIP-1 IS ACTIVELY RECRUITED TO TCF/LEF ELEMENTS	238
FIGURE 6.17: HDAC1 REPRESSES BARX2 AND B-CATENIN-MEDIATED ACTIVATION OF AXIN2 AND TOPFLASH.....	240
FIGURE 6.18: HDAC1 INTERACTS WITH PAX7	241
FIGURE 6.19: PAX7 INHIBITS TOPFLASH ACTIVITY IN THE PRESENCE OF HDAC INHIBITORS	242
FIGURE 7.1: MODEL FOR THE FUNCTION OF BARX2 AND PAX7 DOWNSTREAM OF WNT SIGNALLING.....	262

List of tables

TABLE 3.1: LIST OF ALL PRIMERS USED DURING THIS CHAPTER.....	81
TABLE 4.1: LIST OF ALL PRIMERS USED DURING THIS CHAPTER.....	126
TABLE 4.2: WNT TARGET AND PATHWAY GENES IN PCR ARRAY	129
TABLE 5.1: LIST OF ALL PRIMERS USED DURING THIS CHAPTER.....	165
TABLE 6.1: LIST OF ALL PRIMERS USED DURING THIS CHAPTER.....	208

Summary

Satellite cells are the resident stem cells of skeletal muscle and provide the mechanism by which muscle tissue is capable of repair and renewal. Satellite cells are quiescent in adults, until activated by injury to generate proliferating myoblasts. In a process known as myogenesis, the proliferating myoblasts align, fuse and undergo terminal differentiation, resulting in formation of multi-nucleated muscle fibres.

The muscle regulatory factors (MRFs) are key regulators of myogenesis, and hierarchical expression of the four family members (Myf5, MyoD, myogenin and MRF4) guides progression through the stages of muscle regeneration. The homeobox factor Pax7 also plays an essential role in myogenesis and is considered the canonical marker of satellite cells. Pax7 is important for maintenance of satellite cell quiescence and prevention of precocious differentiation. Recently another homeobox protein, Barx2, has emerged as being functionally important in myoblasts. Barx2 regulates expression of muscle-specific genes, and Barx2 null mice exhibit smaller muscle fibres, muscle atrophy and defective muscle repair. In contrast to Pax7, Barx2 is upregulated during and promotes differentiation of myoblasts.

The canonical Wnt signalling pathway controls myogenesis, inducing a switch from myoblast proliferation to differentiation. The central effectors of the Wnt pathway are TCF/LEF proteins and β -catenin, that together bind Wnt-responsive genes and activate transcription. Our preliminary data demonstrates that Barx2 can activate a synthetic Wnt reporter gene, TOPflash, in the C2C12 myoblast cell line. This thesis sought to understand the mechanisms underpinning this regulation and to determine if Barx2 can regulate endogenous Wnt-responsive target genes in myoblasts.

Co-immunoprecipitations demonstrated that Barx2 could interact with β -catenin and TCF/LEF proteins and chromatin immunoprecipitation (ChIP) experiments showed recruitment of Barx2 to TCF/LEF binding sites in the TOPflash promoter. Barx2 expression also increased levels of nuclear β -catenin and promoted its recruitment to endogenous TCF/LEF sites. In contrast, Pax7 appeared to be antagonistic to Barx2, repressing TOPflash activity.

Generation of a tetracycline-inducible Barx2 myoblast cell line (gain-of-function model), coupled with RNA-Seq and PCR array analysis of primary myoblasts isolated from Barx2 null mice (loss-of-function model), identified Axin2 and cyclinD1 as Wnt-responsive targets of Barx2. Analysis of the Axin2 promoter revealed that Barx2 bound to TCF/LEF sites, recruited β -catenin and the co-activator GRIP-1, and induced activating histone H3K-acetylation. In contrast, ectopic expression of Pax7 repressed Axin2 promoter activity, and knockdown of endogenous Pax7 allowed for greater activation of the promoter by β -catenin and Barx2. Furthermore, Pax7 interacted with the co-repressor HDAC1 and inhibited Barx2-mediated H3K-acetylation at Axin2 TCF/LEF sites. This work shows that Barx2, Pax7 and MRFs can act as direct transcriptional effectors of Wnt signals in myoblasts. These findings support a novel model in which Barx2 is a key transcriptional mediator of Wnt-driven myoblast differentiation, whilst Pax7 antagonises Wnt signalling in a role consistent with promotion of long-term satellite cell self-renewal. This provides a new regulatory pathway for regulation of muscle progenitor differentiation, and suggests that antagonism between Barx2 and Pax7 may help mediate the switch from proliferation to differentiation.

Finally, canonical Wnt signalling induced Barx2 mRNA and stabilised Barx2 protein in myoblasts, suggesting a positive feed-forward loop between Barx2 and Wnt signalling. These studies prompt a biphasic model for Barx2 downstream of Wnt signals in myoblasts: Barx2 initially enhances the activation of Wnt target genes (Axin2 and possibly other negative regulators of Wnt signalling), and through this enhanced activation may help to limit the Wnt response, thus preventing the deleterious effects of excessive Wnt signalling.

Declaration

I certify that this thesis does not incorporate without acknowledgement any material previously submitted for a degree or diploma in any university; and that to the best of my knowledge and belief it does not contain any material previously published or written by another person except where due reference is made in the text.

Julie-Ann Hulin

August 2016

Acknowledgements

I would like to sincerely acknowledge many people who have provided me with invaluable support and encouragement throughout this research project. It has been a wonderful, rewarding and often overwhelming experience.

Firstly, I thank Dr Robyn Meech for her consistent guidance, feedback and patience. You have been an inspiration as well as an incredible example of both a skilful and passionate scientist, and I am truly grateful for your friendship and the expertise you have shared with me. Many thanks also to Professor Peter Mackenzie for his co-supervision, advice and critical reading of this thesis.

I would like thank my colleagues and friends, both past and present, for their friendship and helpful discussions. In particular, Tran Nguyen and Lizhe Zhuang, I thank you for providing a solid basis for the studies described within this thesis – you have contributed enormously to this work. Thanks also to Siti Mubarakah, Dhilushi Wijayakumara, Bo Chanawong, Anne Rogers, Dr Dong Gui Hu, Dr Lu Lu, Alex Haines, Negara Tajbakhsh and Sara Tommasi, as well as many other friends and colleagues in the Department of Clinical Pharmacology. It has been a pleasure to work with you all over the years and share my many disasters and triumphs.

To my immediate family, Mum, Dad, Kylie and Peta, my good friend and fellow PhD-student Belinda, and my extended family: Thank you for your love, support, and providing some much needed stress relief.

Finally, I am especially grateful to my incredible fiancé, Mike. Thank you for your constant faith, reassurance and motivation. This process has been a rollercoaster ride

which I would not have survived without your listening ear and endless cups of tea to maintain my sanity. You have provided me with the strength and love required to fulfil my goals and it has been a fantastic experience to share with you.

Publications arising directly from this thesis

Hulin, J.A., Nguyen, T.D., Cui, S., Makarenkova, H. and Meech, R. (2016) 'Barx2 and Pax7 regulate Axin2 expression in myoblasts by interaction with β -catenin and chromatin remodelling' *Stem Cells*. Epub ahead of print.

Zhuang, L.*, Hulin, J.A.*, Gromova, A.*, Nguyen, T.D., Yu, R.T., Liddle, C., Downes, M., Evans, R.M., Makarenkova, H. and Meech, R. (2014) 'Barx2 and Pax7 have antagonistic functions in regulation of Wnt signalling and satellite cell differentiation' *Stem Cells*. 32(6):1661-1673.

*Indicates co-first authors

Additional publications related to this thesis

Meech, R., Gonzalez, K.N., Barro, M., Gromova, A., Zhuang, L., Hulin, J.A. and Makarenkova, H.P. (2012) 'Barx2 is expressed in satellite cells and is required for normal muscle growth and regeneration' *Stem Cells*. 30(2): 253-265.

Meech, R., Gomez, M., Woolley, C., Barro, M., Hulin, J.A., Walcott, E.C., Delgado, J. and Makarenkova, H.P. (2010) 'The homeobox transcription factor Barx2 regulates plasticity of young primary myofibers' *PLoS One*. 5: e11612

Conference proceedings

Hulin, J.A., Nguyen, T., Makarenkova, H. and Meech, R. 'Regulation of muscle stem cells by Wnt signalling involves homeobox factors Barx2 and Pax7'. Poster presentation, EMBO Workshop on Wnt signalling, Broome, Western Australia 2014.

Hulin, J.A., Nguyen, T., Makarenkova, H. and Meech, R. 'Regulation of muscle stem cells by Wnt signalling involves homeobox factors Barx2 and Pax7'. Poster presentation, Australian Society for Stem Cell Research (ASSCR), Lorne, Victoria 2014.

Hulin, J.A., Nguyen, T., Makarenkova, H. and Meech, R. 'Regulation of muscle stem cells by Wnt signalling involves homeobox factors Barx2 and Pax7'. Poster presentation, International Society for Stem Cell Research (ISSCR) annual meeting, Vancouver 2014.

Hulin, J.A., Nguyen, T., Makarenkova, H. and Meech, R. 'Regulation of muscle stem cells by Wnt signalling involves homeobox factors Barx2 and Pax7'. Oral presentation, Australasian Society for Stem Cell Research (ASSCR) annual meeting, Brisbane 2013.

Hulin, J.A., Nguyen, T. and Meech, R. 'The stem cell homeobox factor Barx2 regulates canonical Wnt signalling and myoblast differentiation'. Poster presentation, Combined Australian Health and Medical Research Congress (AHMRC) and ASSCR annual meeting, Adelaide 2012.

Hulin, J.A., Nguyen, T. and Meech, R. 'The muscle stem cell factor Barx2 mediates transcription of canonical Wnt targets in C2C12 myoblasts'. Oral presentation, Australian and New Zealand Society for Cell and Developmental Biology (ANZSCDB) annual meeting (ComBio), Adelaide 2012.

Hulin, J.A., Nguyen, T. and Meech, R. 'The stem cell homeobox factor Barx2 regulates canonical Wnt signalling and myoblast differentiation'. Oral presentation, Australian and New Zealand Society for Cell and Developmental Biology Adelaide meet, Adelaide 2012.

Hulin, J.A., Zhuang, L., Makarenkova, H. and Meech, R. 'The stem cell factors Barx2 and Pax7 are direct effectors of Wnt signalling'. Poster presentation, Australasian Society for Stem Cell Research (ASSCR) annual meeting, Blue Mountains, New South Wales 2011.

Hulin, J.A., Zhuang, L., Makarenkova, H. and Meech, R. 'The muscle stem cells factors Barx2 and Pax7 are direct effectors of Wnt signalling'. Oral presentation, Australian and New Zealand Society for Cell and Developmental Biology Adelaide meet, Adelaide 2011.

Awards in support of this thesis

Flinders University Postgraduate Scholarship, 2011-2014.

Australian Stem Cell Centre (ASCC) Postgraduate Supplementary Scholarship, 2011-2014.

Flinders University Research Higher Degree Student Publication Award, 2015.

Best Student Poster Presentation Award, ASSCR annual meeting, Lorne 2014.

National Stem Cell Foundation of Australia (NSCFA) Conference Education Award to attend and present at the ASSCR annual meeting, Lorne 2014.

Flinders University Faculty of Health Sciences Student Conference Grant to attend and present at the EMBO Workshop on Wnt signalling, Broome, Western Australia 2014.

National Stem Cell Foundation of Australia (NSCFA) Travel Award for PhD students/early career researchers to attend the ISSCR annual meeting, Vancouver 2014.

Flinders University Research Student Travel Grant to attend and present at the ISSCR annual meeting, Vancouver 2014.

NSCFA Conference Education Award to attend and present at the ASSCR annual meeting, Brisbane 2013.

Flinders University Faculty of Health Sciences Student Conference Grant to attend and present at the 6th AHMRC annual meeting, Adelaide 2012.

ASSCR Student Travel Grant to attend and present at the ASSCR annual meeting, Blue Mountains, New South Wales 2011.

Flinders University Faculty of Health Sciences Student Conference Grant to attend and present at the ASSCR annual meeting, Blue Mountains, New South Wales 2011.

Abbreviations

aa	amino acid
APC	Adenomatous polyposis coli
ATCC	American Type Culture Collection
AWC	Animal welfare committee
BBR	Barx basic region
bFGF	Basic fibroblast growth factor
bHLH	Basic helix-loop-helix
BMP	Bone morphogenetic protein
bp	base pair
BSA	Bovine serum albumin
ca.	Constitutively active
cDNA	Complementary DNA
ChIP	Chromatin immunoprecipitation
CM	Conditioned media
Co-IP	Co-immunoprecipitation
CTX	Cardiotoxin
dIdC	deoxyinosine-deoxycytidine polymer
DMD	Duchenne muscular dystrophy
DMEM	Dulbecco's Modified Eagle's Medium
DMSO	Dimethyl sulfoxide
DNA	Deoxyribonucleic acid
dNTP	Deoxynucleotide triphosphate
Dox	Doxycycline
Dsh	Dishevelled
DTT	Dithiothreitol
E	Embryonic day
<i>E. coli</i>	<i>Escherichia coli</i>
EDTA	Ethylenediaminetetraacetic acid
EGFP	Enhanced green fluorescent protein
Eh	Engrailed homology domain
EMSA	Electrophoretic mobility shift assay
FACS	Fluorescence activated cell sorting
FBS	Foetal bovine serum
Fzd	Frizzled
G	Gauge
GFP	Green fluorescent protein
GSK	Glycogen synthase kinase
HAT	Histone acetyltransferase
HBS	Homeobox binding site
HD	Homeodomain
HDAC	Histone deacetylase
hr	Hours
IBC	Institutional biosafety committee
IVT	<i>In vitro</i> translated

kb	kilobase
kD	kiloDaltons
KO	Knockout
LB	Luria-Bertani
LEF	Lymphoid enhancer factor
LRP	Low density lipoprotein receptor-related protein
MD	Muscular dystrophy
MEF	Myocyte enhancer factor
MHC	Myosin heavy chain
MPC	Muscle progenitor cell
MRF	Muscle regulatory factor
mRNA	Messenger RNA
NCBI	National Centre for Biotechnology Information
ns	Not significant
nt	nucleotide
OD	Optical density
P	Postnatal day
PAGE	Polyacrylamide gel electrophoresis
PBS	Phosphate buffered saline
PCR	Polymerase chain reaction
PIC	Proteinase inhibitor cocktail
Pen-strep	Penicillin-streptomycin
PLB	Passive lysis buffer
PNK	Proteinase K
RIPA	Radioimmunoprecipitation assay buffer
RNA	Ribonucleic acid
RT-PCR	Reverse-transcription PCR
rTA	Tetracycline-controlled transactivator
rtTA	reverse tetracycline-controlled transactivator
rTETR	reverse Tet repressor
SDM	Site directed mutagenesis
SEM	Standard error of the mean
SF	Serum free
Shh	Sonic hedgehog
siRNA	Small interfering RNA
SMA	Smooth muscle actin
SDS	Sodium dodecyl sulphate
TA	Tibialis anterior
TAE	Tris-acetate EDTA buffer
TBE	Tris-borate EDTA buffer
TBST	Tris-buffered saline/Tween-20
TCF	T-cell factor
TE	Tris-EDTA buffer
tetO	tet operator sequences
TetR	Tet repressor protein
TK	Thymidine kinase
TRE	Tetracycline-response element

Tris	tris{hydroxymethyl}aminomethane
TSA	Trichostatin A
WT	Wildtype

Chapter 1

Review of the Literature

1.1 Skeletal muscle: A brief overview

Skeletal muscle is a form of striated muscle tissue responsible for skeletal movements. Skeletal muscles are attached to bones via bundles of collagen fibres known as tendons and are under the voluntary control of the somatic nervous system. An individual muscle is comprised of a bundle of long, cylindrical and multinucleated cells called myofibres which span the muscle lengthwise (Figure 1.1). These are formed from the fusion of many individual muscle progenitor cells (myoblasts) in a process known as myogenesis. In turn, a single myofibre contains many chains of myofibrils within its cytoplasm (sarcoplasm). The myofibrils are composed of actin and myosin filaments which are arranged in structured repeats called sarcomeres; the basic functional unit of a muscle fibre necessary for muscle contraction (Figure 1.1). Surrounding the myofibrils is the sarcoplasmic reticulum which holds a reserve of calcium ions needed for muscle contraction. Contraction of skeletal muscle operates in a process described by the sliding filament theory [Huxley & Niedergerke 1954; Huxley & Hanson 1954]. In this model, “thin” filaments of actin slide over “thick” filaments of myosin, generating tension in the muscle by altering the length of individual sarcomeres and thereby changing both the length and shape of the muscle. Simply put, this process is stimulated by the arrival of neural impulses at neuromuscular junctions, which in turn elicits an influx of Ca^{2+} from the sarcoplasmic reticulum. Ultimately, the Ca^{2+} binds to the troponin C present on the actin-containing “thin” filaments, allowing troponin T to allosterically modulate the tropomyosin. This then unblocks the binding sites for myosin on the actin filaments, allowing for formation of an actin-myosin cross-bridge.

Skeletal muscle is exceptionally plastic and is remarkable in its ability to adapt and regenerate even following extensive damage resulting from traumatic injury or degenerative conditions. Skeletal muscle structure and function can adapt with ease to different stimuli in response to use and disuse; increased work load increases both muscle size and strength [Goldberg et al. 1975; Widrick et al. 2002; Hawley & Holloszy 2009] whilst muscle disuse results in muscle weakness and atrophy [Nicks et al. 1989; Narici & de Boer 2011]. These can include stimuli which modify its contractile activity (inactivity, endurance, exercise) and stimuli which modify imposed load (resistance exercise, unloading). In addition, environmental factors such as heat, oxidative stress [Musaro et al. 2010], and growth factor and nutrient availability also affect muscle function [Husmann et al. 1996; Harridge 2007; Rennie 2007; Schiaffino et al. 2013]. As such, complex cascades of cellular responses triggered by nerve impulses, mechanical stimuli and systemic (e.g. hormonal) cues work together to form, maintain or repair muscle tissue. As skeletal muscle constitutes approximately 50% of the body's total mass for the average adult, an understanding of the molecular and cellular mechanisms which govern these functions is of high importance. In particular, an understanding of how these mechanisms are dysregulated within the context of abnormal muscle homeostasis and/or function due to injury or disease is crucial. To this end, muscle progenitor cells have been well studied in terms of the molecular programs regulating quiescence, proliferation and differentiation during both embryonic development and adult regeneration. Despite the extensive existing knowledge, there is still much to understand about the control of muscle progenitor cells, particularly in terms of signalling pathways and transcriptional regulatory networks. Such studies could lead to the discovery of novel factors and pathways that

might be modulated therapeutically to treat muscle disease.

1.1.1 Formation of skeletal muscle

During vertebrate embryonic development, transient structures of mesodermal cells called somites can give rise to vertebrae, dermis and muscle. Specifically, epithelial cells on the dorsal aspect of the somites develop into the dermomyotome. The dermomyotome is the subsequent source of all dermal, endothelial and skeletal muscle precursors, thus giving rise to the skeletal muscle of the body and limbs [Chevallier et al. 1977; Christ et al. 1977; Jacob et al. 1978; Denetclaw & Ordahl 2000].

Muscles of the limbs are formed by successive waves of migration of multipotent muscle progenitor cells (MPCs) from the dermomyotome into the developing limb buds [Christ & Ordahl 1995; Mackenzie et al. 1998; Buckingham et al. 2003]. Upon activating the myogenic program once they reach the limb, these precursor cells give rise to proliferating myoblasts that express muscle-specific genes [Rudnicki et al. 1993; Tajbakhsh & Buckingham 1994; Tajbakhsh et al. 1996; Buckingham et al. 2003; Kassam-Duchossoy et al. 2004]. The myoblasts will ultimately withdraw from the cell cycle to fuse with each other forming the multinucleated myotubes that subsequently mature to become skeletal muscle fibres [Cooper & Konigsberg 1961].

1.2 Muscle stem cells: The satellite cell

Like all tissues that are capable of homeostasis and renewal, adult skeletal muscle is dependent upon a mechanism which can compensate for the degradation or loss of terminally differentiated muscle fibres [Pellettieri & Sanchez Alvarado 2007]. This mechanism is provided by satellite cells. Satellite cells are the resident stem cells of adult skeletal muscle, representing the oldest known adult stem cell niche [Mauro

1961], and provide a reserve capacity for postnatal muscle growth and regeneration. Satellite cells reside immediately adjacent to the muscle fibre between the basal lamina and sarcolemma, where they are responsive to molecular cues from the myofibre (Figure 1.1). Their activation results in a ready supply of myoblasts for muscle growth, homeostasis and repair [Bischoff 1975; Konigsberg et al. 1975; Collins et al. 2005]. As well as their unique anatomical niche, satellite cells can be further identified morphologically and histologically by their small nuclear size, a high nuclear:cytoplasmic volume ratio, and the expression of a distinctive set of genetic markers [Mauro 1961; Cornelison & Wold 1997; Seale et al. 2000; Lepper et al. 2009; Yin et al. 2013].

Although stem cell populations from both muscle and non-muscle have emerged as effectors of muscle regeneration, the latter including mesangioblasts [Minasi et al. 2002], endothelial cells [Le Grand et al. 2004], pericytes [Birbrair et al. 2013] and bone marrow stem cells [Bittner et al. 1999], extensive evidence from multiple laboratories has demonstrated that the satellite cell is the primary and indispensable mediator of postnatal skeletal muscle repair [Yin et al. 2013]. In their resting state in undamaged muscle, satellite cells are mitotically quiescent and comprise only a small fraction of all myonuclei (~30% at birth, ~3% by adulthood [Gibson & Schultz 1983; Reimann et al. 2000]). In response to muscle injury, myofibres secrete factors that result in activation of satellite cells, inducing them to undergo asymmetric division [Allen & Boxhorn 1989; Seale et al. 2003; Zammit et al. 2004; Kuang 2007]. Typically this produces one daughter cell that is a committed myoblast able to proliferate and exit the niche, and one which retains stem cell properties and returns to quiescence to

replenish the satellite cell pool [Sacco et al. 2008]. The daughter cells which re-enter the cell cycle divide repeatedly as myoblasts before undergoing myogenic differentiation to form either new post-mitotic myofibres, or fuse with existing fibres to facilitate growth and repair of damaged tissue in a process similar to foetal development.

The number of satellite cells in postnatal muscle tends to remain constant over multiple cycles of muscle degeneration and regeneration, supporting the aforementioned capacity for self-renewal and replenishment of the satellite cell pool [Schultz & Jaryszak 1985; Kuang et al. 2007]. However, satellite cell numbers have been reported to decrease with age [Snow 1977; Gibson & Schultz 1983], suggesting that self-renewal capacity is altered by systemic changes associated with ageing and thus leading to a reduced regenerative capacity.

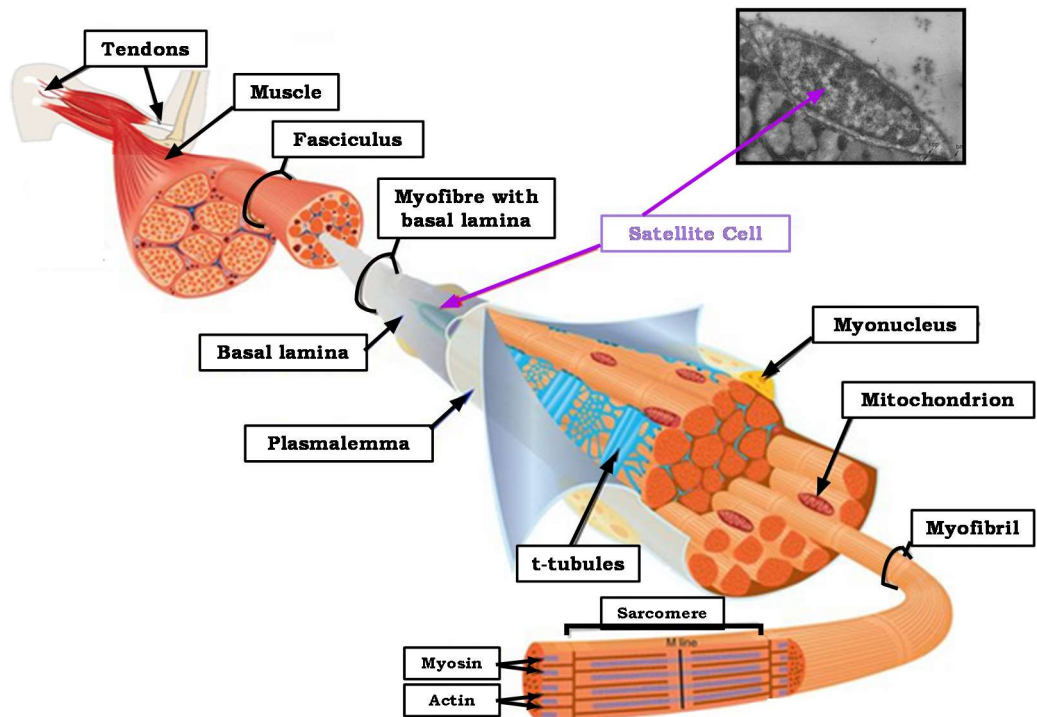


Figure 1.1: Structure of skeletal muscle

The structure of skeletal muscle (modified with permission from Shahrghim Tajbakhsh [Tajbakhsh 2009] and Peter Zammit [Relaix & Zammit 2012]). The satellite cell niche is located beneath the basal lamina which surrounds the myofibre. Image upper right: a transverse section of a skeletal muscle fibre from rat sartorius identifying a satellite cell [Mauro 1961].

1.3 Muscular dystrophy

The term ‘myopathies’ covers a range of neuromuscular disorders in which the primary symptom of muscle weakness occurs due to dysfunction of the muscle fibre for one of many reasons. Myopathies can be acquired, or can be inherited like many of the muscular dystrophies (MD). Muscular dystrophies encompass a range of disorders caused by genetic mutations resulting in either a dysfunction in, or lack of, proteins that are essential for muscle cell stability [Mercuri & Muntoni 2013]. They are characterized by abnormal myofibre degeneration and regeneration and are

usually progressive, culminating in decline in muscle function. This progressive weakness leads to disability and in some severe forms of MD, cases early death from respiratory or cardiac failure [Gomez-Merino & Bach 2002; Passamano et al. 2012]. The most common life-threatening childhood form of MD is Duchenne muscular dystrophy (DMD), an X-linked recessive disorder estimated to affect approximately 1 in 3500 male newborns [Emery 1991]. Life expectancy for boys with DMD is around 20 years, with most patients unable to walk by 12 years of age. Treatment to date remains largely palliative with physiotherapy and occupational therapy. Despite advancement over the last decade there remains no cure, and current treatment aims only to manage symptoms, slow progression and prevent complications [Wagner et al. 2007; Bushby et al. 2010].

The DMD phenotype arises from deletions, duplications or mutations within one or more of the exons that constitute the dystrophin gene, resulting in a lack of functional dystrophin [Hoffman et al. 1987]. The dystrophin gene is the largest gene identified to date, and due to its vast size (2.6 million bp, 79 exons) sporadic mutations occur frequently, accounting for a third of all cases. Dystrophin is a vital structural protein which protects the myofibres from damage during contraction. It links the internal cytoskeleton of a muscle fibre to the extracellular matrix, permitting transmission of the forces of contraction from within the myofibre to the surrounding matrix [Nowak & Davies 2004]. In the absence of dystrophin, myofibres eventually rupture and necrose. In theory, satellite cell activation and the subsequent expansion of their myoblast progeny in response to cues generated by myofibre damage should allow for considerable muscle repair. However, despite the remarkable regenerative

capacity of muscle, in humans the constant demand for repair in DMD appears to create a situation in which regeneration cannot keep pace with the rate of degeneration [Ruegg & Glass 2011]. The process of muscle regeneration involves considerable remodelling of the extracellular matrix, and this may become aberrant. Muscles in DMD patients begin to exhibit extensive fibrosis, calcium deposits and fatty inclusions (e.g. scar tissue) due to overactivity of fibroblasts and myofibroblasts, as well as a dysregulation of myoblast plasticity. The replacement of myofibres with scar tissue further impairs muscle function, reducing the regenerative capacity and accelerating deterioration [Alexakis et al. 2007]; it also leads to an enlarged muscle in a condition known as pseudohypertrophy [Cros et al. 1989].

The DMD phenotype is generally thought to involve senescence of satellite cells driven by the constant pressure of repeated rounds of activation. The continuous participation of satellite cells in response to muscular regeneration is suggested to result in a significant reduction in their cumulative proliferation potential [Schultz & Jaryszak 1985; Day et al. 2010]. As support for this model, myoblasts from DMD patients show a reduced replicative potential which reaches near exhaustion by 7 years of age [Blau et al. 1983; Webster & Blau 1990]. Additionally, Renault and colleagues reported that myoblasts cultured from a DMD patient ceased to divide after 13 population doublings, in comparison to the 30 population doublings observed with an age-matched control [Renault et al. 2000]. However, recent work has challenged this model by demonstrating that the satellite cells themselves do not harbour any inherent defects in regenerative capacity, and are as functional as wildtype-derived satellite cells once removed from the dystrophic environment

[Boldrin et al. 2015]. Some of these discrepancies may relate to the different behaviour of the satellite cell reservoir versus their myoblast progeny, and the responses of the cells to different *in vitro* culture conditions.

An early treatment strategy investigated for DMD was the transplantation of satellite cell-derived myoblasts into dystrophic muscle. Studies have shown fusion of donor nuclei with host myofibres up to six months following transplantation accompanied by increases in dystrophin-positive fibres with little fibrosis observed between fibres [Huard et al. 1991; Tremblay et al. 1993; Gussoni et al. 1997]. Currently, however, there are considerable limitations in myoblast and muscle stem cell transplantation therapies related to immune response, delivery, engraftment efficiency and limited migration of transplanted cells from the transplant site [Meng et al. 2011; Bareja & Billin 2013; Maffioletti et al. 2014]. There has been little evidence of clinical benefit for these transplant approaches in humans.

1.3.1 *Mdx* mice: a DMD model

The most widely used model of DMD is the *mdx* mouse. Like DMD patients, the *mdx* mouse lacks functional dystrophin. *Mdx* mice experience initial myofibre necrosis at age 2-4 weeks [Cullen & Jaros 1988], however they quickly recover. After this initial period, *mdx* mice have a muscle pathology that progresses slowly, and they demonstrate only a mild dystrophic phenotype with very little muscle wasting and a marginally (20%) shortened lifespan [Bulfield et al. 1984; Hoffman et al. 1987; Lefaucheur JP 1995; Chamberlain et al. 2007]. Except for the diaphragm muscle, deletion of dystrophin in mice does not result in formation of fibrous connective tissue, nor does it result in loss of muscle mass. This phenotype is therefore much

less severe than that observed in humans and as such does not provide an ideal model for analysis of DMD therapies. The difference in severity is potentially due to a greater regenerative capacity in mice which is mediated partly by factors inherent in murine muscle stem cells and their descendent myoblasts including greater self-renewal capacity and longer telomeres. Consistent with this idea, an *mdx* model which also lacks telomerase (mTR) activity [Sacco et al. 2010] shows a more severe, rapidly progressing phenotype accompanied with a greatly reduced lifespan.

Improving the regenerative capacity of muscle in humans opens up the potential to slow or even halt disease progression. To do so requires an understanding of the pathways that regulate skeletal muscle development and repair and to understand how these may become dysregulated in disease states such as DMD. However, this requires animal models that faithfully recapitulate the severe phenotypes observed in human muscle disease. This would ultimately allow for identification of new therapeutic targets and pathways, and provide a platform for testing the efficacy of new genetic, stem cell or pharmacologic therapies for treatment.

1.4 Molecular regulation of myogenesis

Our understanding of skeletal muscle regeneration has greatly improved in recent years due to advances in genetics, molecular biology and cell biology. Extensive research on satellite cells following their discovery in 1961 [Mauro 1961] has elucidated many mechanisms which underlie the process of muscle regeneration. Perhaps the most significant finding to date is the discovery of the myogenic regulatory factors (MRFs) which function as nodal points for flow of myogenic information [Thayer et al. 1989; Montarras et al. 1991; Tapscott & Weintraub 1991;

Weintraub et al. 1991]. The MRFs form a family of four highly related transcription factors each containing a conserved basic helix-loop-helix (bHLH), motif which are collectively expressed in the skeletal muscle lineage.

1.4.1 Myogenic Regulatory Factors

The members of the MRF family, MyoD, Myf5, myogenin and MRF4 (also known as Myf6), have been studied in depth since their initial discoveries [Tapscott et al. 1988; Braun et al. 1989; Edmondson & Olson 1989; Rhodes & Konieczny 1989; Wright et al. 1989; Braun et al. 1990] and have been shown to play critical roles in both myogenic determination and myogenesis. During early embryonic muscle development, members of the MRF family have distinct but overlapping patterns of gene expression [Rawls et al. 1998; Kablar & Rudnicki 2000; Kablar et al. 2003]. Specifically, in the somite Myf5 is the first MRF expressed, beginning at embryonic day (E)8 and preceding myogenic differentiation [Ott et al. 1991]. This is followed by myogenin expression in the myotome at E8.5 and MyoD at E10 [Sassoon et al. 1989]. MRF4 is expressed transiently in the myotome between E9 and E11.5 but is subsequently downregulated. Later in development, MRF4 is again expressed in differentiated muscle fibres [Bober et al. 1991; Hinterberger et al. 1991], suggesting a role in the late stages of muscle development. In addition, there is also variation in the expression of MRFs within the compartments of the myotome itself; Myf5 is initially expressed in the dorsal-medial half, MyoD in the ventral-lateral half, and both myogenin and MRF4 are expressed in the whole myotome [Smith 1994].

The distinct but overlapping roles of the MRFs has been further demonstrated through the generation of knockout mice. Whilst an unexpectedly normal skeletal

muscle phenotype has been reported for *Myf5* and *MyoD* knockout mice [Braun et al. 1992; Rudnicki et al. 1992], double *Myf5/MyoD* mutants were observed to form no skeletal muscle due to absence of the precursor myoblast population [Rudnicki et al. 1993]. In these mice, cells in the somite which would otherwise become myoblasts do not locate correctly to sites of myogenesis and instead adopt other cell fates [Tajbakhsh et al. 1996; Kablar et al. 1999]. In contrast to *MyoD* and *Myf5* null mice, studies on *myogenin* knockout mice have revealed that an absence of myogenin expression results in a severe reduction of all skeletal muscle leading to death immediately after birth [Hasty et al. 1993; Nabeshima et al. 1993; Venuti et al. 1995]. These mice also exhibit a reduction in MRF4 expression as well as the skeletal muscle fibre marker myosin heavy chain (MHC), whereas MyoD levels remain normal [Hasty et al. 1993]. The end result is thus diffuse myofibre formation and an abundance of undifferentiated myoblasts. Similarly, mice lacking MRF4 have no prominent muscle defects but show an increase in myogenin expression [Braun & Arnold 1995; Zhang et al. 1995], likely in compensation for the lack of MRF4. Taken together, these findings suggest a two-step model for muscle development in which MyoD and Myf5 act in a redundant fashion upstream of myogenin and MRF4 to establish the myogenic lineage and specify myoblasts for terminal differentiation. Myogenin and MRF4 are more directly involved in the differentiation process, regulating the expression of myotube-specific genes. These factors are therefore organised in a hierarchical gene expression network which can be spatiotemporally induced or repressed during lineage progression and regeneration.

The MRF pathway possesses a remarkable ability to convert a variety of non-

myogenic cell types, such as chondroblasts and the 10T½ and NIH3T3 fibroblasts, into muscle via activation of the myogenic program [Tapscott et al. 1988; Edmondson & Olson 1989; Choi et al. 1990; Russo et al. 1998]. In addition to activating the expression of structural genes required for skeletal muscle, members of the MRF family are capable of activating expression of other members in a hierarchical cascade fashion, as well as maintaining their own expression through a series of auto- and cross-regulatory networks [Braun et al. 1989; Edmondson & Olson 1989; Thayer et al. 1989; Naidu et al. 1995; Berkes et al. 2004]. This provides a level of redundancy whereby MRFs mutually reinforce a fail-safe mechanism for myogenic commitment of the cell.

As mentioned, all MRF members contain a conserved basic helix-loop-helix (bHLH) element. The majority of bHLH proteins function as dimers through their helix-loop-helix motif and bind to the consensus DNA sequence CANNTG [Ephrussi et al. 1985], known as an E-box; a motif found in the promoters of many muscle-specific genes [Massari & Murre 2000]. Due to the complex nature of gene regulatory networks, it is unlikely that the MRFs would be capable of independently regulating this gene expression profile. Supporting this, analysis of MRFs as transcriptional activators has clearly shown that the function of the MRFs in regulating target gene expression is coupled to that of other transcription factors and co-activators. The bHLH proteins form a large superfamily of transcription factors that can be loosely grouped in to two categories: the class II tissue-specific category, such as the MRF family, and the class I ubiquitously expressed E-proteins, including E12, E47 and HEB [Jones 2004]. Although the class II proteins, including the MRFs, are able to form weak

homodimers, they preferentially heterodimerize with the E-proteins, which on their own are non-myogenic [Braun & Arnold 1991; Lassar et al. 1991; Hu et al. 1992]. Specifically, recent work suggests that the E-protein HEB is preferentially expressed in developing muscle, and may be the primary E-protein that cooperates with MRFs in regulating skeletal muscle differentiation [Conway et al. 2004; Parker et al. 2006; Londhe & Davie 2011]. In addition to the HLH domain, a 12 amino acid basic domain of the MRF family mediates DNA binding. The basic domain with the central alanine and threonine (AT) residues, is crucial for binding to promoters of muscle-specific genes, and is absent from non-myogenic bHLH proteins [Davis et al. 1990; Davis & Weintraub 1992; Weintraub et al. 1994; Heidt et al. 2007]. This specific sequence is critically required for myogenic potential as mutation of these residues within MyoD renders it non-myogenic [Davis et al. 1990; Ma et al. 1994; Black et al. 1998]. The heterogeneity in the dimers formed by different MRFs and E-proteins, and thus the specific E-box sequences recognised, determines in part how MRFs are able to control different aspects of myogenesis. In spite of this, there are a number of skeletal muscle genes that can be activated by the MRFs despite the lack of obvious E-boxes in their control regions. This suggests that MRFs may also activate muscle-specific gene expression by indirect mechanisms [Thompson et al. 1991; Parmacek et al. 1994], possibly through downstream transcription factor targets.

1.4.2 Myocyte Enhancer Factors

In addition to MRFs, regulation of myogenesis is mediated by the myocyte enhancer factor-2 (MEF2) family of MADS (MCM1, Agamous, Deficiens, Serum Response Factor)-box transcription factors, consisting of four independent genes: *mef2a*, *mef2b*, *mef2c* and *mef2d* [Yu et al. 1992]. MEF2 proteins can act as co-factors for

MRF-mediated activation. For example, although they cannot induce myogenesis alone in transfected fibroblasts, they can act with MRFs to synergistically activate muscle-specific genes and increase the extent of myogenic conversion observed with an MRF alone [Molkentin et al. 1995; Molkentin & Olson 1996; Black et al. 1998]. Studies on the desmin promoter demonstrate this cooperativity [Li & Capetanaki 1993; Li & Capetanaki 1994], and a mechanism for enhancer-promoter communication has been proposed. MEF2 factors share a highly conserved 86 amino acid region that encodes the MADS and MEF2 domains, which mediate DNA binding and dimerization respectively [Molkentin & Olson 1996]. MEF2 factors recognise and bind AT-rich domains (consensus sequence of CC(A/T)₆GG) called CARG-boxes within the promoters of muscle-specific genes [Andres et al. 1995]. Whilst the MEFs are mostly ubiquitous, MEF2C expression is restricted to skeletal muscle, brain and spleen, and has highly enriched DNA-binding activity in muscle cell types [Martin et al. 1993; Naya et al. 1999]. To date, most of the muscle-specific genes examined have been found to contain MEF2 binding sites in their control regions, including the MRFs [Thompson et al. 1991; Edmondson et al. 1992; Cheng et al. 1993; Buchberger et al. 1994; Parmacek et al. 1994; Black et al. 1995]. Likewise, members of the MRF family can activate the expression of MEF2 factors [Cserjesi & Olson 1991; Yu et al. 1992; Dodou et al. 2003], suggesting that MRF and MEF2 factors function in a complex network by auto- and cross-activating their own and each other's expression to coordinate the myogenic program. Evidence also suggests that members of the MEF2 family may act as co-regulators of MRF-mediated transcription through recognition of the MRF basic region described previously, resulting in direct protein-protein interactions [Molkentin et al. 1995; Naidu et al. 1995; Black et al. 1998]. In support of

this, activation of the myogenin promoter by Myf5 and MyoD requires a MEF2 site but not an E-box motif [Johanson et al. 1999].

1.4.3 The Pax family

Members of the paired-homeobox (Pax) family of transcription factors play a critical role in the genetic hierarchy that leads to the formation and maintenance of skeletal muscle. The Pax family comprises nine members (Pax1-9), which possess both a paired domain and a paired-type homeodomain capable of mediating sequence-specific DNA binding [Walther et al. 1991]. Collectively, *Pax* genes have important functions in regulating development and differentiation of diverse cell lineages during embryogenesis. The Pax3 and Pax7 members play a pivotal role in myogenesis. These factors have similar protein structures and overlapping expression patterns during mouse embryogenesis [Jostes et al. 1990; Goulding et al. 1991]. Two studies have previously identified a proliferating population of Pax3⁺/Pax7⁺ cells that are absent of skeletal-muscle-specific markers in embryonic muscles of the limbs [Kassar-Duchossoy et al. 2005; Relaix et al. 2005]. This population was observed to constitute the resident muscle progenitor cells that will become myogenic, form skeletal muscle and also give rise to satellite cells postnatally. In addition, due to the high homology of both the paired domain and paired-type homeodomain of Pax3 and Pax7, they bind to the same sequence-specific DNA elements (paired domain: GTCAC(A/G)(C/G)(A/T)(T/C), homeodomain: ATTA) [Chalepakis et al. 1994; Schafer et al. 1994; Chalepakis & Gruss 1995], suggesting regulation of similar sets of target genes. An example of likely functional overlap can be seen in the translocations that lead to the expression of activating Pax3-FKHR and Pax7-FKHR fusion proteins. These are equally associated with development of alveolar rhabdomyosarcomas, cancers of

skeletal muscle progenitor cells [Bennicelli et al. 1999].

Currently Pax3 and Pax7 are believed to have some overlapping but mostly non-redundant roles in embryonic myogenesis and establishment of the satellite cell lineage [Buckingham & Relaix 2007]. Studies using *Pax3* and *Pax7* mutant mouse models suggest that Pax3 is important for mediation of the progenitor migratory phase [Relaix et al. 2004], whilst Pax7 is essential to achieve myogenic potential and maintain satellite cell self-renewal [Seale et al. 2000; Wen et al. 2012]. In the absence of both Pax3 and Pax7 expression, myogenesis arrests during the late stages of embryogenesis [Relaix et al. 2005]. Overall, Pax3 and Pax7 are both critical for ensuring the survival of embryonic muscle progenitors and adult satellite cells. Despite this understanding, many of their specific functions and targets remain to be elucidated.

1.4.3.1 *Pax3*

Pax3 is required for somite segmentation and formation of the dermomyotome [Schubert et al. 2001; Relaix et al. 2004], but is also required for multiple aspects of embryonic limb myogenesis including migration of muscle progenitors to the limb buds. In the absence of *Pax3* expression, all limb muscle is absent [Bober et al. 1994; Daston et al. 1996; Relaix et al. 2004] due to failure of myogenic progenitors to populate the developing limb buds, and there is no detection of Pax7 positive cells [Hutcheson et al. 2009]. *Pax3* is an upstream effector of MRF expression: it can induce MyoD and Myf5 expression [Maroto et al. 1997] and directly binds to and activates enhancer regions of the *Myf5* [Bajard et al. 2006] and *MyoD* genes [Tajbakhsh et al. 1997; Hu et al. 2008]. Moreover, double-mutant *Pax3/Myf5* mice lack expression of

MyoD and are devoid of all body muscles [Tajbakhsh et al. 1997; Kassar-Duchossoy et al. 2004]. Although Pax3 is essential for embryonic myogenesis, there is no apparent role for Pax3 in adult muscle regeneration due to the absence of expression in the majority of satellite cells and adult myoblasts [Schafer et al. 1994; Montarras et al. 2005; Relaix et al. 2006].

1.4.3.2 *Pax7*

In contrast to Pax3, Pax7 is dispensable for embryonic myogenesis even though it is expressed in proliferating embryonic muscle progenitors [Jostes et al. 1990; Seale et al. 2000; Zammit et al. 2006]. It does, however, play a critical role in the maintenance and function of satellite cells during postnatal growth and regenerative myogenesis [Seale et al. 2000; Kuang et al. 2006; Hutcheson et al. 2009; Sambasivan et al. 2011; von Maltzahn et al. 2013]. This conclusion is largely based on analysis of *Pax7*-null mice which exhibit no overt defect during embryonic development, but contain a reduced number of satellite cells at birth. These mice also show progressive loss of the satellite cell lineage in muscle throughout postnatal development due to apoptosis and cell-cycle defects [Seale et al. 2000; Oustanina et al. 2004; Kuang et al. 2006]. As expected, this is accompanied by a reduction in muscle size, reduced formation of myofibres, fewer nuclei per myofibre, reduced fibre diameter, a severely compromised ability to regenerate following skeletal muscle injury (evidenced by fibrotic and adipose tissue deposits) and poor survival [Kuang et al. 2006; Sambasivan et al. 2011; von Maltzahn et al. 2013]. Importantly, Pax3 is unable to replace the function of Pax7 in satellite cells [Relaix et al. 2006].

Pax7 is often considered to be the canonical marker of satellite cells. In situ

hybridization has shown that Pax7 is uniformly expressed in the quiescent satellite cells residing in adult skeletal muscle [Seale et al. 2000]. Furthermore, by employing a representational difference analysis technique, Seale and colleagues demonstrated that Pax7 was specifically expressed in cultured satellite cell-derived myoblasts and was downregulated following myogenic differentiation [Seale et al. 2000]. Pax7 overexpression has been shown to delay myoblast differentiation, in part by downregulating and inhibiting the functions of MyoD and myogenin [Zammit et al. 2006; Olguin et al. 2007; Otto et al. 2009], and promoting cell cycle exit [Olguin & Olwin 2004]. Evidence to date therefore suggests that Pax7 is important for satellite cell survival and self-renewal, and for allowing satellite cells to reacquire a quiescent state, thus maintaining the satellite cell pool during muscle regeneration.

1.5 The Barx2 homeobox protein

Homeobox genes are a large family of related genes required for directing the formation of many body structures (morphogenesis) during early embryonic development. These genes encode homeodomain proteins that contain a DNA-binding domain (homeodomain, ~60 aa) which recognises the DNA motif TAAT [Odenwald et al. 1989]. Homeobox proteins typically function in cooperation with other regulatory factors, which may be from a broad range of structural classes. Due to the role of homeobox proteins in embryonic development, mutations within these proteins or misregulation of the genes often produce easily visible phenotypic changes. As such, disruption of the normal gene expression is responsible for a wide variety of developmental disorders. Several homeobox transcription factors regulate early formation and patterning of muscles. They can also play important roles in

postnatal satellite cells, although their functions and interrelationships with other factors may differ in the embryonic and adult contexts. Such homeobox factors include members of the muscle segment homeobox (*Msx*), Ladybird homeobox (*Lbx*) and pituitary homeobox (*Pitx*) families, all of which have been shown to be expressed in somites and/or muscle progenitor cells [Bendall et al. 1999; Gross et al. 2000; Dong et al. 2006; Shih et al. 2007; Watanabe et al. 2007].

Studies in the Meech laboratory, in which this doctoral research was undertaken, have focused on the role of the *Barx* homeobox family. The *Barx* family consists of two members, *Barx1* and *Barx2*. Within our research group the *Barx2* protein and its role during myogenesis is of particular interest. The *Barx2* gene is found in all mammalian species as well as chicken and zebrafish. Conservation of *Barx2* protein is fairly high throughout these species, with the mouse *Barx2* protein sharing approximately 88% homology with human, 74% with chicken and 66% with zebrafish [Makarenkova & Meech 2012].

1.5.1 *Barx2* expression and a role in myogenesis

As homeobox genes such as *Barx2* typically control embryonic development and tissue patterning, it is important to know their developmental expression pattern in order to understand their morphogenetic functions. During embryonic development, *Barx2* is expressed in restricted patterns in many epithelial tissues. These include the nervous system, kidney, skin, hair follicles, lacrimal and lung buds, among others [Jones et al. 1997; Smith & Tabin 1999; Olson et al. 2005; Tsau et al. 2011]. *Barx2* expression continues past embryogenesis, and in newborn mice *Barx2* expression remains high in the skin, hair follicles, vibrissae follicles (in whisker pads),

reproductive tissues and kidney [Makarenkova & Meech 2012]. Previous work arising from the laboratory has shown the critical role of Barx2 in development of the musculoskeletal system. In mice, Barx2 is observed in the somites, limb mesenchyme and early dorsal and ventral muscle masses at E10-11, as well as later in the joints and muscle masses of developing limbs [Jones et al. 1997; Meech et al. 2005; Makarenkova & Meech 2012]. Histological analyses of Barx2 protein in sections of embryonic (E13.5) and foetal (E18.5) mouse limbs has revealed expression of Barx2 in a subset of nuclei within primary myofibres, as well as in nuclei located between the fibres which are likely to be proliferating myoblasts due to co-expression of MyoD [Meech et al. 2012]. Barx2 is also co-expressed with Pax7 in embryonic and foetal muscle and in cultured myoblasts derived from early postnatal mice [Meech et al. 2012]. In newborn mice Barx2 is expressed in the growing limb muscles [Makarenkova & Meech 2012], and in uninjured adult muscle Barx2 is expressed in almost all Pax7-expressing cells. Together these data suggest that Barx2 marks quiescent and activated satellite cells as well as their proliferating myoblast progeny. In addition, Barx2 is expressed in a number of cells in muscle which are absent of Pax7 expression [Meech et al. 2012] and these may represent fibroblasts, other interstitial cells, and/or pericytes. Barx2 also plays a critical role in muscle regeneration as determined by our previous work in a cardiotoxin injury model. During the early stages of regeneration in cardiotoxin-injured adult muscle, when satellite cells are giving rise to a pool of proliferating myoblasts, Barx2 mRNA and protein are highly induced. Specifically, Barx2 protein can be observed to be co-expressed with Pax7 and MyoD, demonstrating its role in regeneration in satellite cells and their myoblast progeny [Meech et al. 2012].

1.5.2 *Barx2* null mice show skeletal muscle dysfunction and defective muscle repair

Gene knockout studies show that *Barx2* is functionally important for muscle regeneration. A germline *Barx2* null mouse model generated by Olson and colleagues [Olson et al. 2005] has been used by our research group to assess the roles of *Barx2* in myogenesis. The *Barx2* null mouse model was generated by deletion of the region of the gene encoding the homeodomain and the C-terminus, leaving only the N-terminal portion of *Barx2* intact. This was fused in-frame with a β -galactosidase gene, thus ablating function of *Barx2* and simultaneously allowing for assessment of *Barx2* expression patterns [Olson et al. 2005]. At present, any residual functions in myogenesis that the N-terminal domains of *Barx2* may have in this model are unknown. Using this mouse model, a number of observations related to skeletal muscle have been made. Firstly, not unlike *Pax7* null mice, no obvious defects in embryonic muscle development are observed. No differences in muscle size or morphology can be seen in *Barx2* null embryos (E12.5 – E18) and there is no difference in body weight between wildtype, heterozygous, and null siblings at birth [Meech et al. 2012]. However, after birth *Barx2* null mice begin to exhibit a growth delay: by postnatal day (P)4, *Barx2* null mice show a subtle 10% reduction in body weight relative to their wildtype (WT) or heterozygous siblings, and by P28 this difference is more pronounced with *Barx2* null mice approximately 25% smaller [Meech et al. 2012]. Moreover, the reduction in the masses of skeletal muscles (tibialis anterior (TA), quadriceps and soleus muscle) in null mice was disproportionately greater than the reduction in overall body mass and the mass of other organs such as the kidneys [Meech et al. 2012]. This suggests that the reduction

in total body weight may be due to reduced muscle growth.

In addition to a delay in postnatal muscle formation, histological analysis of adult *Barx2* null mice has revealed differences in muscle architecture when compared to muscles of wildtype mice. Multiple defects including narrower myofibres, an increased variability of fibre sizes and a larger distance between myofibres have been observed in *Barx2* null mice, as well as collagen deposits suggesting increased and ongoing fibrosis [Meech et al. 2012]. The musculoskeletal phenotype worsens as the mice age, with *Barx2* null mice displaying spinal curvature and a “waddling” gait from around 12 months of age [Meech et al. 2012], although these phenotypes have varying penetrance. Acute muscle injury experiments with cardiotoxin to assess muscle regeneration have revealed a significant delay in the ability of *Barx2* null mice to regenerate fibres. In contrast to wildtype mice which show almost complete myofibre regeneration by 10 days post injury, *Barx2* null mice show very few regenerated fibres by this time. Instead, mice null for *Barx2* expression exhibit disorganised morphology with necrotic fibres, myotubes of different sizes, undifferentiated myoblasts and calcium deposits [Meech et al. 2012]. During this regeneration phase, it appears that loss of *Barx2* alters the normal temporal pattern of gene expression, as assessed by induction of markers of regeneration. Specifically, induction of cyclinD1 and myogenin was delayed and lower in knockout mice, and the myofiber marker myosin heavy chain 4 (*Myh4*) remained lower in *Barx2* null mice even at 12 days post injury [Meech et al. 2012].

In summary, the *Barx2* null mouse model shows profound deficits in adult skeletal muscle maintenance and repair but no defects during embryonic development,

suggesting the most important role for Barx2 is in postnatal and adult myogenesis. This shows parallels with the *Pax7* germline null mouse model, discussed previously [Mansouri et al. 1996; Oustanina et al. 2004]. The fact that Barx2 expression also correlates with expression of Pax7 in myoblasts and satellite cells during muscle development further suggests that they may function in common myogenic pathways.

1.5.2.1 *Barx2/mdx double mutant mice*

As discussed earlier, *mdx* mice are the most widely used model for DMD. The role of Barx2 in chronic muscle injury and repair has previously been assessed by interbreeding *Barx2* mutant mice and *mdx* mice and then extensively backcrossing onto the *mdx* strain background [Meech et al. 2012]. In crosses between *mdx* mice and mice heterozygous for Barx2, *Barx2^{-/-}:mdx* pups were underrepresented by weaning age. In those *Barx2^{-/-}:mdx* mice that did survive, there was reduction in total body and muscle masses when compared to *Barx2^{+/+}:mdx* mice. Moreover, whilst a 30% reduction in total body weight was observed, a much greater 50% reduction in TA muscle weight was observed [Meech et al. 2012]. This was accompanied by irregular organization, variability in myofibre size, and fibrosis in the TA. Development of spine deformation and progressive weakness was also seen in 6 month old *Barx2^{-/-}:mdx* mice [Meech et al. 2012]. Although similar characteristics can also be observed in *Barx2^{+/+}:mdx*, they appeared with greater penetrance and much earlier in *Barx2^{-/-}:mdx* mice. This information provides further support for a role for Barx2 in maintenance of satellite cell and myoblast function in postnatal muscle repair. It suggests that loss of Barx2 in *mdx* mice tips the balance between degeneration and regeneration, leading to a more severe dystrophic phenotype

which is reminiscent of human DMD. Interestingly, a similar conclusion was drawn about the critical role of satellite cell-mediated regeneration in MD progression from studies of *mdx* mice lacking telomerase expression in satellite cells [Sacco et al. 2010]. In this case the severe phenotype was proposed to be due to satellite cell exhaustion, whilst in the *Barx2*^{-/-}/*mdx* mice the phenotype more likely results from satellite cell and myoblast dysfunction.

1.5.3 Functional domains and gene targets of Barx2

Interspecies homology of the centrally located Barx2 homeodomain is very high. The mouse Barx2 homeodomain has 100% homology to other mammals and 98% homology to zebrafish. Immediately following the homeodomain, Barx1 and Barx2 share a region encoding for a stretch of 17 amino acids enriched with basic residues (PTKPKGRPKKNSIPTS) called the Barx Basic region (BBR) [Jones et al. 1997]. The role of the Barx2 BBR has been investigated and research suggests that whilst the homeodomain is sufficient to allow binding to homeobox binding sites (HBS), the BBR has a function in determining specificity of interactions between Barx2 and different target genes [Edelman et al. 2000]. The BBR appears to be unique to Barx1 and Barx2 proteins.

The Barx2 protein can be further divided into amino terminal (N-terminal) and carboxyl terminal (C-terminal) functional domains which have been the subject of a number of studies. Three motifs within the N-terminus possess potential functions: a leucine zipper motif, an engrailed homology domain 1 (Eh1) motif and a polyalanine (A) tract (9 residues in mouse) (Figure 1.2). Briefly, the leucine zipper motif can be found in several transcription factors and is involved in mediating protein-protein

interactions, and the polyalanine tract has been associated with developmental abnormalities when increased in residue length [Kouzarides & Ziff 1988; Shanmugam et al. 2000; Utsch et al. 2002]. The Eh1 motif is a short region generally possessing a repressive function through recruitment of members of the Groucho/TLE family of corepressors [Kobayashi et al. 2001; Muhr et al. 2001; Copley 2005; Olson et al. 2005]. In contrast, the C-terminus of Barx2 has fewer obvious functional motifs, but does contain a region rich in acidic residues [Jones et al. 1997] which can be involved in transcriptional activation [Lin & Green 1991] (Figure 1.2).

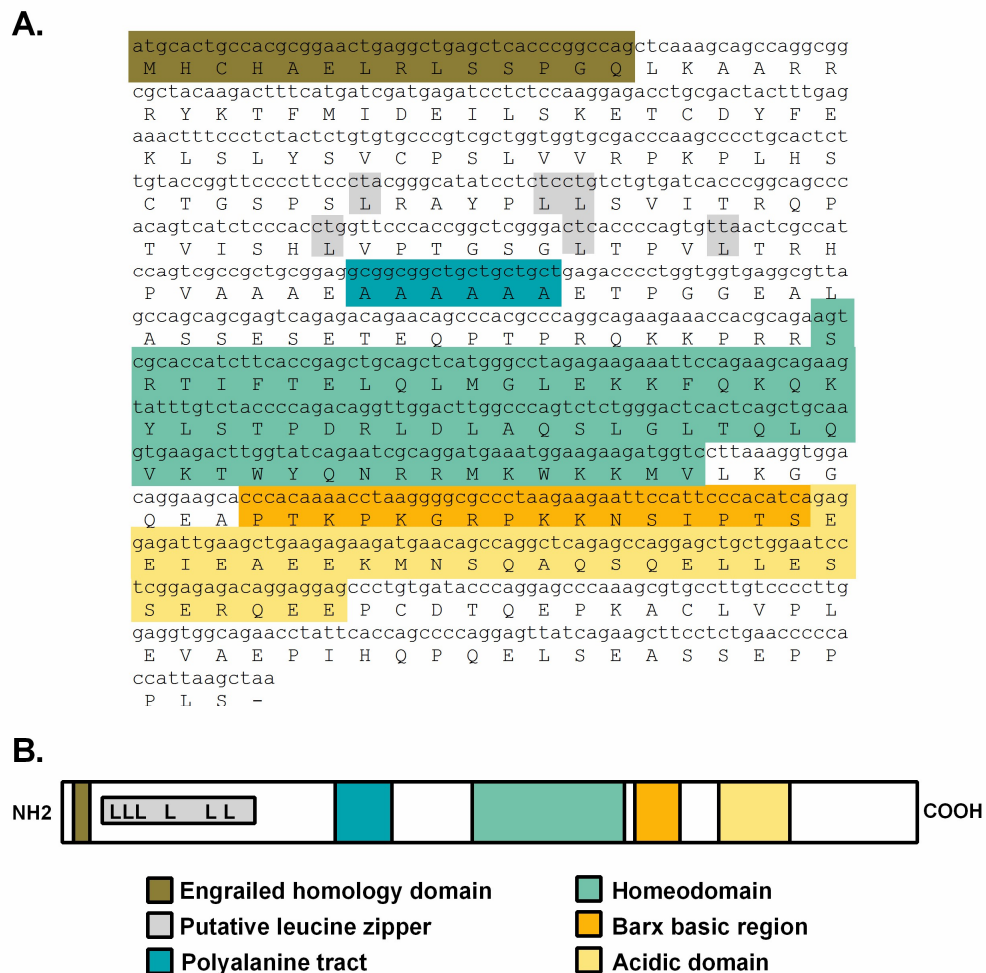


Figure 1.2: Sequence and schematic of Barx2 protein

(A): mRNA and protein sequence of murine Barx2. (B): Schematic representation of murine Barx2 protein.

Initially, overexpression of Barx2 in the mouse embryonic NIH3T3 fibroblast cell line to examine regulation of the mouse L1-CAM (cell adhesion molecule) promoter found that Barx2 mediated transcriptional activation when the CCATTAGPyGA motif was present in the promoter construct, but repressed the activity of promoter constructs lacking the motif [Jones et al. 1997]. This first highlighted the idea that Barx2 contains domains that mediate both activation and repression. Using N-CAM luciferase reporter plasmids in a neural cell line, promoter-reporter assays have been used to investigate the functional domains of Barx2 [Edelman et al. 2000]. A repressive function within the amino terminus was identified, with a construct consisting of the amino terminal region plus the homeodomain and BBR (HDBBR) resulting in a strong repression of the N-CAM promoter. In contrast, a construct consisting of the carboxyl terminus plus HDBBR resulted in a 2-fold activation of the N-CAM promoter. Together, the N-terminal and C-terminal domains appeared to antagonize each other's functions, with the overall effect of the full length (intact) Barx2 construct being mildly repressive [Edelman et al. 2000]. More recently, interactions between Barx2 and two known co-activators of myogenesis, proliferator-activated receptor γ -coactivator 1 (PGC-1) and CREB-binding protein (CBP), were demonstrated [Makarenkova et al. 2009]. These interactions are likely via the C-terminal activation domain of Barx2. In a study by Olson and colleagues [Olson et al. 2005], the N-terminal domain of Barx2 was again shown to have a repressive function. Specifically, Barx2 was shown to repress its own gene promoter via interactions with various co-repressors as described further in a subsequent section. Collectively, the data discussed here indicate that the function of Barx2 is context-dependent. It is likely that it involves interactions with multiple cofactors via multiple different Barx2

domains.

Barx2 has been shown to be a direct regulator of genes involved in many processes critical for myogenesis including cell migration, cytoskeletal remodelling, cell proliferation and cell differentiation. Several muscle-specific gene promoters with binding elements for MRFs and MEF proteins also contain conserved HBS elements clustered with these binding motifs. Chromatin immunoprecipitation (ChIP) assays with Barx2 antibodies have demonstrated binding of Barx2 to some of these muscle-specific genes such as myogenin, myosin heavy chain II, myosin light chain I and smooth muscle α -actin (SMA) [Makarenkova et al. 2009]. In myoblasts, Barx2 can regulate expression of SMA [Makarenkova et al. 2009], a marker of myoblast differentiation which appears to be important for both migration and changes in cell shape prior to fusion [Schevzov et al. 1992; Springer et al. 2002]. Intriguingly, whilst Barx2 modestly activated the SMA promoter via a conserved HBS motif, the activation was much more potent when MyoD was co-expressed and bound to a neighbouring E-box motif [Makarenkova et al. 2009]. In contrast, myoblasts isolated from *Barx2* null mice have reduced/delayed SMA expression, which may be related to their reduced production of cellular processes as well as slower migration and fusion [Makarenkova et al. 2009]. Myoblasts lacking Barx2 expression may be less proliferative, and have been clearly shown to have delayed differentiation compared to wildtype myoblasts [Meech et al. 2003; Makarenkova et al. 2009; Meech et al. 2010]. Preliminary evidence suggests that cyclinD1, myogenin and MyoD are regulated by Barx2 and as such may contribute to these phenotypes; whether these are due to direct interactions between Barx2 and target gene promoters, and

whether they involve other transcription factors is unknown. Taken together, Barx2 appears to function at multiple levels to regulate proliferation, migration and differentiation of myoblasts, and likely acts cooperatively with members of the MRF family and other proteins to coordinate these processes.

1.5.4 Regulation of Barx2

Bioinformatics analyses of the Barx2 proximal 400 bp promoter has identified a cluster of binding motifs for factors which are known for their critical roles in muscle-specific gene regulation [Meech et al. 2003]. This region, which is also highly conserved between mouse and human, contains E-box motifs recognised by the MRFs, and CA₂G boxes recognised by both MEF2 family members and serum response factor (SRF). The conserved E-box motif most proximal to the CA₂G box is essential for activation of the Barx2 promoter by MyoD and myogenin, and the CA₂G box is also important for regulation by these MRFs [Meech et al. 2003; Makarenkova & Meech 2012], suggesting cooperation for control of Barx2 expression in myoblasts. Thus, not only does Barx2 regulate the expression of many muscle-specific genes, including members of the MRF family, but it is also under the transcriptional control of said MRFs. This suggests that Barx2 is closely connected with the activities of the MRFs during myogenesis and functions in a complex feedback loop.

A region approximately 1.4 kb from the Barx2 translation start site containing repeats of the core HBS motif, TAAT, has been shown to be involved in auto-repression by Barx2 itself in skin [Olson et al. 2005]. Recruitment of Barx2, as well as members of the transducin-like enhancer of split (TLE), transducin- β -like (T β 1) and nuclear corepressor 1 (N-CoR) families of co-repressors was demonstrated at this region.

However, whether this auto-regulatory mechanism is important for control of Barx2 expression in muscle has yet to be established.

1.6 Adult skeletal muscle regeneration

The process of satellite cell activation, proliferation and differentiation holds the key to postnatal growth and adult muscle regeneration following injury. This process essentially recapitulates that of embryonic muscle development. Both processes are based on similar regulatory and signalling mechanisms, with many similarities such as identical transcription factors and signalling molecules [Tajbakhsh 2009]. The process of skeletal muscle regeneration is highly orchestrated and involves the activation of many regulatory processes including the MRF and Pax transcription factor families discussed previously. The information that underpins the mechanistic basis for these complex processes of muscle repair has been predominantly obtained from studies that involve injuring muscle tissue in rodents, such as freeze-crush or cardiotoxin (CTX) models. This allows for study of the satellite cells and their progeny as they expand mitotically and differentiate to re-establish muscle homeostasis. It also allows the self-renewal and replenishment of the satellite cell pool to be studied. It is important to keep in mind, however, that these injury models do not necessarily reflect the downstream molecular events that occur post-exercise (eccentric events that damage myofibres), or in chronic degenerative states.

It is currently theorised that all satellite cells express Pax7 [Relaix et al. 2005], with quiescent satellite cells exhibiting high levels of Pax7 and Myf5 and low levels of MyoD [Cornelison & Wold 1997; Olguin et al. 2007]. As satellite cells become activated due to myofibre injury, their molecular markers change with the degree of

activation. The initial activation of satellite cells sees the majority of satellite cells induce MyoD expression. This high co-expression of Pax7 and MyoD identifies the activated satellite cell population [Zammit & Beauchamp 2001; Zammit et al. 2002]. As the activated satellite cells enter the proliferative phase (myoblasts), downregulation of Pax7 and induction of myogenin are observed. Most myoblasts then stop expressing Pax7 and differentiate, expressing markers of differentiation such as MRF4, myosin heavy chain and desmin, although a small subset of cells maintain Pax7 expression and are thought to be self-renewing and return to the satellite cell pool [Olguin & Olwin 2004; Zammit et al. 2004; Zammit et al. 2006; Dick et al. 2015]. Overexpression of Pax7 downregulates MyoD, thus antagonising myogenic progression [Olguin & Olwin 2004; Zammit et al. 2006].

In summary, activation of the MRF pathway drives myogenic commitment and initiates differentiation along the myogenic lineage: initial expression of Myf5 and MyoD commits cells to the myogenic program and promotes proliferation, whilst subsequent downstream expression of myogenin and MRF4 are required for the fusion of myocytes and the formation of myotubes through terminal differentiation [Tajbakhsh & Buckingham 1994; Rawls et al. 1995; Tajbakhsh et al. 1996; Cornelison & Wold 1997; Sabourin & Rudnicki 2000]. With the recent aforementioned studies on the role of Barx2 in myogenesis *in vivo*, new information can be added to this pathway: Barx2 is co-expressed with Pax7 in satellite cells, and it remains expressed during the activation, proliferation and differentiation phases of muscle repair, even following Pax7 downregulation. Indeed, *in vitro* studies indicate that Barx2 is upregulated as differentiation proceeds. The Barx2 promoter is a direct target for

regulation by MyoD and myogenin, and Barx2 itself can interact with these proteins to modulate expression of early muscle differentiation-associated genes such as SMA. Barx2 is, however, downregulated after fusion of myoblasts and is not expressed in mature muscle fibres. Thus, Barx2 appears to be important for the early stages of differentiation, likely because it controls genes that mediate cytoskeletal remodelling, cell movement, and cell migration. This is summarised in Figure 1.3.

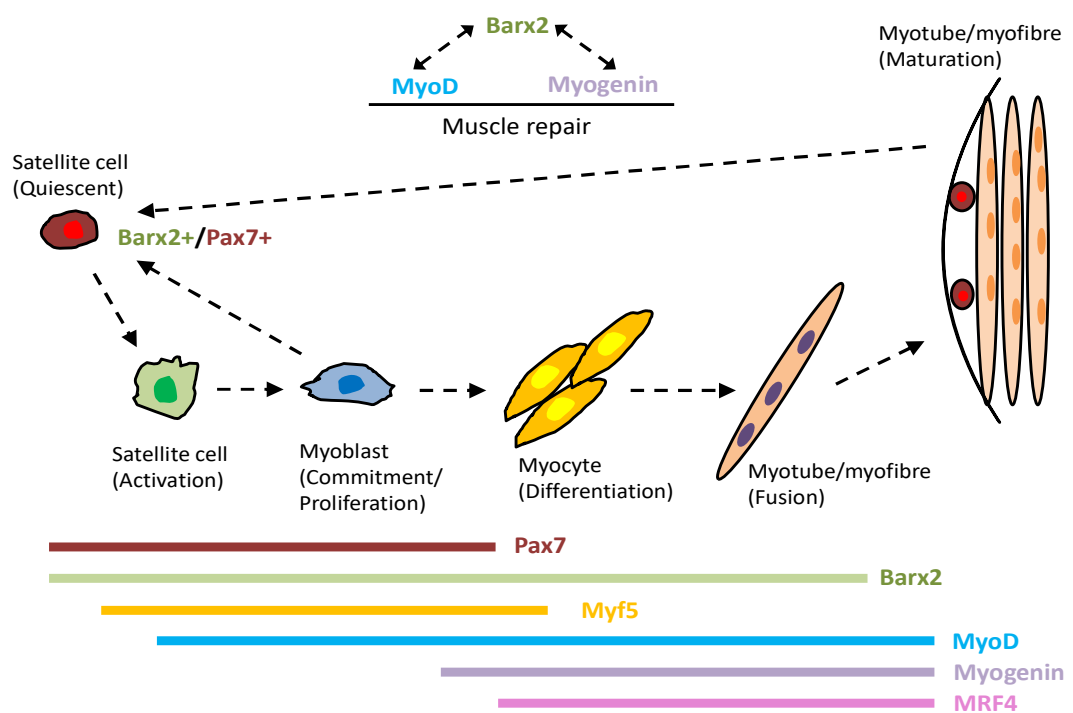


Figure 1.3: Hierarchy of transcription factors in myogenesis

Model summarising the hierarchy of transcription factors regulating progression during muscle development and repair. The expression and proposed functions of Barx2 are indicated. Image is based on a previously published schematic [Makarenkova & Meech 2012].

1.7 The canonical Wnt signalling pathway

In addition to transcription factors such as Barx2 and the MRF and Pax family members, the process of myogenesis (both embryonic and adult) is further

orchestrated by complex signalling networks. Several *in vivo* studies investigating these networks have identified Sonic hedgehog (Shh), BMPs (bone morphogenetic proteins), Notch, and Wnts as the major signalling pathways underpinning myogenesis. The Wnt signalling pathway is of particular focus for this thesis.

Wnts are a highly conserved family of secreted soluble glycoproteins. In most mammals the Wnt family consists of 19 members, and these function either through canonical [Logan & Nusse 2004] or non-canonical [van Amerongen & Nusse 2009] pathways depending on the exact Wnt/receptor complex. For both pathways, activation follows binding of a secreted Wnt ligand to a cell-surface receptor. This induces a signalling cascade which ultimately culminates in gene regulation [Nusse 2008]. The canonical Wnt signalling pathway is the most comprehensively studied and involves the Frizzled (Fzd) cell-surface receptors [Bhanot et al. 1996], the ubiquitous central mediator β -catenin and downstream T-cell factor/lymphoid enhancer factor (TCF/LEF) proteins for transcriptional activation.

The TCF/LEF family is comprised of four members: Tcf1 (Tcf7), Tcf3 (Tcf7l1), Tcf4 (Tcf7l2) and Lef1 [Oosterwegel et al. 1991; Travis et al. 1991; van de Wetering et al. 1991; Waterman et al. 1991; Castrop et al. 1992]. There are certain structural features common to all four members of the TCF/LEF family: a HMG box DNA-binding domain, an N-terminal β -catenin binding domain [Omer et al. 1999] as well as interaction sites for the Groucho/TLE family of co-repressors [Arce et al. 2006; Hoppler & Kavanagh 2007]. TCF/LEF proteins are associated at TCF/LEF binding sites (consensus CTTTG(A/T)(A/T)) [van de Wetering et al. 1991] in regulatory regions of Wnt target genes in the nucleus. Extensive experiments have revealed that when the

Wnt cascade is not activated, TCF/LEF members act as repressors of Wnt target genes [Brannon et al. 1997] through interaction with Groucho/TLE [Cavallo et al. 1998; Chen et al. 1999] and likely other co-repressors. Meanwhile, in the absence of a Wnt ligand the core positive effector of the Wnt pathway, β -catenin, is phosphorylated by the serine/threonine kinases casein kinase 1α (CK1 α) and glycogen synthase kinase-3 β (GSK-3) [Yost et al. 1996; Amit et al. 2002; Liu et al. 2002]. These function as part of a multimeric ' β -catenin destruction complex' with Dishevelled (Dsh) and the scaffolding proteins Axin and adenomatous polyposis coli (APC) [Hart et al. 1998; Kishida et al. 1998; Hsu et al. 1999]. Phosphorylated β -catenin is targeted for degradation by the proteasome, ensuring a low level of β -catenin due to continual cytoplasmic turnover [Aberle et al. 1997; Yanagawa et al. 2002].

Evidence to date suggests that Wnts function as long-range signals that can act on distant neighbouring cells during development [Strigini & Cohen 2000]. Activation of the canonical pathway involves binding of a Wnt ligand to a Frizzled/low density lipoprotein receptor-related protein (LRP) receptor complex in the plasma membrane of a target cell [Clevers & Nusse 2012], which triggers the relocation of Axin away from the destruction complex to the membrane [Cliffe et al. 2003]. With dissociation of the destruction complex, β -catenin is no longer phosphorylated or degraded, thus allowing it to accumulate. β -catenin is normally shuttled from the cytoplasm to the nucleus, and hence the increased stability of β -catenin also allows nuclear accumulation. Nuclear β -catenin is then able to interact with TCF/LEF family members at Wnt target genes [Behrens et al. 1996; Clevers & van de Wetering 1997; Nusse 1999; Hecht & Kemler 2000; Hecht et al. 2000]. Binding of β -catenin plays a

critical role in converting TCF/LEF proteins from transcriptional repressors to transcriptional activators. It is thought that β -catenin displaces Groucho/TLE and other corepressors [Daniels & Weis 2005] and enhances recruitment of coactivators [Hecht et al. 2000; Takemaru & Moon 2000; Barker et al. 2001]. Ultimately, the receipt of a Wnt signal results in transcriptional activation of Wnt target genes. The “off” and “on” states of the canonical Wnt signalling pathway are summarised below in Figure 1.4.

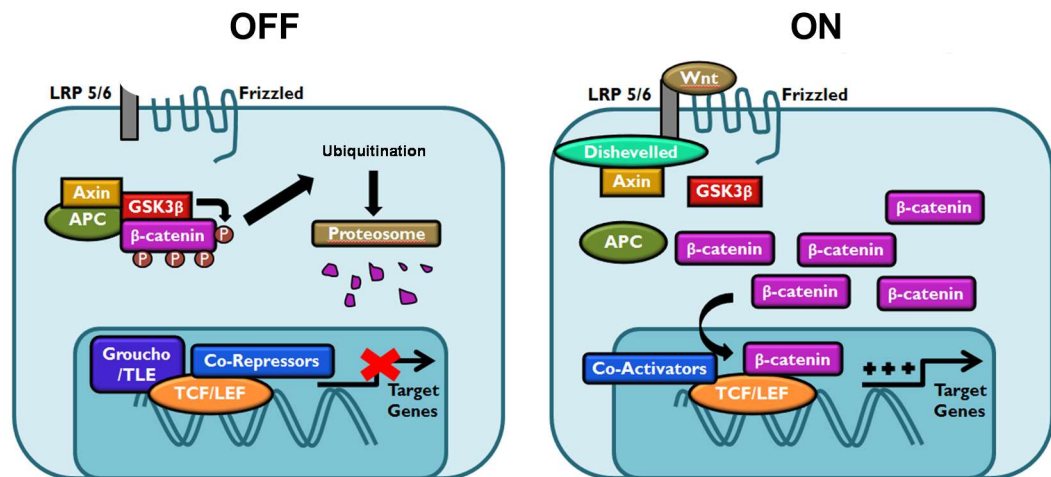


Figure 1.4: The canonical Wnt signalling pathway

In the absence of a Wnt ligand (“Off” state), β -catenin is targeted for phosphorylation and degraded. In the nucleus, TCF/LEF proteins are associated with members of the Groucho/TLE corepressor family, together forming a strong repressor complex. When a Wnt ligand binds the Frizzled/LRP receptor (“On” state), β -catenin is stabilised, enters the nucleus and displaces Groucho/TLE corepressors from TCF/LEF. β -catenin associates with TCF/LEF and coactivators to result in transcriptional activation.

1.7.1 Wnt signalling in myogenesis

The canonical Wnt signalling pathway plays a critical role in embryonic muscle development and in postnatal muscle growth, repair and ageing. Embryonic myogenesis is partly induced by the canonical Wnt ligands Wnt1 and Wnt3, which are

produced by the dorsal neural tube and activate expression of Pax3/7, Myf5 and MyoD in the epaxial myotome during myogenesis, thus driving myogenic specification [Maroto et al. 1997; Seale et al. 2003; Otto et al. 2006; Abu-Elmagd et al. 2010]. In particular, the *Myf5* promoter contains TCF/LEF binding sites required for its early expression [Borello et al. 2006]. Other Wnts are also able to mimic signals from the neural tube, activating both MyoD and Myf5 in explants of paraxial mesoderm [Tajbakhsh et al. 1998]. The critical role of canonical Wnts has been further demonstrated by *Wnt1* and *Wnt3a* knockout mice. These mice do not form the dermomyotome and this is accompanied by a reduction in Myf5 expression [Ikeya & Takada 1998]. Additionally, conditional deletion of β -catenin using Pax3-Cre or Pax7-Cre has shown that β -catenin is necessary for dermomyotome and myotome formation [Hutcheson et al. 2009].

Various Wnts have been reported to influence the proliferation and differentiation of adult satellite cells and myoblasts [Clevers 2006]. In general, non-canonical and canonical Wnts appear to have different roles during lineage progression. For example, the non-canonical Wnt7a ligand is shown to promote self-renewal of satellite cells [Le Grand et al. 2009]. In contrast, canonical Wnt ligands are generally shown to promote myoblast differentiation in culture [Bernardi et al. 2011; Pansters et al. 2011; Suzuki et al. 2015] and the canonical pathway has been suggested to be involved in the switch from proliferation to differentiation [Brack et al. 2008; Tanaka et al. 2011]. This has been further assessed by more recent studies: Increased β -catenin in the nucleus can also be observed in proliferating satellite cells [Otto et al. 2009]. Wnt3a was recently suggested to accelerate myogenic differentiation by

stimulating expression of myogenin and follistatin [Jones et al. 2015]. Myogenic differentiation is also positively regulated by R-spondin, a positive regulator of canonical Wnt signalling [Han et al. 2011]. Very recently, bone morphogenetic protein and activating membrane-bound inhibitor (BAMBI), an enhancer of Wnt signalling in various cell types, was shown to peak during C2C12 myoblast differentiation. Knockdown of BAMBI resulted in reduced Wnt signalling and inhibition of differentiation [Zhang et al. 2015].

As further support for the role of Wnt signalling in adult myogenesis, Wnts appear to be important following skeletal muscle injury or exercise [Poleskaya et al. 2003; Brack et al. 2008; Brack et al. 2009]. Recent studies suggest that activation of Wnt signalling following wheel-running in mice results in direct activation of satellite cells through upregulation of Myf5 and MyoD [Fujimaki et al. 2014]. In addition, Wnts may also be linked to the ageing phenotype. An increase in canonical Wnt signalling in aged skeletal muscle has been reported, and this may play a role in inhibiting myogenesis due to myogenic to fibrogenic transdifferentiation of satellite cells and a loss of cells committed to the myogenic lineage [Brack et al. 2007]. The number of satellite cells present in skeletal muscle decreases with age and these cells may also have reduced potential for activation, proliferation and differentiation [Renault et al. 2002; Shefer et al. 2010], resulting in an overall loss of regenerative capacity [Hikida 2011].

Despite the demonstrated roles of Wnts in almost all aspects of myogenesis including satellite cell activation and myoblast proliferation, differentiation and migration [Poleskaya et al. 2003; Brack et al. 2007; Le Grand et al. 2009], the *muscle specific*

mechanisms of the different Wnt signals/pathways are not well understood. A detailed characterization and understanding of these mechanisms may identify potential targets and allow for therapeutic manipulation of Wnt signals *in vivo* or during *in vitro* satellite cell culture, transplantation and/or engraftment. This may provide new strategies for alleviation of physiological and pathological conditions associated with degenerating muscle which is observed in disease states such as DMD. In fact, it has recently been demonstrated that manipulation of Wnt signals could provide therapeutic benefit in haematopoietic stem cell transplantation [Ko et al. 2011], and that non-canonical Wnt7a can stimulate satellite cell expansion, motility and engraftment to result in improved muscle strength and hypertrophy [von Maltzahn et al. 2012; Bentzinger et al. 2014].

1.8 Potential relationship between Barx2, Pax7 and Wnt signalling

In any given cell type, only a subset of Wnt-responsive target genes are activated in response to a Wnt ligand. As an example, Pax7 and the MRF genes appear to be downstream targets of canonical Wnt ligands only in muscle [Tajbakhsh et al. 1998; Borello et al. 1999; Seale et al. 2003; Hutcheson et al. 2009]. As the expression of β -catenin and TCF/LEF members is ubiquitous, the tissue-specific responses to Wnts are generally thought to be mediated by tissue-specific co-regulators (transcription factors and their cofactors). The recent studies discussed here implicate Barx2 as a novel regulator of myogenesis. Barx2 is expressed in both embryonic myoblasts and adult satellite cells and appears to be required for normal postnatal muscle growth and regeneration. Many of the cellular and *in vivo* phenotypes observed after perturbation of *Barx2* expression are similar to those observed following disruption

of normal canonical Wnt signalling as discussed below. These observations prompted the hypotheses that Barx2 and Wnt/ β -catenin signalling may have overlapping molecular roles, and that Barx2 may be a novel regulator of muscle-specific Wnt signalling.

The canonical Wnt signalling pathway is stimulated following muscle injury, is required for myoblast differentiation and regulates expression of MRF and Pax genes. Barx2 is also co-expressed with Pax7 and MyoD in satellite cells and proliferating myoblasts [Meech et al. 2012]. *In vitro* studies indicate that Barx2 is important for myoblast differentiation and it has been shown to regulate expression of muscle-specific genes such as SMA. Furthermore, this activation of SMA by Barx2 is enhanced by interaction of Barx2 and MyoD, and co-binding of these factors to adjacent homeobox and MyoD (E-box) binding elements in the promoter [Makarenkova et al. 2009]. Interestingly, MyoD has also been shown to interact directly with the central mediator of Wnt signalling, β -catenin, at E-box elements in MyoD target genes [Kim et al. 2008].

Many other components of the canonical Wnt signalling pathway have previously been shown to interact with Barx2. In a study by Olson and colleagues [Olson et al. 2005], the N-terminal domain of Barx2 demonstrated repression of the Barx2 promoter. The repressive function of this domain involved the TCF/LEF-associated corepressors Groucho/TLE and NCoR [Song & Gelmann 2008] that interact with the Barx2 Eh1 motif and are co-recruited to promoter DNA *in vivo* [Olson et al. 2005]. It is also notable that Barx2 plays important regulatory roles in the hair follicle, where Wnt signalling is also critical [Gat et al. 1998; Huelsken et al. 2001; Olson et al. 2005].

In this system, Barx2 associates with the transducin β -like protein 1 (Tb1) and the highly related family member TblR1, known coactivators required for β -catenin-mediated activation in oncogenesis [Li & Wang 2008]. Finally, co-immunoprecipitations have demonstrated that Barx2 can interact with CREB-binding protein (CBP) [Makarenkova et al. 2009], a bimodal regulator of Wnt signalling [Li et al. 2007]. Collectively, all of these data have suggested that Barx2 may influence the Wnt signalling pathway or even function as an effector within the Wnt pathway.

Whilst Barx2 and Pax7 are both expressed in satellite cells and myoblasts, and mice lacking either gene exhibit poor postnatal muscle growth and repair, literature suggests that these factors function in opposition to each other. Specifically, Pax7 is downregulated during differentiation and its ectopic expression inhibits differentiation [Olguin & Olwin 2004; Zammit et al. 2004], whereas Barx2 is upregulated during differentiation, and its overexpression promotes differentiation [Makarenkova et al. 2009; Meech et al. 2010; Meech et al. 2012]. Whether these factors function in common or parallel molecular pathways remains to be determined.

1.9 Experimental aims

Preliminary work undertaken in the Meech laboratory that was unpublished at the beginning of this project [Zhuang et al. 2014] used a synthetic Wnt reporter gene to show that Barx2 may be a novel component of the downstream effector pathway of canonical Wnt signalling in myoblasts. Barx2 activated the Wnt reporter, and this activation was significantly enhanced by co-transfection of MyoD with Barx2. Further characterization of this transcriptional pathway would greatly enhance our

understanding of how canonical Wnt signalling regulates myogenesis. Barx2 appears to promote both myoblast proliferation and differentiation and it is likely that Barx2 cooperates with different coactivators or corepressors to control target gene expression and to regulate the outcomes of Wnt signalling at these different stages. However, the nature of these interactions is not currently known. Barx2 functions in a feedback loop with members of the MRF family, whereby Barx2 regulates MRF expression but the Barx2 gene is also regulated by MRFs. As such, Barx2 may also play a role *downstream* of signalling pathways which mediate myogenesis, such as Wnt. The following hypothesis was thus formed: a functional network between Barx2, MyoD, β -catenin, TCF/LEF and possibly Pax7 controls the response of satellite cells to Wnts and thus adult muscle growth and repair, and that disruption of this network leads to dramatically reduced regenerative capacity.

To explicate this network, the following specific aims were developed:

1. To define in detail the mechanisms by which Barx2 activates the synthetic Wnt/ β -catenin reporter gene
2. To characterise Barx2-containing effector complexes in muscle cells and the interactions between Barx2 and other Wnt effector proteins and cofactors
3. To identify endogenous gene targets of Barx2 in myoblasts and determine the overlap of Barx2- and Wnt/ β -catenin-target genes
4. To identify any regulatory or functional relationship between Barx2 and Pax7,

particularly with respect to Wnt/ β -catenin signaling

5. To characterise the temporal and spatial relationships between Barx2 and canonical Wnt target gene expression in muscle using Wnt-reporter and Barx2-knockout/reporter-knockin mice

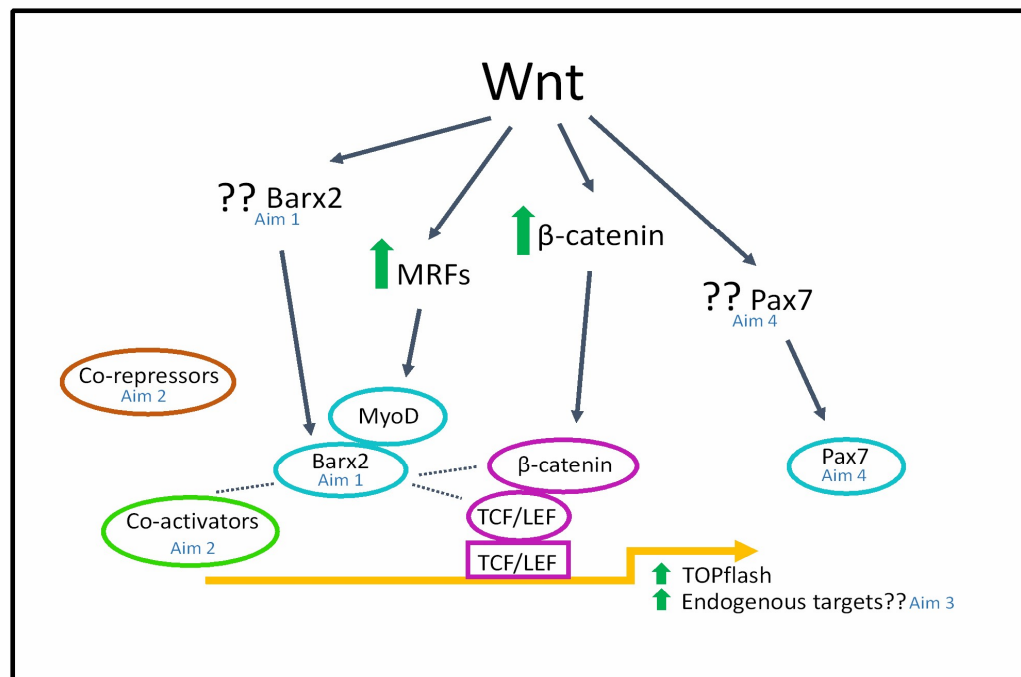


Figure 1.5: Regulatory interactions between Barx2, β -catenin, MRFs and Pax7

Wnt stimulation of myoblasts results in increased MRF and β -catenin expression. Stabilised β -catenin associates with TCF/LEF transcription factors at TCF/LEF motifs of Wnt-responsive promoters. At least one of the MRFs, MyoD, associates with Barx2. Preliminary evidence shows Barx2 and MyoD can together activate a synthetic Wnt reporter, TOPflash, but the exact mechanisms of this activation are as yet unknown (Aim 1 and 2). Whether this activation extends to endogenous targets is also unknown (Aim 3). Currently, the role of Barx2 and Pax7 downstream of Wnt (Aim 1 and 4) are yet to be determined, as is any functional relationship between Barx2 and Pax7 (Aim 4).

Chapter 2

Methods and Materials

2.1 Chemicals and reagents

All chemicals and reagents used during this project were of analytical grade. The suppliers of chemicals, reagents and kits mentioned throughout this thesis are listed in Appendix 1.

2.2 General buffers

The following buffer formulae were used to make up appropriate buffers throughout the duration of this work:

1 x Phosphate buffered saline (PBS): 137 mM NaCl, 2.7 mM KCl, 10 mM Na₂HPO₄ and 2 mM KH₂PO₄, pH 7.4

1 x Tris-acetate EDTA electrophoresis buffer (TAE): 40 mM Tris pH 8, 20 mM acetic acid, 1 mM EDTA

0.5 x Tris-borate EDTA electrophoresis buffer (TBE): 40 mM Tris pH 8.3, 45 mM boric acid, 1 mM EDTA

1 x SDS-PAGE running buffer: 25 mM Tris pH 8.3, 192 mM glycine, 0.1% SDS

1 x SDS-PAGE transfer buffer: 25 mM Tris pH 8.3, 192 mM glycine, 20% methanol

1 x Tris-buffered saline (TBS): 50 mM Tris pH 7.4, 150 mM NaCl

2.3 Mice

Barx2-LacZ knock-in mice were obtained from Dr. Geoff Rosenfeld and were maintained and genotyped as previously reported [Olson et al. 2005]. The Wnt-reporter TOP-EGFP mice were obtained from the RIKEN BioResource Center (BRC)

(RBRC02229) and were genotyped for the presence of GFP. All mice were housed in the Animal Facility in the School of Medicine, Flinders University and all maintenance and breeding of mice was performed by trained technical staff within the facility.

2.4 Eukaryotic and prokaryotic cell lines

The DH5 α *Escherichia coli* (*E. coli*) strain was originally purchased from the American Type Culture Collection (ATCC; Manassas, Virginia, USA). All immortal mammalian cell lines used throughout this project were also originally obtained from the ATCC. A previous member of the laboratory, Ms Thi Diem Tran Nguyen, generated a modified C2C12 cell line which has a stably integrated synthetic Wnt reporter (TOPflash). Designated TOPPuro, this cell line was previously characterised and identified to respond to Wnt3a stimulation and over-expression of Barx2. The TOPPuro stable line proved extremely useful in elucidating functional binding to TOPflash promoter DNA and was a model used consistently throughout this thesis.

2.5 Mammalian reporter and expression vectors

The reporter vectors pGL3-Basic and pRL-Null were originally purchased from Promega. The reporter vector pcDNA3 was originally purchased from Invitrogen. Full length Barx2 cDNA was previously isolated from embryonic day (E)14 mouse tongue and cloned into the pcDNA3 vector in frame with an N-terminal myc-tag by Mr Lizhe Zhuang. Expression plasmids encoding constitutively active (ca.) mouse β -catenin, and human dominant negative (dn) TCF4 were a gift from Dr. Wolfgang Rottbauer (Harvard Medical School, USA) and the cDNAs were subsequently shuttled in to pcDNA3 in frame with an N-terminal flag-tag. A human TCF4 variant expression plasmid (pK-myc) was a gift from Dr. Vladimir Korinek (Institute of Molecular

Genetics, Czech Republic).

The Super 8x TOPFlash and FOPFlash (TOPFlash mutant) promoters were obtained from the Randall Moon Lab (University of Washington, Seattle, WA) and have since been deposited to Addgene (Addgene plasmids 12456 and 12457 respectively) [Veeman et al. 2003]. The cyclinD1/pGL3-Basic construct containing the 1 kb promoter of mouse cyclinD1 was a gift received from Prof. Johan Auwerx of the Ecole Polytechnique Fédérale (Lausanne, Switzerland) [Botrugno et al. 2004]. The Axin2/pGL3-basic plasmid containing a 5.6 kb promoter/intronic region of mouse Axin2 was purchased from Addgene (Addgene plasmid 21275) and was originally constructed by Frank Constantini of Columbia University (New York, USA) [Jho et al. 2002]. The eGFP-containing plasmid was a gift from Dr. Michael Michael (Flinders University, South Australia). The construction of all other daughter pGL3-basic/pcDNA3 plasmids carrying the appropriate promoter/cDNA inserts are described under the relevant sections of this thesis.

2.6 Oligonucleotides

Oligonucleotides were purchased from Geneworks (Hindmarsh, SA, Australia) or Integrated DNA Technologies (Coralville, Iowa, USA). All oligonucleotides were of standard purification quality (desalted). The sequences of all oligonucleotides are listed within the appropriate chapters.

2.6.1 Polyacrylamide Gel (PAGE) purification of site directed mutagenesis oligonucleotides

Oligonucleotides for site directed mutagenesis were purchased as standard (desalted) oligonucleotides and PAGE-purified in the laboratory. Complementary top

and bottom oligonucleotides for a single mutation were annealed together by combining equal amounts in the presence of 1 x NEBuffer 2 (10 mM Tris-HCl, 50 mM NaCl, 10 mM MgCl₂ and 1 mM DTT, pH 7.9), heating to 99°C for 5 minutes and then slow-cooling back to room temperature for up to 2 hours. Annealed oligonucleotide pairs were resolved on a 10% 19:1 Acrylamide/Bis gel in 0.5 x TBE. Oligonucleotides were excised from the gel and eluted in 400 µl 1 x NEBuffer 2 at 4°C overnight. Two volumes of cold 100% ethanol was added to precipitate the DNA which was pelleted at 13,000 rpm for 15 minutes and resuspended in 1 ml 70% ethanol. After a second centrifugation the final DNA pellet was resuspended in 50 µl TE buffer ready for use in PCR.

2.7 Polymerase Chain Reaction (PCR) amplification

2.7.1 Equipment

Non-quantitative PCR reactions were performed on an Applied Biosystems Veriti thermal cycler. For quantitative real-time PCR (qPCR) reactions, a Rotor-Gene™ 3000 (Corbett Life Science, Mortlake, NSW, Australia) thermal cycler was used. Analysis of real-time PCR results was performed using Rotor-Gene 6 software (Corbett Life Science).

2.7.2 PCR for cloning

PCRs to generate DNA fragments for cloning were performed with the high fidelity enzyme *Phusion* DNA polymerase. *Phusion* PCR reactions were performed in a total of 50 µl in the supplied *Phusion* HF buffer, unless specified otherwise, with 0.02 Units/µl *Phusion*, 200 µM dNTPs and 0.5 µM each primer.

2.7.3 PCR for genotyping or screening

Phire Hot Start II DNA polymerase was used for PCR when fidelity was not critical. *Phire* mediated PCR reactions were performed in a total of 20 µl in the supplied buffer with 0.02 Units/µl *Phire*, 200 µM dNTPs and 0.5 µM each primer.

2.7.4 Site-directed mutagenesis

Mutagenesis reactions were performed using Stratagene's QuikChange® Site-Directed Mutagenesis kit as per the manufacturer's instructions with *PfuTurbo* DNA polymerase, unless otherwise specified. 10 Units of *DpnI* were added to the amplified vector and incubated at 37°C for 1 hour to ensure degradation of the wild-type parent vector. A microlitre of digested PCR product was then used to transform 50 µl competent DH5α *E. coli* as described in Section 2.21 and presence of the desired mutation(s) was confirmed by sequencing.

2.7.5 Quantitative real-time PCR

To quantify levels of mRNA transcripts present in RNA extracted from C2C12 cells, primary myoblasts or primary tissue, real-time PCR was used. Primer sets used are detailed in the appropriate chapters. However, the generic set-up used for all reactions was: 20 µl reactions containing 1x GoTaq qPCR Master Mix, 0.5 µM each primer and template cDNA equivalent to 20-40 ng input RNA. The generic PCR cycling conditions used for quantitative analysis were: an activation period of 15 minutes at 95°C; 40 cycles of 95°C for 15 seconds, specific annealing temperature (60-62°C) for 15 seconds, and 72°C for 20 seconds; and a ramped melt analysis between 55 and 95°C with 4 second, 1°C steps. Data was acquired during the 72°C extension phase of each cycle.

2.8 Extraction of total RNA

2.8.1 Extraction of RNA from monolayer cells

C2C12 cells or primary myoblasts were harvested for total RNA post transfection or treatment. To extract total RNA, cells were washed in PBS and harvested in 1 ml TRIzol (Life Technologies, Victoria, Australia) per 10-25cm² of surface area as per the manufacturer's protocol. Briefly, the TRIzol (containing lysed cells) was transferred to 1.5 ml microcentrifuge tubes and 200 µl of chloroform per 1 ml of TRIzol was added to each sample and mixed vigorously. Tubes were centrifuged at 12,000 x g, 4°C for 15 minutes and the aqueous (top) layer containing the RNA was removed to a fresh tube. RNA was precipitated by the addition of 500 µl isopropanol per 1 ml TRIzol initially used, incubated at room temperature for 10 minutes and centrifuged again at 12,000 x g, 4°C for 10 minutes. A final 75% ethanol wash of the RNA pellet was done with 1 ml ethanol per 1 ml TRIzol and centrifuged under the same conditions as previous. The RNA pellet was air-dried, resuspended in 20-30 µl RNase-free water and heated to 60°C for 10 minutes to redissolve.

2.8.2 Extraction of RNA from primary tissue

Harvested murine tissue was stored in RNALater (Invitrogen). RNA from tissue was extracted using the same TRIzol method and protocol. However, tissue samples were first sliced in to small pieces using a razor blade, and then homogenised in a microcentrifuge tube in a small amount of TRIzol (100-200 µl) using a UV-sterilised hand micro-pestle. Generally a final volume of 1 ml TRIzol was sufficient for most tissue samples. The remainder of the protocol was performed as previous. All RNA samples were stored at -20°C.

2.9 Generation of cDNA

Two micrograms of total RNA extracted by TRIzol was treated with one unit amplification grade DNase I in 20 mM Tris-HCl (pH 8.4), 2 mM MgCl₂ and 50 mM KCl for 15 minutes at room temperature. EDTA was added to a final concentration of 2.5 mM and the sample was incubated at 65°C for 10 minutes to inactivate the DNase I.

cDNA was generated from DNase-treated RNA in a random hexamer-primed M-MuLV reverse transcriptase reaction using the Lucigen NxGen M-MuLV Reverse Transcriptase. One microgram (8 µl) of RNA was added to a 20 µl reaction initially containing 1 µl 10 mM dNTPs, 1 µl 53 ng/µl random hexamers (NEB) and 6 µl water. Following a 5 minute incubation at 65°C and 2 minutes cooling on ice, the reaction was brought up to a total of 20 µl by the addition of 2 µl 10x M-MuLV Reverse Transcriptase buffer, 1 µl RNase inhibitor (Lucigen) and 1 µl Reverse Transcriptase (Lucigen). RNA was reverse transcribed at 42°C for 1 hour and the reaction stopped by heating to 90°C for 10 minutes. Before use in PCR, the cDNA was diluted 1:5 in sterile RNase-free water.

2.10 Co-immunoprecipitation (Co-IP)

Co-immunoprecipitation experiments were performed in either COS7 or HEK293T cells due to ease of transfection and high expression. Cells were transfected upon reaching 80% confluency in T25 flasks using Lipofectamine 2000 (Invitrogen) with 5 µg total DNA per flask (two flasks per condition). The exact details of each Co-IP experiment can be found within the relevant results chapters. Nuclear cell lysates were prepared 48 hours post transfection by harvesting cells in 400 µl hypotonic lysis buffer [Klenova et al. 2002] (see Appendix 2) with the addition of proteinase inhibitor

cocktail (PIC; Roche) and phosphate inhibitors (glycerol-2-phosphate). Cell membranes were disrupted by passaging through a 29G needle followed by supplementation with NaCl to 350 mM. Cell lysates were pre-cleared with Protein A-Sepharose for 1 hour and then split into two tubes: 200 μ l for IP and 200 μ l for IgG preimmune control. A 10 μ l aliquot was also saved as a positive input control. Antibodies for protein IP and IgG (3 μ g each) were added to lysates and incubated overnight whilst rotating at 4°C. Complexes were precipitated with Protein A-Sepharose the following day for 2 hours at 4°C and washed three times with PBS. Proteins were eluted from the beads by the addition of 20 μ l SDS sample dye (62.5 mM Tris pH 6.8, 10% glycerol, 2% SDS, 0.01 mg/ml bromophenol blue, 5% β -mercaptoethanol) followed by boiling at 95°C for 5 minutes. Proteins were resolved by SDS-PAGE for immunoblotting.

2.11 Chromatin Immunoprecipitation (ChIP)

ChIP experiments were performed using a modified MicroChIP protocol [Dahl & Collas 2008] in primary myoblasts or TOPPuro, the stable C2C12 cell line expressing the TOPflash promoter/luciferase construct. Cells were either treated with L-cell or Wnt3a CM, or transfected using Lipofectamine 2000 (Life Technologies) at a density of 1.8×10^6 cells per T75 flask. Each flask was transfected with a total of 20 μ g of DNA and 100 μ l Lipofectamine in 3.5 ml serum free (SF)-DMEM. Two flasks were used per condition. Six hours post transfection, the media was removed and replaced with fresh media to prevent transfection toxicity to the cells. Twenty four hours post transfection cells were trypsinised and resuspend in to 2xT175 flasks per transfection condition. After a further 24 hours, cells were cross-linked by the addition of 1% final

formaldehyde (Sigma) to the growth media. Cells were cross-linked for 30 minutes at room temperature with gentle rocking. Glycine was then added to the growth media at a final concentration of 125 mM for 10 minutes at room temperature to quench the formaldehyde and stop the fixation reaction. Following fixation, cells were washed twice with ice-cold PBS and then scraped from the flask in 5 ml ice-cold PBS + PIC per flask. Cell suspensions from duplicate flasks were combined in a 10 ml tube and centrifuged at 3,000 rpm, 10 minutes at 4°C. Supernatant was aspirated and the cells were washed again in 5 ml PBS/tube and centrifuged as previously. After removal of the supernatant, the cell pellet was either stored frozen at -80°C until required, or was lysed immediately. Cells were lysed by the addition of 6 ml of ChIP Lysis Buffer 1 + PIC followed by a 10 minute incubation on ice. Nuclei were pelleted by centrifugation at 4,000 rpm, 10 minutes, 4°C and supernatant was removed. Nuclear lysis was performed by the addition of 500 µl of ChIP Lysis Buffer 2 + PIC and incubation on ice for 10 minutes. Sonication of the chromatin was performed as follows on a Sonics Vibracell VCX130 (John Morris Scientific) using a 3 mm stepped microtip probe: 25% amplitude, 20 second pulse followed by a 30 second rest for a total of 10-15 bursts. Chromatin was kept on ice for the whole procedure. To check efficiency of sonication, 20 µl of chromatin from each sample was reverse crosslinked by adding 80 µl water, 4 µl 5 M NaCl and 1 µl 10 mg/ml RNase A (Cell Signaling Technology) and incubating overnight at 65°C. The remaining sheared chromatin was stored at -80°C until required again. The following day, tubes were cooled, 0.5 µl Proteinase K (PNK; 20 mg/ml) was added and samples were incubated at 42°C for 1 hour. DNA was purified by use of a PCR purification spin kit (Qiagen) as per the manufacturer's instructions and visualised on a 1.5% agarose gel. The aim was to

generate chromatin fragments that ranged between 300 and 3000 bp in length. Once chromatin of the appropriate size range was obtained, the samples were centrifuged at 13,000 rpm, 10 minutes, 4°C to pellet any insoluble material. The chromatin was then diluted 6-fold in Dilution Buffer (to a total of 3 ml) and pre-cleared for 40 minutes at 4°C by adding 20 µl Protein G CHIP-Grade Magnetic Beads (Cell Signaling Technology). Protein G Magnetic Beads were captured and removed from the chromatin samples by use of the magnetic rack (Cell Signaling Technology). The chromatin was split as follows: 20 µl saved for total chromatin (input), 500 µl each for normal rabbit IgG control and each antibody required. Two micrograms of IgG or antibody was used and samples were slowly rotated overnight at 4°C. Thirty microlitres of Protein G Magnetic Beads were added to all IgG and antibody samples (not input) the following day to capture the immunocomplexes and tubes were left to rotate for a further 2-3 hours. Using the magnetic rack, the magnetic beads were washed twice with Dilution Buffer + PIC, once with High Salt Wash Buffer, once with LiCl Wash Buffer and 1x with TE Buffer. Each wash involved slow rotation of the beads in the appropriate buffer for 10 minutes at 4°C. Finally, the beads were captured and resuspended in 200 µl Elution Buffer and incubated at 65°C overnight. The following day 0.5 µl PNK was added and samples were incubated 1 hour at 55°C. DNA purification was performed with the Qiagen PCR purification kit as previously described. For a detailed list of buffers used, see Appendix 2.

2.12 Western Blotting

2.12.1 Preparation of lysates

For protein isolation, cultured mammalian cells were scraped from the flask in PBS

and pelleted gently at 1,500 rpm for 10 minutes. The cell pellet was washed once more in PBS and centrifuged again. Cells were lysed by the addition of 50-100 μ l RIPA buffer (Radioimmunoprecipitation assay buffer; 50 mM Tris pH 7.3, 150 mM NaCl, 0.1% SDS, 0.5% sodium deoxycholate, 1% NP-40) depending on cell number. To further promote cell lysis, lysates were passed through a 29G syringe 10 times and incubated on ice for 20 minutes. Cellular debris was removed via centrifugation at 13,000 rpm for 10 minutes at 4°C and protein lysates were stored at -20°C.

2.12.2 Protein concentration determination

The concentration of total protein in RIPA lysates was determined using Bio-Rad Protein Assay reagent (Bio-Rad, NSW, Australia) as per the instructions. Using a 96-well plate, 2 μ l RIPA lysate was added to 100 μ l 1 x Protein Assay reagent and the absorbance measured at 595 nm in a plate reader (DTX 880 Multimode Detector; Beckman Coulter). Protein concentration was calculated against the 595 nm absorbances of a BSA standard curve of known concentrations (0, 0.1, 0.2, 0.4, 0.6 and 1 μ g/ml).

2.12.3 Polyacrylamide gel electrophoresis (PAGE)

Approximately 20-30 μ g total protein was diluted 1:4 in 4x SDS-PAGE sample loading buffer and heated at 95°C for 5 minutes. Proteins were separated by SDS-PAGE (4% stacking gel, 10% separation gel) at room temperature; at 70 V through stacking gel and 120 V through separating gel using Mini-Protean II Cell equipment (BioRad). Proteins were transferred on to Trans-blot nitrocellulose membrane (Bio-Rad) in an ice-cooled Mini Trans-Blot Cell apparatus at 25 V overnight at 4°C. The membrane was washed once in TBST (TBS + 0.2% Tween-20) and blocked in 3% (w/v) non-fat dry

milk in TBST (blocking buffer) for 90 minutes at room temperature. Following a wash in TBST, the membrane was incubated with primary antibody (generally 1:1000) and 1% blocking buffer overnight at 4°C. The membrane was washed 3 times at room temperature with TBST for 10 minutes each, and then incubated with the appropriate secondary antibody (1:2000) and 1% blocking buffer for 2 hours at room temperature. The membrane was finally washed in TBST another 3 times at 10 minutes each at room temperature before imaging. The blot was treated with enhanced SuperSignal West Pico chemiluminescent (ECL) HRP substrate (Thermo Scientific) to the manufacturer's instructions and imaged using an ImageQuant LAS 4000 (GE Healthcare Life Sciences).

2.13 Preparation of primary myoblasts

The skin was removed from sacrificed mice and the forelimbs and hind limbs were dissected away from the bone, ensuring to keep the muscle moist in a dish of PBS. Using sterile scissors and razor blades, the muscle was minced into a coarse slurry and placed in to a tube containing 500 µl collagenase, 80 µl dispase (680 U/µl) and 30 µl CaCl₂ (20x, final concentration 2.5 mM) per mouse and incubated in a 37°C water bath for 45 minutes to facilitate breakdown of the connective tissue, fibronectin and collagen. Every 15 minutes the muscle was triturated with a 1 ml pipette. After the final incubation, 3 ml myoblast growth media was added to each tube, mixed, and the slurry solution passed over a 50 µm nylon mesh cell strainer. The strainer was washed with a further 2 ml growth media and the filtrate centrifuged at 2,000 rpm for 5 minutes. The cell pellet was resuspended in 10 ml PBS + 2% foetal bovine serum (FBS) and centrifuged for a further 5 minutes. The final cell pellet was

resuspended in 150 μ l PBS + 2% FBS for antibody labelling.

2.13.1 Antibody labelling of myoblasts for fluorescence activated cell sorting (FACS)

Twenty microlitres of isolated cells in PBS + 2% FBS (as above) was placed in a fresh tube and set aside as an unlabelled control sample. The remaining 130 μ l was labelled with: 0.3 μ l Sca1 (FITC rat anti-mouse), 1.2 μ l CD45 (APC rat anti-mouse) and 2 μ l CD34 (PE rat anti-mouse) and left to incubate in the dark at room temperature for 45 minutes. The cells were washed twice with 1 ml PBS + 2% FBS (2,000 rpm, 5 minutes) in a tabletop microcentrifuge before being resuspended in a final volume of 1 ml growth media with 2 μ g/ml doxycycline (to minimise contamination risk) and passed through a 50 μ m nylon mesh membrane before FACS.

2.13.2 FACS

Labelled cells from murine muscle were sorted based on Sca1, CD45 and CD34 expression on a BD FACSAria (BD Biosciences, San Jose, CA). Cells were collected as two populations; the first, CD34+, CD45- and Sca1-, which were considered our primary myoblast population based on morphology and myogenic differentiation capacity. The second, CD34+, CD45- and Sca1+, were deemed to consist of primarily fibroblasts based on morphology. Sorted cells were collected in 1 ml myoblast growth media with 2 μ g/ml doxycycline to reduce the risk of contamination from the sorter and grown on collagen-coated flasks.

2.14 Mouse tail tip/ear notch genomic DNA isolation

Tail tips or ear notches of Barx2, Top-EGFP or BAR-TOP mice were collected by the Animal House, Flinders Medical Centre. Genomic DNA was isolated by incubating the

tissue samples overnight in 600 µl TNES buffer (50 mM Tris pH 8.8, 400 mM NaCl, 100 mM EDTA, 0.5% SDS) with fresh proteinase K (PNK) at 55°C to digest tissue. Two hundred microlitres of 5 M NaCl was then added, tubes shaken vigorously and samples centrifuged at 13,000 rpm for 5 minutes to pellet protein and other debris. Supernatant was removed and transferred to fresh tubes and genomic DNA was precipitated by addition of 700 µl 95% cold ethanol. DNA was pelleted at 13,000 rpm for 5 minutes and the supernatant was decanted. DNA pellets were left to dry at room temperature for approximately 30 minutes to allow the ethanol to evaporate and were ultimately resuspended in 100 µl EB buffer (Qiagen).

2.15 Maintenance of mammalian cell lines

C2C12 cells (mouse myoblast) and all C2C12-derived stable cell lines were cultured in Dulbecco's Modified Eagle Medium (DMEM) supplemented with 20% FBS, 1 mM sodium pyruvate and 0.1 mM non-essential amino acids. Cos-7 (African green monkey kidney) cells were cultured in complete DMEM + 10% FBS, whilst L-Cell and L Wnt-3A (mouse fibroblast) cells were cultured in complete DMEM + 10% FBS + 0.4 mg/ml G418 where appropriate. Cells were grown in an incubator that maintained a constant temperature of 37°C and a humidified atmosphere of 5% CO₂.

An Olympus CK2 microscope was used to assess the approximate level of confluence of the cells on a regular basis. Cells were passaged at approximately 70-80% confluence, ensuring that C2C12 cells and primary myoblasts in particular did not reach full confluence. To passage cells, media was aspirated from the flask and cells were rinsed with 5 ml sterile PBS to remove any remaining DMEM. Cells were released from the flask by the addition of 1.5 ml 0.05% trypsin/0.53 mM EDTA in PBS

solution and incubation at 37°C. The activity of the trypsin digest was stopped by the addition of complete DMEM. Cells were then passaged at a dilution of 1:20 to 1:30 depending on their current density and growth rate.

To determine cell density, 30 µl of cell suspension was combined with an equal volume of 0.2% trypan blue to enable counting of viable cells. Ten microlitres of the cell suspension/trypan blue mix was loaded on to a haemocytometer (Hausser Scientific) and the viable cells were counted. The viable cell concentration (cells/ml) was used to calculate the volume needed to sufficiently dilute the cell suspension for seeding of cells. Once reaching passage 20-25, cell cultures were replaced with fresh stock from liquid nitrogen. All handling of cultures was performed under sterile conditions within a laminar flow hood.

2.16 Maintenance of mouse primary myoblast cultures

Primary myoblast cultures isolated from mouse were cultured in either Myoblast Selection Media (Ham's F10 media, 20% FBS, penicillin-streptomycin (pen-strep) and 5 ng/ml murine basic fibroblast growth factor (bFGF)) or Myoblast Growth Media (1:1 Ham's F10 media:complete DMEM, 20% FBS, pen-strep and 5 ng/ml murine bFGF). In order for the primary myoblasts to adhere, all plates and flasks were first coated with a collagen solution (filtered 20 mM acetic acid + 50 µg/ml rat tail collagen). Enough collagen was added to completely cover the surface and this was left on either overnight at room temperature or for 1 hour at 37°C. After removal of the collagen, the vessel was rinsed and then incubated with sterile PBS for at least 10 minutes. If the vessel was not to be used immediately it was stored at 4°C with the PBS. The collagen solution was re-used up to 5 times and was always stored at 4°C.

2.17 Frozen cell stocks

To generate stocks of cells for later use, cells were centrifuged at 1,500 rpm for 5 minutes and preserved in FBS containing 10% DMSO. They were stored in Nunc cryotube vials, initially placed at -80°C, and later moved to liquid nitrogen for long term storage. On removal from liquid nitrogen, cell stocks were thawed quickly in a 37°C water bath. Complete DMEM (or other appropriate media) was slowly added. Media was changed the following day to remove remaining traces of DMSO.

2.18 Generation of L-cell control and Wnt3a conditioned media

L-cell control media and Wnt3a conditioned media (CM) was generated and collected as per instructions from the Nusse laboratory [Willert et al. 2003]. Briefly, L-cell and Wnt-3A expressing L-cells were passaged 1:10 from 70% confluence in to T175 flasks with no G418 selection. Cells were cultured for 4 days (approximately to confluency) at which point the media was removed and collected. Fresh media was placed on the cells and they were cultured for a further 3 days. This second batch of media was removed and combined with the first batch and cells were discarded. The harvested media was filtered through a 0.25 µM filter and stored in 50 mL aliquots at -20°C until required. Thawed aliquots were stable at 4°C for several months.

2.18.1 Testing activity of Wnt3a conditioned media

Batches of L-cell and Wnt3a CM were tested for activity on the TOPPuro stable line as this allowed for quick screening without the need for any transfection. C2C12 TOPPuro cells were plated in a 24-well plate at a density of 3×10^4 cells/well. L-cell and Wnt3a CM was added to wells at a 1:2 dilution for 24 hours. Cells were harvested and a luciferase assay was performed as described in Section 2.28.

2.19 Bacterial culture

All bacteria were grown at 37°C in LB broth with vigorous shaking (215-230 rpm) in an Innova 4330 Refrigerated Incubator Shaker (New Brunswick Scientific) or on LB agar plates in a Shimadex (Scientific Equipment Manufacturers) incubator. Each culture was maintained under appropriate antibiotic selection. In all cases this was either 100 µg/ml ampicillin or 30 µg/ml kanamycin.

2.20 Restriction digests

In general, restriction digests were performed in the buffers recommended by the manufacturer (in all cases NEB) in a total of 30 µl when used for analysis and in 50 µl when fragments were to be used for cloning purposes. In the latter situation, the fragments were subsequently purified using either the QIAquick PCR purification kit or the gel extraction kit (Qiagen) as per the manufacturer's instructions.

2.21 Ligations and transformations

Ligations were performed using the NEB Quick Ligation Kit containing 2 x NEB quick ligation buffer (132 mM Tris-HCl, 20 mM MgCl₂, 2 mM DTT, 2 mM ATP, 15% polyethylene glycol (PEG 6000), pH 7.6) and Quick T4 DNA ligase unless otherwise specified. A 3 to 5-fold molar excess of insert DNA to vector DNA was required for successful ligation. This was prepared with 1 x NEB quick ligation buffer, 1 µl T4 DNA ligase and water to a total reaction volume of 14 µl. The reaction mixture was incubated at room temperature for 15 minutes and then chilled on ice ready for transformation.

Transformations were performed using either chemically competent DH5α or high efficiency 10-beta (NEB) strain *E. coli* bacteria. Two microlitres of ligation product was

added to 50 µl of competent cells and mixed gently. The cells were incubated on ice for 20-30 minutes, followed by a heat shock at 42°C for 30-45 seconds to facilitate uptake of the ligated DNA. Cells were then immediately placed back on ice for a further 2-5 minutes. Four hundred and fifty microlitres or 950 µl (for NEB competent cells) SOC media (containing no antibiotics) was added to the shocked cells. The bacteria were allowed to recover at 37°C in a shaking incubator for 1 hour. Generally, 200 µl of recovered cells were spread on LB agar plates and these plates were incubated overnight at 37°C. Colonies were analysed for appropriate inserts by PCR and/or restriction digest of miniprep DNA.

2.22 Preparation of competent cells

Competent DH5α *E. coli* cells were prepared by a variant of the Hanahan protocol (Hanahan et al. 1991) using CCMB80 buffer (10 mM KOAc pH 7, 80 mM CaCl₂·2H₂O, 20 mM MnCl₂·4H₂O, 10 mM MgCl₂·6H₂O, 10% glycerol, pH 6.4). Briefly, 100 ml LB broth was inoculated with 1 ml of a DH5α overnight culture and incubated at 37°C with shaking until the OD₆₀₀ of the culture reached 0.25-0.3. The culture was centrifuged at 3,000 x g in a Sigma 4K15 (Quantum Scientific) centrifuge at 4°C for 10 minutes and the pellet resuspended in 32 ml of cold CCMB80 buffer and left on ice for 20 minutes. The cells were centrifuged for a further 10 minutes, resuspended in 4 ml of cold CCMB80 buffer and aliquoted into 50, 100 or 200 µl aliquots. The competent cells were stored at -80°C.

2.23 Plasmid preparations

Small scale plasmid DNA preparations (minipreps) were generated using the QIAprep Spin Miniprep Kit (Qiagen) from 5 ml overnight bacterial cultures grown in LB broth.

These minipreps were suitable for preparing plasmid DNA of positively identified clones for restriction analysis and for sequencing. The procedure was carried out as per the manufacturer's protocol. Briefly, a bacterial pellet was produced by centrifugation of the overnight culture at 2,600 x g for 15 minutes at 4°C and the resultant supernatant was discarded. The bacterial pellet was air dried, resuspended in 250 µl Buffer P1 containing 100 µg/ml RNase A (Qiagen), lysed by the addition of 250 µl Buffer P2, and all genomic DNA and bacterial proteins present were precipitated by addition of 350 µl Buffer N3. The precipitate was centrifuged for 10 minutes at 13,000 rpm and the supernatant applied to a QIAprep spin column (Qiagen). This solution, containing the plasmid DNA, was centrifuged briefly and thus drawn through the column via a vacuum. The spin column was washed with 750 µl Buffer PE and the bound plasmid DNA was eluted from the column by addition of 40 µl Buffer EB and centrifugation for 1 minute.

Large scale plasmid DNA preparations (midipreps) were used to purify plasmid DNA in preparation for DNA sequencing and mammalian cell transfections. These were generated from a 50 or 100 ml overnight bacterial culture using the QIAGEN Plasmid Midi Kit (Qiagen). The following procedure is as per the manufacturer's protocol with some minor changes to the centrifugation steps: The bacteria were pelleted by centrifugation for 15 minutes at 2,600 x g, 4°C, and supernatant was discarded. The pellet was air dried, resuspended in 4 ml chilled Buffer P1 (+ 100 µg/ml RNase A) and lysed by addition of 4 ml Buffer P2. The bacterial lysate was incubated at room temperature for 5 minutes before addition of 4 ml chilled Buffer P3, followed by a 15 minute incubation on ice. The precipitate was pelleted by a 30 minute centrifugation

at 2,600 x g, 4°C followed by a further 20 minute centrifugation at 2,600 x g. The supernatant was applied to a Qiagen-tip 100 (Qiagen), which had been equilibrated by application of 4 ml Buffer QBT, and was allowed to pass through the column under gravity flow. The column was washed twice with 10 ml Buffer QC and the plasmid DNA eluted with 5 ml Buffer QF. Eluted DNA was precipitated by addition of 3.5 ml room temperature isopropanol and pelleted by centrifugation at 2,600 x g, 4°C for 30 minutes. The supernatant was removed and the DNA pellet washed with 3 ml 70% ethanol and recovered by a further 20 minute centrifugation at 2,600 x g, 4°C. Final DNA pellets were air-dried for 1 hour and then resuspended in 300 µl Buffer EB.

2.24 Gel electrophoresis and quantification of DNA/RNA

Agarose gel electrophoresis was used to analyse DNA fragments and plasmids for their relative size and purity. All gels used were 1-2% agarose and contained 0.03 µg/ml ethidium bromide. All samples were loaded on to agarose gels suspended in TAE buffer, and 100 bp or 1 kb DNA ladders (NEB) were used as size markers. Electrophoresis was performed in a Bio-Rad Mini-Sub Gel GT electrophoresis system where a voltage of approximately 5 volts/cm was applied to the gel. The gel was then examined with a Gene Genius Bio Imaging system (SynGene, Cambridge, England) using GeneSnap version 6.04 software (SynGene).

Spectrophotometry was used to determine the concentration and purity of DNA and RNA samples. Samples were diluted 1:50 in water to a total volume of 100 µl. A GeneQuant II (Pharmacia Biotech, Buckinghamshire, England) spectrophotometer was used to measure the OD₂₆₀ and the DNA/RNA to protein ratio (purity) at OD₂₆₀ versus OD₂₈₀. Absorbance readings were given as 1 unit = 50 µg/ml double strand

DNA or 40 µg/ml single strand RNA. The concentration of DNA was calculated at Absorbance x 50 x 50 (dilution factor), and Absorbance x 40 x 50 for RNA.

2.25 DNA Purification

DNA products generated by PCR, restriction digest for subcloning, or from DNA isolation following ChIP, were purified using the QIAquick PCR purification kit or the Qiagen gel extraction kit as per the manufacturer's instructions.

2.26 Sequencing

Sequencing of DNA was undertaken following either a miniprep or midiprep and quantification of the DNA. A DNA concentration of 100 ng/µl in a volume of greater than 10 µl was required. The sequencing reaction was performed by the Flinders Sequencing Facility (Genetics & Molecular Pathology Directorate, Flinders Medical Centre site, SA Pathology, South Australia) using Big Dye Terminator Cycle Sequencing Version 3.1 chemistry (Applied Biosystems, Foster City, CA) and an ABI 3130xl Genetic Analyser sequencer (Applied Biosystems). Results obtained from sequencing were analysed using the National Center for Biotechnology Information (NCBI) website for alignments to consensus sequences.

2.27 Transient transfections

C2C12 cells were resuspended in supplemented DMEM upon reaching 50-80% confluence. In all cases, C2C12 cells were transfected by the 'reverse' method using Lipofectamine 2000 (Life Technologies). This involved adding the transfection complexes to the tissue culture vessels immediately following seeding of the cells. Therefore, cells were transfected whilst still in suspension. For C2C12 cells, this method resulted in a higher transfection efficiency as determined by monitoring

eGFP expression. For luciferase assays, cells were plated at a density of 3×10^4 cells/well in 1 ml DMEM and transfected with a total of 1.5 μg DNA and 3 μl Lipofectamine 2000 in SF-DMEM. For ChIP experiments, cells were transfected at a much higher density (Section 2.11). For protein or RNA isolation, C2C12 cells were transfected at 2×10^5 cells/well of a 6-well plate with 4 μg DNA and 20 μl Lipofectamine 2000 in 500 μl SF-DMEM.

2.28 Luciferase Assays

At 48 hours post transfection, cells were lysed by the addition of 100 μl Passive Lysis Buffer (PLB; Promega) to each well, and plates were rocked gently and continuously for 15 minutes to promote complete lysis. Using the Dual-Luciferase Reporter Assay system (Promega), a 20 μl sample of lysate was analysed on a TopCount NXT Luminescence and Scintillation counter (Packard, Australia) for firefly (*Photinus pyralis*) and *renilla* luciferase activity. To minimise the effect of carryover luminescence from neighbouring wells, cell lysates were added to alternate wells of 96-well plates. Lysates were mixed with 50 μl of firefly luciferase reagent (Luciferase Assay Reagent II (LARII), Promega) in order to measure the activity of firefly luciferase expressed from transiently transfected pGL3-derived vectors. The luminescence of each well was determined 2 minutes after addition of LARII. Addition of 50 μl of Stop and Glo Reagent (Promega) was then added to wells as soon as possible to quench the firefly luciferase activity and provide the substrate for *renilla* luciferase. As previously, the luminescence resulting from the *renilla* luciferase protein was also determined 2 minutes following addition of the substrate.

Relative luciferase activities (ratios of firefly to *renilla* luciferase activity) were

calculated for each individual sample and then averaged to provide a single value for each condition. Cell lysates were stored at -20°C if they were to be assayed again.

2.29 Immunofluorescence Microscopy

For immunofluorescence imaging of C2C12 cells, glass coverslips were prepared by washing with 100% ethanol and then left to dry in a UV laminar flow hood for approximately 15 minutes. Coverslips were placed within wells of a 24-well plate and coated with 500 µl of collagen solution (50 µg/ml in 20 mM acetic acid). C2C12 cells were seeded at 0.8×10^4 cells/well in 1 ml complete DMEM the day prior to transfection, viral transduction or treatment. For Lcell/Wnt3a CM treatments, cells received the appropriate media for 6 hours. Media was removed and cells were washed once with PBS before fixing with 500 µl of 3.7% formaldehyde (37% formaldehyde stock diluted 1:10 in PBS) for 10 minutes at room temperature. Cells were washed again with PBS and stored in fresh PBS at 4°C if required. Cell membranes were permeabilised by the addition of 0.5% Triton-X in PBS for 5 minutes followed by a rinse with PBS, and coverslips were then blocked in 1% BSA in PBS (blocking buffer) for 30 minutes whilst still in the wells. Cells were rinsed once more with PBS before antibody labelling.

For immunofluorescence imaging of primary myoblasts, cells were seeded in 24-well plates at a density of 1.5×10^4 cells/well in 1 ml complete DMEM, 24 hours prior to treatment. Due to difficulties in attachment of primary myoblasts to glass coverslips, these cells were seeded directly in to collagen-coated wells. The subsequent steps were identical to that of C2C12 cells, as detailed above.

2.29.1 Antibody labelling

Primary antibodies were used at a concentration of 4 µg/ml. Using a scalpel and fine tweezers, glass coverslips were carefully removed from wells and placed in a humidified chamber (empty pipette tip box with moist paper towel lining the bottom) by laying glass slides on the tip rack and positioning the cover slips on the glass slides. Antibodies were diluted in blocking buffer and 100 µl buffer was placed on the top of each coverslip. Primary antibodies were left on the coverslips overnight at room temperature. The following day, primary antibodies were removed from the coverslips (drained off in to tissues) and coverslips were washed 3 times with PBS for 15 minutes each time. Secondary antibodies were diluted in PBS to a concentration of 10 µg/ml and 100 µl was placed on each coverslip for 1-2 hours at room temperature followed by another 3x washes with PBS. Finally, DAPI (1 µg/ml) counterstaining for nuclei was done the same way with only a 5 minute incubation. Coverslips were washed a final 3 times before mounting on to glass slides.

2.29.2 Mounting coverslips to slides

Mounting media (Buffered Glycerol pH 8.6) was prepared from the following two solutions:

Solution A: 0.5 M sodium carbonate (Na_2CO_3), 5.3 g / 100 ml, pH 11.5

Solution B: 0.5 M sodium bicarbonate (NaHCO_3), 8.4 g / 200 ml, pH 8.16

To make 0.5 M Sodium Carbonate Buffer (pH 8.6), 50 ml of Solution B was placed in a beaker and pH was adjusted to 8.6 by addition of Solution A (approximately 3 ml). Two parts glycerol was then added to 1 part 0.5 M buffer solution to prepare the

buffered glycerol mounting media. A small drop of mounting media was placed on the glass slide and the coverslip placed on top, being careful not to create any bubbles. The edges of the coverslips were sealed with clear nail varnish.

2.29.3 Imaging

Slides were imaged using an Olympus BX50 fluorescence microscope (upright) and in-well cells were imaged using an Olympus IX71 fluorescence microscope.

2.30 Statistics

Statistical analysis of all results presented in this thesis was performed using Microsoft Office Excel 2010 or GraphPad Prism software (Hearne Scientific). The statistical significance was determined by use of a one-way ANOVA, a two-way ANOVA or the Student's T-test with two-sample unequal variance, as appropriate. A change was deemed statistically significant if $P < 0.05$.

Chapter 3

Analysis of Barx2-mediated
regulation of the Wnt reporter
TOPflash

3.1 Introduction

The foundation for the majority of the work which has been undertaken and presented within this thesis was formed by the preliminary studies of a Masters student, Lizhe Zhuang. This founding data has since been published along with the majority of the results presented in this chapter in a joint first-author paper in “Stem Cells” [Zhuang et al. 2014].

3.1.1 The TOPflash reporter

The canonical Wnt signalling pathway is mediated by TCF/LEF proteins and β -catenin. In the presence of a Wnt ligand the pathway is activated, ultimately resulting in stabilised, nuclear β -catenin which pairs with members of the TCF/LEF family to induce gene expression via direct binding to TCF/LEF motifs [Wodarz & Nusse 1998; Staal et al. 2002]. A well-characterised synthetic reporter of canonical Wnt signalling is the TOPflash reporter gene, originally generated by the laboratory of Hans Clevers and later optimised by the Randall Moon Laboratory [Veeman et al. 2003]. TOPflash consists of 6x TCF/LEF binding motifs (AGATCAAAGG, with spacer GGGTA) upstream of a minimal TA viral promoter (the TATA box from the herpes simplex virus thymidine kinase promoter) driving expression of the firefly luciferase gene in the pGL3 backbone (Promega). A control for the TOPflash reporter, FOPflash, contains 6x mutated TCF/LEF binding sites (AGGCCAAAGG, with spacer GGGTA) in the same vector backbone [Veeman et al. 2003]. As an output, luciferase expression/activity can be measured, thus providing an indication of the level of Wnt signalling occurring within the cell. The activity of the TOPflash reporter is therefore considered to be representative of the transcriptional response one might expect of *bona fide* Wnt

target genes containing TCF/LEF binding sites. Using the TOPflash reporter, work performed by student Lizhe Zhuang in C2C12 myoblasts identified Barx2 as a new transcriptional regulator of canonical Wnt signalling [Zhuang et al. 2014]. Co-transfection experiments with Barx2 and TOPflash in C2C12 myoblasts consistently showed activation of TOPflash by Barx2. This ranged from 5- to 50-fold depending on transfection efficiency. This Barx2-mediated activation was completely abolished by co-transfection of a dominant-negative form of TCF4 (dnTCF4), which is lacking the N-terminal β -catenin-interaction domain and therefore is able to bind DNA but not interact with β -catenin. Traditionally, homeobox proteins such as Barx2 are thought to mediate transcription by binding directly to DNA via their highly conserved ~60 amino acid DNA binding domain, the homeodomain (HD) [Gehring et al. 1994]. The recognition site for homeobox proteins, termed the homeodomain binding site (HBS) contains the short sequence ATTA as its core [Odenwald et al. 1989]. The sequence of the synthetic TOPflash promoter contains no such identifiable HBS motifs, and thus the Barx2-mediated activation of TOPflash is not due to direct binding of the HD and must therefore be via the TCF/LEF binding elements. As further support for this idea, Barx2 did not activate the control reporter FOPflash (containing mutated TCF/LEF motifs) under the same transfection conditions, indicating the Barx2-mediated activation is dependent upon intact TCF/LEF motifs.

Further analysis of the TOPflash reporter in C2C12 myoblasts led to the identification of MyoD (one of the MRF members) as a potent co-activator of TOPflash activity when co-expressed with Barx2 [Zhuang et al. 2014]. Whilst transfection of MyoD alone was not sufficient to induce TOPflash activity, co-transfection of Barx2 and

MyoD together produced a strong synergistic activation, more than 10-fold higher than activation produced by Barx2 alone. Significantly, co-expression of MyoD was also sufficient to switch an N-terminally-truncated form of Barx2 (missing the first 25 amino acids) from a repressor to an activator. Previous studies have demonstrated a physical interaction between Barx2 and MyoD [Makarenkova et al. 2009] and between MyoD and β -catenin [Kim et al. 2008], and as such the observed synergy between Barx2 and MyoD was not entirely unexpected. However these results prompted two questions that are addressed in this chapter:

- 1) As MyoD is endogenously expressed at a high level in C2C12 cells, is Barx2-mediated activation of TOPflash dependent on MyoD, and hence specific to muscle cells?
- 2) Do other MRF members have the ability to synergize with Barx2 in regulation of TOPflash?

3.1.2 Mechanisms of activation and repression by Barx2

The full length Barx2 protein has been reported to have dual functions, with studies indicating that Barx2 has the potential to act as an activator or as a repressor of transcription in different contexts. In order for Barx2 to have a dual function it must therefore contain both activation and repression domains. It is important to note that studies prior to those described in this thesis [Zhuang et al. 2014] used a version of Barx2 with a short N-terminal truncation. At that time the full length mRNA encoding the Barx2 protein had not yet been cloned, and only a 5'-truncated mRNA had been isolated and studied. This mRNA expressed a truncated Barx2 protein that excludes the first 25 amino acids (aa), and as such the protein begins at the second in frame

methionine (M) (Refer to Chapter 1, Figure 1.2). In previous publications this truncated protein was referred to as 'full length' Barx2. A longer 'full length' Barx2 mRNA including the first in frame methionine was cloned by Lizhe Zhuang. This version contains what we now consider to be the full N-terminal sequence. The previous, truncated version will henceforth be referred to as 'tr-Barx2' within this thesis.

Consistent with previous studies discussed in Chapter 1, a fragment of Barx2 containing the C-terminal domain and homeodomain (HDBBRC) strongly activated the TOPflash reporter in C2C12 myoblasts, and was sufficient to provide 90% of the activation observed with the full length Barx2 construct [Zhuang et al. 2014]. Successive truncations of the C-terminus showed proportionally reduced activation, suggesting the activation function may be distributed throughout the length of the C-terminal region (refer to Figure 3.1 for schematic of Barx2 protein truncations). Overall, the activating function of the C-terminal domain of Barx2 with respect to TOPflash was consistent with previous studies showing that this domain activated other target gene promoters. Studies on the N-terminal domain, however, showed more complexity. Co-transfection of the 'tr-Barx2' construct produced mild repression of the TOPflash reporter, indicating a repression domain lay within the N-terminal region (outside the first 25 aa) that is sufficient to block the activating function of the C-terminal domain. This was consistent with previous studies using the 'tr-Barx2' protein that had shown that the N-terminal region had a repressive function [Edelman et al. 2000; Olson et al. 2005]. Our studies on TOPflash compared the effects of the complete N-terminus and homeodomain (NHDBBR) to the

truncated N-terminus and homeodomain (tr-NHDBBR). We found that NHDBBR induced transcriptional activation of TOPflash whereas tr-NHDBBR induced repression [Zhuang et al. 2014]. Therefore, the first 25 aa of Barx2 contains a potent activation function which appears able to override the repression domain located further downstream. Similarly, the full Barx2 construct (including the first 25 aa) resulted in activation of TOPflash [Zhuang et al. 2014], contrasting to previous work where the tr-Barx2 was mildly repressive of the N-CAM promoter [Edelman et al. 2000].

The nature of the N-terminal activation and repression domains is still unresolved, although the N-terminal domain has been reported to recruit HDACs [Olson et al. 2005]. Moreover, an Eh1 motif is present in the Barx2 N-terminal region (core located at 25-28 aa) has been reported to have repressive functions in other transcription factors [Copley 2005; Goldstein et al. 2005]. Previous work indicated that the Barx2 Eh1 motif mediated interaction with Groucho/TLE family proteins [Olson et al. 2005], classical repressors of the Wnt signalling pathway [Cavallo et al. 1998].

Further delineation of the functions of various Barx2 protein domains revealed that, despite the lack of HBS binding sites within the TOPflash reporter sequence, the Barx2 homeodomain was essential for Barx2-mediated activation. Although Barx2 NHDBBR and HDBBRC constructs could both activate TOPflash, constructs comprised of the N-terminus (N-term) or C-terminus (C-term) alone (therefore no HDBBR) could not. Furthermore, expression of the homeodomain and BBR alone (HDBBR) did not produce any activation, showing that these domains are *necessary but not sufficient* for TOPflash activation. Consistent with a critical role for the HDBBR domain in

TOPflash activation, Barx1, which shows 87% homology with Barx2 within the HDBBR, was able to activate TOPflash to a similar level as that of Barx2 [Zhuang et al. 2014].

Whilst the work described above greatly enhanced our understanding of Barx2 protein domains involved in regulation of the Wnt reporter TOPflash and in transcriptional regulation in general, again they prompted further questions that are addressed in this chapter:

- 1) Are the classical effectors of the Wnt signalling pathway (β -catenin and TCF/LEF family members) also involved in the response of TOPflash to Barx2 and MyoD?
- 2) If so, how are these interactions mediated?

3.1.3 The role of Pax7 in regulation of Wnt target genes

As discussed in Chapter 1, Pax7 is a well-characterized homeobox protein in muscle development and often considered the canonical marker of satellite cells [Oustanina et al. 2004]. Pax7 is highly expressed in quiescent satellite cells and their proliferating myoblast progeny, but is downregulated as cells begin to differentiate [Olguin & Olwin 2004; Zammit 2004]. Furthermore, forced expression of Pax7 delays myoblast differentiation, thus suggesting a role for Pax7 in maintaining satellite cell quiescence and preventing precocious differentiation [Olguin & Olwin 2004; Zammit et al. 2006; Olguin et al. 2007]. It has previously been shown that Barx2 is co-expressed with Pax7 in quiescent muscle satellite cells and myoblasts [Meech et al. 2012]. However, in contrast to Pax7, Barx2 is induced during differentiation and promotes pro-differentiation events such as cell spreading and migration [Makarenkova et al. 2009]. Prompted by our initial findings that Barx2 acts as a positive regulator of a Wnt

reporter, we hypothesised that the opposing roles of Barx2 and Pax7, two key myogenic factors, might be related to differential effects of Wnt target gene regulation.

Pax7 is one of 9 members of a family of Paired Box (Pax) transcription factors. The defining characteristic of this family is the presence of a 128 amino acid paired domain, encoding a unique DNA-binding motif which may function in either transcriptional repression or activation, as well as a carboxy-terminal transactivation domain [Balczarek et al. 1997]. The Pax gene family is further split in to subgroups based on the presence or absence of the following structural regions: a full homeodomain (66 aa helix-turn-helix), a partial homeodomain (first helix only), and/or an octapeptide motif [Maulbecker & Gruss 1993]. Pax7 as well as Pax3 contain both a full homeodomain and an octapeptide motif.

3.1.4 Aims

Based on the prior knowledge described above and the questions raised by it, the specific aims of this chapter were to:

1. Expand on the mechanisms by which Barx2 activates TOPflash in myoblasts
2. Determine if Pax7 plays any role in regulation of TOPflash in myoblasts
3. Identify protein-protein and protein-DNA interactions involving Barx2, Pax7 and Wnt effectors in this system, and
4. Identify the role of β -catenin and TCF/LEF factors in the regulation of TOPflash by Barx2

3.2 Methods

3.2.1 Expression plasmids

Myf5 and MRF4 plasmid constructs were generated by *Pfu* Turbo (Agilent Technologies) amplification of cDNA isolated from C2C12 myoblasts. The resultant PCR products were directionally cloned *XhoI-XbaI* in pcDNA3 already containing an N-terminal myc-tag.

The Barx2 Δ HD construct was generated by amplification of a Barx2 BBR and C-term fragment and fusion of this fragment to the previously generated Barx2 N-term fragment at an introduced *NheI* site. Barx2 Δ BBR was generated by amplification of a Barx2 N-term and HD fragment and fusion of this fragment to the previously generated Barx2 C-term fragment at an introduced *NheI* site. Barx2 Δ HDBBR was generated by fusion of the Barx2 N-term fragment and the Barx2 C-term fragment at an introduced *NheI* site. All Barx2 deletion constructs were ligated *XhoI-XbaI* in pcDNA3 containing an N-terminal myc-tag. Mutagenesis of the predicted Barx2 phosphorylation sites was performed in the context of full length Barx2 with primers spanning either the GSK or CKII sites, as listed in Table 3.1. The Site Directed Mutagenesis protocol (Clontech) was followed (Chapter 2, Section 2.7.4).

The Pax7 variant used within all of these studies is Pax7D [Lamey et al. 2004] (referred to hereafter as just Pax7), which was originally cloned from postnatal mouse muscle into pcDNA3 in frame with the N-terminal myc-tag. Partial deletion of the Pax7 paired domain (Δ PD) was performed by fusing the *EcoRV* site of the pcDNA3 polylinker (after the myc-tag) with the *EcoRV* site in the Pax7 region encoding the paired domain. Deletion of the Pax7 homeodomain (Δ HD) was performed by amplifying both the

Pax7 N-terminus and the C-terminal transcriptional activation domain (TAD) with primers containing *NheI* sites and then fusing both fragments together at the introduced *NheI* site. Mutagenesis of the Pax7 engrailed homology domain (Eh1 SDM) was performed in the context of full length Pax7 with primers spanning the Eh1 domain as listed in Table 3.1, as per the Site Directed Mutagenesis protocol (Clontech).

All primers used for cloning and generation of mutations are listed below in Table 3.1.

3.2.2 In vitro transcription/translation of Barx2, β -catenin and TCF4

Barx2, β -catenin and TCF4 proteins were synthesised using the TnT[®] Quick Coupled Transcription/Translation system (Promega) according to the manufacturer's protocol. Briefly, 1 μ g linearized plasmid template DNA was incubated in a mixture containing 40 μ l TnT[®] Quick Master Mix, 1 μ l 1 mM methionine, 1 μ l T7 enhancer and water to 50 μ l. Incubation was performed at 30°C for 90 minutes. To perform co-immunoprecipitation with *in vitro* translated (IVT) products, 10 μ l of each appropriate IVT protein was combined in 150 μ l binding buffer (20 mM Tris pH 7.5, 300 mM NaCl, 0.5% NP40, PIC) and rotated at 4°C for 1 hour. Washed 50% protein A beads (40 μ l) were added to pre-clear the lysates for 1 hour at 4°C. Beads were removed via centrifugation and the lysate was divided in to fresh tubes and incubated overnight with the appropriate antibody or preimmune serum. Washed protein A beads (40 μ l) were added to each sample and incubated for a further 3 hours at 4°C. Following incubation, supernatant was removed and beads were gently washed 3 times with washing buffer (20 mM Tris pH 7.5, 150 mM NaCl, 0.5% NP40) before being resuspended in SDS loading dye for analysis via western blot. Western blots were

performed as previously described (Chapter 2, Section 2.12).

3.2.3 Immunofluorescence labelling

Using 24-well plates, 12mm glass coverslips were sterilised in ethanol and coated with 50 µg/ml rat-tail collagen for 1 hour at 37°C. C2C12 cells were seeded in the 24-well plates at 1×10^4 cells/well 24 hours prior to viral transduction or treatment with Wnt3a CM. When cells were to be transfected using a high efficiency Lipofectamine 2000 (Invitrogen) protocol, 2×10^5 cells were seeded in 6-well plates and transfected with 4 µg DNA and 20 µl Lipofectamine 2000 per well. Media was changed after 6 hours. At 24 hours post transfection, cells were trypsinised and re-seeded on 12mm coated coverslips in 24-well plates at 1×10^4 cells/well. Cells were fixed with 3.7% formaldehyde in PBS for 10 minutes at room temperature, rinsed with PBS and permeabilised with 0.5% Triton-X for 5 minutes. Cells were then blocked with 1% BSA in PBS for 30 minutes before addition of antibodies. Primary antibodies for β-catenin or Barx2 (Santa Cruz Biotechnology) were used at a final concentration of 4 µg/ml overnight in a humidified chamber, and fluorescently labelled secondary antibodies (Dylight-594 or Dylight-488; Vector Labs) were used at 10 µg/ml for 2 hours. Nuclei were counterstained with 1 µg/ml DAPI for 5 minutes. Labelled cells were imaged with an Olympus BX-50 microscope. Immunostaining of primary myoblasts was performed in collagen-coated wells and imaged in-well using an Olympus IX71 microscope at 10x magnification. Images were processed using ImageJ software.

3.2.4 Pax7 siRNA design and transfection

Pax7 siRNA was designed based on previously published work [Olguin & Olwin 2004] (D2). The sequence was adapted for double-stranded siRNAs that were purchased

along with a universal negative control siRNA from Integrated DNA Technologies (IDT, Coralville, Iowa). Pax7 or control siRNAs were co-transfected in C2C12 cells at a concentration of 30 nM along with TOPflash luciferase reporter and effector plasmids as previously described, and luciferase results were assayed after 48 hours.

3.2.5 Primers

Table 3.1: List of all primers used during this chapter

<u>Name</u>	<u>Sequence</u>
<u>Cloning</u>	
Bx2 BBRC F Nhe	ccgctagccttaaaggtggacaggaag
Bx2 Cloning Rev Xba	ggctctagattagcttaatggagggttc
Bx2 Cloning For Xho	agctcgagcactgccacgcggaactgag
Bx2 HD Rev Nhe	ccgctagcgcaccatcttcttctcttc
Myf5 F Xho	ggcctcgaggacatgacggacggctgccag
Myf5 R Xba	ggctctagatcataatacgtgatagataag
MRF4 F Xho	ggcctcgagatgatgatggacctttttgaaac
MRF4 R Xba	ggctctagattacttctccaccacctctc
Msx1 F Xho	ggcctcgaggccccggctgctgctatgac
Msx1 R Xba	ggctctagactaagtcagggtggtacatgctgtagcc
Msx2 F Xho	ggcctcgaggcttctccgactaaaggcggt
Msx2 R Xba	ggctctagattagaatagatggtacatgccatatcc
mPax3 F Xho	ggccccgagaccacgctggccggcgct
Pax3 R Nhe	ggcgctagcctagaacgtccaaggcttactttgtc
<u>Mutagenesis/Deletions</u>	
Pax7 Eh1 SDM Top	ccaaa g ccagc g cgatggc g ctggg g cgacaaa g gg
Pax7 Eh1 SDM Bottom	ccaagg g ggccatc g g g ct g g g cttt g gctttcttctc g cc
Pax7 TAD F NheI	gggctagcgcctaaccagctggccg

Pax7 Nterm R NheI	gggctagcgcggcgctgcttgccg
Barx2 GSK phos S-A SDM F	gaatg ^c ccattcccacag ^c cagaggagattgaag
Barx2 GSK phos S-A SDM R	ctctg ^c tgtgggaatgg ^c attcttcttagggc
Barx2 CKII phos SDM F	cagaagg ^c ctttgg ^c taccccagacaggttg
Barx2 CKII phos SDM R	ggtagccaaagccttctgcttctggaatttc
Barx2 CKII phos S-A SDM F	tatttggtaccccagacaggttg
Barx2 CKII phos S-A SDM R	ggtagccaaaacttctgctctgg
Barx2 CKII phos Y-A SDM F	cagaagg ^c ctttgtctaccccagacaggttg
Barx2 CKII phos Y-A SDM R	ggtagacaaaag ^c ctctgcttctggaattc
Barx2 CKII phos Y-D SDM F	cagaagg ^a ctttgtctaccccagacaggttg
Barx2 CKII phos Y-D SDM R	ggtagacaaag ^t ccttctgcttctggaatttc
<u>Chromatin Immunoprecipitation</u>	
TOPflash CHIP F	ccgagctcttacgcgagatc
TOPflash CHIP R	caagctggaattcgagcttcc
β2-microglobulin CHIP F	cggagaatgggaagccgaacat
β2-microglobulin CHIP R	gtgaggcgggtggaactgtgt
Desmin F	ctggcaggacagaggga
Desmin R	gccccttagctgtctgc
<u>siRNA</u>	
Pax7 sense	tgtctccaagattctgtgccgatat
Pax7 antisense	acacagagggttctaagacacggctata

3.3 Results

3.3.1 The homeodomain is essential for Barx2-mediated activation of TOPflash

To expand on previous work and further delineate the Barx2 domains involved in activation of TOPflash, new deletion constructs were prepared. Previous analysis of

Barx2 involved constructs expressing full length (FL) protein, the N-terminus alone (N-term), the C-terminus alone (C-term), the homeodomain and Barx basic region (HDBBR), as well as the N-terminus and HD/BBR (NHDBBR) and C-terminus and HD/BBR (HDBBRC), and these data had demonstrated a crucial role for the highly conserved homeodomain and closely associated BBR in terms of TOPflash activation. To extend these findings, constructs with deletion of the homeodomain and BBR (Δ HDBBR), homeodomain (Δ HD) or BBR (Δ BBR) were generated. Transient transfections and luciferase assays performed in C2C12 myoblasts with the TOPflash reporter showed that, consistent with the N-term and C-term only constructs having no activating function, both new constructs with a deleted homeodomain (Δ HDBBR and Δ HD) were also unable to activate the TOPflash reporter (Figure 3.1). In contrast, deletion of the Barx2 BBR alone reduced Barx2-mediated activation but was not sufficient to eliminate it. FL Barx2, NHDBBR and HDBBRC constructs were all able to significantly activate TOPflash compared to empty vector transfection, with the HDBBRC construct being the most potent. The HDBBR domain alone did not activate TOPflash (Figure 3.1). In summary these data confirmed the results obtained previously by Masters student Lizhe Zhuang under the same experimental conditions, and extended them to show the essential but non-sufficient nature of the Barx2 homeodomain in TOPflash activation.

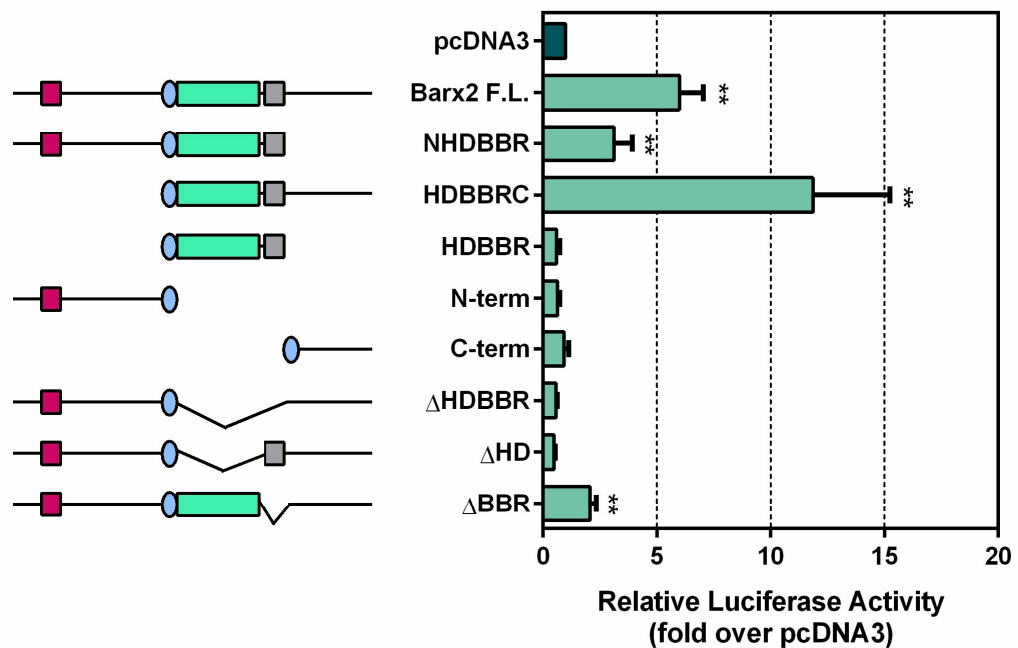


Figure 3.1: Analysis of new Barx2 deletion constructs

Left: schematic of Barx2 deletion constructs. Green – homeodomain; grey – BBR; blue – nuclear localisation sequence; red – Eh-1 motif. Right: Barx2 deletion constructs (1 μ g) were co-transfected with the TOPflash reporter (0.5 μ g) in to C2C12 myoblasts. Transfection of empty pcDNA3 vector served as a negative control. Luciferase activity was assayed 48 hours post transfection. All data are normalised to a Renilla luciferase internal control, expressed as the mean firefly/Renilla luciferase ratio, and then to pcDNA3 empty vector transfection (set to a value of 1). The results shown are the average of at least three independent experiments performed in triplicate. Error bars represent SEM. ** $p < 0.001$ relative to pcDNA3.

Previous work from this laboratory identified that Barx1, which shares high sequence homology to Barx2 within the HDBBR region, also activates TOPflash alone and synergistically with MyoD [Zhuang et al. 2014], further highlighting a critical role for these domains in activation of TOPflash. We therefore wanted to assess the generality of Homeobox-mediated activation of the TOPflash reporter by testing proteins from a different Homeobox family to that of the Barx family. The Msx family comprises two members (Msx1 and Msx2) that are primarily expressed in a subset of blood vessels [Goupille et al. 2008]. Msx proteins contain an Antennapedia class

homeodomain related to that in the Barx proteins, but no BBR. Both Msx1 and Msx2 were tested for their ability to activate TOPflash in C2C12 myoblasts via luciferase assay. As shown in Figure 3.2, transfection of Msx2 alone modestly activated TOPflash (3-fold), however no activation was observed for Msx1 under the same conditions. Interestingly, both Msx1 and Msx2 produced potent activation of TOPflash when co-transfected with MyoD (11 and 18-fold respectively).

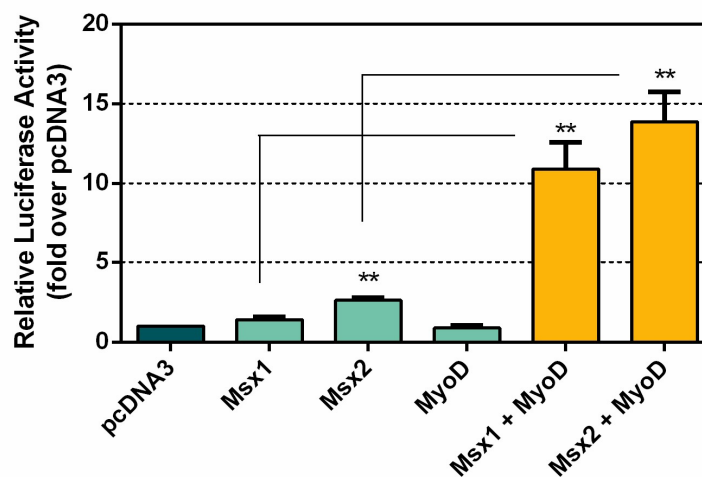


Figure 3.2: Msx homeobox proteins can activate TOPflash

TOPflash reporter (0.5 μ g) was co-transfected with Msx1 or Msx2 either separately or in combination with MyoD (total 1 μ g) in to C2C12 myoblasts. Transfection of empty pcDNA3 vector served as a negative control and to control for total amount of transfected DNA. Luciferase activity was assayed 48 hours post transfection. All data are normalised to a Renilla luciferase internal control, expressed as the mean firefly/Renilla luciferase ratio, and then to pcDNA3 empty vector transfection (set to a value of 1). The results shown are the average of two independent experiments performed in triplicate. Error bars represent SEM. ** $p < 0.001$ relative to pcDNA3 control unless marked otherwise. $n=6$.

3.3.2 Barx2 synergistically activates TOPflash with MyoD and other MRFs

Previous work from this laboratory had identified a strong synergistic activation of TOPflash in C2C12 cells following co-transfection of Barx2 and MyoD, with no activation observed following MyoD transfection alone [Zhuang et al. 2014]. To

determine if MyoD is the only MRF member able to synergise with Barx2, the other 3 members of the MRF family, Myf5, MRF4 and myogenin were tested by transient cotransfection and luciferase assay. These assays demonstrated that all 4 members are capable of synergising with Barx2 in C2C12 cells (Figure 3.3A), but synergy with MyoD was the most potent. Expression of any MRF on its own was insufficient to increase TOPflash promoter activity above basal levels, whilst co-transfection of Barx2 and MyoD resulted in 18-fold increase in activity over transfection of Barx2 alone (which was set to 1 in Figure 3.3A). Co-transfection of Myf5, MRF4 or myogenin with Barx2 resulted in 4 to 6-fold increase in promoter activity relative to Barx2 transfection alone. The synergistic effect of Barx2 in combination with MyoD is unlikely to be due to a differentiation-promoting effect as cells transfected with TOPflash alone did not show significant promoter induction even after 48 hours of differentiation media (Figure 3.3B). Moreover, both Barx2 and the combination of Barx2 and MyoD induced TOPflash promoter activity in COS7 cells (Figure 3.3C), which have no endogenous MRF expression and are unable to undergo myogenic conversion. The fact that Barx2 is still able to activate the TOPflash promoter in the absence of exogenous MyoD in COS7 cells indicates that Barx2-mediated activation is not dependent on MyoD.

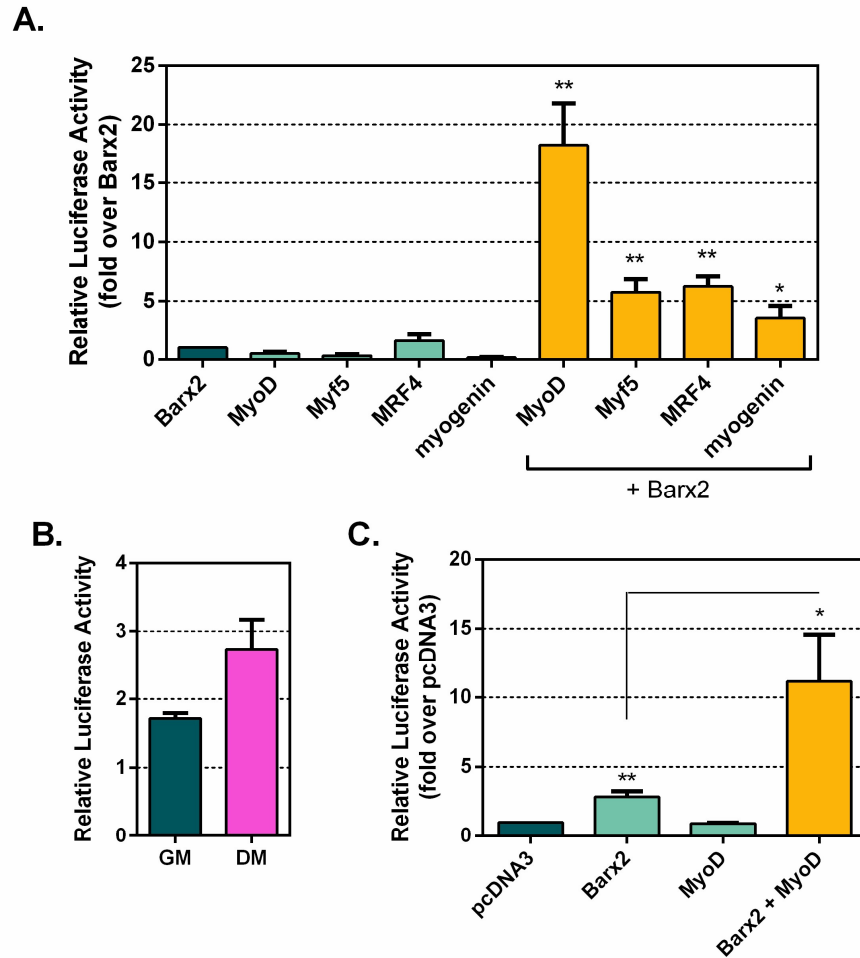


Figure 3.3: Barx2 regulates the TOPflash reporter gene synergistically with MRFs in C2C12 cells

(A): TOPflash reporter (0.5 μ g) was co-transfected with Barx2 either separately or in combination with a MRF (total 1 μ g) in to C2C12 cells. (B): TOPflash reporter (0.5 μ g) was transfected in to C2C12 cells and cells were grown in either growth media (GM) or differentiation media (DM) for 48 hours. (C): TOPflash reporter (0.5 μ g) was co-transfected with Barx2 or MyoD or combination (total 1 μ g) in to COS7 cells. Transfection of empty pcDNA3 vector served as a negative control and to control for total amount of transfected DNA. Luciferase activity was assayed 48 hours post transfection. All data are normalised to a Renilla luciferase internal control, expressed as the mean firefly/Renilla luciferase ratio, and then to Barx2 transfection (set to a value of 1). The results shown are the average of at least two independent experiments performed in triplicate. Error bars represent SEM. * $p < 0.05$ and ** $p < 0.001$ relative to (A) Barx2 or (C) pcDNA3 control unless marked otherwise.

3.3.3 Barx2 may synergise with Wnt3a/ β -catenin to activate TOPflash

Up to this point in the study, the ability of Barx2 to activate the TOPflash reporter gene had been examined independently of Wnt3a/ β -catenin signal or effector. Here

the question was asked whether combining Barx2 expression with constitutively active (ca.) β -catenin or Wnt3a ligand treatment could potentiate a higher activation response. Due to the high levels of TOPflash activation produced by expression of ca. β -catenin or treatment with Wnt3a ligand, the concentrations of each were titrated to induce only modest activations of TOPflash, similar to the response elucidated by expression of Barx2 or the combination of Barx2 and MyoD (hereafter called Barx2+MyoD). As such, when combining Barx2 with ca. β -catenin, only 2-50 ng of ca. β -catenin was transfected per well. Similarly, when combining Barx2 expression with Wnt3a, Wnt3a CM was used at dilutions of 1:10 or 1:20 in complete DMEM. The data obtained from these co-treatment experiments indicated that under specific experimental conditions, synergy between Barx2 and ca. β -catenin or Wnt3a was possible. As shown in Figure 3.4, Barx2 was observed to synergise with 10-50 ng β -catenin, whilst Barx2 and Barx2+MyoD provided a synergistic effect with Wnt3a CM at a 1:10 dilution. However, results were not entirely consistent between replicate experiments; it is likely that variables such as cell passage, transfection efficiency and variations in batches of Wnt3a CM contributed to the variable results. One interesting observation from these studies was the ability of MyoD to block activation mediated by ca. β -catenin (Figure 3.4C). A previous study by Kim and colleagues identified that a direct interaction between β -catenin and MyoD enhances the binding of MyoD to E-box elements [Kim et al. 2008], and thus recruitment of β -catenin away from TCF/LEF elements may provide an explanation for this result.

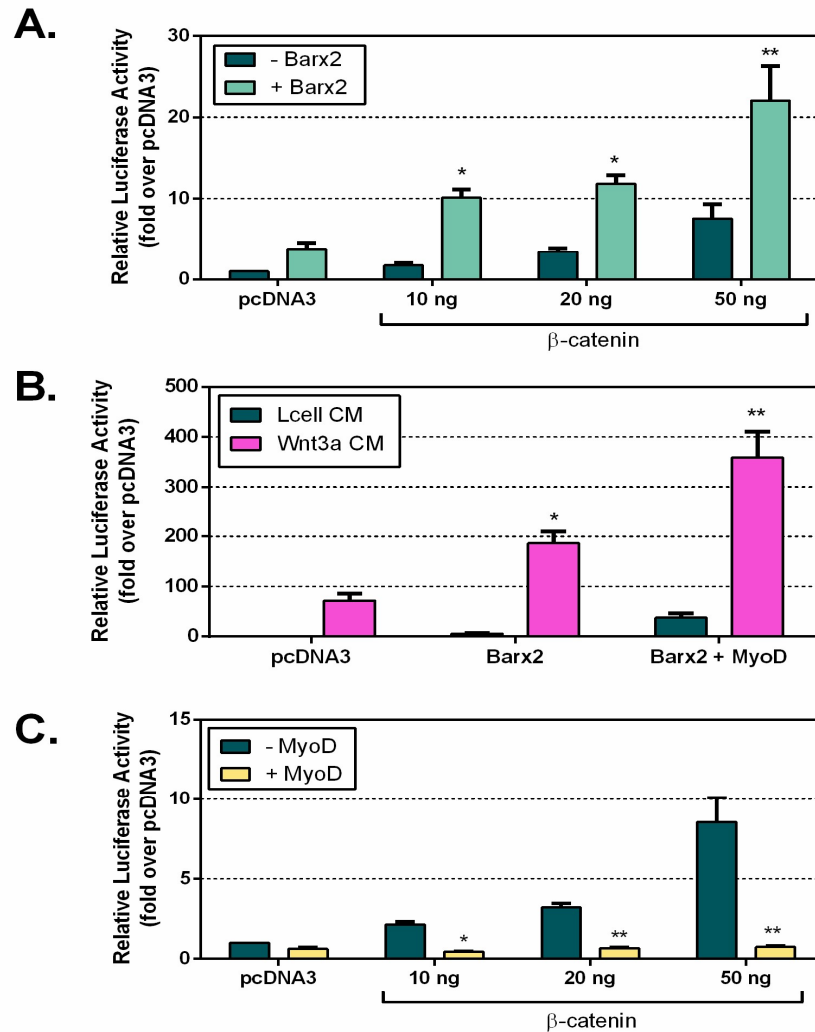


Figure 3.4: Barx2 and β -catenin may synergise to activate TOPflash whilst MyoD represses β -catenin activation

(A): TOPflash reporter (0.5 μ g) was co-transfected with Barx2 and increasing concentrations of β -catenin. (B): TOPflash reporter (0.5 μ g) was co-transfected with Barx2 or Barx2+MyoD and cells received control Lcell CM or Wnt3a CM. (C): TOPflash reporter (0.5 μ g) was co-transfected with MyoD and increasing concentrations of β -catenin. Transfection of empty pcDNA3 vector served as a negative control and to control for total amount of transfected DNA. Luciferase activity was assayed 48 hours post transfection. All data are normalised to a Renilla luciferase internal control, expressed as the mean firefly/Renilla luciferase ratio, and then to Barx2 transfection (set to a value of 1). The results shown are the average of at least two independent experiments performed in triplicate. Error bars represent SEM. * $p < 0.05$ and ** $p < 0.001$ relative to each control condition.

3.3.4 Pax7 antagonises Barx2, β -catenin and Wnt3a-mediated activation of TOPflash activity

As discussed previously, Pax7 is expressed in satellite cells but is downregulated as cells begin to differentiate [Olguin & Olwin 2004; Zammit et al. 2004]. It also inhibits myoblast differentiation whilst Barx2 promotes differentiation [Zammit et al. 2006; Olguin et al. 2007; Makarenkova et al. 2009]. To examine whether these opposing effects of Barx2 and Pax7 may be related to differential effects on Wnt target regulation, the ability of Pax7 to modulate TOPflash activity was tested. In contrast to the effect of Barx2, Pax7 repressed basal TOPflash reporter activity (approximately 3-fold) when expressed in C2C12 myoblasts (Figure 3.5). Furthermore, when Pax7 was co-transfected with Barx2, activation of TOPflash was completely inhibited, suggesting a potent repressive function of Pax7 that is capable of over-whelming the activating function of Barx2.

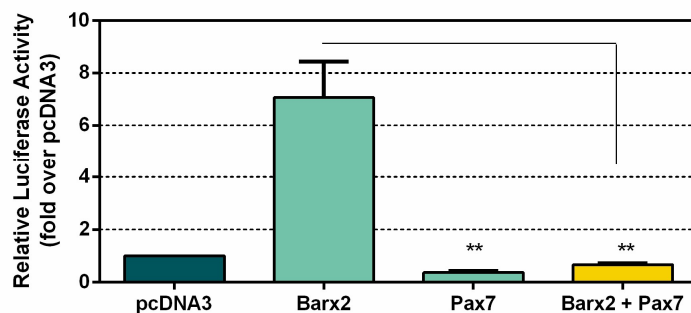


Figure 3.5: Pax7 antagonises the activating effect of Barx2 on TOPflash activity

TOPflash reporter (0.5 μ g) was co-transfected with combinations of Barx2, MyoD and Pax7 (total 1.5 μ g) in to C2C12 myoblasts. Transfection of empty pcDNA3 vector served as a negative control and to control for total amount of transfected DNA. Luciferase activity was assayed 48 hours post transfection. All data are normalised to a Renilla luciferase internal control, expressed as the mean firefly/Renilla luciferase ratio, and then to pcDNA3 empty vector transfection (set to a value of 1). The results shown are the average of at least three independent experiments performed in triplicate. Error bars represent SEM. ** $p < 0.001$ relative to pcDNA3 control unless marked otherwise.

Pax7 is highly expressed in proliferating myoblasts (and proliferating C2C12 cells) and this endogenous Pax7 may impair the response of TOPflash to over-expression of Barx2 (and Barx2+MyoD). Hence, the idea that the ability of Barx2 to activate TOPflash could potentially be higher if endogenous Pax7 expression was inhibited was considered. To confirm this, expression of Pax7 was knocked down with Pax7 siRNA used at a concentration of 30 nM. Before use in a luciferase assay, efficiency of the Pax7 siRNA to knockdown Pax7 was first confirmed in transfection experiments in C2C12 myoblasts. C2C12 cells were transfected with either Pax7 siRNA or universal negative control siRNA, and mRNA and protein levels of Pax7 were assessed after 48 hours. As shown in Figure 3.6A, Pax7 mRNA expression as assessed by quantitative PCR was reduced by 50% in cells transfected with Pax7 siRNA compared to cells transfected with control siRNA. Similarly, Pax7 protein as assessed by western blot was reduced by ~90% in lysates from Pax7 siRNA transfected cells when compared to expression of Pax7 in lysates from control siRNA transfected cells (Figure 3.6B).

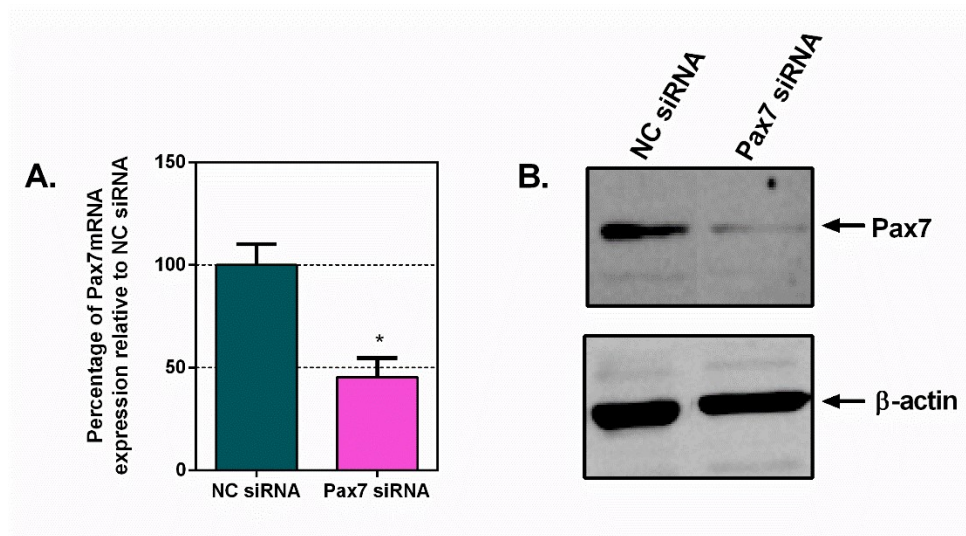


Figure 3.6: Efficacy of Pax7 siRNA knockdown in C2C12 cells

Pax7 siRNA or universal negative control siRNA (30 nM) was transfected into C2C12 cells. (A) RNA isolated from transfected cells was reverse transcribed and Pax7 mRNA was measured by quantitative real-time PCR. Data were normalised to the housekeeping gene RPS26. Expression of Pax7 in Pax7 siRNA-transfected cells is presented relative to that of control siRNA-transfected cells, set arbitrarily to a value of 1. Results shown are the average of two experiments performed in duplicate. Error bars represent SEM. * $p < 0.05$. $n=4$. (B) Nuclear total protein lysates of siRNA transfected C2C12 cells were resolved on a 10% SDS-PAGE gel, transferred to nitrocellulose membrane and probed with a Pax7 specific antibody. The same membrane was then probed with an anti- β -actin antibody as a control for total loaded protein. A representative blot of two independent experiments is shown.

Following confirmation that the Pax7 siRNA reduced Pax7 expression, C2C12 myoblasts were transiently transfected with the TOPflash reporter, together with Barx2 and MyoD, and either 30 nM of negative control siRNA or Pax7 siRNA. In cells that were transfected with Pax7 siRNA, the activation of the TOPflash reporter by Barx2 and MyoD was approximately 2.25-fold higher than in cells transfected with negative control siRNA (Figure 3.7B). Interestingly, however, knockdown of Pax7 had no effect on basal TOPflash activity (Figure 3.7A).

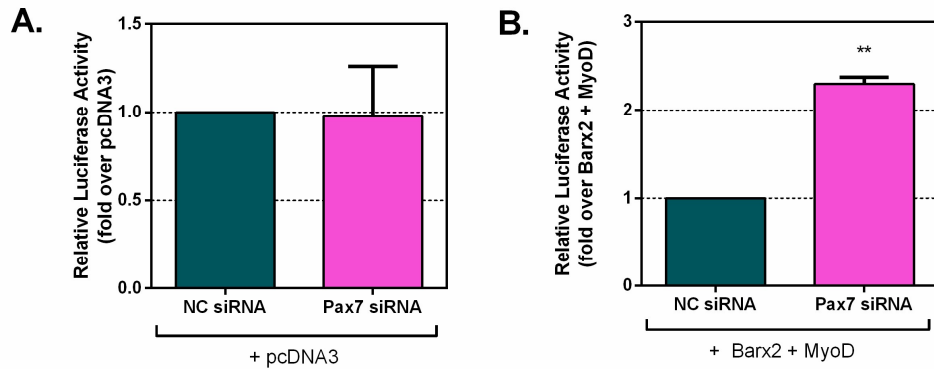


Figure 3.7: Knockdown of Pax7 increases the ability of Barx2 and MyoD to activate TOPflash

TOPflash reporter (0.5 μ g) was co-transfected with Barx2, MyoD and siRNA (total 1 μ g) in to C2C12 myoblasts. Transfection of empty pcDNA3 vector served as a negative control. Luciferase activity was assayed 48 hours post transfection. All data are normalised to a Renilla luciferase internal control, expressed as the mean firefly/Renilla luciferase ratio, and then to pcDNA3 empty vector transfection with (A): control siRNA (set to a value of 1) or (B): Barx2 and MyoD transfection with control siRNA (set to a value of 1). The results shown are the average of three independent experiments performed in triplicate. Error bars represent SEM. ** $p < 0.001$. $n=9$.

To assess whether Pax7 is a specific antagonist of Barx2-mediated TOPflash activation, or whether it acts more generally on the Wnt/ β -catenin pathway, the ability of Pax7 to antagonise activation either by constitutively active (ca.) β -catenin or Wnt3a ligand was assessed. As shown in Figure 3.8A, cotransfection of Pax7 abolished the 14-fold activation of TOPflash by β -catenin. Furthermore, TOPflash activation by Wnt3a CM (180-fold at 1:10 dilution, 90-fold at 1:20 dilution) was significantly reduced although not abolished by transfection of Pax7 (Figure 3.8B). Pax7 expression produced a consistent 5-fold inhibition of Wnt3a-mediated TOPflash activation despite different concentrations of Wnt3a CM. For example, at a 1:10 dilution of Wnt3a CM, Pax7 expression reduced activation from approximately 180-fold to 40-fold above basal activity, and at a dilution of 1:20 Wnt3a CM, Pax7 reduced activation from 90-fold to 11-fold.

Another member of the Pax family, Pax3, was also tested for its ability to modulate TOPflash activity. Pax3 contains a paired domain, a full homeodomain and an octapeptide motif that are highly related to those of Pax7. Similar to Pax7, transfection of Pax3 was repressive to basal TOPflash activity and completely abolished activation of TOPflash by Barx2 and β -catenin (Figure 3.8C).

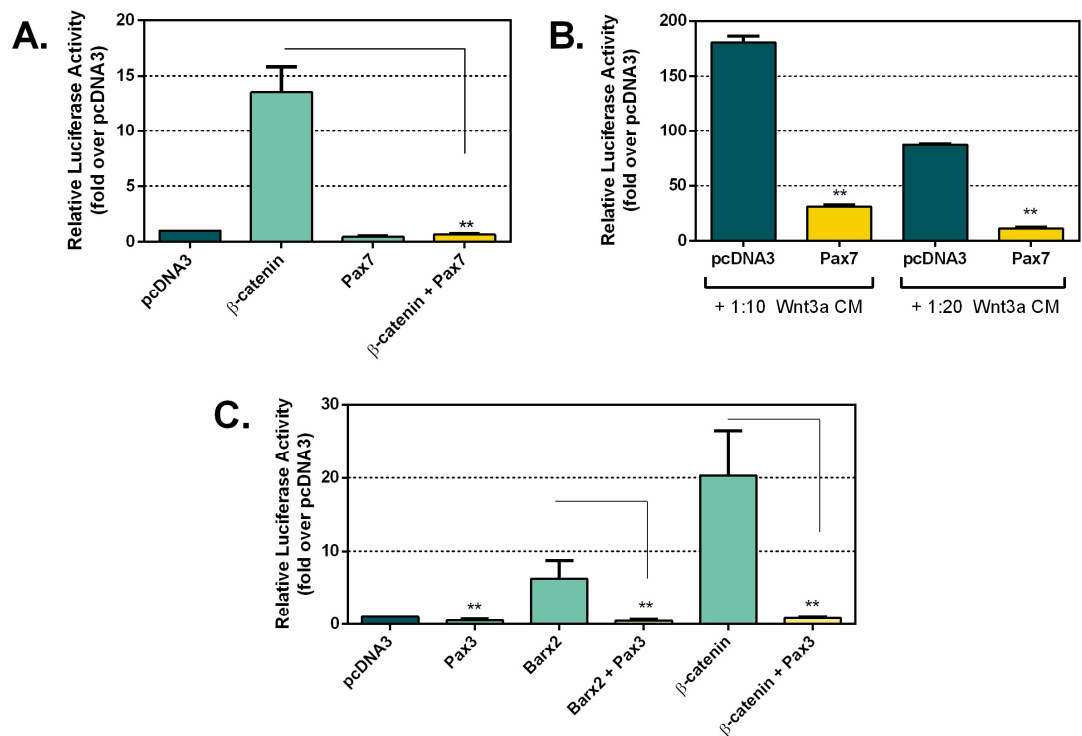


Figure 3.8: Pax7 antagonises the activating effect of β -catenin and Wnt3a on TOPflash

(A) TOPflash reporter (0.5 μ g) was co-transfected with combinations of Pax7 or constitutively active β -catenin (50 ng) in C2C12 myoblasts. (B) TOPflash reporter (0.5 μ g) was co-transfected with Pax7 in C2C12 myoblasts and cells were treated with Wnt3a CM. (C) TOPflash reporter (0.5 μ g) was co-transfected with combinations of Pax3, Barx2 or ca. β -catenin in C2C12 myoblasts. Transfection of empty pcDNA3 vector served as a negative control and to control for total amount of transfected DNA. Luciferase activity was assayed 48 hours post transfection. All data are normalised to a Renilla luciferase internal control, expressed as the mean firefly/Renilla luciferase ratio, and then to pcDNA3 empty vector transfection (set to a value of 1). The results shown are the average of at least three independent experiments (A, C) or a representative experiment (B) performed in triplicate. Error bars represent SEM. ** $p < 0.001$ relative to pcDNA3 control unless otherwise marked.

3.3.5 Delineation of the functional domains of Pax7 repression

The Pax7 protein consists of a paired domain and a homeodomain, both of which encode a DNA-binding motif, as well as an engrailed homology-1 (Eh1) domain. Eh1 motifs are known to mediate interactions of a number of protein families with transcriptional co-repressors of the TLE/Groucho protein family, and functional analysis has shown that the Eh1 motif is required for active transcriptional repression *in vivo*, as well as for the physical interaction with Groucho co-repressors [Logan et al. 1992; Smith & Jaynes 1996; Tolkunova et al. 1998; Chen & Courey 2000]. Groucho/TLE co-repressors have been reported as playing an important role in repression of canonical Wnt target genes in the absence of a Wnt signal and nuclear β -catenin [Cavallo et al. 1998]. To delineate the functional domains mediating Pax7 repression in this system, three mutant expression constructs were generated (as described in Section 3.2.1) and co-expressed in C2C12 cells with TOPflash and either Barx2 or ca. β -catenin. Figure 3.9 shows that mutation of the Pax7 Eh1 domain (Eh1 SDM) or deletion of the Pax7 paired domain (Δ PD) had no effect on the ability of Pax7 to block TOPflash activation by either Barx2 or ca. β -catenin. However, deletion of the homeodomain (Δ HHD) moderately impaired the ability of Pax7 to inhibit Barx2 or ca. β -catenin-mediated activation. Overall, these data indicated a previously unreported role for Pax7 as a repressor of canonical Wnt signalling, which is in part mediated through the Pax7 homeodomain.

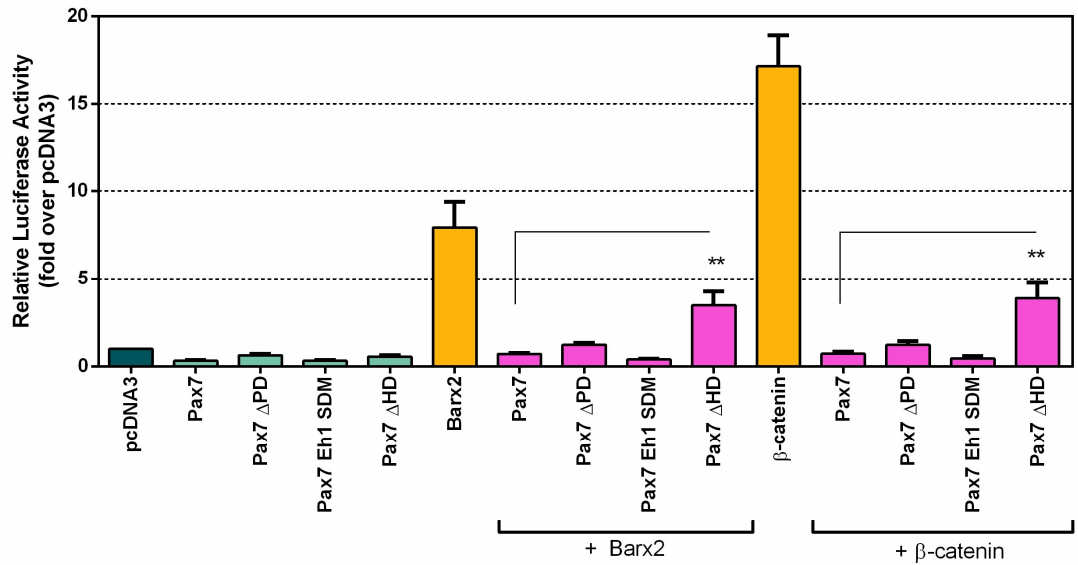


Figure 3.9: The Pax7 homeodomain is important for repression of TOPflash activity

TOPflash reporter (0.5 µg) was co-transfected with combinations of constitutively active β-catenin (50 ng), Barx2 and Pax7 mutant constructs (total 1 µg) in C2C12 myoblasts. Transfection of empty pcDNA3 vector served as a negative control and to control for total amount of transfected DNA. Luciferase activity was assayed 48 hours post transfection. All data are normalised to a Renilla luciferase internal control, expressed as the mean firefly/Renilla luciferase ratio, and then to pcDNA3 empty vector transfection (set to a value of 1). The results shown are the average of at least two independent experiments performed in triplicate. Error bars represent SEM. ** p < 0.001.

3.3.6 Barx2 and Pax7 interact physically with β-catenin and TCF family members

With evidence to date suggesting a role for Barx2, MyoD and Pax7 in modulating TOPflash reporter activity, it was important to determine whether these factors form a complex with the core Wnt effectors, β-catenin and TCF/LEF. To this end, co-immunoprecipitation (IP) with myc-epitope-tagged proteins was performed in COS7 cells. Previous studies have shown the ability of Barx2 and MyoD [Makarenkova et al. 2009] and MyoD and β-catenin [Kim et al. 2008] to interact and as such these interactions were not assessed. Myc-tagged Barx2 or Pax7 was expressed in COS7

cells and IP was performed for endogenous β -catenin with an anti- β -catenin antibody. Blotting for Barx2 or Pax7 with anti-myc antibody showed both Barx2 and Pax7 were efficiently co-immunoprecipitated with endogenous β -catenin (Figure 3.10A). Moreover, co-immunoprecipitation of Barx2 and β -catenin also occurred in lysates sonicated and treated with ethidium bromide, which selectively inhibits DNA-dependent protein associations in the precipitation reactions [Lai & Herr 1992] (Figure 3.10A), suggesting the interaction between Barx2 and β -catenin is not entirely dependent on DNA. To delineate interaction domains of Barx2 with β -catenin, the myc-tagged Barx2 NHDBBR, HDBBRC, N-term and C-term constructs were expressed in COS7 cells. Figure 3.10B shows that both NHDBBR and HDBBRC proteins co-immunoprecipitated with endogenous β -catenin, whilst the N-term and C-term proteins lacking the HD and BBR were not precipitated, indicating that the HDBBR region is necessary for interaction. Attempts to co-immunoprecipitate the HDBBR fragment alone with endogenous β -catenin were unsuccessful, potentially due to weaker expression of this protein fragment (not shown), however this could also explain the reduced activation of TOPflash shown previously in Figure 3.1. Consistent with these results and the aforementioned luciferase assays, the myc-tagged Barx2 Δ HD and Pax7 Δ HD constructs also did not co-immunoprecipitate with endogenous β -catenin in COS7 cells (Figure 3.10C). Full length Barx2 successfully co-immunoprecipitated with TCF4 following over-expression of both proteins also in COS7 cells (Figure 3.10D). It should be noted that two TCF4 species of \sim 60 and 80 kDa were observed on the immunoblots. The larger variant is consistent with a post-translationally modified form [Yamamoto et al. 2003] that is reported to confer the majority of transcriptional activity in other cells [Chesire et al. 2002]. As shown in

Figure 3.10D, Barx2 preferentially co-immunoprecipitated the larger molecular weight form of TCF4.

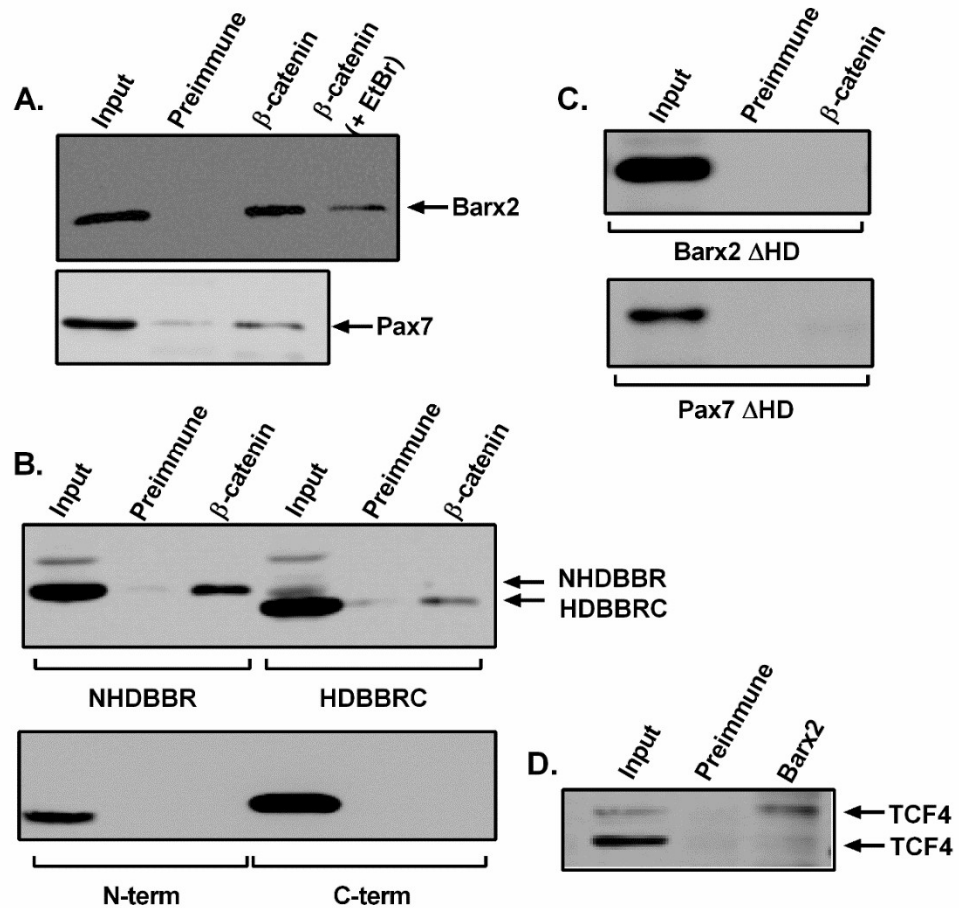


Figure 3.10: Barx2 interacts with β -catenin and TCF4 *in vitro*

(A, B, C): Myc-epitope-tagged Barx2 or (A, C) Pax7 constructs were expressed in COS7 cells and immunoprecipitated using polyclonal antibodies to endogenous β -catenin. (D): Myc-epitope-tagged TCF4 and Barx2 were expressed in COS7 cells and immunoprecipitated using polyclonal antibodies to Barx2. Proteins were resolved on a 10% SDS-PAGE gel, transferred to nitrocellulose membrane and probed with monoclonal antibodies to the myc-tag. All immunoprecipitation assays were performed at least twice with similar results. Representative blots are shown.

To determine whether the aforementioned protein interactions were direct, co-immunoprecipitations using proteins generated by *in vitro* transcription/translation were attempted. Whilst *in vitro* translated (IVT) TCF4 co-immunoprecipitated with IVT β -catenin, attempts to co-immunoprecipitate IVT Barx2 with IVT β -catenin, TCF4

or both together were unsuccessful (Figure 3.11B), indicating possible additional proteins or post-translational modifications are required to mediate or stabilise the interactions. As shown in Figure 3.11B, when all three IVT products were incubated together and complexes were captured with an antibody to β -catenin, TCF4 but not Barx2 was present in the IP. When complexes were captured with an antibody directed at Barx2, only Barx2 was detected in the IP. Furthermore, re-probing the same blot with anti- β -catenin antibodies showed the presence of β -catenin in the β -catenin IP but not the Barx2 IP (not shown).

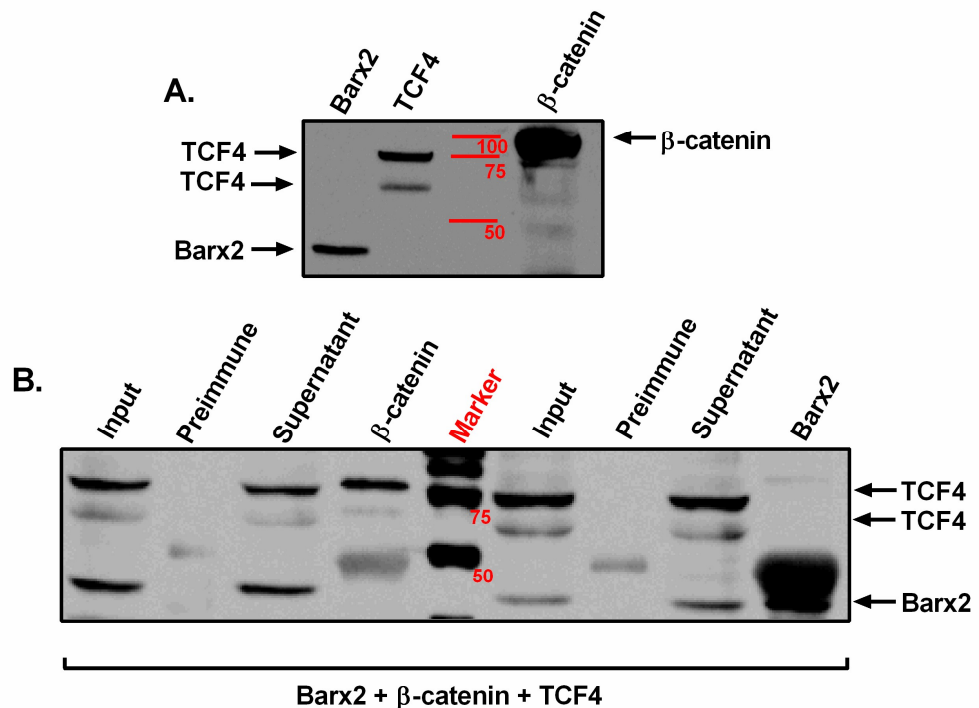


Figure 3.11: Barx2, β -catenin and TCF4 proteins do not directly interact

(A): Proteins were synthesised using the TnT® Quick Coupled Transcription/Translation system (Promega). (B): β -catenin, TCF4 (myc tagged) and Barx2 (myc tagged) IVT products were incubated together and complexes were captured with either anti- β -catenin or anti-Barx2 rabbit polyclonal antibodies and Protein A sepharose beads. Proteins were resolved on a 10% SDS-PAGE gel, transferred to nitrocellulose membrane and probed with antibodies to the myc-tag. A representative blot is shown.

3.3.7 Disruption of a phosphorylation site within Barx2 renders the protein inactive

Proteins are often modified following translation. One type of post-translational modification is phosphorylation; the addition of a phosphate group to the –OH group of serine, threonine or tyrosine (ie. changing –OH to –PO₄²⁻), catalysed by a kinase. Analysis of the Barx2 protein sequence using phosphorylation prediction software NetPhos 2.0 (www.cbs.dtu.dk/services/NetPhos/) revealed a number of potential phosphorylation sites (Figure 3.12). Of these, 4 high ranking candidates (score >0.8 out of a possible 1) were chosen. Three of these were serine (S) and were conserved between Barx2 and Barx1, and one tyrosine (Y) present only in Barx2.

MHCHAE LRLSSPGQLKAARRRYKTFMIDEILSKETCDYFEKLSLYSVCPSLVVRPKPLHS	60
CTGSPSLRAYPLLSVITRQPTVISHLVPTGSGLTPVLTRHPVAAAAEAAAAAETPGGEAL	120
ASSESETEQPTPRQKKPRRSRTIFTELQLMGLEKKFQKQKYLSTPDRDLAQSGLTQLO	180
VKTWYQNRMRKWKMMVLKGGQEAPTKPKGRPKKNSIPTSEEIEAEKMNNSQAQSQELLES	240
SERQEEPCDTQEPKACLVPLEVAEPIHQPELSEASSEPPPLS	300
.....SS.....T.....S.....Y.....S	60
.....S.....T.....T.....T.....	120
.SS.S.....T.....S.....Y.ST.....	180
.....S.....S.....S.....S.....S	240
S.....T.....S.....	300

Figure 3.12: Phosphorylation prediction of Barx2

Barx2 sequence was analysed by NetPhos 2.0 software (www.cbs.dtu.dk/services/NetPhos/). Predicted phosphorylation of serine (S), threonine (T) and tyrosine (Y) residues are indicated. Highlighted residues indicate a score of >0.8 out of 1 that were chosen for mutational analysis. Green: conserved S residues between Barx2 and Barx1. Blue: non-conserved Y residue. Underline: Barx2 homeodomain.

To assess the role of these predicted residues and thus the role of serine and tyrosine phosphorylation in Barx2-mediated activation of TOPflash, primers were designed to introduce point mutations at these sites, and the new constructs were tested for their ability to activate TOPflash in a transient transfection followed by luciferase assay.

Initially, two Barx2 phosphorylation site mutants were generated – one which mutated two serines (S) within a potential GSK3 phosphorylation site to alanine (A) (S215A, S219A), and one which mutated a serine and tyrosine (Y) within a potential CKII phosphorylation site to alanine (S163A, Y161A). Alanine lacks the –OH group that allows serine and tyrosine residues to be phosphorylated. As shown in Figure 3.13, mutation of the S residues within the possible GSK3 phosphorylation site had no significant effect on the ability of Barx2 to activate the TOPflash reporter, with the mutated construct producing approximately the same level of activation as wildtype (WT) Barx2. However, mutation of both the S and Y residues within the possible CKII phosphorylation site completely abolished Barx2-mediated activation. To further isolate the critical residue, two further mutants were generated. This time, the Y residue and the S residue were mutated to A residues independently. The ability of these new constructs to activate TOPflash was then assessed. It was observed that the S163A mutation did not reduce the level of activation when compared to WT Barx2, but that the Y161A mutation was sufficient to abolish all activity (Figure 3.13), suggesting a potential requirement for the phosphorylation of Y(161) in the function of Barx2. To study the effect of phosphorylation more directly, a “phosphomimetic” mutation is often generated that mimics the chemical structure of a phosphorylated residue. Generally, aspartate (D) is used to mimic phosphorylation of serine and threonine residues. It can also be used to mimic tyrosine phosphorylation with the caveat that the structure of aspartate is very different to tyrosine because it lacks the aromatic ring. A Barx2 Y161D mutant construct was generated and its ability to activate TOPflash was tested. Barx2 Y161D yielded the same result as the Barx2 Y161A construct, which was no activation of the reporter (Figure 3.13). Y161 is

located in the centre of the Barx2 homeodomain and it is possible that it is the side chain conformation of Y161 that is critical for Barx2 function rather than its phosphorylation. Overall these data could not unequivocally determine whether Barx2 function is dependent on phosphorylation. However it is still possible that post-translational modifications are required to mediate or stabilise the interaction between Barx2, β -catenin, and/or TCF family members and this could be further investigated in the future.

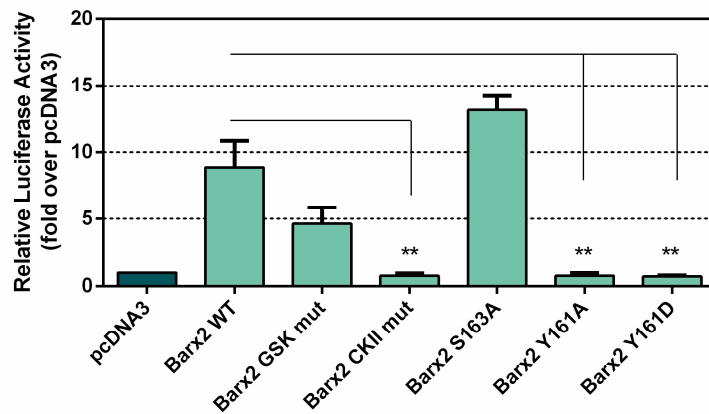


Figure 3.13: Analysis of Barx2 phosphorylation mutants on TOPflash activity

TOPflash reporter (0.5 μ g) was co-transfected with either WT Barx2 or Barx2 phosphorylation mutants (1 μ g) in to C2C12 myoblasts. Transfection of empty pcDNA3 vector served as a negative control. Luciferase activity was assayed 48 hours post transfection. All data are normalised to a Renilla luciferase internal control, expressed as the mean firefly/Renilla luciferase ratio, and then to pcDNA3 empty vector transfection (set to a value of 1). The results shown are the average of two independent experiments performed in triplicate. Error bars represent SEM. ** $p < 0.001$. $n=6$.

3.3.8 Barx2 binds to the TOPflash promoter and promotes recruitment of β -catenin

To test the hypothesis that Barx2 is recruited to the TOPflash promoter via interactions with TCF/LEF and/or β -catenin, chromatin immunoprecipitation (ChIP)

using a stable C2C12 cell line that carries an integrated TOPflash promoter/luciferase reporter (TOPPuro) was performed. This cell line was previously tested and the reporter shown to respond to Wnt3a stimulation as well as over-expression of Barx2 and Barx2+MyoD. Given that endogenous Barx2 target genes containing TCF/LEF sites had not been clearly defined by this stage of the project, this transgenic cell line was extremely valuable for elucidating functional binding to TOPflash promoter DNA. The CHIP protocol was based on a rapid microCHIP protocol [Dahl & Collas 2008] but was optimised for C2C12 cells and the factors of interest. Specifically, the factors that were modified for optimisation included cell number, cross-linking time, volume of lysis buffer for sonication and sonication conditions, protein:DNA complex washing and DNA elution from Protein-G beads. The details of the optimization have been omitted from this thesis but the final, optimised protocol is described in Chapter 2, Section 2.11. During optimisation of the CHIP protocol, TOPPuro cells were cultured with 1:2 dilution of Wnt3a CM for 8 hours, followed by immunoprecipitation with a β -catenin antibody. As expected, immunoprecipitation of β -catenin following Wnt3a stimulation produced a robust 10-fold enrichment of TOPflash promoter DNA relative to IgG control (Figure 3.14A). In TOPPuro cells that were transfected with either Barx2 or Barx2+MyoD, CHIP with Barx2 antibodies produced, on average, 4-fold enrichment of TOPflash promoter DNA, suggesting that Barx2 binds the promoter. Moreover, in cells transfected with Barx2 or Barx2+MyoD, CHIP with β -catenin antibodies also produced 3 to 4-fold enrichment of TOPflash promoter DNA indicating recruitment of β -catenin, independent of β -catenin transfection or Wnt3a stimulation. As a control, no β -catenin recruitment was observed with either Barx2 or β -catenin antibodies when cells were transfected with control empty vector. The recruitment

of MyoD to TOPflash after transfection of TOPPuro cells with empty vector, MyoD, or Barx2+MyoD was also examined. CHIP with antibodies to MyoD showed that MyoD was only recruited to the TOPflash promoter after co-transfection of Barx2 with MyoD, and not following empty vector or MyoD transfection alone. Furthermore, transfection of MyoD alone was not sufficient to induce recruitment of β -catenin to the TOPflash promoter. As shown in Figure 3.14B, efficacy of the MyoD antibody in CHIP was demonstrated by the recruitment of MyoD to an E-box-containing promoter, desmin [Li & Capetanaki 1993]. Overall these data suggest that Barx2 recruits both MyoD and β -catenin to the TOPflash promoter.

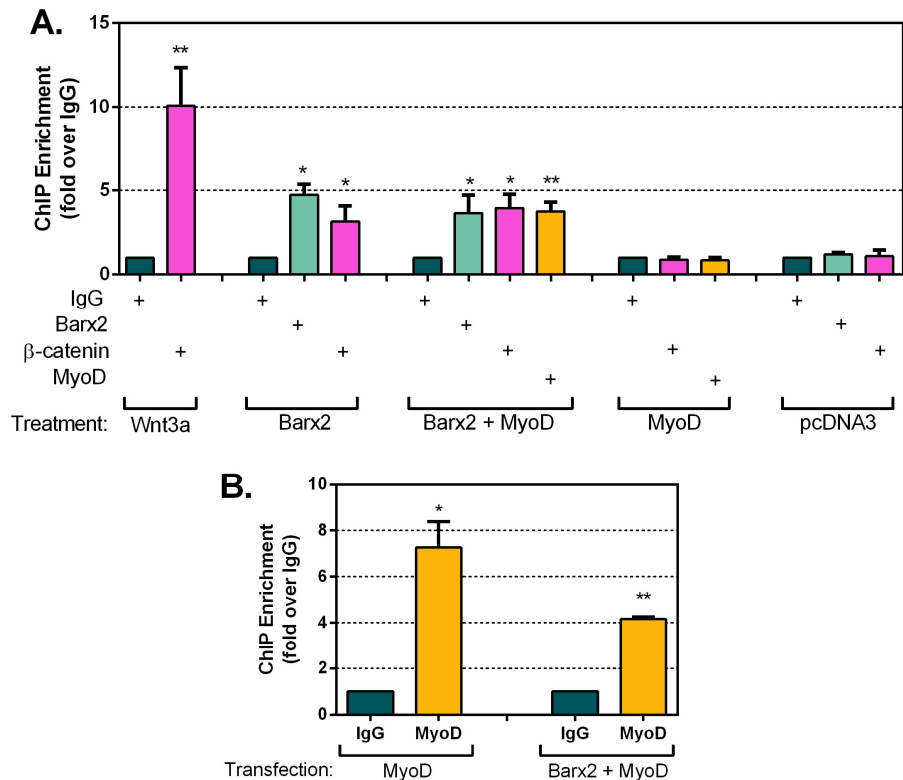


Figure 3.14: Barx2 is recruited to the TOPflash promoter in C2C12 cells and promotes recruitment of β -catenin

ChIP was performed on chromatin from the C2C12 TOPPuro stable cell line following transfection of empty vector, Barx2, Barx2+MyoD or MyoD, or treatment with a 1:2 dilution of Wnt3a CM for 8 hours. ChIP was performed with 2 μ g of the indicated antibodies. Data are PCR amplification values for the (A) TOPflash promoter or (B) Desmin promoter normalised to amplification values for a control non-target locus (β 2-microglobulin), with enrichment values for each antibody subsequently normalised to the mock ChIP with preimmune IgG, arbitrarily set to a value of 1. The results shown are the average of at least three independent experiments. Error bars represent SEM. * $p < 0.05$ and ** $p < 0.001$ relative to IgG controls.

3.3.9 Over-expression of Barx2 leads to accumulation of β -catenin in the nucleus

The role of canonical Wnt ligands in inhibiting β -catenin phosphorylation and promoting its stabilisation is well defined [Liu et al. 2005; Li et al. 2012]. Western blot analysis and immunofluorescence microscopy were used to quantify the effect of adding Wnt3a CM to C2C12 myoblasts on the total amount of β -catenin. As shown in

Figure 3.15A, lysates of C2C12 cells treated with 1:2 dilution of Wnt3a CM for 48 hours had approximately 9-fold more total β -catenin than control-treated lysates (when quantified to β -actin housekeeping protein). In an attempt to quantify the level of only non-phosphorylated (active) β -catenin, by western blot, two different anti-active β -catenin antibodies (Anti-active- β -catenin clone E87 (Merck Millipore) and Non-phospho β -catenin Ser33/37/Thr41 (Cell Signaling Technology)) were tested. However both proved to be insufficiently sensitive to reliably quantify non-phosphorylated β -catenin and therefore the data is not shown. Immunofluorescence analysis showed that Wnt3a CM increased the total amount of β -catenin as measured by total cellular fluorescence (Figure 3.15B). Furthermore, immunofluorescence analysis showed that Wnt3a increased the ratio of nuclear:cytoplasmic β -catenin, with cells that were treated with Wnt3a CM containing on average 16-fold more β -catenin in the nucleus relative to the cytoplasm (Figure 3.15C).

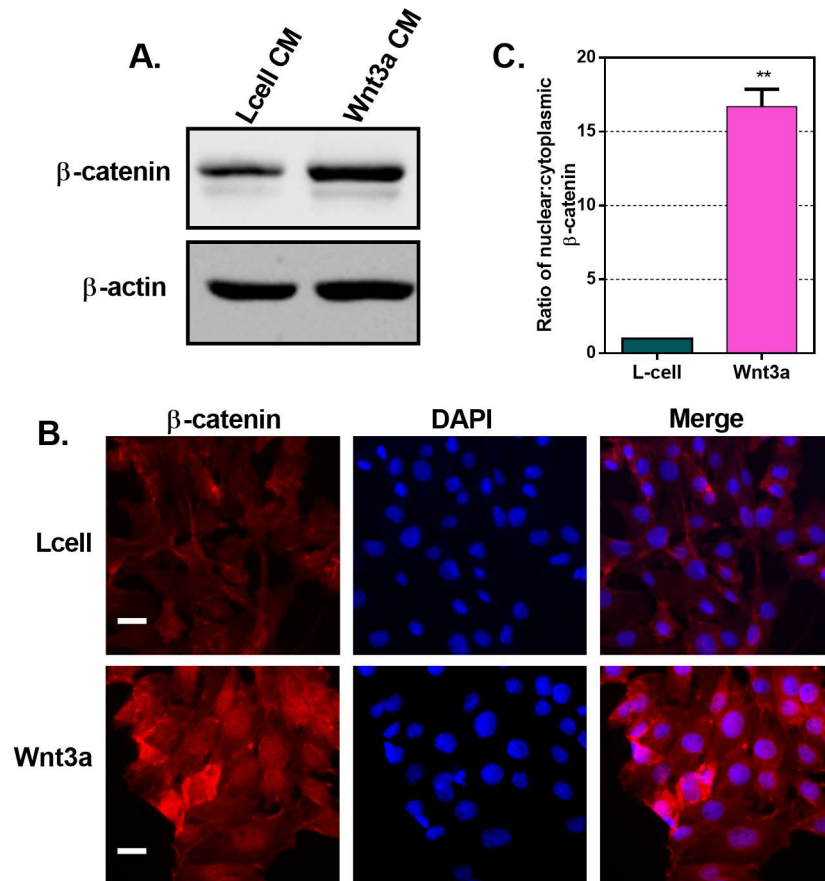


Figure 3.15: Wnt3a stimulates nuclear localisation of β-catenin in C2C12 cells

(A): Protein lysates of C2C12 cells treated with control or a 1:2 dilution of Wnt3a CM for 8 hours were resolved on a 10% SDS-PAGE gel, transferred to nitrocellulose membrane and probed with antibodies to endogenous total β-catenin. This was performed in duplicate and a representative blot is shown. (B): C2C12 cells treated with control or Wnt3a CM for 48 hours were fixed, immunostained for total β-catenin (red) and DAPI (blue) and imaged with an Olympus IX71 microscope. This was performed in duplicate and a representative image is shown. Scale bar represents 25 μM. (C): ImageJ software was used to quantify nuclear and cytoplasmic fluorescence. ** p < 0.001.

The next question that was examined was whether Barx2 played any role regulating β-catenin expression level and/or nuclear localisation. In contrast to what was observed with Wnt3a, over-expression of Barx2 or Barx2+MyoD did not increase total β-catenin as observed by western blot (Figure 3.16A). Interestingly, however, immunofluorescence staining of C2C12 cells transfected with Barx2 and probed with antibodies recognising Barx2 and β-catenin showed that cells expressing high levels

of Barx2 had a significant increase in nuclear β -catenin compared to the control untransfected cells (Figure 3.16B, as quantified in Figure 3.16C). On average, Barx2-positive cells had 7.6-fold higher nuclear:cytoplasmic β -catenin ratio than Barx2-negative cells. This result suggests that Barx2 does not increase total β -catenin levels but may sequester it in the nucleus. This interpretation is also consistent with increased binding of endogenous β -catenin to TOPflash promoter DNA following Barx2 over-expression as observed in ChIP.

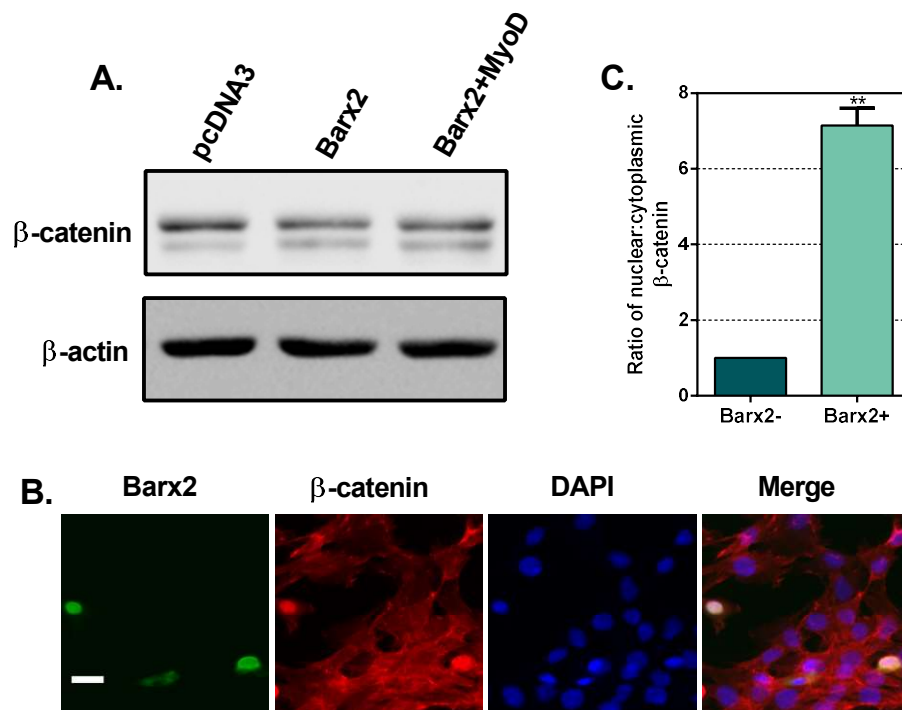


Figure 3.16: Barx2 over-expression leads to β -catenin accumulation in the nucleus

(A): Protein lysates of C2C12 cells transfected with empty vector control, Barx2 or Barx2 and MyoD were resolved on a 10% SDS-PAGE gel, transferred to nitrocellulose membrane and probed with antibodies to endogenous total β -catenin. This was performed in duplicate and a representative blot is shown. (B): C2C12 cells transfected with empty vector control or Barx2 were fixed, immunostained for total Barx2 (green), β -catenin (red) and DAPI (blue) and imaged with an Olympus IX71 microscope. ImageJ software was used to quantify nuclear and cytoplasmic fluorescence. A representative image is shown. Scale bar represents 25 μ M.

3.4 Discussion

Data generated in the laboratory prior to the commencement of this doctoral study identified a novel role for the homeobox factor Barx2 and the bHLH MRF MyoD in regulation of Wnt target gene activity in myoblasts via use of the widely used Wnt reporter gene, TOPflash. The work presented in this chapter greatly extended these initial observations and answered several key questions posed at the beginning of the chapter. It clearly defines Barx2 and MyoD as novel members of the canonical Wnt/ β -catenin effector complex in myoblasts, and also suggests a new player within this complex, Pax7. In the absence of a canonical Wnt ligand, β -catenin has been reported to exist primarily in the cytoplasm, where it is phosphorylated and targeted for degradation and thus unable to activate gene transcription [Rubinfeld et al. 1996; Aberle et al. 1997; Behrens et al. 1998]. The studies here have demonstrated, by use of the synthetic Wnt reporter, that Barx2 can potentiate Wnt target promoter activity on its own, in the absence of exogenously expressed 'active' β -catenin or treatment with Wnt ligand to stabilize and promote nuclear accumulation of endogenous β -catenin. Furthermore, as previously shown in the laboratory, the activation observed by Barx2 was potentially enhanced by the over-expression of MyoD, yet MyoD alone had no effect on promoter activity. Here, transfection studies combined with luciferase assays demonstrated that MyoD was not the only MRF member able to synergise with Barx2 in this context. In fact, all four MRFs (MyoD, Myf5, MRF4 and myogenin), which are expressed at varying stages of myogenesis, displayed the ability to significantly enhance Barx2-mediated activation of TOPflash when co-expressed in C2C12 cells. This suggests a possible role for Barx2 activation of Wnt target genes during all stages of myogenesis. Barx2 has previously been reported to interact with

MyoD [Makarenkova et al. 2009]; however the functional interaction between Barx2 and other MRFs is yet to be assessed. These studies also show for the first time that MRFs can assist in promoting transcription from TCF/LEF sites. An interesting observation was that MyoD, when expressed in the absence of Barx2, could inhibit activation of β -catenin. Previously, an interaction between β -catenin and MyoD was reported, however this interaction was only shown to enhance transcription via E-box motifs [Kim et al. 2008]. One possibility consistent with the findings presented here and also the current literature is that in the presence of high expression of MyoD, β -catenin is sequestered away from TCF/LEF binding sites and instead associates with MyoD at E-box binding motifs.

The ability of Barx2 to activate TOPflash in COS7 cells, a fibroblast-like cell line from monkey kidney which is unable to undergo myogenic conversion and does not express any member of the MRF family, indicates that Barx2 is not *dependent* on MRFs to mediate Wnt target promoter activation. Moreover, the observation that synergy between heterologously-expressed Barx2 and MyoD could still be achieved in COS7 cells further indicates that no other muscle-specific protein partners are required for this regulation. These data are significant as they suggest that Barx2 could regulate Wnt signalling in other contexts, including epithelial tissues in which it is expressed.

In this chapter, the role of the canonical satellite cell marker, Pax7, in regulation of Wnt target genes was assessed. Pax7 is expressed in quiescent and proliferating satellite cells/myoblasts but is downregulated when cells begin to differentiate [Zammit et al. 2004]. Barx2 is also expressed in satellite cells [Meech et al. 2012], but

in contrast to Pax7, is induced during early stages of differentiation, promoting pro-differentiation events such as cell spreading and migration [Makarenkova et al. 2009]. Pax7 was highly repressive to basal TOPflash activity. In addition to this, it completely blocked activation by Barx2, Barx2+MyoD and constitutively active β -catenin, and greatly reduced activation by Wnt3a ligand (Wnt3a CM addition), highlighting the potency of Pax7-mediated repression within this system. The repression of Pax7 observed here was partially dependent on the homeodomain, but not the paired domain or the Eh1 motif.

Barx2 has been shown to promote differentiation [Meech et al. 2012] and canonical Wnt signals have also been shown to promote differentiation [Brack et al. 2008; Tanaka et al. 2011; Jones et al. 2015]. Conversely, Pax7 has been shown to block differentiation [Olguin & Olwin 2004; Zammit et al. 2006; Olguin et al. 2007] and indeed the Pax7^{high} expression state may be considered to be differentiation-incompetent. Hence a model can be proposed in which high levels of Pax7 block the pro-differentiation effects of both Barx2 and received Wnt signals in proliferating cells. The subsequent down-regulation of Pax7 in cells committed to differentiation may allow Barx2 to activate pro-differentiation target genes in co-operation with β -catenin and MRFs. Thus, antagonism between Pax7 and Barx2 with respect to Wnt signalling may be a key component of the Wnt-induced switch from proliferation to differentiation [Brack et al. 2008]. Pax7 is known to destabilise MyoD protein [Olguin & Olwin 2004], and this may in part explain the ability of Pax7 to inhibit Barx2+MyoD-mediated activation of TOPflash. However, the ability of Pax7 to block activation by β -catenin in both myogenic and non-myogenic cells indicates a role within the Wnt

effector complex that is independent of Barx2 and MRFs. Interestingly, in the studies shown here, Pax3 produced the same potent repression of TOPflash as Pax7. Furthermore, recent work from this laboratory (not shown here) found an interaction between Barx2 and Pax6 in regulation of TOPflash in epithelial cells, suggesting that the Barx-Pax interaction is a broadly applicable paradigm.

The co-immunoprecipitations performed within this chapter demonstrate the ability of Barx2 to interact with both β -catenin and TCF4 when expressed in COS7 cells, yet not when the proteins are transcribed and translated *in vitro*. The fact that no direct interaction could be identified between Barx2 and β -catenin, Barx2 and TCF4, or Barx2 with either β -catenin or TCF4 when protein lysates were mixed, suggests additional proteins or post-translational modifications are required to stabilise the reaction. A consistent thread throughout the results was the importance of the Barx2 homeodomain, with constructs lacking the homeodomain unable to mediate TOPflash activation or interaction with β -catenin. Furthermore, the co-immunoprecipitation results suggest that the Barx2 homeodomain works collaboratively with either N-terminal or C-terminal domains to bind β -catenin, and as such that it is necessary, but not sufficient, for this interaction. Interactions with β -catenin are lost upon removal of either the homeodomain or absence of both the N-terminus and C-terminus.

CKII phosphorylates a variety of transcriptional regulators and plays key roles in myogenesis, with its enzymatic activity increasing as myoblasts differentiate. For example, overexpression of CKII has been shown to increase the transcriptional activities of MRF4 and MyoD *in vivo* through phosphorylation of E47 proteins

[Johnson et al. 1996]. CKII also phosphorylates both Pax7 and Pax3 in proliferating myoblasts [Dietz et al. 2009; Gonzalez et al. 2016] and inhibition of Pax7 phosphorylation results in a downregulation of Pax7 accompanied by precocious myogenic induction. In these studies, a potential Barx2 CKII phosphorylation site was identified. A variant Barx2 protein with a mutated CKII phosphorylation site (situated within the homeodomain) was unable to activate TOPflash; however it remains unresolved whether this was due to loss of phosphorylation or simply due to disruption of a critical residue within the homeodomain. With no additional support for phosphorylation of Barx2, these studies were not pursued further.

Data shown here support the idea that Pax7 acts as an antagonist of the core Wnt effector complex. Initially, it was speculated that Pax7 may function by stabilizing the binding of the TCF/LEF-corepressor complex to DNA and preventing recruitment of β -catenin. This model would be consistent with the known role of the Eh-1 motif in recruiting TLE/Groucho factors that bind to TCF/LEF factors and act as corepressors [Brantjes et al. 2001; Daniels & Weis 2005]. However, this model was incompatible with two observations: 1) removal of the Eh1 motif did not affect the repressive function of Pax7 with respect to TOPflash, 2) co-immunoprecipitations revealed that Pax7 bound to β -catenin. Hence it seems likely that Pax7 doesn't block recruitment of β -catenin to DNA, but that it may block the ability of β -catenin to dismiss corepressors and recruit coactivators. Moreover, Pax7 and Barx2 may compete for interaction with β -catenin; however this also remains to be tested. A handful of other homeodomain proteins have been reported to engage in functional interactions with β -catenin or TCF/LEF proteins [Vadlamudi et al. 2005; Olson et al. 2006; Park et al.

2012]. In particular, Pitx2 interacts with β -catenin via its homeodomain [Amen et al. 2007], raising the interesting possibility that Barx2 and Pitx2 could also compete for this interaction.

It was hypothesised that Barx2 and MyoD are recruited indirectly to the TOPflash promoter through β -catenin/TCF, as TOPflash contains no recognisable binding sites for either homeobox or bHLH factors, and both Barx2 and MyoD are able to interact with β -catenin. Consistent with the promoter-reporter studies, chromatin immunoprecipitation (ChIP) experiments revealed that Barx2 was recruited to TOPflash promoter DNA. Barx2 was also sufficient to promote recruitment of endogenous β -catenin, providing a mechanism by which Barx2 is able to mediate activation of TOPflash in the absence of β -catenin over-expression or canonical Wnt ligand stimulation. ChIP studies also showed that Barx2 was necessary for MyoD to be recruited to the promoter. Hence, Barx2 may be the core mediator of Barx2-MyoD- β -catenin complex formation. Western blot experiments revealed that Barx2 did not increase levels of β -catenin; however, fluorescence immunostaining indicated that Barx2 induced a higher nuclear:cytoplasmic ratio of β -catenin. Thus, this suggests that Barx2 plays a role in sequestering β -catenin in the nucleus to activate transcription and complements a study by Shao and colleagues implicating another homeobox factor, Msx2, in promoting β -catenin nuclear localization in fibroblasts [Shao et al. 2005]. Whether Barx2 actually regulates nuclear import of β -catenin is unclear. However, given that β -catenin is proposed to freely shuttle between compartments, increased recruitment to DNA alone could result in a net increase in nuclear levels.

In summary, these studies show that Barx2 is able to activate TOPflash by promoting nuclear sequestering of β -catenin and recruitment of it to promoter DNA. Barx2 is able to functionally interact with both β -catenin and TCF4, and possibly other TCF/LEF members, forming an activation complex. The Barx2 homeodomain is essential for this interaction and thus for the activating function of Barx2. In contrast, Pax7 is highly repressive of TOPflash, possibly through blocking the ability of β -catenin to dismiss co-repressors and recruit co-activators.

Chapter 4

Analysis of the effect of Barx2 loss-of-function on Wnt and Notch signalling in myoblasts and *in vivo*

4.1 Introduction

4.1.1 Transgenic TCF/LEF reporters

As a means of tracking activity of canonical Wnt signalling during animal development, various “reporter transgenes” that respond to Wnt signals have been developed. These transgenes can provide a useful means for monitoring both pathway activity at previously confirmed sites of signalling, and also for identifying novel signalling contexts. Similar to the TOPflash luciferase reporter construct described in the previous chapter, these transgenes are based on a multimerized TCF/LEF binding site driving expression of reporters such as LacZ or GFP. Several transgenic mouse lines have been described in the literature. Of these, perhaps the most widely reported: TOPGAL, a β -galactosidase gene under the control of three multimerized TCF/LEF consensus binding sites and the c-fos minimal promoter [DasGupta & Fuchs 1999] and BAT-GAL, a β -galactosidase gene under the control of seven multimerized TCF/LEF consensus binding sites and the minimal promoter of the *siamois* gene [Maretto et al. 2003]. Other transgenic models that have been reported, such as a β -galactosidase gene under the control of six TCF/LEF response elements and the hsp68 minimal promoter [Mohamed et al. 2004], and a LEF-EGFP Wnt reporter originally described by Currier and colleagues [Currier et al. 2010] have limited direct evidence regarding their Wnt responsiveness *in vivo*.

Certain caveats should be considered when analysing these reporters. In particular, the fact that the number of TCF/LEF binding sites in reporter transgenes is usually higher than in native Wnt-responsive target gene promoters. BAT-GAL, for example, contains seven multimerized TCF/LEF binding sites, whilst most natural target

promoters/enhancers contain far fewer, and/or distributed TCF/LEF sites [Botrugno et al. 2004; Maduro et al. 2005; Kim et al. 2015]. It is possible that placing a large number of closely-packed, optimal-affinity binding sites immediately upstream of a minimal promoter is sufficient to observe a transcriptional response that may not be seen in most native Wnt-responsive promoters. Furthermore, potential transgene insertion site-specific effects may result in 'enhancer traps' at the integration site, presenting consequences for specificity.

In an attempt to reduce chromosomal positional effects, Moriyama and colleagues [Moriyama et al. 2007] generated two TCF/LEF reporter transgenes (ins-TOPEGFP and ins-TOPGAL), which were both flanked by two copies of the core element of the chicken β -globin HS4 insulator [Recillas-Targa et al. 2002]. Insulators, a class of DNA elements that possess the ability to protect genes from regulatory signals emanating from their local genomic environment [Burgess-Beusse et al. 2002; West et al. 2002], have been previously employed in transgenic lines [Potts et al. 2000; Hsiao et al. 2004]. However, this was the first time the insulator sequence has been used in the context of a transgene reporter of the canonical Wnt signalling pathway. These transgenes contained six TCF/LEF consensus sites upstream of a minimum thymidine kinase (TK) promoter driving expression of either EGFP or nuclear localized β -galactosidase. Analysis of these transgenes revealed consistency between the expression patterns of each reporter, indicating success in suppressing chromosomal positional effects by utilising the insulator, and analysis of embryos revealed activation of the reporter genes in regions of known canonical Wnt activity [Moriyama et al. 2007]. In general, reporter gene expression of both ins-TOPEGFP

and ins-TOPGAL embryos are similar to those observed with previous Wnt reporter transgenic mice, and are also consistent with regions where canonical Wnt signalling has been implicated in development.

As part of this project the transgenic reporter mouse line ins-TOPEGFP was obtained from Dr Saga [Moriyama et al. 2007] via the RIKEN BRC, Japan. These mice were then inter-bred with the Barx2 knock-in LacZ mice previously described. The goal was to allow both EGFP and β -galactosidase activity to be visualised simultaneously and the regulation of Wnt signalling by Barx2 within the whole muscle and satellite cell populations to be assessed, providing a model for Wnt signalling in the context of Barx2 WT and Barx2 null expression. Furthermore, it would allow for examination of how the canonical Wnt pathway is dys-regulated in Barx2 knockout mice when the postnatal muscle is subjected to injury (by means of cardiotoxin injection) or Wnt stimulation (purified Wnt3a or lentivirus).

4.1.2 The Notch signalling pathway

In addition to Wnt signalling, six other major signalling pathways control cell fate decisions during development: TCF- β , Hedgehog, receptor tyrosine kinase, nuclear receptor, Jak/STAT and Notch. Each of these pathways is repeatedly activated and used during development of any given organism, activating different subsets of target genes within different developmental contexts. Whilst these signalling pathways have a very different mechanism of signal transduction, the end-result of signalling is to activate specific target genes by means of signal-regulated transcription factors that recognise specific response elements in the promoters or enhancers of target genes. The Notch signalling pathway involves activation of one of four different

transmembrane Notch receptors (NOTCH1, NOTCH2, NOTCH3, NOTCH4), which consist of an extracellular domain (NECD), transmembrane (TM), and intracellular domain (NICD). The binding of a Notch ligand to the extracellular domain of a receptor induces proteolytic cleavage and release of the intracellular domain [Struhl & Greenwald 2001]. The intracellular domain (NICD) is then able to enter the nucleus and mediate target gene activation via formation of a complex with RBP-Jk (also known as CBF1) and Mastermind at the consensus sequence YRTGDGAD [Jarriault et al. 1995; Bray 2006; Ehebauer et al. 2006; Wilson & Kovall 2006; Tanigaki & Honjo 2010]. In the absence of a Notch signal, RBP-Jk inhibits target gene transcription by binding transcriptional corepressors [Kuroda et al. 2003]. Like the Notch receptors, Notch ligands are also single-pass transmembrane proteins, and are members of the DSL (Delta/Serrate/LAG-2) family of proteins; Delta-like (DLL1, DLL3, DLL4) and Jagged (JAG1, JAG2). Thus, in contrast to Wnt signalling, Notch ligands are membrane rather than secreted proteins, and consequently cells expressing Notch ligands must be adjacent to the Notch-receptor expressing cells for signalling to occur.

4.1.2.1 Notch signalling in myogenesis

The Notch signalling pathway has emerged as an important player in myogenesis. In contrast to Wnt signalling, Notch signalling has been found to be a key regulator of satellite cell self-renewal [Fukada et al. 2011; Wen et al. 2012] and quiescence [Bjornson et al. 2012; Mourikis et al. 2012], as well as satellite cell activation and myoblast proliferation [Conboy & Rando 2002]. When Notch signalling is blocked, inhibition of both satellite cell proliferation and self-renewal is observed [Conboy et al. 2003]. Similarly, disruption of Notch3 results in loss of regulation of satellite cell proliferation [Kitamoto & Hanaoka 2010]. Consistent with this, in asymmetrically

dividing satellite cells the differentiating daughter cell expresses higher levels of the Notch ligand Delta-1 [Kuang et al. 2007]. This likely initiates Notch signalling in the neighbouring sister cell to promote self-renewal. In addition, active Notch signalling inhibits differentiation, and has shown to be required for the BMP4-mediated block of myoblast differentiation [Dahlqvist et al. 2003].

4.1.2.2 Notch and Wnt cross-talk

Together, the Wnt and Notch pathways regulate many aspects of development, with recent work highlighting intricate connections between components of each pathway. In regards to myogenesis, Notch signalling likely helps specify commitment of cells to the myogenic lineage [Conboy & Rando 2002; Conboy et al. 2003] whilst preventing lineage progression to the differentiated state [Brack et al. 2008]. A comprehensive study by Brack and colleagues [Brack et al. 2008] detected no Wnt signalling in uninjured adult muscle, but an increase in Wnt signalling in mononucleated cells within injured muscle at days 2 to 5 post-injury. The levels of Wnt signalling progressively increased as the myogenic progenitors spent more time in culture. When Notch signalling is inhibited during the early myoblast proliferative phase a premature increase in Wnt signalling is observed [Brack et al. 2008], suggesting that Notch may be suppressing Wnt at this stage. In addition, inhibiting Notch during the differentiation phase has negligible effects, signifying a functional decline in Notch signalling at a time when Wnt signalling is increasing. Moreover, activation of Notch in myoblasts that have been treated with Wnt3a results in fewer cells expressing active nuclear β -catenin compared to myoblasts with no Notch activation [Brack et al. 2008].

A common component of the Notch and Wnt signalling pathways is GSK3 β , a positive regulator of the Notch pathway [Guha et al. 2011] and a negative regulator of the Wnt pathway [Ikeda et al. 1998]. Both inhibition of Notch and activation of Wnt are sufficient to inactivate GSK3 β [Brack et al. 2008], providing a mechanistic link between the two pathways. Additionally, Pax7 was recently identified as a downstream target of Notch signalling [Wen et al. 2012]. Consistent with a role for Pax7 in quiescent and proliferating satellite cells/myoblasts but not differentiating myoblasts [Olguin & Olwin 2004; Zammit et al. 2004], NICD over-expression results in upregulation of Pax7, an increased number of Pax7+ cells and impaired muscle regeneration [Wen et al. 2012]. Studies described in Chapter 3 suggest that Pax7 may also be common component of these two pathways. Other downstream targets of Notch signalling include members of the Hes and Hey families of bHLH repressors such as Hes1, Hey1 and HeyL. In quiescent satellite cells, these factors are highly expressed due to induction by Notch. Hes1 and Hey1 can both potentially inhibit function of MyoD via the formation of inactive Hes1/MyoD or Hey1/MyoD heterodimers [Sasai et al. 1992; Sun et al. 2001] or by preventing binding of MyoD to myogenin or Mef2C promoter regions [Buas et al. 2010], thus inhibiting progression of myogenesis. Together, these studies highlight the interplay between the Notch and Wnt pathways and in particular, an important role for this interplay in the transition between cell states (e.g. self-renewal and proliferative expansion vs differentiation) during muscle development or regeneration.

4.1.3 Aims

The specific aims of this chapter were to:

1. Profile expression of Wnt and Notch pathway components and targets in Barx2^{+/+} and Barx2^{-/-} myoblasts using PCR arrays and RNA-Seq
2. Generate a double-transgenic mouse line by intercrossing ins-TOPEGFP reporter mice and Barx2 LacZ knock-in mice
3. Examine regulation of Barx2 expression in myoblasts downstream of canonical Wnt signalling

4.2 Methods

4.2.1 Maintenance of mice

Mice containing the TOPEGFP reporter (on an ICR outbred albino strain background) were obtained from the RIKEN BRC in Japan and housed in physical containment level 2 (PC2) rooms within the Animal House Facility at Flinders Medical Centre. The mice were maintained by heterozygous or homozygous crosses. All breeding including timed matings, notching and weaning of mice, was performed by the Animal House staff. Mice were maintained and used as specified by Flinders University Animal Welfare Committee (AWC) and Institutional Biosafety Committee (IBC) approvals.

4.2.2 Genotyping for GFP

Mice were genotyped by PCR analysis of DNA which was isolated as previously described (Chapter 2, Section 2.14). Based on recommendations from the RIKEN BRC standard protocols, mice were genotyped for the presence of the GFP transgene. Primers for amplification of GFP are listed in Table 4.1.

4.2.3 ChIP in whole muscle

Tibialis anterior (TA), gastrocnemius and tricep muscles were dissected from

euthanized p4, p8, p12 or p16 TOPEGFP homozygous mice, with any visible fat and tendons removed. The muscles were collected in a petri dish containing DMEM + 20% FCS and quickly minced into a slurry using small surgical scissors and a razor blade. The slurry was placed in to a 10 ml tube containing DMEM + 20% FCS with 1% formaldehyde, shaking at room temperature for 30 minutes. Cross-linking was stopped by the addition of 125 mM glycine for 10 minutes at room temperature. The slurry was pelleted by centrifugation at 3,000 x g for 10 minutes at 4°C, supernatant removed and the pellet stored at -80°C until required. Prior to proceeding with the CHIP protocol, the thawed muscle slurry was homogenised using a glass dounce tissue grinder to produce a more homogenous cell suspension. The remainder of the CHIP procedure was performed as previously described for CHIP in cell lines (Chapter 2, Section 2.11).

4.2.4 RNA-Seq and PCR Pathway arrays

All sample preparations for RNA-Seq and PCR Pathway arrays were undertaken by Assistant Professor Helen Makarenkova and Anastasia Gromova from the Department of Cell and Molecular Biology at the Scripps Research Institute in La Jolla, California. For PCR arrays, RNA was prepared from primary myoblast cultures from 4-5 mouse pups (P7) using RNeasyPlus Kit (Qiagen) and then pooled (equal amounts of RNA from each culture) and applied to Qiagen RT² Profiler Mouse Wnt Signaling Targets (PAMM-243A) and Wnt Signaling Pathway (PAMM-043A) arrays. Each sample was run three times for each array, and then analysed using an Applied Biosystems 7300 Real-Time PCR System and SABiosciences online software (Qiagen) to calculate fold-change and P-value. For RNA-Seq, RNA prepared as described above was purified, fragmented and used for first-, then second-strand cDNA synthesis followed

by adenylation of 3' ends. Samples were ligated to unique adapters and subjected to PCR amplification. Libraries were then validated using the 2100 BioAnalyzer (Agilent), normalised and pooled for sequencing. Prepared samples were sequenced on the IlluminaHiSeq 2000 using barcoded multiplexing and either 50 or 100 bp read length. Read alignment and junction mapping was accomplished using TopHat2 v2.0.6 using a 25 bp 5' segment seed for initial mapping followed by differential gene expression analysis using CuffDiff v2.0.2 to map reads to the reference genome annotation, NCBI mouse build 37.2 [Trapnell et al. 2012]. Median sequencing read yield per replicate sample was 38.9M. Data were expressed as fragments per kilobase of exon per million fragments mapped (FPKM). Two replicate libraries were sequenced from the same pooled RNA samples.

4.2.5 RNA analysis of whole muscle

TA muscles were roughly dissected from euthanized P21 Barx2^{+/+} or Barx2^{-/-} mice and stored in RNAlater (Life Technologies) until required. RNA was prepared from whole muscle tissue by using TRIzol (Life Technologies) and grinding the tissue with a plastic pestle. cDNA synthesis was performed as previously described (Chapter 2, Section 2.9). Primers used for gene expression analysis are listed in Table 4.1.

4.2.6 Lentiviral packaging and transduction

The Barx2/pTiger lentivirus (expressing full-length untagged mouse Barx2) was previously constructed by Ms Bianca de Bellis and Ms Thi Diem Tran Nguyen as a way to efficiently over-express Barx2 in both C2C12 and primary myoblasts. Due to observations that the standard viral transduction protocol (overnight incubation of cells with viral supernatant) resulted in considerable death of primary myoblasts, the

transduction protocol was modified, replacing the overnight incubation with a 2 hour ‘spinfection’ step followed by removal of the viral supernatant and replacement with regular growth media. This method reduced toxicity issues whilst still resulting in high transduction efficiency as assessed by imaging expression of GFP/pTiger control virus. Briefly, HEK293T cell were seeded in 6-well plates at 4×10^5 cells/well 24 hours prior to transfection. Cells were transfected with 1.125 μg viral DNA plasmid, 1.875 μg appropriate gag-pol and 1 μg VSV-G combined with 10 μl Lipofectamine 2000 (Invitrogen) and media was replaced after 6 hours. Cells were grown for a further 42 hours before viral supernatant was collected. The supernatant was centrifuged at 1000 rpm to pellet any packaging cells and then diluted 1:1 in target cell media. Polybrene (Sigma) was added to the media at 4 $\mu\text{g}/\text{ml}$ final concentration and spinfection was carried out by spinning plates for 2 hours at 2500 rpm, 30°C to infect target cells. Media was replaced following spinfection and cells grown for a further 48 hours.

4.2.7 Primers

Table 4.1: List of all primers used during this chapter

<u>Name</u>	<u>Sequence</u>
<u>Genotyping</u>	
Barx2 F	ccggctcgggactcaccacagtg
Barx2 R WT	cctacagagcgctacggggctca
Barx2 R Mut	gagcgagtaacaaccgctcggattc
GFP qPCR F	cccgaccacatgaagcagca
GFP qPCR R	tgcgctcctggacgtagc
GFP PCR R	acgaactccagcaggacatg

UGT1A7like F	tctgcttcaagtactccactaacttcttg
UGT1A7like R	aggctgctggtggtgcc
<u>TOEGFP promoter analysis</u>	
TCF ChIP F	cggccagtgcccaagttaagat
TCF ChIP R	ccggatcctctagagtgcg
TCF ChIP F2	atcaaagggggccccct
TCF ChIP F3	ttgatcttactgcatgcctgc
TCF ChIP R2	ccgactgcatctgcgtggt
ChIP GFP F	atggtgagcaagggcgaggag
ChIP GFP R	gtaggtggcatcgccctcg
Chick HS4 Ins 3' F	ggggatacggggaaaaaagc
GFP R ATG	ctcctcgcccttgctcaccat
<u>qRT-PCR</u>	
RPS26 F	aggcgcagaaggctgagg
RPS26 R	ggttctcccagtgatgaag
Axin2 F	gagagtgagcggcagagc
Axin2 R	cggctgactcgttctcct
Barx2 F	agccccctgcactcttgtacc
Barx2 R	ccgcagcggcgactggatg
CyclinD1 F	tctttocagagtcacaaagtgtg
CyclinD1 R	gactccagaagggttcaatc
Id2 F	gacagaaccaggcgtcca
Id2 R	agctcagaaggggaattcagatg
Lef1 F	tcttgaatccccaccttct
Lef1 R	tgggataaacaggctgacct
MMP9 F	gtcatccagtttggtgtcgc
MMP9 R	ccagggaccacaactggtc

Myf5 F	ctgctctgagcccaccag
Myf5 R	gacagggctgttacattcagg
MRF4 F	ggctggatcagcaagagaag
MRF4 R	aatccgcaccctcaagaat
MyoD F	ccgcctgagcaaagtgaatg
MyoD R	gcgggtccagggtgcgtagaa
Myogenin F	ccttgctcagctccctca
Myogenin R	tgggagttgcattcactgg
Pax7 F	accacttggctacagtgtgga
Pax7 R	agtaggcttgtcccgtttcc
Wif1 F	ggcagacactgcaataagagg
Wif1 R	ttaagtgaaggcgtgtgtcg
<u>Chromatin Immunoprecipitation</u>	
Barx2prom CHIP F	aatctgttccctaccaatgtc
Barx2prom CHIP R	ggcgcttaggtgcggggcc
β 2-microglobulin CHIP F	cggagaatgggaagccgaacat
β 2-microglobulin CHIP R	gtgaggcgggtggaactgtgt

4.3 Results

4.3.1 Barx2 regulates known Wnt target genes, and genes within both the Wnt and Notch signalling pathways

In order to profile gene expression of Barx2^{+/+} and Barx2^{-/-} mice, primary myoblasts of each genotype were isolated and mRNA expression of both Wnt targets and Wnt pathway components was assessed using PCR arrays (Qiagen; PAMM243 and PAMM043 respectively) as described in Methods (Section 4.2.4). In Barx2^{-/-} myoblasts, relative to Barx2^{+/+} myoblasts, 26 genes were significantly downregulated

and 12 genes were significantly upregulated by more than 1.5-fold (Table 4.2).

Table 4.2: Wnt target and pathway genes in PCR array

(A) Wnt target genes and (B) Wnt signalling pathway genes showing at least 1.5-fold change in expression in *Barx2*^{-/-} myoblasts relative to *Barx2*^{+/+} myoblasts. Data are the average of three experiments.

A. Wnt target genes (PAMM243)

Gene Symbol	Fold change	p-value
Gdnf	2.14	0.041499
Id2	1.54	0.019162
Mmp9	2.38	0.004672
Smo	1.51	0.004563
Sox2	3.24	0.001648
Wisp1	1.62	0.00089
Wisp2	2.20	0.014496
Ahr	-1.64	0.003976
Axin2	-3.36	0.002601
Cacna2d3	-2.71	0.000173
Ccnd1	-1.61	0.000118
Ccnd2	-2.22	0.000018
Ctgf	-2.28	0.000013
Dlk1	-4.36	0.000003
Fgf7	-2.03	0.00211
Fst	-5.60	0.000003
Fzd7	-1.85	0.000156
Gdf5	-7.05	0.001411
Igf2	-1.85	0.000137
Klf5	-2.07	0.000043
Pdgfra	-1.84	0.000236
Pitx2	-2.22	0.000001
Tgfb3	-2.78	0.000001
Wnt5a	-1.52	0.000092

B. Wnt pathway genes (PAMM043)

Gene Symbol	Fold change	p-value
Fzd4	2.56	0.000026
Fzd6	3.64	0.000595
Sfrp1	2.36	0.001004
Tle2	1.63	0.042534
Wisp1	1.66	0.000382
Ccnd1	-1.73	0.000296
Ccnd2	-1.81	0.000032
Dvl1	-1.67	0.00399
Fzd7	-1.80	0.005092
Nkd1	-1.53	0.010481
Pitx2	-2.01	0.000496
Porcn	-4.15	0.000401
Wif1	-6.96	0.002692
Wnt4	-1.66	0.002231

As shown in Figure 4.2, the majority of Wnt target/pathway genes with significantly different expression ($p < 0.05$) were downregulated in *Barx2*^{-/-} myoblasts compared to *Barx2*^{+/+} myoblasts. RNA-Seq analysis of the same samples was performed (by Dr Ruth Yu; Gene Expression Laboratory, Salk Institute, La Jolla, California) and manually mined for Wnt target and Wnt pathway genes. Comparison of the PCR array and RNA-seq data showed highly concordant results (Figure 4.1). Due to the cross-talk often observed between Wnt and Notch signalling, and its previously mentioned relevance to myogenesis, the RNA-Seq data was further mined for genes involved in the Notch

signalling pathway as well as downstream Notch target genes. Numerous Notch target and pathway genes were upregulated in *Barx2*^{-/-} myoblasts relative to *Barx2*^{+/+} myoblasts. For example, *Notch3*, *Dll1*, *Hes1*, *Hey1*, *Heyl* and *Snai1* all showed at least 1.5-fold higher expression (statistically significant) in *Barx2*^{-/-} myoblasts. A summary of fold-changes of both Wnt and Notch target/pathway genes is shown in Figure 4.1.

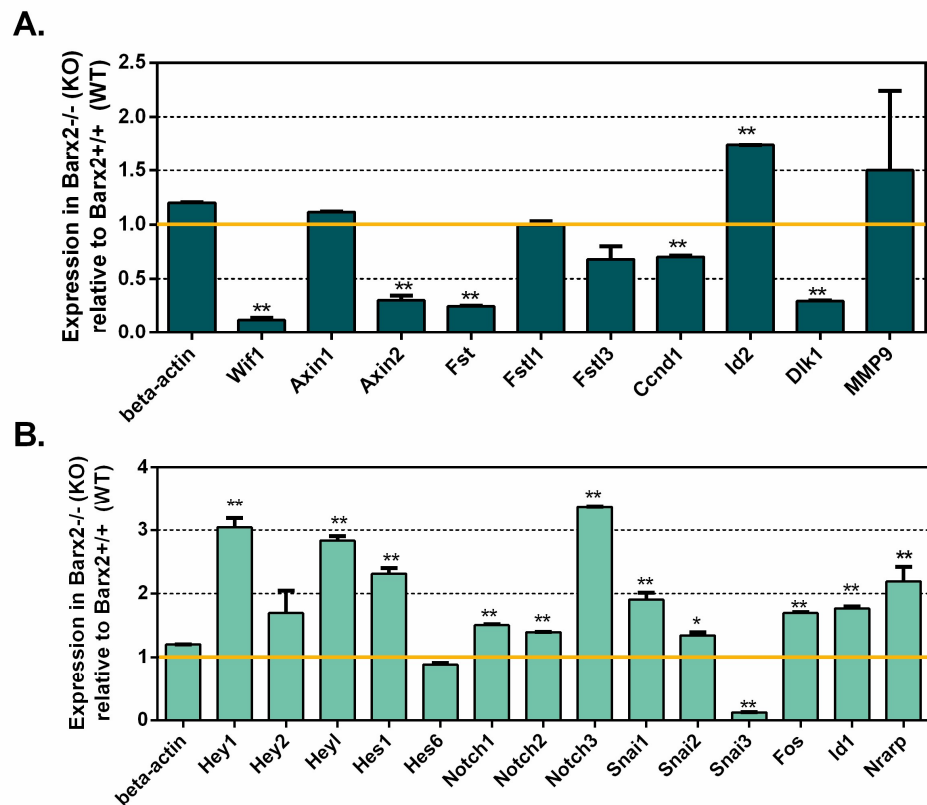


Figure 4.1: A representative set of Wnt and Notch genes from RNA-Seq analysis of *Barx2* wildtype and null myoblasts

Relative expression of a representative set of (A) Wnt and (B) Notch target and pathway genes in *Barx2*^{+/+} and *Barx2*^{-/-} primary myoblasts obtained from RNA-seq analysis. Data are the average of two experiments. Error bars represent SEM. Significant gene expression changes are noted as * $p < 0.05$ and ** $p < 0.001$ relative to *Barx2*^{+/+} myoblasts set arbitrarily to 1 (yellow line). $n=4$.

4.3.2 Analysis of Wnt targets in whole muscle from Barx2 wildtype and null mice

A subset of the Wnt target genes shown by PCR arrays and RNA-seq to be differentially expressed between Barx2^{-/-} and Barx2^{+/+} myoblasts were then assessed *in vivo* by RT-PCR analysis of whole TA muscles from P21 of Barx2^{+/+} and Barx2^{-/-} mice (Figure 4.2). CyclinD1 and Wif1 were lower in Barx2^{-/-} muscle, consistent with their expression in isolated myoblasts as shown in both the PCR arrays and RNA-Seq data. In contrast, MMP9 was higher in Barx2^{+/+} muscle than Barx2^{-/-} muscle, and Axin2 expression was unchanged. Overall, analysis of whole muscles showed a high degree of interindividual variation that was not observed in the myoblast cultures. Of note, littermates showed greater similarity in gene expression than mice from different litters, despite age- and sex-matching. This was particularly evident for expression of Axin2.

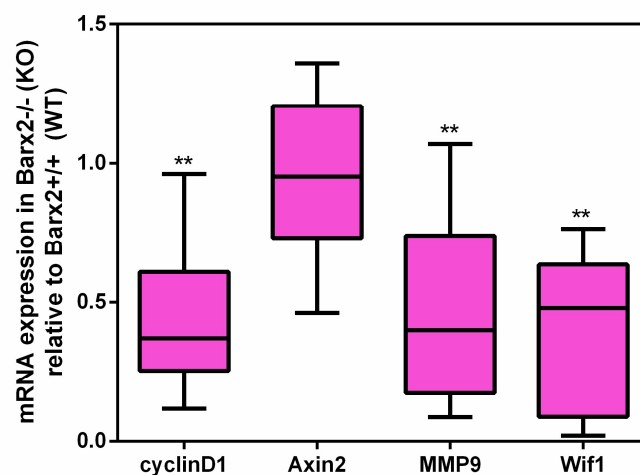


Figure 4.2: Whole muscle gene expression analysis

Expression of Wnt target genes in whole TA muscle from Barx2^{+/+} (n=14) and Barx2^{-/-} (n=15) mice (age P21). To more easily compare data between litters, the expression level in Barx2^{-/-} mice is normalised to a wildtype sibling control in each litter, arbitrarily set to a value of 1. ** p < 0.001 relative to expression in Barx2^{+/+} TA.

4.3.3 Genotyping of TOPEGFP mice: A method for analysis of single-copy versus double-copy GFP allele

Six TOPEGFP mice were purchased from the RIKEN BRC, Japan (3 males and 3 females, all heterozygous for the TOPEGFP reporter). The initial breeding pairs were TOPEGFP^{+/-} x TOPEGFP^{+/-}, with the resulting progeny being either homozygous, heterozygous or wildtype for the TOPEGFP reporter. For analysis of the TOPEGFP line and for cross-breeding with the Barx2 null mouse model, TOPEGFP^{+/+} mice were required, and thus, a method for detecting a single copy vs double copy of the TOPEGFP allele was required. To achieve this, a qPCR method sensitive enough to detect a 2-fold difference in expression was established. GFP amplification was performed using 20 ng of isolated genomic DNA and this was normalised to a control locus, *UGT1A7like*. The ratio between the CT value of GFP and *UGT1A7like* was calculated for each sample and used to determine GFP transgene copy number (homozygous vs heterozygous).

4.3.4 Generation of a Barx2-TOPEGFP mouse line (BAR-TOP)

The Barx2 knock-in LacZ mouse (C57BL/6 strain background) colony established at Flinders University originated from three stock mice that had been relocated from The Scripps Research Institute (2 sibling females and 1 male) and have been consistently inbred to maintain the colony. For this reason it is considered that the Barx2 knock-in LacZ mice are genetically homogenous. To generate the Barx2-TOPEGFP (BAR-TOP) double-transgenic line, first a female (♀) TOPEGFP^{+/+}Barx2^{+/+} (homozygous TOPEGFP) was crossed with a male (♂) TOPEGFP^{-/-}Barx2^{+/+} (wildtype C57BL/6) in order to generate F1 hybrid mice all with the genotype TOPEGFP^{+/-}

Barx2^{+/+}. The progeny were then crossed with C57BL/6 Barx2 knock-in LacZ mice by setting up the following two crosses: ♂ TOPEGFP^{+/+}Barx2^{+/+} x ♀ TOPEGFP^{-/-}Barx2^{-/-} and ♀ TOPEGFP^{+/+}Barx2^{+/+} x ♂ TOPEGFP^{-/-}Barx2^{-/-}. The rationale for the two reciprocal crosses was that we were unsure of how well the Barx2^{-/-} female would breed, because previously we documented that litters from Barx2^{-/-} females were smaller, less frequent, and had poorer survival to weaning, relative to Barx2^{+/+} females. F2 hybrid mice therefore consisted of two potential genotypes: TOPEGFP^{+/+}Barx2^{+/+} or TOPEGFP^{-/-}Barx2^{+/+}. Of these, we selected offspring of the genotype TOPEGFP^{+/+}Barx2^{+/+} to backcross to their parent (TOPEGFP^{-/-}Barx2^{-/-}). We continued to backcross offspring using this method; crossing pups of the genotype TOPEGFP^{+/+}Barx2^{+/+} with the parent of genotype TOPEGFP^{-/-}Barx2^{-/-} until generation F8. Initially, with the early hybrid generations we noticed our double transgenic BAR-TOP mice exhibited hybrid vigour. In particular, the females of genotype Barx2^{-/-} produced larger and more frequent litters than our parent Barx2^{-/-} mice in the C57BL/6 background. TOPEGFP mice were albino and Barx2 LacZ knock-in C57BL/6 mice were black; by generation F4 all BAR-TOP mice had black fur like the parent Barx2 LacZ knock-in C57BL/6 mice. At hybrid generation F8 we changed to sibling-sibling inbreeding. Sibling-sibling crosses initially consisted of TOPEGFP^{+/+}Barx2^{+/+} x TOPEGFP^{+/+}Barx2^{+/+}. Later, two separate lines were generated and maintained: one carrying two copies of the EGFP transgene (TOPEGFP^{+/+}Barx2^{+/+} x TOPEGFP^{+/+}Barx2^{+/+}) and one carrying no copies of the EGFP transgene (TOPEGFP^{-/-}Barx2^{+/+} x TOPEGFP^{-/-}Barx2^{+/+}), the latter presumed to be genetically identical to the original colony of Barx2 LacZ knock-in C57BL/6 mice. These two lines would therefore generate pups of either TOPEGFP^{+/+} or TOPEGFP^{-/-} which are wildtype, heterozygous or null for Barx2. The breeding and generation

method of the double transgenic BAR-TOP mouse line is summarised in Figure 4.3.

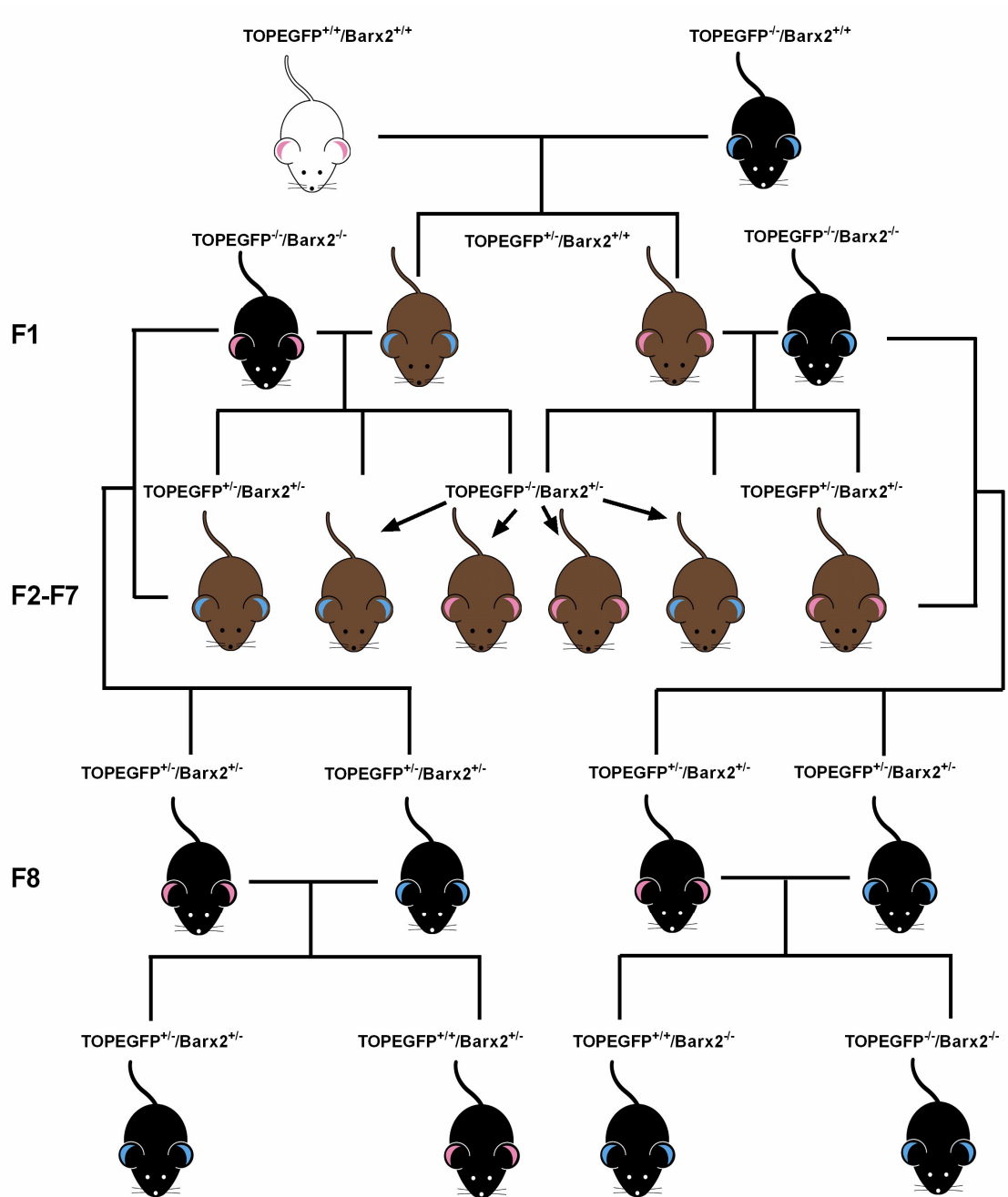


Figure 4.3: Generation of the BAR-TOP double-transgenic mouse model

A simplified schematic outlining the generation of the double transgenic BAR-TOP mouse line. Pink ears – female; blue ears – male; white mouse – original TOPEGP strain; black mice – C57BL/6 strain; brown mice – mixed strain during back-crossing process.

4.3.5 Initial phenotypic analysis of BAR-TOP transgenic model

After the BAR-TOP transgenic line was generated, we assessed how phenotypically similar they were to the original Barx2 LacZ knock-in C57BL/6 mice. Male BAR-TOP pups post F4 generation were genotyped for the Barx2 allele and weighed at weaning (P21). Analysis of the total body weights showed that Barx2^{-/-} mice were consistently 20-25% smaller than their heterozygous and wildtype littermates (Figure 4.4). This was consistent with previous published reports of the Barx2 LacZ knock-in C57BL/6 strain [Meech et al. 2012] and suggested that the initial hybrid vigour effect was lost by generation F4.

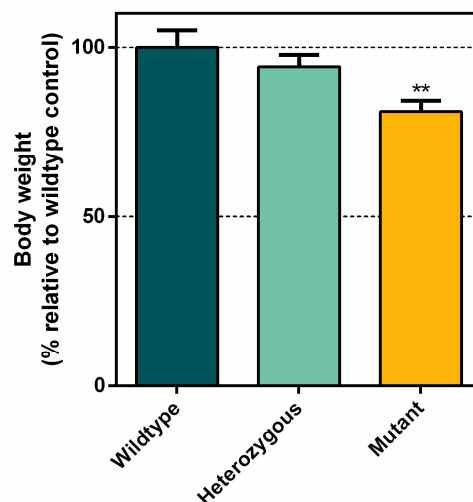


Figure 4.4: Analysis of total body weight of male BAR-TOP pups at P21

BAR-TOP pups were weighed at P21. Data are relative to wildtype (Barx2^{+/+}) mice, set to 100%. Error bars represent SEM. ** p < 0.001 relative to wildtype. n=10 for wildtype, 20 for heterozygous (Barx2^{+/-}) and 19 for mutant (Barx2^{-/-}).

4.3.6 Ins-TOPEGFP mice are found to be TP1-Venus, a transgenic Notch reporter mouse strain

Following successful ChIP analysis of β -catenin, Barx2 and MyoD recruitment to the

integrated Topflash promoter in C2C12 cells (Chapter 3, Section 3.3.8), one of the planned uses of the TOPEGFP^{+/+} mice was to examine the binding of endogenous transcription factors to the TOPEGFP transgene *in vivo*. To select the best time point at which to study Barx2 binding to the TOPEGFP transgene promoter, the level of Barx2 expression was profiled in postnatal muscle. RNA was isolated from whole muscles (TA, gastrocnemius and tricep muscles) from TOPEGFP^{+/+} mice at P4, P8, P12 and P16 so that the Barx2 mRNA expression level could be quantified. RNA from vibrissae pads from P8 pups was isolated as a positive control as this is a site of known high Barx2 expression. Barx2 mRNA was expressed highly in muscle at all timepoints and there was less than 2-fold difference in expression between P16 and P8 mice as shown in Figure 4.5.

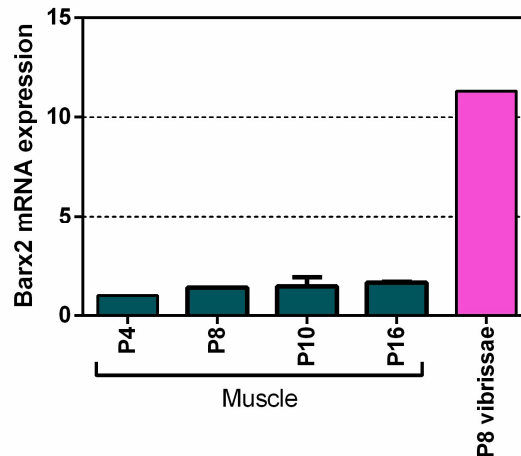


Figure 4.5: Barx2 mRNA expression in whole muscle

Tibialis anterior, gastrocnemius and tricep muscles were dissected from TOPEGFP^{+/+} mice and total RNA was isolated. Expression of Barx2 mRNA is relative to P4, set arbitrarily to a value of 1. The results shown are from a single mouse at each timepoint.

Muscle tissue was combined from a total of four individual mice (two P12 and two P16) and crosslinked with formaldehyde in order to prepare chromatin for ChIP

analysis. ChIP was performed using antibodies to Barx2 under the same optimised conditions that were used for Barx2 ChIP in the stable TOPPuro C2C12 cell line (Chapter 3, Section 3.3.8). Analysis of enrichment of the TOPEGFP promoter in the Barx2 ChIP-isolated DNA used qPCR amplification with the same primers that had been designed to amplify the synthetic TOPflash promoter in the TopPuro stable line. However, whilst amplification of the control genomic locus (β 2-microglobulin) was successful in all IP conditions, amplification of the TOPEGFP promoter region was unsuccessful, even from the input genomic DNA control sample. To try to understand why the amplification of the promoter was unsuccessful, further information about the transgene was obtained by directly contacting the originator Dr Isao Kii [Moriyama et al. 2007]. Dr Kii confirmed that the transgene was constructed from the TOPflash plasmid (Upstate Biotechnology, previously Millipore, cat# 21-170) by replacing the Firefly luciferase gene with EGFP, and insertion of flanking insulator sequences derived from the chicken β -globin HS4 insulator element. This information suggested that the primers previously used should have been effective for amplification. Regardless, more primers were designed based on the TOPflash plasmid sequence (Table 4.1 - TCF ChIP F, R, F2, F3 and R2) spanning the TCF/LEF consensus regions upstream of EGFP and a further attempt was made to amplify the TOPEGFP transgene from genomic DNA, again with no success. Next, an attempt was made to amplify a fragment of the transgene spanning from the upstream insulator element [Chung et al. 1997; Recillas-Targa et al. 2002] to the downstream EGFP gene (hence containing the TOPflash promoter region) using a series of HS4 insulator forward primers and GFP reverse primers. Only one primer combination (chick HS4 Ins 3' F and ChIP GFP R; listed in Table 4.1) amplified the locus as assessed by gel

mouse line obtained from the RIKEN BRC did not contain the Wnt signalling reporter TOPEGFP, but in fact contained a Notch signalling reporter. Our analysis of the literature suggested that this reporter was analogous to that previously reported in the mouse transgenic line called TP1-Venus. This finding was submitted to the RIKEN BRC (Appendix 3) who in turn informed the depositor of the strain and as a direct result, an investigation into the apparent strain substitution was launched. The outcome of this investigation was that the error was found to be the responsibility of the depositor, and that the RIKEN BRC had been maintaining and distributing a mislabelled mouse strain for up to 5 years. The RIKEN subsequently informed all laboratories that had purchased this strain that they had been distributing a strain carrying a transgene described as the Wnt reporter TOPEGFP when it was in fact the Notch reporter TP1-Venus. Refunds on purchase and shipping costs were offered (Appendix 3), however, as per their distribution agreement, they accepted no further liability for the impact of the mislabelling on individual research projects.

While a valuable outcome of the work described above was the service to the research community by informing all other users of the RIKEN TOPEGFP mouse of the true identity of the transgene, the outcome was clearly deleterious to this project. In particular, after 2 years of back-crossing the BAR-TOP double-transgenic mouse line, it could not be used as originally planned to study Barx2-mediated Wnt signalling *in vivo*. However, because my work had uncovered a role for Barx2 in modulating Notch signalling, a decision was made to keep the new transgenic line (which we re-designated BAR-TP1) but not the original TP1-Venus parent line. Moreover, because the BAR-TP1 mice had been highly back-crossed to the original Barx2-LacZ knockin

strain and were phenotypically indistinguishable from that strain, they continued to be used to study loss of Barx2 function *in vivo* and in primary myoblast culture assays that were not dependent on the presence of the TP1 reporter transgene.

4.3.7 Canonical Wnt signalling promotes differentiation of myoblasts and expression of Barx2

It has been previously shown that Barx2 is upregulated at the onset of myoblast differentiation and promotes early differentiation events [Makarenkova et al. 2009]. Pax7, on the other hand, is downregulated at the onset of differentiation and forced expression of Pax7 delays differentiation [Zammit et al. 2006]. Furthermore, as discussed in Chapter 3 and above, Barx2 appears to function downstream of a Wnt signal to regulate transcription of a Wnt reporter and potentially other endogenous Wnt target genes through functional interaction with β -catenin and TCF/LEF, whilst Pax7 blocks and abolishes this activation. With this in mind, the question was asked whether Barx2 and Pax7 are themselves targets of canonical Wnts, thus providing a regulatory loop. As various Wnt ligands have been reported to influence either proliferation or differentiation of myoblasts [Otto et al. 2008; Bernardi et al. 2011; Tanaka et al. 2011], the effect of Wnt3a, a canonical Wnt ligand, was first examined on myoblast cultures. As shown in Figure 4.7, C2C12 cells treated with Wnt3a CM at a 1:2 dilution for a total of 72 hours showed an increased rate of differentiation as assessed by the number of elongated and fused cells (data not shown) and by measuring changes in cell confluence over time post-Wnt treatment. Cell confluence was assessed by the Incucyte-FLR real time cell monitoring system (Essen) and is plotted in Figure 4.7. The time point at which the increase in cell confluence begins to slow correlates with the beginning stages of differentiation. Decreasing

concentrations of Wnt3a CM resulted in diminishing effects on differentiation (Figure 4.7). This effect of Wnt3a CM on C2C12 cells is consistent with data produced previously in isolated primary myoblasts [Zhuang et al. 2014].

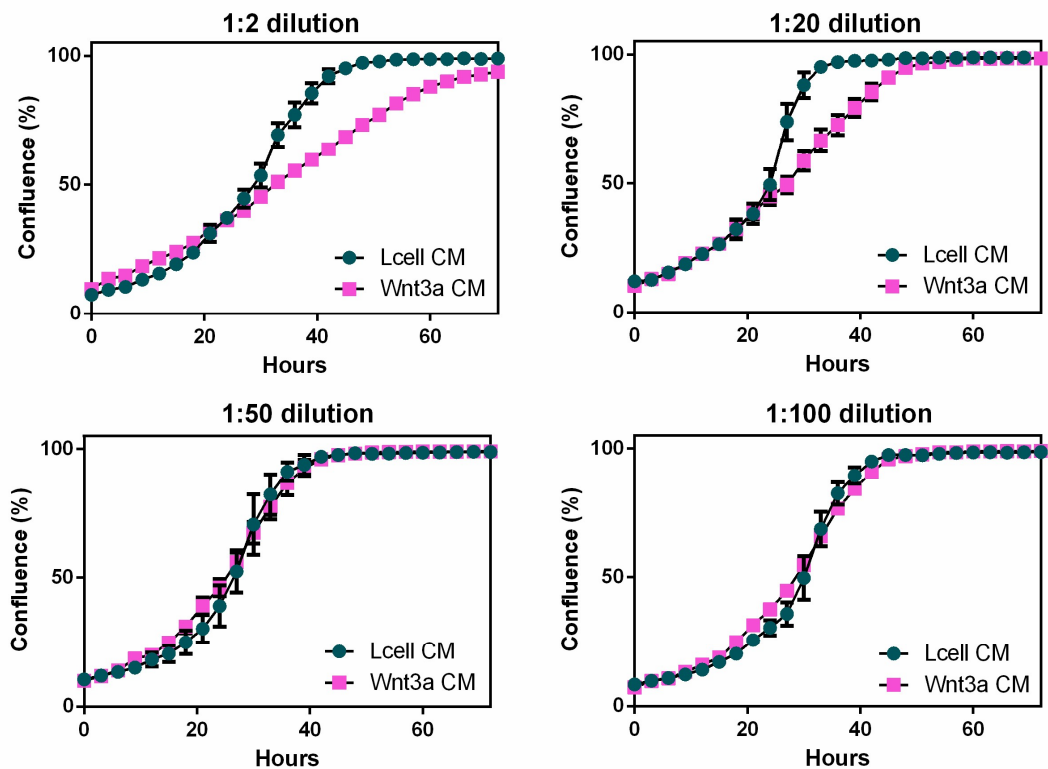


Figure 4.7: The canonical Wnt3a promotes differentiation of C2C12 myoblasts

C2C12 cells were treated with control Lcell CM or decreasing concentrations of Wnt3a CM for 72 hours. Cell confluence was assessed using the Incucyte (Essen) every 3 hours. The results shown are a representative experiment performed in triplicate. Error bars represent SEM.

The level of Barx2 mRNA was assessed in the same Wnt3a-treated C2C12 cells, yet even at the highest concentration of Wnt3a CM, no increase in Barx2 mRNA was observed (not shown). In contrast, when primary myoblasts from Barx2^{+/+} mice were cultured and treated with Wnt3a CM for 48 hours, the level of Barx2 mRNA was significantly increased approximately 28-fold relative to control treatment (Figure 4.8A). Expression of a known Wnt target gene, Axin2, was also significantly increased

following 48 hours of Wnt3a CM (Figure 4.8B). In contrast, mRNA expression of Pax7 showed a modest (<2-fold) but significant reduction following Wnt3a CM treatment (Figure 4.8C).

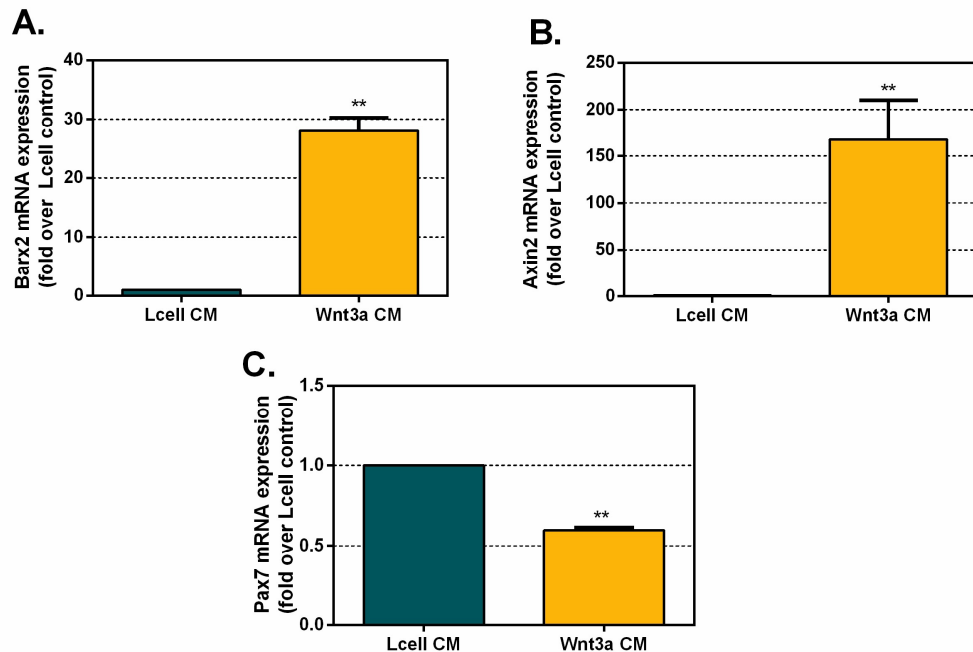


Figure 4.8: mRNA expression of primary myoblasts following 48 hours Wnt3a stimulation

Primary myoblasts from TOPEGFP mice were treated with Lcell conditioned media (CM) or Wnt3a CM diluted 1:2 in growth media for 48 hours. Expression of (A) Barx2 (B) Axin2 or (C) Pax7 mRNA was measured relative to housekeeping RPS26 mRNA. The results shown are the average of at least two independent experiments performed in duplicate. Error bars represent SEM. ** $p < 0.001$ relative to control L-cell CM condition.

In a very preliminary experiment, cultured primary fibroblasts were isolated from Barx2^{+/+} mouse muscle and treated with Wnt3a CM for 48 hours. Axin2 mRNA expression was robustly increased, but there was no change in Barx2 expression (Figure 4.9). This suggests that induction of the Barx2 mRNA by Wnt3a is myoblast specific. However, whilst this was a robust result and an interesting finding, it would be important to replicate this experiment for future work before drawing any conclusions.

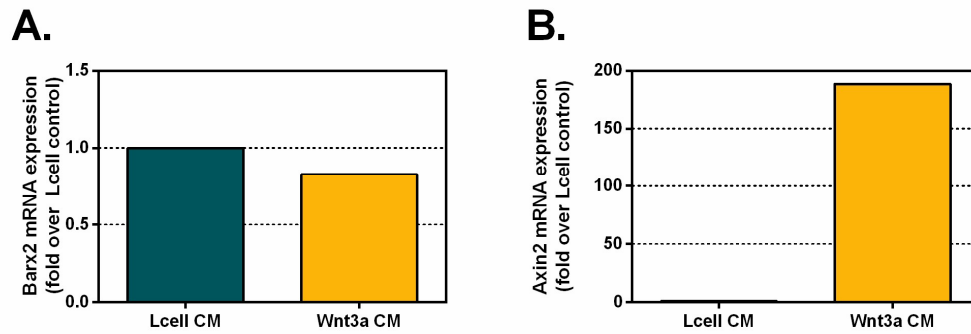


Figure 4.9: mRNA expression of fibroblasts following 48 hours Wnt3a stimulation

Isolated primary fibroblasts were treated with Lcell or Wnt3a CM diluted 1:2 in growth media for 48 hours. Expression of (A) Barx2 or (B) Axin2 mRNA was quantified. The results shown were only performed once as a preliminary experiment. n=1.

4.3.8 Wnt3a-mediated regulation of Barx2 expression is indirect and does not involve MyoD binding to the proximal promoter

A detailed analysis of Barx2 mRNA expression in primary myoblasts over a time-course from 12 to 48 hours of Wnt3a treatment revealed no significant change in the level of Barx2 mRNA following 12 hours of Wnt3a stimulation, but an increase of 14-fold at 24 hours post-treatment. This increase continued to rise to 25-fold by 48 hours of treatment. By comparison, expression of Axin2, a direct target of canonical Wnt signalling [Jho et al. 2002], was robustly induced by 12 hours post-Wnt3a stimulation (94-fold) and was maintained at that level over 48 hours of continuous Wnt3a stimulation (Figure 4.10A). A Wnt-pulse experiment, whereby myoblasts were stimulated with Wnt3a CM for 12 hours followed by removal of the CM and incubation with regular DMEM for a further 36 hours, revealed that the level of Barx2 mRNA continued to rise following removal of the Wnt3a, although it did not reach the same level as with 48 hours of continuous Wnt3a stimulation (2-fold at 24 hours,

8-fold at 48 hours). In comparison, the mRNA levels of Axin2, which were rapidly induced by Wnt3a, dropped dramatically back to baseline after removal of the Wnt3a (equivalent to the control condition at the same time point) (Figure 4.10A). Treatment of the myoblasts with cycloheximide (CHX), an inhibitor of protein synthesis or actinomycin D, an inhibitor of mRNA transcription (Figure 4.10B) following the initial 12 hour Wnt3a pulse revealed that transcription and translation of intermediate factors was required for induction of Barx2 mRNA. In the presence of either CHX or actinomycin D, expression of Barx2 mRNA did not continue to increase following the initial Wnt3a pulse, instead remaining at baseline. It was therefore unlikely that induction of Barx2 mRNA by Wnt3a was due to stabilisation of β -catenin alone and more likely involved additional factors that were induced by Wnt3a.

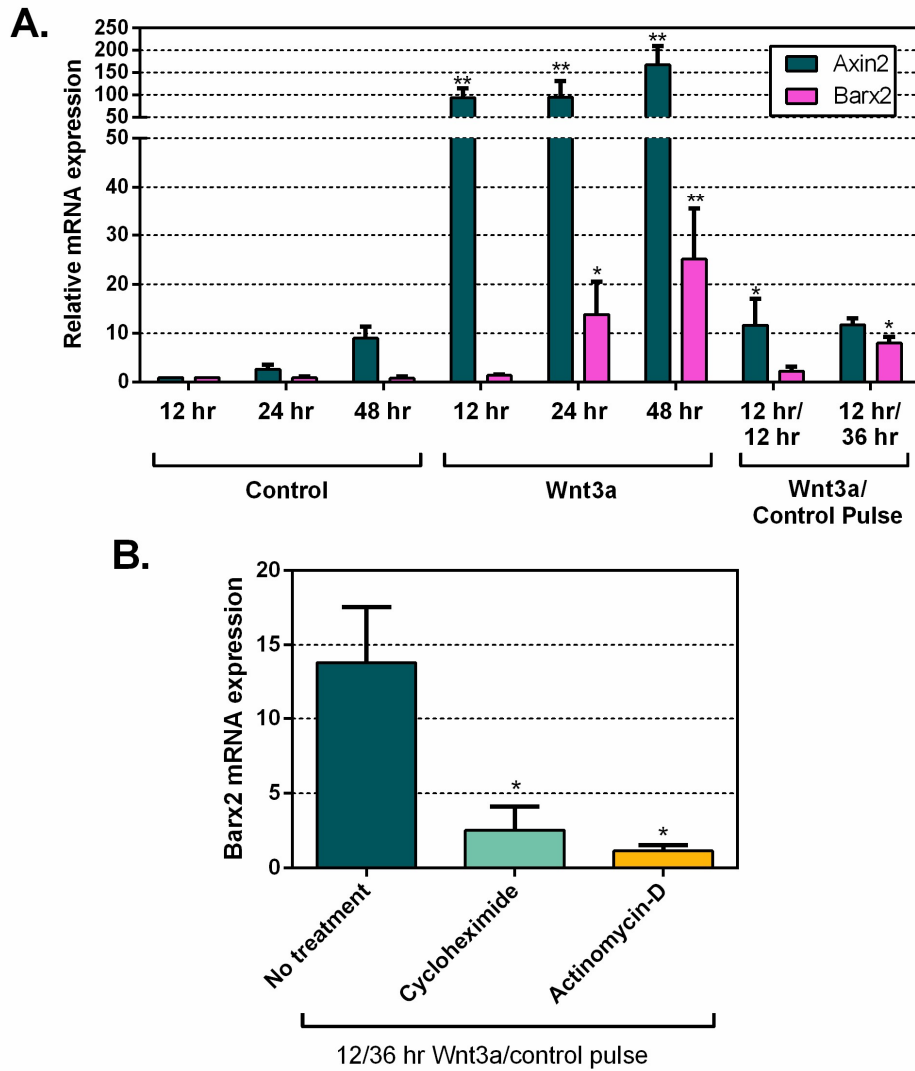


Figure 4.10: Indirect Barx2 mRNA induction by Wnt3a

(A): Primary myoblasts were treated with Lcell or Wnt3a CM at a dilution of 1:2 in growth media for the timepoints indicated. mRNA expression of Axin2 and Barx2 was quantified relative to housekeeping RPS26 mRNA. Data are normalised to the 12 hour control treatment (set to 1). (B): Barx2 mRNA was quantified relative to housekeeping RPS26 mRNA in primary myoblasts treated with a 12 hour Wnt3a pulse followed by the addition of cycloheximide or actinomycin-D. Data are normalised to vehicle control treatment (set to 1). The results shown are the average of two independent experiments performed in duplicate. Error bars represent SEM. * $p < 0.05$ and ** $p < 0.001$ relative to control treatment at the same timepoint. $n=4$.

Previous studies on the regulation of Barx2 have indicated that Barx2 expression is induced by MyoD via E-box binding motifs within the Barx2 proximal promoter [Meech et al. 2003]. Furthermore, there is existing evidence that MyoD is a

downstream target of canonical Wnt signalling [Tajbakhsh et al. 1998] and that β -catenin interacts with MyoD, enhancing transcriptional activation of genes containing E-box elements within their promoters [Kim et al. 2008]. To assess whether MyoD may be the intermediate factor required for Wnt3a-mediated Barx2 induction, MyoD mRNA expression was assessed following 48 hours of Wnt3a stimulation of primary myoblasts. As shown in Figure 4.11A, no change in MyoD mRNA levels was observed following treatment with Wnt3a CM. MyoD recruitment to the Barx2 proximal promoter might be increased after Wnt3a treatment even if overall MyoD levels are not increased. Hence, ChIP was performed with MyoD antibodies following 48 hours of Wnt3a stimulation and enrichment of the Barx2 proximal promoter (containing E-box elements previously shown to respond to MyoD) was tested by qPCR. These experiments showed no increase in recruitment of MyoD to the Barx2 proximal promoter in Wnt3a-treated cells relative to control treated cells (Figure 4.11B). It remains formally possible, however, that Wnt3a treatment affects recruitment of MyoD to other more distal sites in the Barx2 locus.

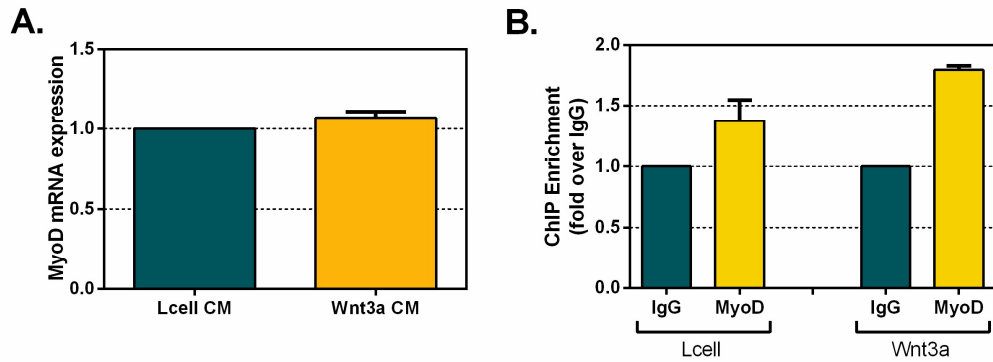


Figure 4.11: MyoD is not induced or recruited to the Barx2 proximal promoter following treatment with Wnt3a

(A): Primary myoblasts were treated with Lcell or Wnt3a CM at a dilution of 1:2 in growth media for 48 hours. mRNA expression of MyoD was quantified relative to housekeeping RPS26 mRNA. Data are normalised to the Lcell control condition (set to 1). (B): ChIP was performed on chromatin from primary myoblasts following treatment with a 1:2 dilution Lcell or Wnt3a CM for 48 hours. ChIP was performed with 2 μ g of the indicated antibodies. Data are PCR amplification values for the Barx2 proximal promoter normalised to amplification values for a control non-target locus (β 2-microglobulin), with enrichment values subsequently normalised to the mock ChIP with preimmune IgG, set to a value of 1. The results shown are representative experiments performed in duplicate. Error bars represent SEM. * $p < 0.05$ and ** $p < 0.001$ relative to control treatment (A) or IgG (B). $n=2$.

As further support for an indirect mechanism of regulation, a series of Barx2 promoter-luciferase constructs (obtained from Dr Robyn Meech) spanning 3 kb upstream of the transcription start site [Meech et al. 2003] were tested for activity in response to Wnt3a treatment. In addition to the multiple E-box consensus sites mentioned above, this promoter region contains a single TCF/LEF consensus motif. The Barx2 promoter constructs were transfected in to C2C12 cells and treated with either Lcell or Wnt3a CM. Additionally, the promoter constructs were co-transfected with ca. β -catenin or empty control vector. As shown in Figure 4.12, co-transfection of the promoter constructs with ca. β -catenin or treatment of transfected cells with Wnt3a CM was insufficient to induce the activity of the promoter-luciferase constructs above basal levels.

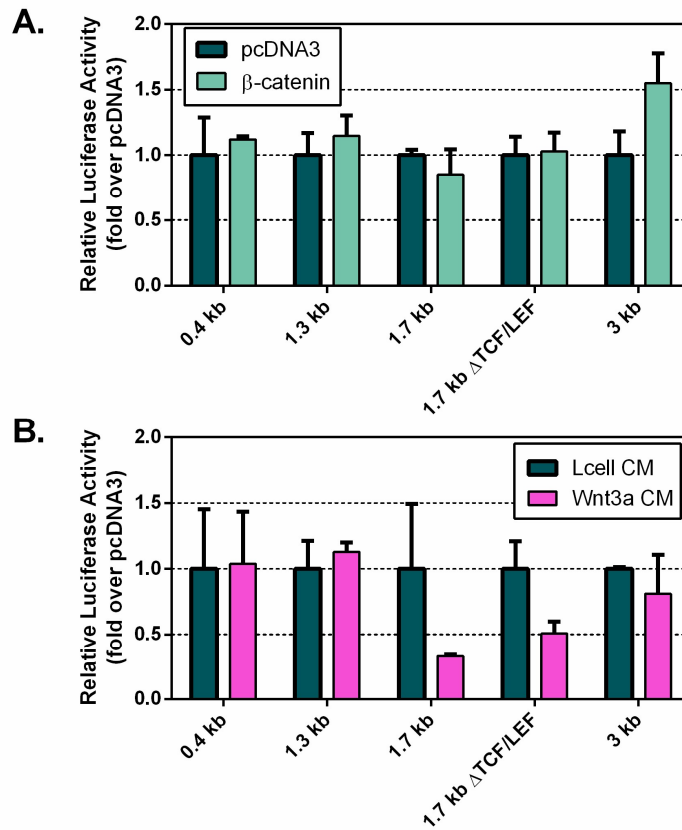


Figure 4.12: The proximal Barx2 promoter is not activated by β -catenin/Wnt signalling

Barx2 promoter constructs (0.5 μ g) were transfected into C2C12 myoblasts. In addition cells were also transfected with either pcDNA3 empty vector or β -catenin (A) or treated with a 1:2 dilution of either Lcell or Wnt3a conditioned media (B). Luciferase activity was assayed 48 hours post transfection. All data are normalised to a Renilla luciferase internal control, expressed as the mean firefly/Renilla luciferase ratio. Data were then normalised to the promoterless pGL3-basic vector, and then to pcDNA3 transfection or Lcell treatment (set to a value of 1). The results shown are single experiments performed in duplicate. Error bars represent SEM. n=2.

4.3.9 Barx2 protein may be regulated proteolytically in primary myoblasts

To assess whether the aforementioned upregulation of Barx2 mRNA in Wnt3a-stimulated primary myoblasts translated to an increase in protein expression, endogenous Barx2 was quantified by fluorescence immunostaining. An increase in Barx2 protein was observed after 48 hours of continuous Wnt3a treatment by fluorescence immunostaining for Barx2 (Figure 4.13A); however the average level of

induction was much lower than that of the mRNA. On average, cells that were treated with Wnt3a CM had a 2-fold increase in Barx2 protein (Figure 4.13B). However, the intensity of Barx2 immunostaining varied, with some cells showing large increases in Barx2-immunofluorescence and some showing no apparent increase (Figure 4.13C). This observation prompted further examination of post-transcriptional or post-translational regulation of Barx2 levels which might involve cell autonomous mechanisms.

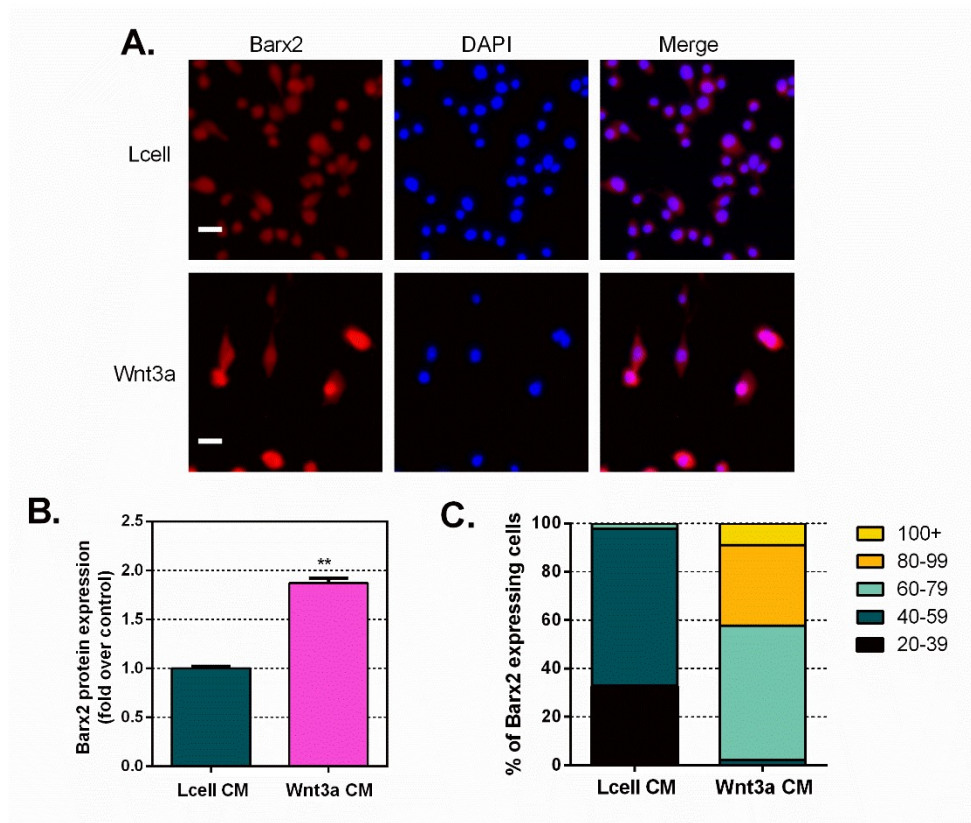


Figure 4.13: Stimulation by Wnt3a induces Barx2 protein expression in primary myoblasts

(A): Primary myoblasts treated with a 1:2 dilution of Lcell or Wnt3a CM for 48 hours were fixed, immunostained for Barx2 (red) and DAPI (blue) and imaged with an Olympus IX71 microscope. A representative image is shown. Scale bar represents 25 μ M. (B): Quantification of mean fluorescence of Barx2 in Wnt3a CM condition relative to Lcell CM. (C): Barx2 expression on a cell-by-cell basis, gated using raw fluorescence counts quantified by ImageJ. Two independent experiments were performed but representative images and quantification from a single experiment are shown; n=45 individual cells quantified per condition. Error bars represent SEM. ** p < 0.001.

Due to the difficulty of transfecting primary myoblasts with standard transfection reagents, our laboratory uses lentiviral constructs to introduce transgenes into myoblasts. In this study, the expression of Barx2 protein at a single cell level was examined by immunostaining for Barx2 following transduction with a Barx2 lentivirus. In comparison to transduction with a GFP lentiviral construct (which showed close to 100% transduction efficiency based on counting GFP-positive cells), very few cells transduced with the Barx2 lentivirus expressed the Barx2 protein at detectable levels. This could have been related to variation in the packaging and transduction efficiencies of the Barx2 and GFP lentiviral constructs. However, when the level of Barx2 mRNA and GFP mRNA was measured in the Barx2 and GFP lentivirus transduced cell populations respectively, it was found to be equivalent. Furthermore, immunostaining for Barx2 in non-myogenic HEK293T cells transduced with Barx2 lentivirus revealed that close to 100% of cells expressed Barx2 protein (not shown), and transfection of non-myogenic COS7 cells with Barx2 plasmids produced high expression of Barx2 protein as determined by western blotting (Chapter 3, Section 3.3.6). Together these data suggested that translation and/or accumulation of heterologously (virally) expressed Barx2 protein might be *specifically inhibited in myoblasts*. The possibility that Barx2 protein might be rapidly turned over by proteolysis in myoblasts was tested by inhibition of the proteasome. Approximately 36 hours post Barx2 transduction, the proteasome inhibitor MG312 was applied to the cells for 8 hours and then cells were fixed and immunostained for Barx2 protein. A dramatic increase in both the number of cells expressing Barx2 protein and the level of expression per cell (Figure 4.14) was observed, suggesting that indeed Barx2 is regulated by proteosomal turnover. I next examined whether Wnt3a also affected

Barx2 protein stability. In cells transduced with the Barx2 lentivirus and treated with Wnt3a for 24 hours, there was an average of 2-fold increase in Barx2 protein levels per cell (Figure 4.14). In untransduced cells there was no elevation of endogenous Barx2 protein after only 24 hours of Wnt3a treatment. This suggests that the increase in Barx2 protein in Wnt3a-treated, lentivirally transduced cells is due to stabilization of the heterologously-produced protein rather than induction of the endogenous gene.

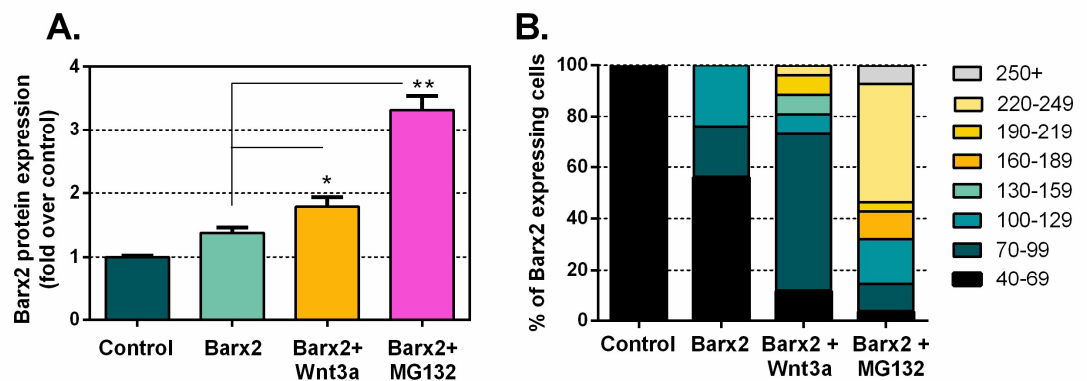


Figure 4.14: Barx2 protein is regulated proteolytically in primary myoblasts

Primary myoblasts were transduced with Barx2 lentivirus, treated with a 1:2 dilution of Wnt3a CM for 24 hours, and/or treated with the proteasome inhibitor MG132 for 8 hours. (A): Quantification of mean fluorescence of Barx2 relative to control untreated condition. (B): Barx2 expression on a cell-by-cell basis, gated using raw fluorescence counts quantified by ImageJ. Two independent experiments were performed but quantification from a single experiment is shown. Error bars represent SEM. ** $p < 0.05$ and $p < 0.001$.

4.4 Discussion

One goal of the studies summarized in this chapter was to generate a double transgenic (in fact transgenic/knockout) Barx2/TOPEGFP mouse line which would facilitate analysis of canonical Wnt signalling in the context of loss of Barx2 expression *in vivo*. Generation of this new double transgenic line involved back-crossing to the

parent Barx2 LacZ knockin C57BL/6 strain for several generations so as to minimise effects of strain background on gene expression. It was originally envisaged that these double transgenic mice would be used in the final year of this project for various experiments including: comparing the expression patterns of the Barx2-LacZ transgene and the TOPEGFP transgene, and analysing the expression of the TOPEGFP transgene in Barx2^{+/+} and Barx2^{-/-} mice during muscle development and regeneration and after intramuscular Wnt injection. The TOPEGFP transgene was also to be used as a positive control in the development of ChIP protocols to assess binding of various transcription factors, including Barx2, to Wnt target genes in whole muscle or primary myoblasts. However, a pilot ChIP experiment performed in the second year of the project using whole muscle from the TOPEGFP^{+/+} mice suggested that the sequence of the TOPEGFP transgene was not as reported. Isolation and sequencing of the transgene promoter region ultimately showed that the promoter contained 12 RBP-Jk binding elements consistent with a Notch reporter transgene, and indicative of a strain substitution. Although many of the proposed studies employing these mice could no longer be carried out, the decision was made to continue breeding the double-transgenic line. This was because other work described in this chapter highlighted the role of Barx2 in regulating not only components of the Wnt signalling pathway, but also components and targets of the Notch signalling pathway. Thus, the Notch reporter mouse is still a useful model and the role of Barx2 in regulation of the Notch pathway *in vivo* could be assessed in the future. Additionally, the requirement for an *in vivo* TOPEGFP reporter as a model to study the role of Barx2 in regulating Wnt target genes became less critical because endogenous targets of Barx2 and Wnt signalling were subsequently identified and characterised (as discussed in later

chapters). These endogenous targets can be analysed both *in vitro* and *in vivo*, and might provide better models for the effect of Barx2 on canonical Wnt signalling.

Barx2 null mice show defective muscle growth and repair [Makarenkova & Meech 2012; Meech et al. 2012]. Gene expression analysis of myoblasts isolated from Barx2^{+/+} and Barx2^{-/-} mice using both PCR arrays and RNA-Seq revealed misregulation of not only Wnt pathway components and target genes, but also many targets and components of the Notch signalling pathway. Many genes misregulated in Barx2^{-/-} myoblasts within these two pathways have known roles in myogenesis that could underlie aspects of the delayed Barx2^{-/-} muscle growth and repair phenotype. For example, Dlk1, which is both a Wnt target gene and a Notch ligand, shows approximately 4-fold lower expression in Barx2^{-/-} myoblasts when compared to Barx2^{+/+} myoblasts. Dlk1 is a negative regulator of Notch signalling [Baladron et al. 2005], controls postnatal muscle growth [Fleming-Waddell et al. 2009] and its ablation in the myogenic lineage results in postnatal growth retardation, reduced body and muscle weight, and impaired regeneration [Waddell et al. 2010]; a phenotype that resembles that of Barx2 null mice. Similarly, Follistatin (Fst) is another Wnt target gene that is critical for both muscle growth and regeneration [Amthor et al. 2004; Benabdallah et al. 2008; Gilson et al. 2009; Hiroki et al. 2011; Zhu et al. 2011] and its expression was 6-fold less and 4-fold less in Barx2^{-/-} myoblasts as determined by PCR array analysis and RNA-Seq respectively. Notch3, which was elevated in Barx2^{-/-} myoblasts, is suggested to be an inhibitor of satellite cell proliferation and self-renewal via inhibition of Notch1 [Kitamoto & Hanaoka 2010]. Notch pathway target gene Snail1, which was also elevated in Barx2 null myoblasts, has been reported to

inhibit binding of MyoD to target genes and thus inhibit the progression of myogenesis [Soleimani et al. 2012]. Overall, the spectrum of misregulated genes in *Barx2*^{-/-} myoblasts is consistent with their reduced differentiation in culture and the reduced capacity of *Barx2*^{-/-} mice to grow, maintain and repair muscle [Meech et al. 2012]; although further work is required to assess the contribution of each of these genes to the null phenotype.

Although the expression of many Wnt and Notch target genes were significantly altered in *Barx2*^{-/-} cultured myoblasts, only a subset of genes were altered in whole TA muscle isolated from P21 mice. This may relate to the fact that *Barx2* is only expressed in muscle progenitors and not the myofibres that make up the bulk of the muscle tissue. Consistent with this idea, *cyclinD1*, like *Barx2*, is primarily expressed in proliferating myoblasts and *cyclinD1* was consistently downregulated in *Barx2* null muscle. Although not necessarily a direct target of Wnt signalling, Wnt inhibitory factor 1 (*Wif1*) plays an important negative feedback role by acting as an antagonist of the Wnt signalling pathway through binding to Wnt proteins [Hsieh et al. 1999; Xu et al. 2011]. In both *Barx2*^{-/-} myoblasts and TA muscle, *Wif1* expression was significantly decreased (6-10 fold), perhaps indicating broader dysregulation of the Wnt signalling pathway, and in particular its negative feedback. Variability of gene expression in P21 muscle may also reflect the heterogeneity of developmental states of muscle progenitor cells *in vivo*, relative to in culture. In the latter they are deprived of the complex regulatory signals present in muscle and provided largely pro-proliferative signals (bovine serum and bFGF). As an example, *Axin2* mRNA has a short half-life [Hughes & Brady 2005] and shows ultradian oscillations in somitogenesis

[Jensen et al. 2010]. Similar oscillations may occur during muscle growth as progenitors are repeatedly activated and progress through proliferation and differentiation phases, and it is unlikely that all parts of the muscle are synchronous in these waves. Thus, although Axin2 expression showed very high variance in whole muscle, with no consistent pattern of reduction in Barx2^{-/-} muscle, a significant reduction in Axin2 mRNA was seen in cultured Barx2^{-/-} cells and studies presented in subsequent chapters confirm that it is a downstream target of Barx2. Consistent with data presented in the previous chapter, Pax7 is known to be a direct target of Notch signalling and may promote myoblast proliferation and inhibit differentiation downstream of Notch signals [Wen et al. 2012]. It has previously been postulated that a temporal switch from Notch to Wnt signalling may control the switch from myoblast proliferation to differentiation [Brack et al. 2008]. Thus, the functional antagonism between Barx2 and Pax7 with respect to the activation of Wnt target genes may be an important control node in this Notch-Wnt signalling switch.

In addition to demonstrating that Barx2 regulates endogenous Wnt target genes, as revealed by RNA analysis of Barx2 wildtype and null myoblasts, studies presented within this chapter also identified Barx2 as a downstream target of canonical Wnt signalling in primary myoblasts. Primary myoblasts cultured in the presence of Wnt3a for a period of 12 to 48 hours showed increasing expression of Barx2 mRNA and protein over this period, consistent with both the role of Barx2 in early myoblast differentiation [Makarenkova et al. 2009] and the role of Wnt3a in promoting differentiation [Tanaka et al. 2011]. In contrast to Axin2, a direct downstream target of Wnt signalling [Jho et al. 2002], the induction of Barx2 by Wnt3a stimulation is

likely to be indirect as suggested by several pieces of data. Whilst induction of Axin2 mRNA was very rapid (less than 12 hours), induction of Barx2 mRNA was slow, with maximal induction observed at the latest time point (48 hours). In addition, induction of Barx2 by a 12 hour pulse of Wnt3a could be blocked by the addition of cycloheximide, suggesting that protein synthesis was required. MyoD was considered a candidate intermediate factor for induction of Barx2 downstream of Wnt signalling [Tajbakhsh et al. 1998], however there was no increase in MyoD binding to E-box motifs within the Barx2 proximal promoter [Meech et al. 2003] after Wnt treatment. Luciferase assays demonstrated that neither the proximal Barx2 promoter containing the E-box motifs, nor longer constructs containing a putative TCF/LEF site, were activated by Wnt3a or constitutively active β -catenin. It remains possible that activation of Barx2 mRNA is mediated by more distal promoter elements, or by elements in the introns. Of note, the first intron of the Barx2 gene is very long (approximately 50 kb in mice and 100 kb in humans), which is often indicative of a regulatory function for this region of the gene. One approach to identifying the region through which the Barx2 gene is induced by Wnt signalling is to examine Wnt3a-induced changes in activating histone modifications across the Barx2 locus using ChIP-seq.

Interestingly, upregulation of Barx2 mRNA by Wnt3a was not observed in C2C12 cells, even though these cells show enhanced differentiation in response Wnt3a stimulation. Unstimulated C2C12 cells show extremely low levels of Barx2 mRNA (relative to unstimulated primary myoblasts) suggesting that the Barx2 gene might be epigenetically repressed. However, pilot studies (not shown) have not revealed a

reactivation of Barx2 expression in C2C12 cells after treatment with inhibitors of histone deacetylases or DNA methylation. Thus the mechanism behind repression of Barx2 expression in C2C12 cells remains an area for future study. Barx2 was also not induced by Wnt3a in primary muscle associated fibroblasts. This is not likely to be explained by epigenetic repression because fibroblasts actually express slightly higher levels of Barx2 mRNA than (unstimulated) myoblasts. Overall, these data suggest that induction of Barx2 mRNA by Wnt3a in myoblasts may be dependent on muscle specific factors that are yet to be defined, and which may not be present in C2C12 cells.

The use of lentiviral transduction for introducing Barx2 transgenes into primary myoblasts consistently resulted in very modest increases in Barx2 protein expression despite optimisation of the same protocols with a GFP reporter plasmid showing an efficacy close to 100%. Analysis of Barx2 protein expression on an individual cell basis by immunostaining with antibodies to Barx2 revealed that the percentage of myoblasts expressing Barx2 following viral transduction was extremely low. Various control experiments suggested that this was not explained by poor packaging or transduction efficiencies and was a myoblast-specific phenomenon. Inhibition of the proteasome significantly increased Barx2 protein expression and a similar but more modest effect was seen with Wnt3a treatment. The conclusions from these studies are that Barx2 is regulated post-transcriptionally in a cell autonomous manner in myoblast cultures, and that canonical Wnt signalling not only increases Barx2 mRNA, but also plays a role in stabilising Barx2 protein. An intriguing question for future studies is whether the myoblasts that permit upregulation of Barx2 at the protein

level in response to Wnt3a have a different behaviour to those that do not, for example being more competent for rapid differentiation.

Overall, the studies described here show that Barx2 is a target of canonical Wnt signalling in myoblasts at transcriptional and post transcriptional levels, and that lack of Barx2 expression results in dysregulation of many components of both the Wnt and Notch signalling pathways in myoblasts. These findings provide better insight into the roles of Barx2 downstream of Wnt signalling in muscle.

Chapter 5

Identification of direct Barx2 target
genes in myoblasts

5.1 Introduction

As discussed in detail in the previous chapter (Chapter 4), PCR array and RNA-Seq analysis performed on primary myoblasts isolated from Barx2^{+/+} and Barx2^{-/-} mice identified genes involved in both the Wnt and Notch signalling pathways that were dysregulated in response to loss of Barx2 expression. Whilst this gave an insight into the pathways in which Barx2 plays a role, it was not sufficient to elucidate *direct* downstream targets of Barx2. The Wnt and Notch signalling pathways are complex, consisting of multiple levels of regulation by both positive- and negative-feedback loops. As such, absence of Barx2 expression may directly affect the expression of some genes, but the dys-regulation of these genes may then have a knock-on effect, altering expression of many other components and targets of the aforementioned pathways indirectly. Moreover, given that the Barx2-LacZ knockin model has a germline deletion of Barx2, the possibility exists that the (near-normal) development and growth of the Barx2 null mice involves compensatory effects such as upregulation of other gene pathways involved in myoblast function. Thus, in order to extend our discovery of endogenous Barx2 target genes in myoblasts, the approach taken in studies described in this chapter was to over-express Barx2 in a myoblast model.

Immunohistochemistry techniques have shown that Barx2 is expressed *in vivo* in satellite cells and myoblasts both embryonically and postnatally [Meech et al. 2012]. However, in my studies using immunoblotting and immunohistochemistry, little or no endogenous Barx2 protein expression was detected in isolated primary myoblasts from postnatal mice or the C2C12 cell line cultured under standard growth

conditions. In addition, consistent with data presented in Chapter 4 regarding the instability of Barx2 protein expression in myoblasts, previous attempts to generate C2C12 cell lines stably over-expressing Barx2 by conventional methods in this laboratory have yielded limited results. In these stable lines, Barx2 protein expression appeared to be lost during the time taken for stable line selection (unpublished data). It was possible that this was because high expression of Barx2 drives myoblasts towards terminal differentiation and these cells are hence lost from the growing population at passage. Hence a different approach was needed to achieve stable Barx2 over-expression in myoblasts.

The Tet-ON (Clontech) method allows a Barx2-expression vector be induced into cells, but its expression is silenced until it is induced by addition of the stable tetracycline analogue Doxycycline (Dox) to the media. A Tet-ON Barx2 model was generated in C2C12 cells, and gene expression studies were then performed to identify genes whose expression was altered by acute overexpression of Barx2.

5.1.1 Tet systems

In *E. coli*, the genes of the tetracycline-resistance operon are negatively regulated by the Tet repressor protein (TetR). In the absence of tetracycline, TetR is able to block transcription by binding to the tet operator sequences (*tetO*). Both TetR and *tetO* thus provide the basis of regulation and induction for use in mammalian systems. The first component of the Tet Systems is the regulatory protein based on TetR. In the Tet-OFF system, this protein is a fusion of amino acids 1-207 of TetR and the C-terminal 127 amino acids of the Herpes simplex virus VP16 activation domain. Addition of the VP16 domain converts the TetR from being a transcriptional repressor

to a transcriptional activator, thus activating gene expression in the absence of Dox. The resulting protein is the tetracycline-controlled transactivator (tTA) [Gossen & Bujard 1992]. In the Tet-ON system the regulatory protein is based on a “reverse” Tet repressor (rTetR), created by four amino acid changes in TetR [Hillen & Berens 1994; Gossen et al. 1995]. The resulting protein, reverse tetracycline-controlled transactivator (rtTA), activates gene expression in the presence of Dox and is encoded by the pTet-ON regulator plasmid. The second component of this system is the response plasmid, which expresses a gene of interest under the control of the tetracycline-response element (TRE). The pTRE2pur plasmid contains the TRE, which consists of seven direct repeats of a 42 bp sequence containing the *tetO*, located upstream of a minimal CMV reporter.

The ultimate goal in setting up a functional Tet system is creating a double-stable Tet cell line which contains both the regulatory and response plasmids. In the case of a Tet-ON line, when cells contain both plasmids the gene of interest is only expressed upon binding of the rtTA protein to the TRE. rtTA binds the TRE and activates transcription in the *presence* of Dox in a precise and dose-dependent manner. Other advantages of using the Tet system include reversible induction, tight on/off regulation with minimal background or leaky expression in the absence of induction, no pleiotropic effects of the transactivator, and high inducibility with a fast response. Ultimately, this meant that Barx2 could be expressed highly for short periods of time. This was expected to prevent the problem of inhibition of Barx2 protein expression during long term selection, and also circumvent the need to perform repeated high-efficiency transient transfections.

5.1.2 Aims

Studies described in this chapter sought to:

1. Identify direct endogenous Barx2 targets that are regulated via the interaction of Barx2 with TCF/LEF proteins and/or β -catenin
2. Study the regulation of a selection of these target genes at the promoter level
3. Assess the role of TCF/LEF variants at these target gene promoters

5.2 Methods

5.2.1 Expression plasmids

The Axin2 promoter/intron luciferase reporter construct was obtained from Addgene (plasmid 21275 [Jho et al. 2002]). The cyclinD1 promoter luciferase reporter construct was a kind gift from Dr. Johann Auwerx [Botrugno et al. 2004].

Mouse Tcf7L1 (Tcf1) and Tcf7L2 (Tcf4) plasmid constructs were generated by *Phusion* (Thermo Scientific) amplification of cDNA isolated from C2C12 myoblasts. The resultant PCR products were directionally cloned *XhoI-XbaI* in pcDNA3 already containing an N-terminal myc-tag. All primers used for cloning are listed below in Table 5.1.

An mCherry/2A/mBarx2 cassette had previously been cloned by researchers in this laboratory into the *BamHI* and *XbaI* sites of the pcDNA3 vector multiple cloning site (MCS) and shown to be functionally active. The 2A peptide sequence disrupts normal peptide bond formation through a mechanism of ribosomal skipping. The presence of this 2A self-cleaving peptide allows multiple proteins to be encoded as polyproteins, which dissociate into component proteins upon translation. As such, it

allows for expression of mBarx2 whilst at the same time roughly equimolar amounts of mCherry, which can be used as a fluorescent positive marker. To insert this cassette into the Tet-ON system response plasmid pTRE2pur, it was digested *Bam*HI-*Xba*I while the pTRE2pur backbone was digested *Bam*HI-*Nhe*I.

5.2.2 Development of double-stable C2C12 Barx2-TetON cell lines

5.2.2.1 C2C12 Tet-ON Transfection and Selection

Low passage C2C12 cells were seeded at a density of 1×10^5 cells/well in 2 ml of complete media into two wells of a 6-well plate. Twenty four hours later, 2 μ g of pTet-ON regulatory plasmid per well was transfected using Lipofectamine 2000. Forty eight hours post transfection, cells were split 1:16 – a single well in a 6-well plate into two 10 cm culture dishes. Cells successfully transfected with pTet-ON encoding a neomycin-resistance gene were selected for with 1 mg/ml G418, added at the time of passaging and continually maintained, and cells successfully transfected with mCherry/2A/mBarx2 encoding a puromycin-resistance gene were selected for with 1 μ g/ml puromycin.

Approximately one week after onset of selection, antibiotic-resistant colonies were picked from the culture dishes. The aim was to select colonies before they grew too dense and began differentiating. As such, colonies were not visible to the naked eye and a microscope (Olympus CKII) was required. Using a 10x lens, colonies were carefully picked off the dish with a 40 μ l filter pipette tip and transferred into a 24-well plate (one colony per well). Because the level of expression of rtTA can be profoundly affected by the site of integration, it was necessary to isolate and analyse as many clones as possible in order to identify clones that would provide high

inducibility and a low level of ‘leaky’ expression in the un-induced state. Twenty eight individual colonies were picked at this stage and were maintained and expanded in 24-well plates.

Once cell lines carrying the TetON regulatory plasmid and optimally expressing rtTA were selected (see Results), these lines were re-transfected as described above with the mCherry/2A/mBarx2 response plasmid and new double transgenic lines were selected as described above.

Table 5.1: List of all primers used during this chapter

<u>Name</u>	<u>Sequence</u>
<u>Cloning</u>	
TCF7L1 (TCF3) F Xho	aagctc <u>gag</u> ccccagctcggtggtgg
TCF7L1 (TCF3) R Xba	ggctc <u>tag</u> attagtgggcagacttggtgacc
TCF7L2 (TCF4) F Xho	tatc <u>gag</u> ccgcagctgaacggcg
TCF7L2 (TCF4) R Xba	ggctc <u>tag</u> actattctaaagacttggtcacc
<u>Quantitative Real-time PCR</u>	
RPS26 F	aggtgcagaaggctgagg
RPS26 R	ggttctcccagtgatgaag
Myogenin F	ccttgctcagctccctca
Myogenin R	tgggagttgcattcactgg
MyoD F	cgacaccgcctactacagtg
MyoD R	tatgctggacaggcagtcg
cyclinD1 F	tctttccagagtcatcaagtgt
cyclinD1 R	gactccagaagggttcaatc
Axin2 F	gagagtgagcggcagagc
Axin2 R	cggctgactcgttctcct

Barx2 F	agccccctgcactcttgtacc
Barx2 R	ccgcagcggcgactggatg
ID2 F	gacagaaccaggcgtcca
ID2 R	agctcagaaggggaattcagatg
TCF7 (TCF1) F	cagctccccatactgtgag
TCF7 (TCF1) R	tgctgtctatatccgcaggaa
c-Myc F	cctagtgtgcatgaggaga
c-Myc R	tccacagacaccacatcaattt
Lef1 F	tctgaaatccccaccttct
Lef1 R	tgggataaacaggctgacct
ID3 F	gaggagcttttgccactgac
ID3 R	gctcatccatgccctcag
Pax7 F	accacttggtacagtgtgga
Pax7 R	agtaggcttgtcccgtttcc
Myf5 F	ctgctctgagcccaccag
Myf5 R	gacagggctgttacattcagg
TCF7L1 (TCF3) F	ctgagcagcccgtacctct
TCF7L1 (TCF3) R	aggggccatttcatctgtag
MMP9 F	cgacatagacggcatccag
MMP9 R	ctgtcggctgtggttcagt
Wnt4 F	ccgggcactcatgaatct
Wnt4 R	cacgccagcacgtctttac
Dlk1 F	ccctgcgtgatcaatggt
Dlk1 R	cacagaagttgcctgagaagc
Follistatin F	tctgccagttcatggagga
Follistatin R	ctcttccttgcctcagttctgtct
Pitx2a/b F	attgtcgcaaactagtgctg

Pitx2a/b R	gcccacatcctcattctttc
Pitx2c F	cctcacccttctgtcaccat
Pitx2c R	gcccacatcctcattctttc
Fzd7 F	ctggtgcttgctcttctgg
Fzd7 R	gcacaacgggatggagat
Fzd6 F	ttaagcgaaaccgcaagc
Fzd6 R	ttggaaatgaccttcagccta
Fzd4 F	aacctcggctacaacgtgac
Fzd4 R	ccgaacaaaggaagaactgc
Gdf5 F	taacagcagcgtgaagttgg
Gdf5 R	cacgtacctctgcttcctga
Tgfb3 F	aaccacacctgatcctcat
Tgfb3 R	cagcagttctcctccaggtt
MMP2 F	ggagaaggctgtgcttctcg
MMP2 R	aggctggtcagtggcttg

5.3 Results

5.3.1 Selection of suitable C2C12 pTet-ON stable lines

To screen for activity of the Tet-ON lines the reporter vector pTRE2-Luc (Clontech) containing a luciferase gene was used: with successful integration of the Tet-ON regulator plasmid, this reporter should be activated in the presence of Dox, allowing luciferase activity to be measured. A total of 28 C2C12 stable pTet-ON clones were screened for their background expression (no Dox condition) and inducibility by Dox by transiently transfecting the pTRE2-Luc reporter vector and measuring luciferase activity. The majority of selected lines had minimal background expression, as

reflected by their luciferase activity relative to the parent C2C12 line, set to 1 (Figure 5.1A). The graph shows no error bars as only single samples were analysed in this crude initial screen. Although most clones were able to be induced by Dox to some extent, there was great variation between the clones (Figure 5.1B). The goal was to identify clones that had low background expression of pTRE2-Luc, and high induction of luciferase activity following treatment with Dox.

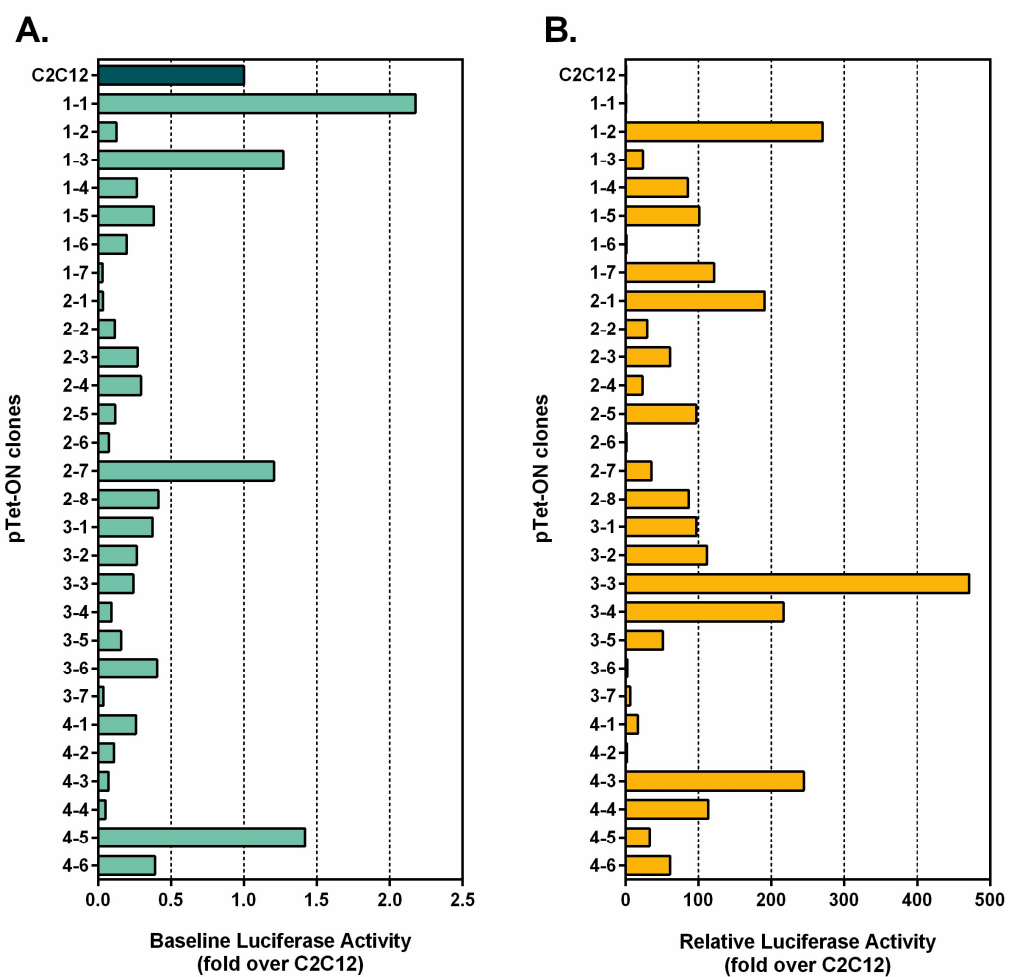


Figure 5.1: Initial screen of stable C2C12 pTet-ON clones

C2C12 pTet-ON stable clones were transiently transfected with pTRE2-Luc (0.5 μ g) and received vehicle or 2 μ g Dox. Luciferase activity was assayed 48 hours post transfection. All data are normalised to a Renilla luciferase internal control, expressed as the mean firefly/Renilla luciferase ratio, and then to parent C2C12 cells (set to a value of 1). (A): Baseline luciferase activity with vehicle. (B): Fold induction after treatment with Dox.

The eight lines with the lowest background and induction of greater than 95-fold were selected for a second round screen. These were clones **1-2**, **1-7**, **2-1**, **2-5**, **3-3**, **3-4**, **4-3** and **4-4**. In this second screen, all inductions in response to Dox were considerably lower than in the first screen, however all were greater than 20-fold (as recommended by the Clontech Tet User Manual) (Figure 5.2). This variation between experiments may relate to different cell densities. The three best responsive clones were **3-3**, **4-3** and **4-4** with 35, 106 and 61-fold activations respectively.

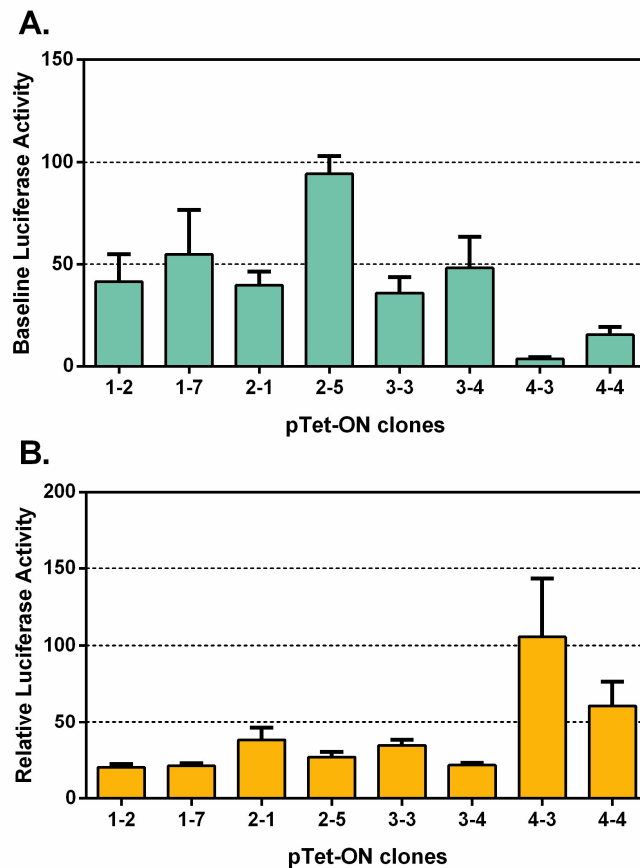


Figure 5.2: Second screen of stable C2C12 pTet-ON clones

C2C12 pTet-ON stable clones were transiently transfected with pTRE2-Luc (0.5 μ g) and received vehicle or 2 μ g Dox. Luciferase activity was assayed 48 hours post transfection. All data are normalised to a Renilla luciferase internal control, expressed as the mean firefly/Renilla luciferase ratio, and then to parent C2C12 cells (set to a value of 1). (A): Baseline luciferase activity with vehicle. (B): Fold induction after treatment with Dox. Error bars represent SEM.

5.3.1.1 Response to Wnt3a

Before continuing with further selection, the three selected stable lines were tested to ensure that their ability to respond to Wnt3a treatment had not been compromised during the selection and screening processes. All three lines were found to respond well to Wnt3a CM, activating the transiently transfected TOPflash reporter up to 1500-fold over L-cell control treatment (Figure 5.3). Although non-transgenic C2C12 cells were not used as a control in this particular experiment, the TOPflash activation range shown here is consistent with that observed in C2C12 cells previously (Chapter 3).

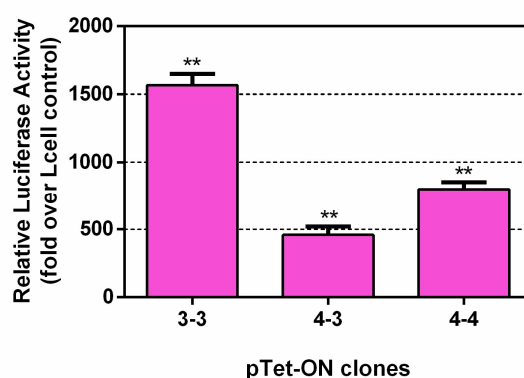


Figure 5.3: C2C12 pTet-ON stable clones respond to Wnt3a

C2C12 pTet-ON stable clones were transiently transfected with TOPflash (0.5 μ g) and treated with 1:2 dilution of Lcell or Wnt3a CM for 48 hours. Luciferase activity was assayed 48 hours post transfection. All data are normalised to a Renilla luciferase internal control, expressed as the mean firefly/Renilla luciferase ratio, and then to Lcell control (set to a value of 1). Error bars represent SEM. ** $p < 0.001$.

5.3.2 Identifying appropriate double-stable C2C12 mCherry/2A/mBarx2 Tet-ON lines

After transfecting the mCherry/2A/mBarx2 response plasmid to generate double-transgenic stable clones, the presence of the mCherry cistron allowed for quick and

easy screening of clones for expression by fluorescence microscopy. Using an Olympus IX71 Fluorescence Inverted Microscope, clones were assessed for low background and high inducible expression of mCherry, and hence presumably also Barx2. Only one line, designated C2C12 Barx2 Tet-ON **4-4-12**, showed background expression of mCherry without Dox. All other lines had either extremely low or no detectable background expression. Fifteen of the double-stable lines had detectable mCherry expression following induction by Dox for 48 hours. The 10 best expressing lines are shown in Figure 5.4.

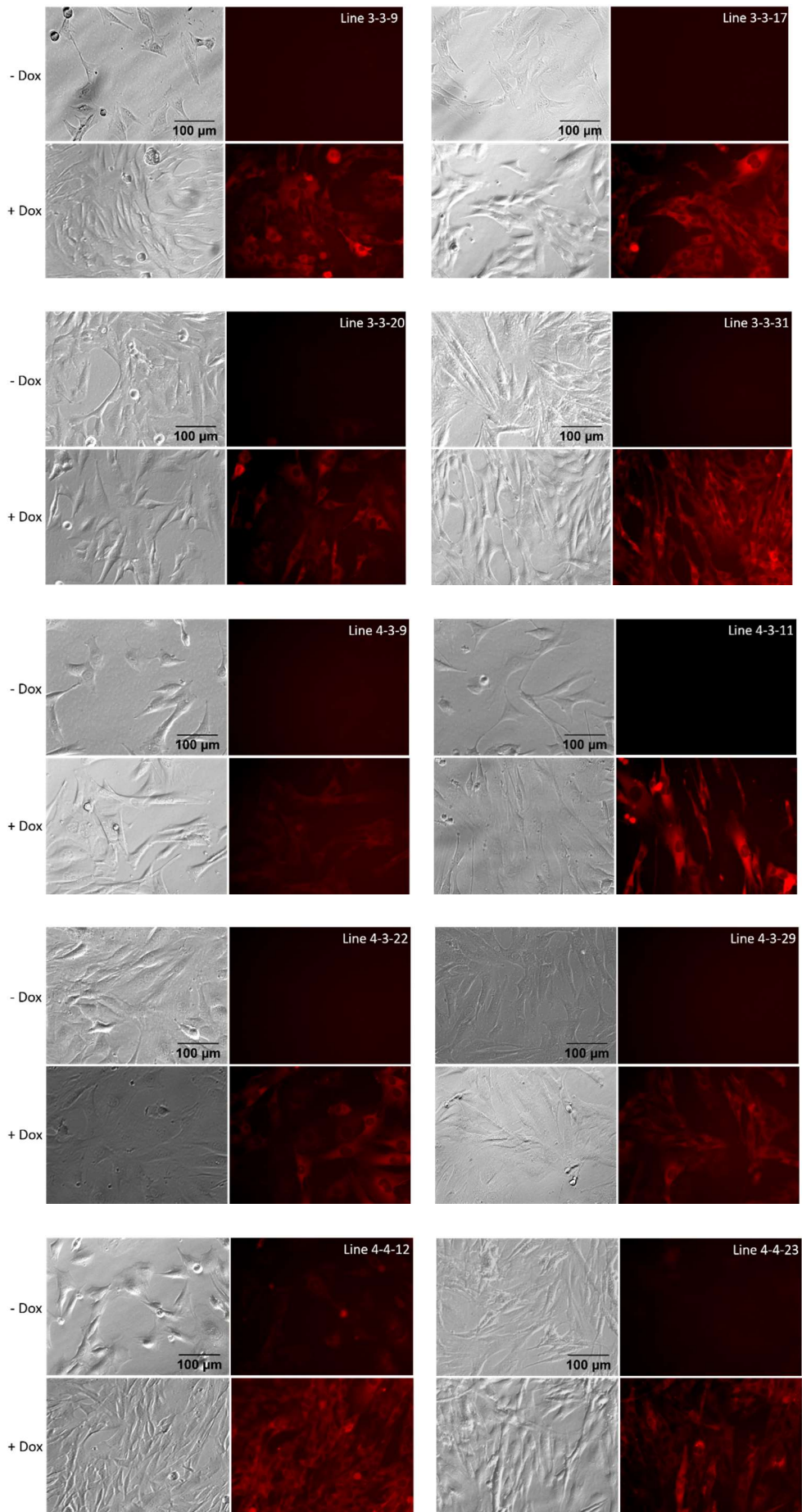


Figure 5.4: Immunofluorescence screening of double-transgenic C2C12 Barx2 Tet-ON clones

C2C12 mCherry/2A/mBarx2 Tet-ON stable clones were treated with vehicle or 2 μ g Dox for 48 hours and imaged for mCherry expression with an Olympus IX71 microscope. Representative images are shown. Scale bars represent 100 μ M.

The Barx2 and mCherry cistrons should be translated as a polyprotein, however the presence of the 2A self-cleaving peptide causes them to dissociate into two separate proteins upon translation, thus resulting in a theoretical 1:1 ratio of expression of Barx2 and mCherry protein. However, due to concerns about the stability of Barx2 protein in myoblasts, western blotting was used to confirm Barx2 protein expression in the ten lines showing highest mCherry induction. Total protein (20 μ g) from each sample was loaded on SDS-PAGE gels, and proteins were immunoblotted with anti-Barx2 antibody. Lysate from COS7 cells transiently transfected with full length Barx2 in pcDNA3-myc served as a positive control. This Barx2 protein in the Barx2-TetON samples appears slightly lower in molecular weight than in the Barx2/pcDNA3-myc samples, likely due to the absence of the myc tag (Figure 5.5).

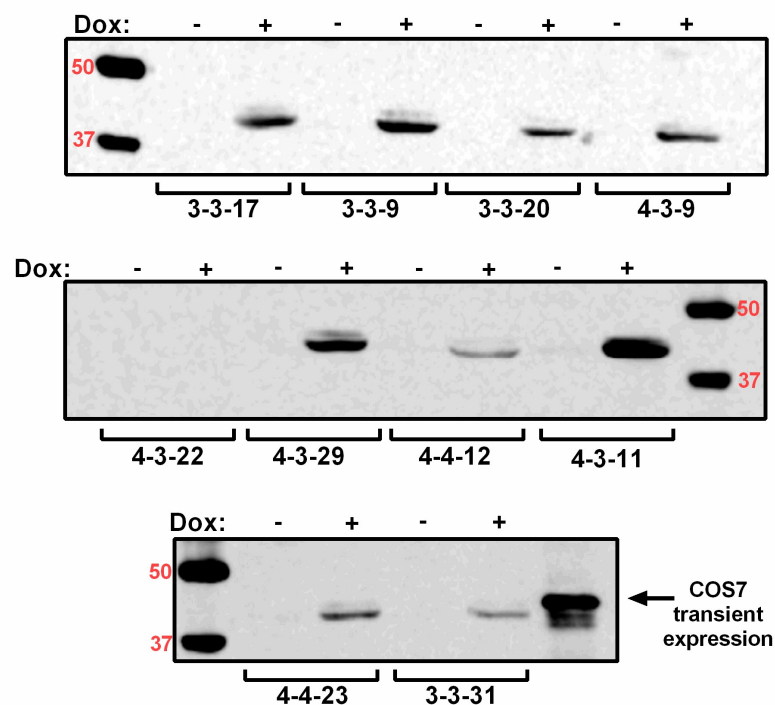


Figure 5.5: Western Barx2 Tet-ON lines

C2C12 mCherry/2A/mBarx2 Tet-ON stable clones were treated with vehicle or 2 μ g Dox for 48 hours. Proteins were resolved on a 10% SDS-PAGE gel, transferred to nitrocellulose membrane and probed with polyclonal antibodies to Barx2.

Of the ten selected Barx2-TetON stable lines, nine successfully induced Barx2 as assessed by western blotting, with only line **4-3-22** not expressing any detectable level of Barx2. Line **4-4-12** had significantly lower Dox-induced Barx2 expression than all other Barx2-expressing lines, and no Barx2 expression at all in the vehicle control (Figure 5.5). This was unexpected because it had previously shown high expression of mCherry in both vehicle and Dox conditions. It is possible that ongoing 'leaky' expression of the mCherry/2A/mBarx2 cassette during the selection process had created a feedback process that suppressed Barx2 protein as observed in previous attempts to generate constitutive Barx2 stable lines.

To narrow down the selection of stable mCherry/2A/mBarx2 Tet-ON (referred to as simply Barx2 Tet-ON from this point) lines further, it was decided to screen all 9 Dox-responsive lines, the three Tet-ON parent lines (**3-3**, **4-4** and **4-3**) and the C2C12 parent line for mRNA expression of key myogenic genes. All cell lines were treated with either 2 µg/ml Dox or vehicle for 48 hours under growth conditions. Although each of these 13 cell lines were seeded at equal densities, at the time of harvesting 48 hours later they had reached different degrees of confluence. Expression of Barx2 mRNA, as well as two genes involved in cell cycle regulation and myogenesis: cyclinD1 and myogenin respectively, were analysed in all lines. The cell-cycle factor cyclinD1 acts as a regulatory subunit of cyclin-dependent kinase 4 or 6, the activity of which is required for cell cycle G1/S transition [Stacey 2003]. Changes in cyclinD1 expression could suggest quiescent cells re-entering the cell cycle, changes in cell activation and/or proliferation. Myogenin is upregulated during, and promotes, myoblast differentiation; hence any increase in myogenin expression would be consistent with

onset and progression of differentiation. As expected, Barx2 mRNA expression was increased in all double-stable Barx2 Tet-ON lines after Dox-induction (Figure 5.6A). The fold induction relative to the control condition varied from 2-fold (**4-4-12**) to 42-fold (**3-3-31**), and the mRNA level did not obviously correlate with protein expression as shown in Figure 5.6. In the parent C2C12 cells and the parent Tet-ON lines, minimal Barx2 expression was detected either without or with Dox-induction, as expected. There were also minimal changes in expression of cyclinD1 and myogenin mRNAs after Dox-induction in any parent line (Figure 5.6B). The trend observed following Dox-induction of the Barx2 Tet-ON lines was a slight increase in cyclinD1 expression and a slight down-regulation of myogenin expression. These changes in gene expression were independent of cell density at the time of harvest, suggesting that this may be due to Barx2 induction.

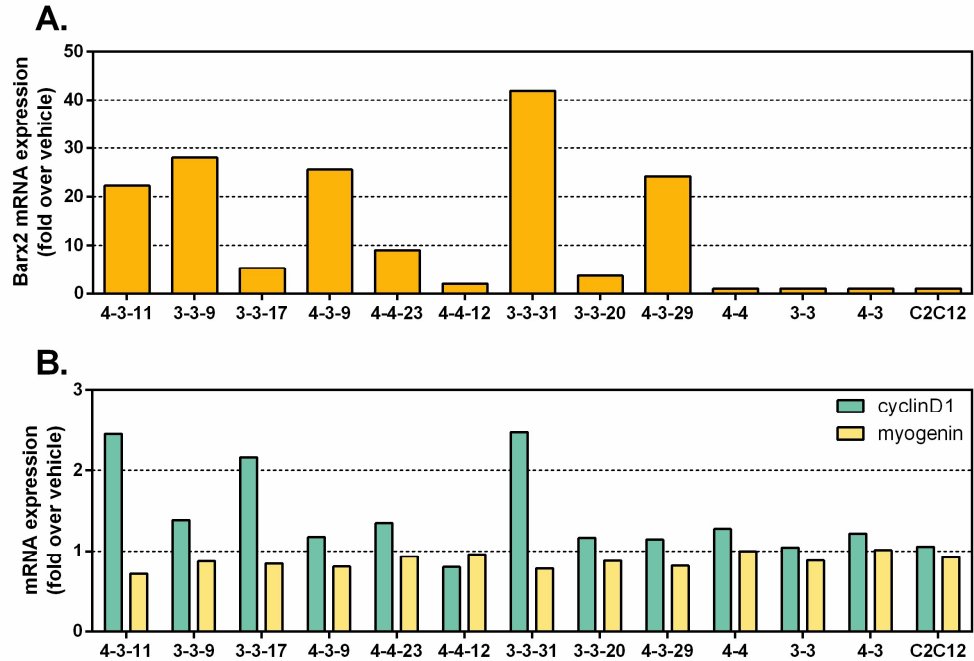


Figure 5.6: Initial mRNA screen of stable C2C12 Barx2 Tet-ON lines

C2C12 Barx2 Tet-ON stable clones received vehicle or 2 μ g Dox for 48 hours and total RNA was isolated and reverse transcribed. Expression of (A) Barx2 or (B) cyclinD1 and myogenin mRNA was assessed by quantitative realtime PCR, normalised to the housekeeping gene RPS26 and is presented as fold-change relative to expression in vehicle condition (set to a value of 1). The results shown are from a single experiment with no replicates.

The best-responding Barx2 Tet-ON clone from each rtTA-expressing parent line based on the studies described above was selected for a further in-depth analysis of gene expression. These lines were **3-3-31** and **4-3-11**.

5.3.3 TOPflash is activated in the Barx2 Tet-ON stable lines

The ultimate goal of generating Barx2 Tet-ON stable lines was to identify target genes that Barx2 may regulate via interaction with β -catenin and TCF/LEF at TCF/LEF binding elements. It was therefore important to ensure that induction of Barx2 by Dox could activate the synthetic TOPflash reporter, as observed previously following transient transfection of Barx2. To achieve this, TOPflash was transiently transfected in to both **3-3-31** and **4-3-11** Barx2 Tet-ON lines, with and without Dox, and luciferase activity

was measured after 48 hours. As shown in Figure 5.8, Dox alone was not sufficient to activate the TOPflash reporter. However, TOPflash could be activated in these same cells by a combination of Dox and MyoD transient transfection (Figure 5.7). As discussed in Chapter 3, transient co-transfection of Barx2 and MyoD produced a significantly greater activation of the TOPflash reporter than Barx2 alone. It may be that, in contrast to transient transfection, the level of Barx2 protein produced per cell in the Tet-ON system is not quite sufficient to induce TOPflash without the concomitant overexpression of MyoD. Overall these data suggest that the pathway required for activation of Wnt target genes, as assessed using the synthetic reporter TOPflash, is still intact in the selected Tet-ON cell lines.

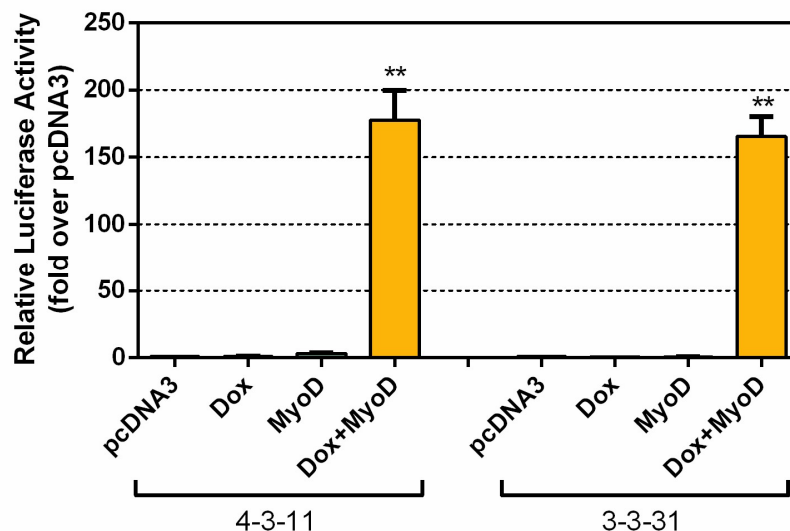


Figure 5.7: TOPflash is activated in the Barx2 Tet-ON stable lines

TOPflash reporter (0.5 μ g) was co-transfected with MyoD (1 μ g) into C2C12 Barx2 Tet-ON stable lines 4-3-11 and 3-3-31. Transfection of empty pcDNA3 vector served as a negative control and to control for total amount of transfected DNA. Cells received either vehicle or 2 μ g Dox. Luciferase activity was assayed 48 hours post transfection. All data are normalised to a Renilla luciferase internal control, expressed as the mean firefly/Renilla luciferase ratio, and then to pcDNA3 empty vector transfection (set to a value of 1). The results shown are the average of two independent experiments performed in triplicate. Error bars represent SEM. ** $p < 0.001$ relative to pcDNA3 control. n=6.

5.3.4 Identification of Barx2 targets from C2C12 Barx2 Tet-ON lines

For gene expression analysis, Barx2 Tet-ON lines 3-3-31 and 4-3-11 were treated with vehicle or Dox for 48 hours in growth conditions, and in addition a 1:4 dilution of either L-cell or Wnt3a CM was added for the final 6 hours. Selected target genes were assayed by qRT-PCR to determine whether they may be regulated by either Barx2, Wnt3a, or the combination of both. These targets were selected based on their involvement in the Wnt signalling pathway, either as downstream targets or factors involved in the pathway itself, or their known role in myogenesis. Additional target genes were selected based on data presented in Chapter 4 that identified genes that were misregulated in Barx2^{-/-} myoblasts relative to Barx2^{+/+} myoblasts.

Although not shown, similar gene expression data were obtained with both Tet-ON cell lines, with line 4-3-11 showing more pronounced changes in gene expression. This was more than likely due to the greater induction of Barx2 expression (an average of 45-fold for line 4-3-11, and 20-fold for line 3-3-31 across multiple experiments). As shown in Figure 5.8, many target genes that were screened showed no significant change in expression levels in the presence of Dox (and thus increased Barx2 expression). These included Follistatin, cyclinD2, Pax7, Fzd7, Fzd4, Tgfb3, c-Myc, Pitx2 and MyoD. Most of these genes however did show a response to Wnt3a ligand (Follistatin, Pitx2, Tgfb3, Fzd4, Fzd7), whilst others were not responsive to Wnt3a stimulation and therefore not likely to be targets of the canonical Wnt signalling pathway within this myogenic cell system.

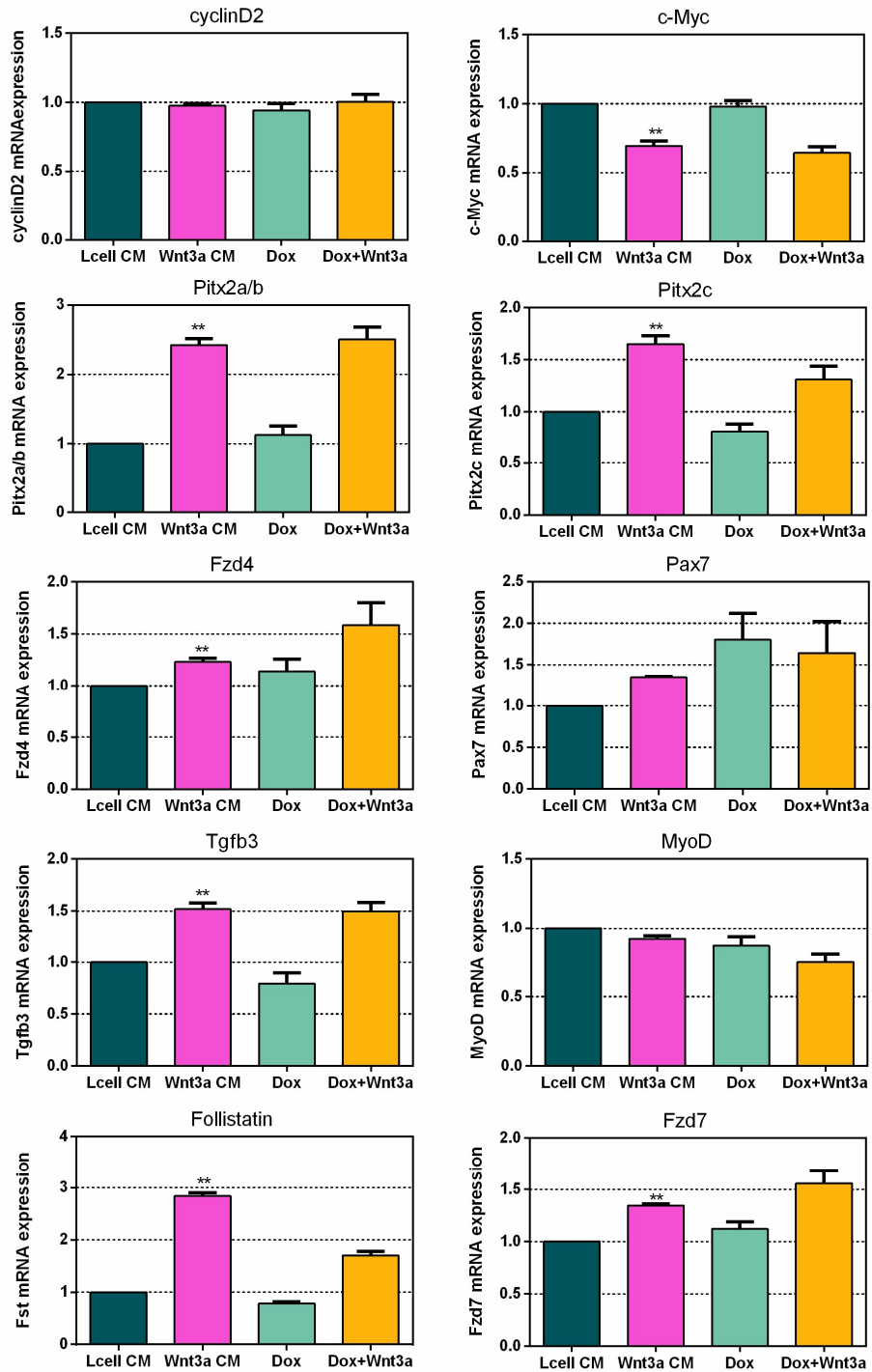


Figure 5.8: Target genes not regulated by Dox-induced Barx2 expression

C2C12 Barx2 Tet-ON stable line 4-3-11 received vehicle or 2 μ g Dox for 48 hours, and Lcell or Wnt3a conditioned media for the final 6 hours. Total RNA was isolated and reverse transcribed. mRNA expression was assessed by quantitative realtime PCR, normalised to the housekeeping gene RPS26 and is presented as fold-change relative to expression in vehicle Lcell condition (set to a value of 1). Three independent experiments were performed but a representative experiment is shown. Error bars represent SEM. ** $p < 0.001$ relative to vehicle Lcell control. $n=4$.

In contrast, a selection of target genes did show a significant change in expression levels following increased Barx2 expression (Figure 5.9). Two of the most robustly upregulated target genes identified in this screen were cyclinD1 and Axin2. Expression of both Axin2 and cyclinD1 was 2-fold higher in Dox-induced line 4-3-11 (Figure 5.9), and both of these genes were previously identified as being down-regulated in Barx2^{-/-} myoblasts (Chapter 4, Section 4.3.1). Interestingly, although Axin2 was only increased 2-fold by Barx2 over-expression, there was a synergistic induction of Axin2 expression by both Barx2 over-expression and treatment with Wnt3a CM; 56-fold with Wnt3a CM alone and 79-fold with Wnt3a CM and Dox (Figure 5.9). No change in Axin2 or cyclinD1 mRNA was observed in the parental rtTA-expressing cell lines 3-3 and 4-3 which do not express Barx2 in response to Dox (Figure 5.10).

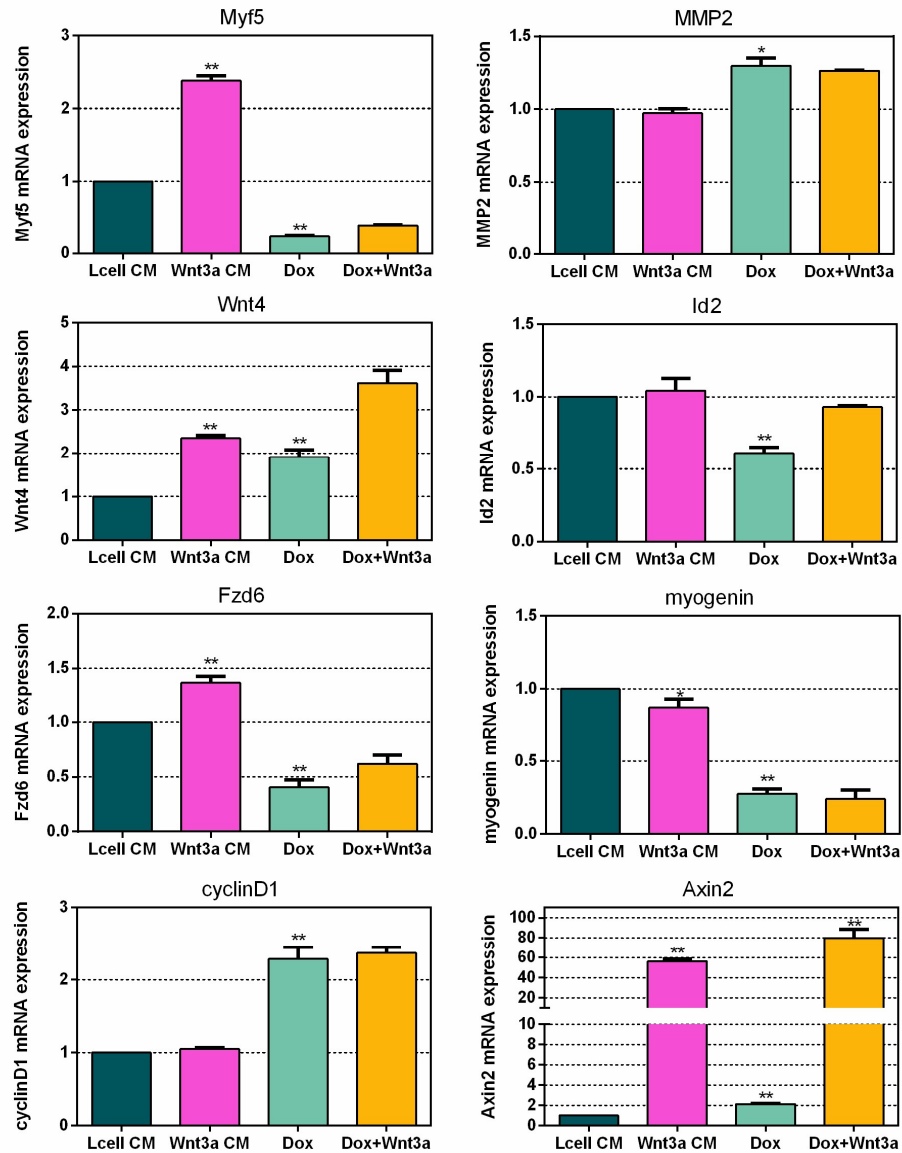


Figure 5.9: Target genes regulated by Dox-induced Barx2 expression

C2C12 Barx2 Tet-ON stable line 4-3-11 received vehicle or 2 μ g Dox for 48 hours, and Lcell or Wnt3a CM for the final 6 hours. Total RNA was isolated and reverse transcribed. mRNA expression was assessed by quantitative realtime PCR, normalised to the housekeeping gene RPS26 and is presented as fold-change relative to expression in vehicle Lcell condition (set to a value of 1). Three independent experiments were performed but a representative experiment is shown. Error bars represent SEM. * $p < 0.05$ and ** $p < 0.001$ relative to vehicle Lcell control or relative to Wnt3a CM + Dox combined. $n=4$.

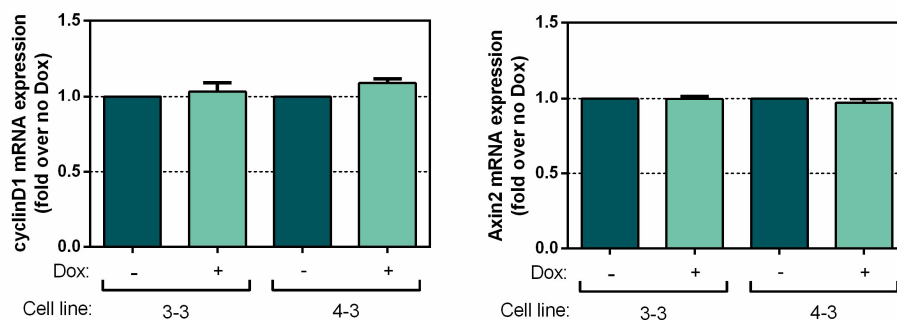


Figure 5.10: Parental rtTA-expressing cell lines do not show induction of cyclinD1 or Axin2 in response to Dox

C2C12 pTet-ON stable lines 3-3 and 4-3 received vehicle or 2 μ g Dox for 48 hours. Total RNA was isolated and reverse transcribed. mRNA expression was assessed by quantitative realtime PCR, normalised to the housekeeping gene RPS26 and is presented as fold-change relative to expression in vehicle Lcell condition (set to a value of 1). Error bars represent SEM. n=4.

5.3.5 The Axin2 and cyclinD1 promoters are regulated by Barx2

To better understand the regulation by Barx2, cyclinD1 and Axin2 promoter-luciferase constructs [Jho et al. 2002; Botrugno et al. 2004] were used in transient co-transfection experiments in C2C12 cells. As shown in Figure 5.11A, Barx2 induced the Axin2 promoter/intron luciferase construct (Axin2-luc) approximately 2-fold in growth conditions and 4-fold in differentiation conditions. β -catenin activated Axin2-luc 3-fold and 6-fold in growth and differentiation conditions respectively (Figure 5.11A). Moreover, Barx2 and β -catenin also synergistically activated Axin2-luc under differentiation conditions, but not in growth conditions. Both Barx2 and β -catenin induced the cyclinD1 promoter nearly 2-fold (Figure 5.11B). In contrast to the Axin2-luc construct, fold changes of the cyclinD1 promoter construct were identical in growth and differentiation conditions, and there was no synergy between Barx2 and β -catenin.

Previous work performed in the laboratory showed that Barx2-mediated activation of TOPflash was completely abolished by co-transfection of a dominant-negative form of TCF4 (dnTCF4), which is lacking the N-terminal β -catenin domain and therefore is able to bind DNA but not interact with β -catenin. This, together with co-IP and CHIP data presented in Chapter 3, suggested that Barx2 regulated the TOPflash promoter through the TCF/LEF motifs. To ascertain whether Barx2-mediated activation of Axin2 and cyclinD1 promoters may also be mediated by TCF/LEF motifs, dnTCF4 was co-transfected with Barx2 or β -catenin. As shown in Figure 5.11A and Figure 5.11B, dnTCF4 blocked activation of Axin2-luc by both Barx2 and β -catenin. Similarly, dnTCF4 blocked activation of the cyclinD1 promoter by both factors. The role of MyoD in this system was also assessed. However, unlike the TOPflash reporter which was synergistically activated by Barx2 together with MyoD, MyoD played no role in activation of either Axin2-luc or the cyclinD1 promoter constructs.

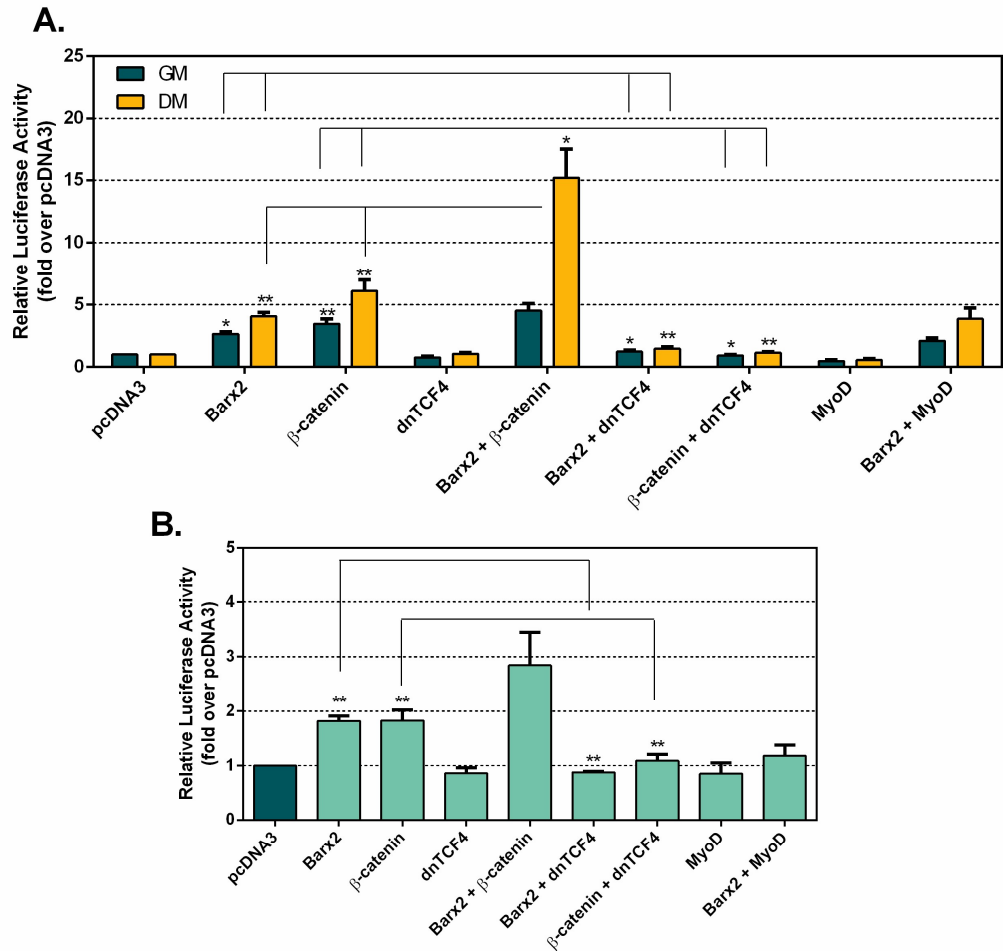


Figure 5.11: Barx2 regulates the Axin2 and cyclinD1 promoters

Axin2-luc (A) or cyclinD1 (B) promoter constructs (0.5 μ g) were co-transfected with varying combinations of Barx2, β -catenin, dnTCF4 and MyoD expression plasmids (total 1 μ g) in growth media (GM) or differentiation media (DM). Transfection of empty pcDNA3 vector served as a negative control and to control for the amount of transfected DNA. Luciferase activity was assayed 48 hours post transfection. All data are normalised to a Renilla luciferase internal control, expressed as the mean firefly/Renilla luciferase ratio. Data were then normalised to the promoterless pGL3-basic vector, and then to pcDNA3 empty vector transfection (set to a value of 1). The results shown are the average of at least three independent experiments performed in triplicate. Error bars represent SEM. * $p < 0.05$ and ** $p < 0.001$ relative to pcDNA3 control unless marked otherwise.

5.3.6 The role of TCF/LEF variants in regulation of Wnt-target promoters

The literature on TCF/LEF proteins suggests that TCF/LEF family members play a critical role in shaping both tissue-specific and stage-specific transcriptional output from Wnt signalling. However, the functions of each of the four family members can

differ. To determine which TCF/LEF family members are expressed in muscle, quantitative PCR analysis was performed with primers specific for each family member, but that did not distinguish between splice variants, in both C2C12 cells and primary myoblasts. These experiments showed that Lef1, Tcf3 (Tcf7l1) and Tcf4 (Tcf7l2) were all expressed in both cell types (Figure 5.12). In contrast, no Tcf1 (Tcf7) was detected in either cell type.

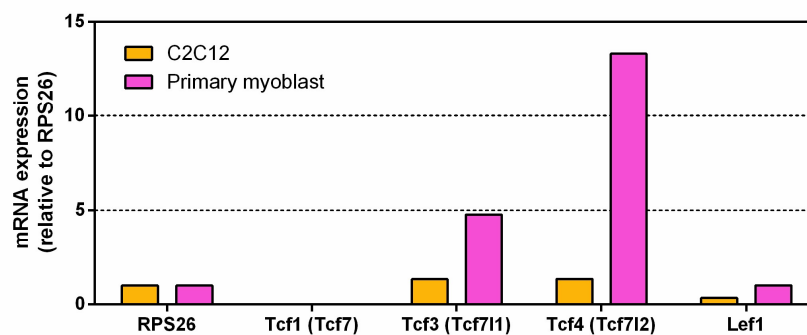


Figure 5.12: TCF/LEF mRNA expression in C2C12 cells and primary myoblasts

Total RNA was isolated from C2C12 cells and primary myoblasts and reverse transcribed. mRNA expression of TCF/LEF family members was assessed by quantitative realtime PCR, normalised to the housekeeping gene RPS26 and is presented as fold-change relative to RPS26 expression (set to a value of 1). The results shown are from a single experiment with no replicates.

In order to characterise the role of TCF/LEF family members and their variants in regulation of TOPflash and Axin2 by Barx2, the TCF/LEF members Lef1, Tcf3 and Tcf4 were cloned and multiple clones were sequenced to identify splice variants. Previously in the laboratory, only human (h)TCF4 had been used in luciferase reporter assays with TOPflash (unpublished data). These experiments showed that wildtype hTCF4 was extremely repressive when co-expressed with Barx2 or β -catenin, similar to that observed with dnTCF4 discussed previously. It was therefore hypothesised that perhaps TCF4 (at least the human variant that was tested) was not the TCF/LEF

family member that mediated the activation of Wnt target genes by Barx2 and β -catenin in myoblasts, and thus the decision was made to clone the mouse TCF/LEF variants expressed in muscle cells. Sequencing of multiple isolated clones generated by PCR with the Tcf3 primers identified only a single isoform of Tcf3 (isoform 2, lacking an internal exon), which has previously been described. In contrast, sequencing of multiple isolated clones generated by PCR with the Tcf4 (Tcf7l2) primers identified multiple splice variants of this transcript as described further below.

A comprehensive study performed by Weise and colleagues previously showed that the *Tcf7l2* gene, which consists of 17 exons, contains a conditional exon 4 and sequence variation around exon 8 whereby alternative splice donor and acceptor sites generate additional sequences giving rise to LVPQ and SFLSS amino acid motifs [Weise et al. 2010], in a manner similar to the human *TCF7L2* gene. Furthermore, alternative splicing of exons 12-17 was demonstrated. Depending upon the preceding exon combination, different open reading frames are used for translation of exons 15, 16 and 17. This distinction can be used to classify *Tcf7l2* transcripts into TCF4E (also known as L), TCF4S and TCF4M protein isoforms [Young et al. 2002; Shiina et al. 2003]. TCF4E splice variants contain a longer coding region of the final exon (exon 17), generating a second DNA-binding domain, referred to as a complete C-clamp [Hecht & Stemmler 2003; Atcha et al. 2007]; either a CRARF or a CRALF motif with conserved cysteines [Weise et al. 2010]. In contrast, TCF4S variants contain only three of the four conserved cysteines, and TCF4M variants lack both the cysteines and the CRARF/CRALF element. Interestingly, sequencing of six Tcf4 clones isolated here from

myoblasts showed that five of the six were TCF4M isoforms. Of the six Tcf4 clones, clones #1 and #2 contained exon 4 and no LVPQ or SFLSS motifs around exon 8. Clone #1 lacked exons 13-16 (M1 isoform) [Weise et al. 2010]. Sequencing for clone #2 was inconclusive; it did, however, contain a long coding region within exon 17, making it an E isoform. Clones #5 and #6 were also M1 isoforms, and both lacked exon 4, with clone #5 containing the LVPQ motif. Interestingly, two clones (#7 and #8) lacked exon 8, a variation that has not previously been reported. These two clones also contained exon 4 and lacked exons 14-16, making them M2 isoforms [Weise et al. 2010]. It is important to note that the hTCF4 variant used in the laboratory previously is an E isoform and thus contains the C-clamp. A schematic of previously characterized Tcf4 variants and the new clones identified here is shown below in Figure 5.13. For the full protein sequence and alignment, see Appendix 4.

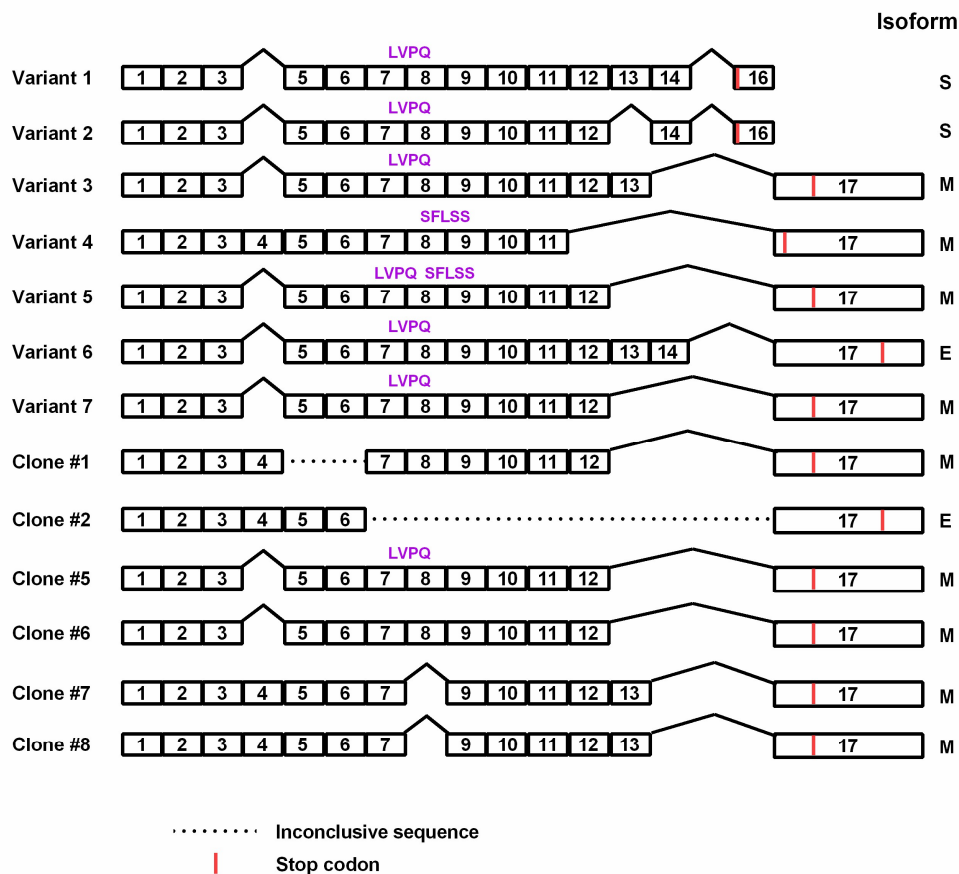


Figure 5.13: Simplified schematic of exon structure of Tcf4 variants cloned from myoblasts

Schematic of seven previously identified Tcf4 variants (Variant 1-7) and six cloned Tcf4 variants from myoblasts (Clone #1, 2, 5, 6, 7 and 8). The presence of the LVPQ and SFLSS motifs are marked. “...” denotes inconclusive sequencing results, and red lines indicate the positions of the stop codons. The isoform of each variant is shown on the right hand side.

The role of each TCF/LEF variant was assessed in luciferase assays with either TOPflash or Axin2-luc. Due to low activation of the cyclinD1 luciferase promoter by Barx2 and β -catenin, the role of TCF/LEF variants was not assessed using this promoter. When co-transfected with TOPflash, Lef1 synergistically enhanced activation by both β -catenin and Barx2+MyoD (Figure 5.14). This effect was dose-dependent, with transfection of 10 and 50 ng of Lef1 providing synergistic activation, whereas 500 ng did not. Co-transfection of Tcf3 at 10 ng did not augment activation of TOPflash by either Barx2+MyoD or β -catenin, and it was repressive at 50 and 500

ng (Figure 5.14). Contrastingly, all Tcf4 splice variants were highly repressive at all concentrations tested; similar to previous observations with hTCF4 (Figure 5.14). Tcf4 variants #1 and #2 were assessed with β -catenin only and not Barx2+MyoD.

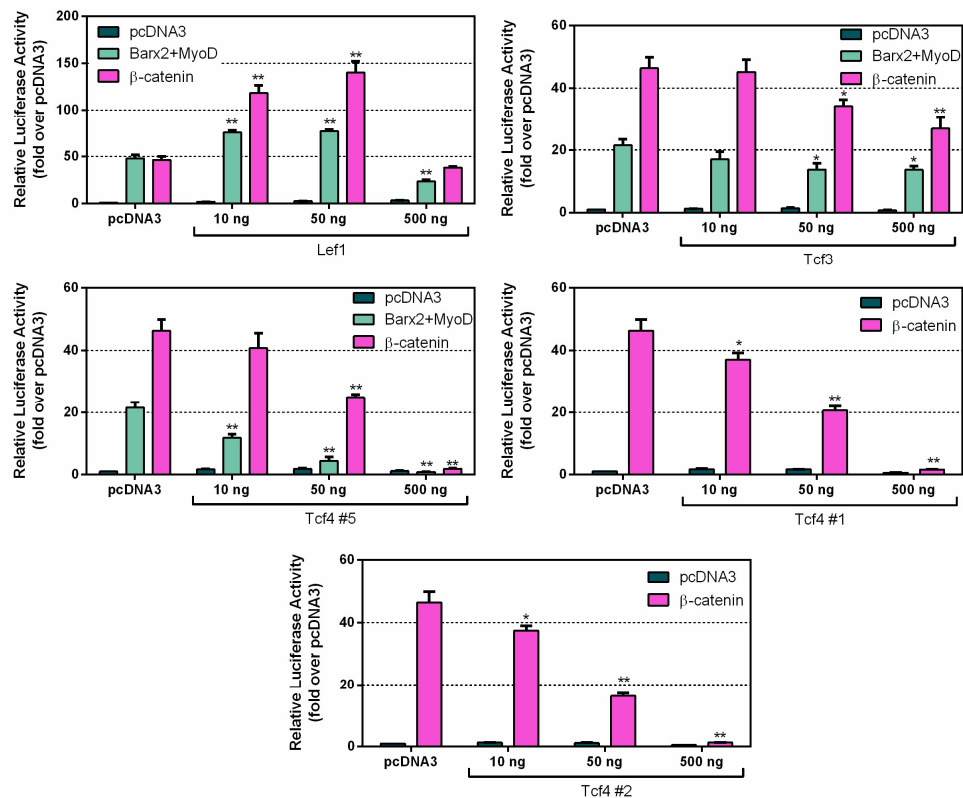


Figure 5.14: TCF/LEF family members differentially regulate Barx2+MyoD and β -catenin-mediated activation of TOPflash

TOPflash reporter (0.5 μ g) was co-transfected with Barx2+MyoD (1 μ g) or β -catenin (50 ng) and increasing concentrations of Lef1, Tcf3 or Tcf4 expression plasmids. Transfection of empty pcDNA3 vector served as a negative control and to control for the amount of transfected DNA. Luciferase activity was assayed 48 hours post transfection. All data are normalised to a Renilla luciferase internal control, expressed as the mean firefly/Renilla luciferase ratio, and then to pcDNA3 empty vector transfection (set to a value of 1). The results shown are the average of two independent experiments performed in triplicate. Error bars represent SEM. * p < 0.05 and ** p < 0.001 relative to pcDNA3 control. n=6.

When tested with the Axin2-luc reporter, Lef1 synergised with β -catenin to produce greater activation than β -catenin alone in GM or DM conditions (2-fold to 6-fold, 5-fold to 22-fold), but no synergy was seen between Lef1 and Barx2 (Figure 5.15). Co-

transfection of Tcf3 did not affect Barx2- or β -catenin-mediated activation of Axin2-luc in either GM or DM conditions (Figure 5.15).

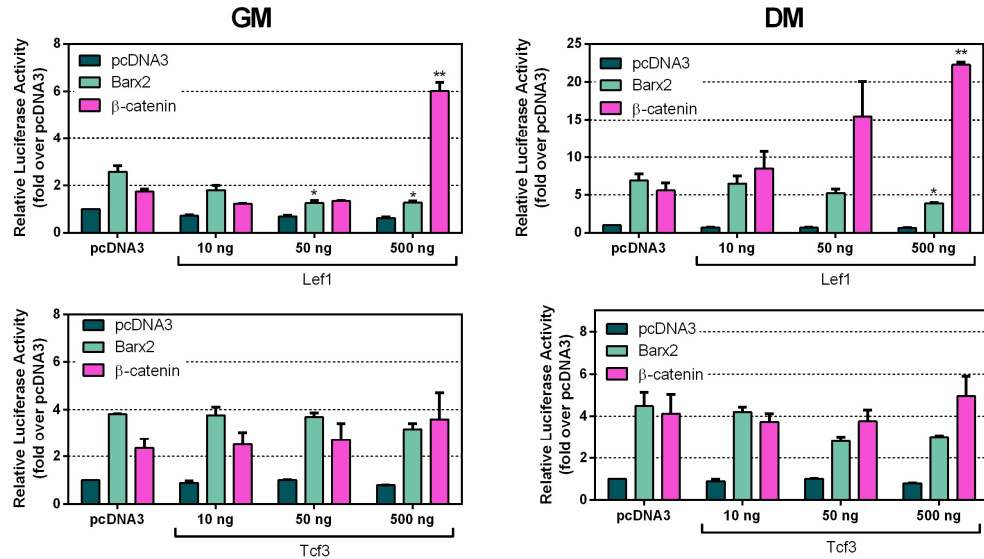


Figure 5.15: Lef1 and Tcf3 differentially regulate Barx2 and β -catenin-mediated activation of Axin2-luc

Axin2-luc (0.5 μ g) was co-transfected with Barx2 (1 μ g) or β -catenin (50 ng) and increasing concentrations of Lef1 or Tcf3 expression plasmids. Transfection of empty pcDNA3 vector served as a negative control and to control for the amount of transfected DNA. Luciferase activity was assayed 48 hours post transfection. All data are normalised to a Renilla luciferase internal control, expressed as the mean firefly/Renilla luciferase ratio. Data were then normalised to the promoterless pGL3-basic vector, and then to pcDNA3 empty vector transfection (set to 1). The results shown are the average of two independent experiments performed in triplicate. Error bars represent SEM. * p < 0.05 relative to pcDNA3. n=6.

Unlike the effect of Tcf4 variants on TOPflash activity, co-transfection of Tcf4 did show some ability to synergise with β -catenin in activation of the Axin2-luc construct. As shown in Figure 5.16, Tcf4 variants #1, 5 and 8 enhanced β -catenin-mediated activation when transfected at a concentration of 50 ng. Synergy between hTCF4 and β -catenin was also observed, but most significantly at 500 ng; which was in contrast to its repressive effects on TOPflash. No synergy was observed with any Tcf4 variant (including hTCF4) and Barx2 (Figure 5.16), and each variant was repressive to Barx2-

mediated Axin2-luc activation in a concentration-dependent manner. These data show that the functions of the different TCF/LEF family members and their splice variants are both promoter and co-factor dependent.

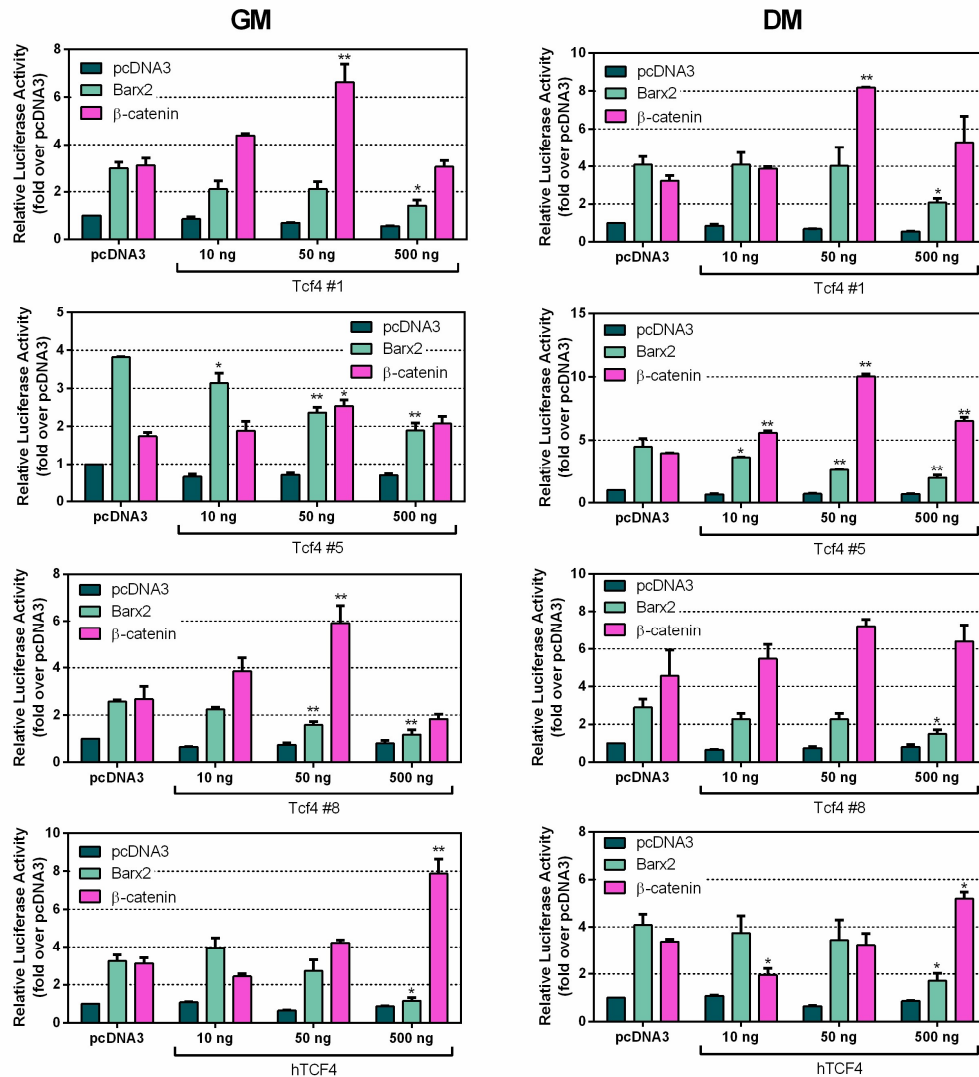


Figure 5.16: Tcf4 variants differentially regulate Barx2 and β -catenin-mediated activation of Axin2-luc

Axin2-luc (0.5 μ g) was co-transfected with Barx2 (1 μ g) or β -catenin (50 ng) and increasing concentrations of Tcf4 expression plasmids. Transfection of empty pcDNA3 vector served as a negative control and to control for the amount of transfected DNA. Luciferase activity was assayed 48 hours post transfection. All data are normalised to a Renilla luciferase internal control, expressed as the mean firefly/Renilla luciferase ratio. Data were then normalised to the promoterless pGL3-basic vector, and then to pcDNA3 empty vector transfection (set to a value of 1). The results shown are the average of two independent experiments performed in triplicate. Error bars represent SEM. * $p < 0.05$ and ** $p < 0.001$ relative to pcDNA3. $n=6$.

5.4 Discussion

The generation of C2C12 Barx2 Tet-ON stable cell lines provided a valuable model for Barx2 over-expression in myoblasts. Because the behaviour of myoblast cell lines can change during the selection process to generate stable lines, they were screened after each selection step to ensure that they maintained the ability to differentiate and that the Wnt reporter TOPflash still responded to treatment with Wnt3a CM, indicating that the Wnt signalling pathway components were not substantially altered. Only lines that maintained these normal parental C2C12 cell behaviours were used for later studies. However, there were still notable differences in the response of the Wnt reporter to Barx2 overexpression in the Tet-ON system relative to the previous transient over-expression system. As highlighted in Chapter 3, transient over-expression of Barx2 alone could activate TOPflash without the need for exogenously expressed MyoD, although the latter did produce a synergistic effect. In contrast, Dox-induced Barx2 expression alone was insufficient to induce transiently transfected TOPflash. One possible explanation for this is that in the stable Barx2 Tet-ON lines, Dox will induce Barx2 expression in every cell, but the level of expression *per cell* may be relatively low due to single or few copies of the integrated transgene. In contrast, transient transfection of C2C12 cells typically results in only a small percentage of cells receiving the plasmids, but they may then carry and express many copies *per cell*. When the TOPflash reporter plasmid is transiently transfected in Barx2 Tet-ON cells, the ratio between expression of effector (Barx2) and reporter (TOPflash) within any given cell may not be sufficient to produce reporter activation. In contrast, when C2C12 cells are co-transfected with TOPflash reporter and Barx2 expression plasmid, although only a small percentage of cells will be efficiently

transfected, these cells will receive and express both TOPflash and Barx2 plasmids. This hypothesis is consistent with the observation that co-transfection of MyoD and TOPflash, both presumably at high numbers of plasmid copies per transfected cell, still allowed synergy with the lower level of Dox-induced Barx2 produced in each cell. Overall, the important result was that Dox-induced Barx2 was able to activate TOPflash under appropriate conditions (additional MyoD) and hence, that the regulatory factors that cooperate with Barx2 in activation of Wnt target genes are likely to still be expressed in these stable cell lines.

Although examination of Barx2 mRNA levels in the absence of Dox-induction suggested that there was some leaky expression of the mCherry/2A/Barx2 expression cassette, analysis by western blots and fluorescence microscopy confirmed no Barx2 protein expression in the absence of Dox. This is consistent with previous data which has shown that a) Barx2 mRNA and protein levels following over-expression frequently do not correlate in myoblasts (Chapter 4) and b) C2C12 Barx2 stable lines produced by standard plasmid integration methods do not express any detectable Barx2 protein following the initial selection period (unpublished data). Collectively, these data suggest that Barx2 protein expression is suppressed in proliferating myoblast cultures, possibly because high levels of Barx2 protein are not compatible with continuing proliferation. In contrast, for short term expression of up to 48 hours, the Barx2 Tet-ON stable lines consistently and reliably produced Barx2 at both the message and protein level following induction by Dox, permitting discovery of potential Barx2 target genes by comparison of induced and uninduced states.

As discussed previously, Barx2 is induced during early stages of myoblast

differentiation and may be an important player in the proliferation-differentiation “switch”. This function may involve regulating other genes which further drive the differentiation process. The MRF family members MyoD, myogenin and Myf5, key regulators of myogenesis, were thus analysed as downstream targets of Barx2. Given that previous work has indicated that Barx2 can promote differentiation, the observation that myogenin mRNA expression was downregulated by Barx2 overexpression was unexpected. It would be of interest to assess whether protein levels of myogenin are up or down regulated by Barx2, and whether specific post-transcriptional regulators of myogenin function are altered. In contrast, the increased expression of Myf5 is more consistent with the pro-proliferation effects of Barx2 as Myf5 is typically associated with proliferating myoblasts.

The data presented in Chapter 4 identified Wnt-responsive target genes and pathway components that were misregulated in Barx2 knockout myoblasts compared to wildtype myoblasts, by means of both RNA-Seq and PCR arrays. This data was used to guide the selection of genes to screen within the Barx2 Tet-ON over-expression system. This led to selection of cyclinD1, cyclinD2, Axin2, Follistatin, growth differentiation factor 5 (Gdf5), paired-like homeodomain 2 (Pitx2), frizzled class receptor 7 (Fzd7), Wnt4, and transforming growth factor beta 3 (Tgfb3). Furthermore, matrix metalloproteinase-9 (MMP9) was selected as it was previously identified as a downstream target of Barx2 in breast cancer cells [Stevens & Meech 2006], and as a target of canonical Wnt signalling in T cells [Wu et al. 2007]. Other selected genes were shown to be Wnt-responsive in a variety of cell models including Id2 in colon cancer cells [Rockman et al. 2001; Willert et al. 2002], MMP2 in T cells [Wu et al.

2007], c-Myc in colon cancer cells [He et al. 1998; van de Wetering 2002] and P19 teratocarcinoma cells [Zhang et al. 2012] and Id3 in myoblasts [Zhang et al. 2012]. However, most of these putative Wnt-target genes showed no significant change in expression in Tet-ON C2C12 cells following treatment for 24 hours with Wnt3a, indicating their response to Wnt signalling may be cell-type specific. Of those that responded to stimulation by Wnt3a (cyclinD1, Axin2, Pitx2, Fst, Gdf5, Wnt4 and Tgfb3), only cyclinD1 and Axin2 also showed significantly increased expression in response to Barx2 induction. Importantly, this result was consistent with the previously presented RNA-Seq and microarray analyses of Barx2^{-/-} primary myoblasts, which identified both cyclinD1 and Axin2 as potential targets of Barx2 regulation in myoblasts. Moreover, cyclinD1 was also shown to be significantly downregulated in whole TA muscle isolated from Barx2^{-/-} mice when compared to Barx2^{+/+} littermate controls. In addition, expression of Axin2 mRNA was synergistically regulated by both Wnt3a treatment and Barx2 expression in C2C12 cells. This result was also consistent with studies described in Chapter 3, whereby Barx2 and Wnt3a/ β -catenin could synergistically activate the TOPflash reporter plasmid under specific conditions. It is of note that, unlike many downstream targets of the canonical Wnt signalling pathway, the Axin2 promoter contains multiple (eight) predicted TCF/LEF binding sites [Jho et al. 2002]; equivalent to the number of TCF/LEF elements present in TOPflash.

The Axin2-luc construct [Jho et al. 2002] which contains all eight predicted TCF/LEF sites was significantly activated by Barx2 and by constitutively active β -catenin. However, these factors only synergised under differentiation conditions, suggesting

that other differentiation-associated factors are required to mediate transcriptional cooperation at this promoter. Co-transfection of a dominant negative form of TCF4 (dnTCF4), that is able to bind DNA but not interact with β -catenin, abolished activation by β -catenin and Barx2, strongly suggesting that the promoter TCF/LEF binding sites were involved in the response.

CyclinD1 is a well-defined Wnt-target in many epithelial cell types [Shtutman et al. 1999; Tetsu & McCormick 1999; Schmidt-Ott et al. 2007; Bao et al. 2012] and the cyclinD1 proximal promoter containing a single TCF/LEF site was previously shown to respond modestly (2.5-fold) to Wnt signals [Botrugno et al. 2004]. Here, the cyclinD1 proximal promoter luciferase reporter construct was activated by both Barx2 and constitutively active β -catenin: although the level of promoter activation was low, an equivalent response was observed with both factors. Co-expression of dnTCF4 with either of these factors abolished activation, again highlighting the potential role of the single TCF/LEF site in Barx2-mediated activation of cyclinD1. Surprisingly, in contrast to previous observations using the TOPflash reporter (Chapter 3), there was no Barx2-MyoD synergy observed with either the Axin2 or cyclinD1 luciferase construct. The promoter specific mechanism(s) by which MyoD generates transcriptional synergy with Barx2 clearly requires further analysis, however, it is possible that both the number and the density of TCF/LEF motifs may be an important variable.

TCF/LEF genes have tissue-specific expression patterns [Oosterwegel et al. 1993; Korinek et al. 1998; Galceran et al. 1999] and loss-of-function studies have demonstrated a unique requirement for individual TCF/LEF genes in certain

developmental processes [Verbeek et al. 1995; Korinek et al. 1998; Merrill et al. 2004]. Although all TCF/LEF family members recognise similar DNA elements and interact with β -catenin, the above observations suggest that TCF/LEF family members are not redundant and may have different albeit overlapping functions. This may provide a mechanism by which Wnt-responsive target genes can be differentially regulated in a tissue-specific manner. In support of this idea, functional differences among TCF/LEF members in reporter gene assays, as well as differential promoter occupancy, have been observed [Atcha et al. 2003; Hecht & Stemmler 2003; Wohrle et al. 2007; Weise et al. 2010].

Mechanistically, TCF/LEF proteins function in the absence of β -catenin by recruiting corepressors such as Groucho family members and various HDACs. During the canonical Wnt response these corepressors are believed to be 'dismissed' by stabilized β -catenin, which in turn recruits coactivators. Some studies have reported that the response of specific target promoters to β -catenin requires addition of exogenous TCF/LEF proteins [Weiske & Huber 2005; Sanchez-Tillo et al. 2011], presumably because these factors mediate recruitment of β -catenin-mediated activation complexes to the DNA. However, previous work performed in the laboratory showed that hTCF4 overexpression strongly suppressed the activation of TOPflash by β -catenin or Barx2, possibly the high level of TCF4 expression overwhelmed the ability of these factors to dismiss TCF4-associated co-repressors from the promoter. Given this dichotomy, it was important to determine which TCF/LEF genes were expressed in myoblasts and whether any of them might in fact be able to promote Barx2 and/or β -catenin activation of Wnt-responsive genes.

Analysis of TCF/LEF family members expressed in C2C12 cells and primary myoblasts revealed similar levels of mRNA expression of Lef1, Tcf3 (Tcf7l1) and Tcf4 (Tcf7l2) but not Tcf1 (Tcf7). A recent study reported that all four family members are highly expressed at the protein level in C2C12 cells [Wallmen et al. 2012]. Due to time constraints, this potential discrepancy between the literature and results reported here was not able to be resolved.

The TCF/LEF family genes generate multiple isoforms through alternative splicing and promoter usage, thereby generating proteins which differ in domain composition. As discussed previously, there are certain structural features common to all members of the TCF/LEF family; an N-terminal β -catenin binding domain, interaction sites for Groucho/TLE co-repressors, and a HMG box DNA-binding domain [Arce et al. 2006; Hoppler & Kavanagh 2007]. In particular, TCF4 genes undergo extensive and tissue-specific alternate splicing [Duval et al. 2000; Howng et al. 2004; Weise et al. 2010] and the variant proteins exhibit different protein-protein interactions [Hecht & Stemmler 2003; Valenta et al. 2003] as well as DNA binding specificities [Atcha et al. 2007]. In particular, alternative splicing of *Tcf7l2* results in a variable C-terminus, classifying resultant proteins as either E, S or M isoforms [Young et al. 2002; Shiina et al. 2003]. Current literature suggests that the longer E-tail of TCF4E isoforms interacts with CBP/p300 [Hecht & Stemmler 2003] and that TCF4E variants exhibit promoter-specific activities that are not interchangeable with other isoforms or TCF/LEF family members [Atcha et al. 2003; Hecht & Stemmler 2003], possibly due to differences in their ability to form multimeric complexes with co-factors.

Here, six Tcf4 variants were cloned from C2C12 cells. Of note is that five of the six

clones were M isoforms; that is, they contained a truncated final exon lacking both the conserved cysteines and the CRARF/CRALF element (C-clamp). Furthermore, two of these variants were novel as they completely lacked exon 8, a finding that has previously not been reported. These variants, along with Lef1 and Tcf3, were tested for their ability to synergise with either β -catenin or Barx2 on the TOPflash reporter or Axin2-luc construct in luciferase assays. When tested in assays with the TOPflash reporter, all Tcf4 variants were highly repressive to β -catenin and Barx2-mediated activation, whilst Lef1 was synergistic with both in a concentration-dependent manner. In contrast, all Tcf4 variants, when co-transfected at a low concentration, synergised with β -catenin in activation of the Axin2-luc reporter construct. This indicates that all tested mouse Tcf4 isoforms, which include variations in exons 4, 8 and 13, but contain identical C-termini, have a similar ability to facilitate the β -catenin-mediated recruitment of coactivators to Axin2. Transfection of the hTCF4 variant (an E isoform containing the C-clamp), which was performed alongside the mouse variants, also led to synergy with β -catenin in a concentration-dependent manner. The dose-dependent effects of TCF/LEF proteins in these studies (synergy at low concentrations but inhibition at high concentrations) are consistent with the idea presented earlier that excessive levels of TCF/LEF-associated co-repressor complexes at the target promoter may overwhelm the ability of β -catenin to dismiss the repressors and recruit co-activators. No TCF/LEF family member or splice variant that was tested was able to synergistically activate the Axin2-luc reporter with Barx2 at any concentration. However, it still remains to be determined whether any Tcf1 isoform (not detected in this study but reported to be expressed in myoblasts by others) is involved in activation of Axin2 by Barx2. Overall these studies suggest that

TCF/LEF variants have non-redundant and dose-dependent functions in regulation of Wnt target promoters, including Axin2, in myoblasts.

Chapter 6

Regulation of the *Axin2* gene by
Barx2, Pax7 and Wnt signalling in
myoblasts

6.1 Introduction

Work presented in Chapters 4 and 5 of this thesis identified the Wnt-responsive genes *Axin2* and *cyclinD1* as downstream targets of Barx2 in myoblasts using a variety of models and experimental techniques. In particular, studies in Chapter 5 define the proximal promoter of *cyclinD1*, and the promoter/intronic region of *Axin2* as important for regulation by both Barx2 and β -catenin/Wnt signalling. However, these promoters contain many regulatory elements and whether their activation by Barx2 is mediated through HBS elements, TCF/LEF elements, or a combination of both, was not defined. This chapter will attempt to unveil these mechanisms using site directed mutagenesis and deletion analysis of promoter constructs, as well as epigenetic analysis of natural promoters. The majority of data presented and discussed within this chapter is published in a first-author paper in “Stem Cells” [Hulin et al. 2016].

6.1.1 Regulation of the *Axin2* gene by Wnt signals

Unlike most other Wnt-responsive targets which harbor only one or two TCF/LEF binding sites within their promoter, the region of the *Axin2* promoter capable of responding to Wnt signalling in reporter assays contains eight predicted TCF/LEF binding sites [Jho et al. 2002]. Furthermore, the majority of these are very close matches to the high-affinity consensus TCF/LEF sites used in TOPflash and TOPGAL reporters [van Beest et al. 2000]. *Axin2* is activated in many sites of Wnt signalling [Jho et al. 2002] and is therefore also the exception to the general observation that the transcriptional responses of Wnt target genes are tissue-specific. In addition to this, the *Axin2* gene product plays a critical role as a component of the β -catenin destruction complex [Behrens et al. 1998; Yamamoto et al. 1998; Stamos & Weis

2013] and its activation directly downstream of a Wnt signal thus places it in the role of a negative regulator of the Wnt pathway [Yan et al. 2001; Jho et al. 2002; Lustig et al. 2002]. Data in Chapter 4 also indicated that Barx2 is an indirect downstream target of Wnt signalling. The regulation of Axin2 expression by Barx2 suggests that Barx2 may in fact be part of the feedback network that attenuates or limits the duration of a Wnt-initiated signal in myoblasts. This idea will be further explored in this chapter.

6.1.2 Co-factors and epigenetic mechanisms involved in the transcriptional response to Wnt signalling

The initiation and regulation of transcription in eukaryotes is complex, and requires a myriad of factors including RNA polymerase machinery, general transcription factors, tissue-specific transcription factors, and co-activators and co-repressors [Perissi & Rosenfeld 2005]. Gene activation and repression requires the chromatin modifying activities of a large array of co-activators and co-repressors. Detailed kinetic analysis of the occupancy of co-activators and co-repressors at gene promoters reveals a highly dynamic process of co-factor exchange [Rosenfeld et al. 2006]. In addition, many co-activator and co-repressor proteins are components of multisubunit coregulator complexes that exhibit an ever-expanding diversity of enzymatic activities [Yoon et al. 2003; Rosenfeld et al. 2006; Santoso & Kadonaga 2006; Tsukada et al. 2006].

6.1.2.1 Histone acetylation

Epigenetic regulation, which controls the accessibility of promoter chromatin, has become increasingly recognised as important in both development and regeneration. One type of chromatin modification which plays an important role in the control of

gene transcription is histone acetylation. Histone acetyltransferases (HATs) and histone deacetylases (HDACs) modify the structure of chromatin by opening and compacting chromatin respectively. Hyperacetylation of histones appears to create a more permissive environment for gene expression by relaxing chromatin structure, thus making the DNA more accessible to modifying enzymes, transcription factors and RNA polymerase [Gorisch et al. 2005]. Highly acetylated histones are therefore generally associated with actively transcribed genes or genes poised for transcription [Marks et al. 2000; Schrem et al. 2002; Kurdistani et al. 2004]. Conversely, genes repressed by histone deacetylation are resistant to the influence of certain transcription factors that could otherwise activate their promoters. Thus, the balance between HATs and HDACs in terms of expression and recruitment to genomic loci establishes a pattern of histone acetylation for global gene expression [Grewal & Moazed 2003; Bannister & Kouzarides 2011]. Wnt-mediated gene transcription has been linked to the acetylation or deacetylation of histones, but how Wnt signalling regulates this type of histone modification during myogenesis is poorly understood. p300/CBP (CREB-binding protein), a well-studied coactivator of β -catenin/Wnt signalling, has intrinsic HAT activity [Ogryzko et al. 1996; Hecht et al. 2000; Takemaru & Moon 2000; Parker et al. 2008] and likely plays a synergistic role with β -catenin in alleviating promoter repression. Other HATs such as glucocorticoid receptor-interacting protein 1 (GRIP-1) have also been identified as co-activators via direct interaction with β -catenin [Li et al. 2004; Song & Gelmann 2005]. Conversely, in the absence of nuclear β -catenin, TCF/LEF members associate with HDAC1 at Wnt-responsive promoters, leading to transcriptionally silent chromatin until such point where HDAC1 is competitively displaced by β -catenin [Billin et al. 2000; Arce et al.

2009], and coactivator recruitment may thus occur.

6.1.3 Aims

The specific aims of this chapter were to:

1. Understand the mechanisms by which Barx2 acts as a positive regulator of Axin2 and cyclinD1 expression
2. Examine the role of Pax7 in regulation of Axin2 and cyclinD1 expression
3. Identify co-activators and co-repressors involved in the Barx2/ β -catenin/TCF activation complex and the Pax7/ β -catenin/TCF repression complex respectively

6.2 Methods

6.2.1 Expression plasmids

HA-tagged Grip-1 in the pSG5 vector was a kind gift from Dr. Michael Downes. Other co-activators were obtained from Addgene: PGC-1 alpha in pcDNA4-myc (plasmid 10974) [Ichida et al. 2002], PCAF-FLAG in pCI (plasmid 8941) [Yang et al. 1996] and HA-UTX in pCMV (plasmid 24168) [Agger et al. 2007]. ACTR, Carm1 and CBP plasmids were already available in the laboratory, but were originally from the Evans lab at the Salk Institute for Biological Studies. HDAC1-FLAG in pcDNA3 was also obtained from Addgene (plasmid 13820) [Emiliani et al. 1998].

All primers used for cloning and generation of mutations are listed below in Table 6.1. The Axin2 promoter/intron luciferase reporter construct was obtained from Addgene (plasmid 21275) [Jho et al. 2002]. The consensus TCF/LEF sites in the mouse Axin2 promoter (T2, T3, T4, T5, T6, T7, T8; nomenclature from [Jho et al. 2002]), were

mutated by the introduction of three nucleotide substitutions that disrupted the core of each motif (ga(a/t) to cgc). For mutation of site T2, a 2.6 kb fragment of Axin2 promoter containing the T2 element was excised (using *PstI/Spel* sites) and ligated in to the PCR-Blunt vector. Site directed mutagenesis (SDM) was then performed using the QuikChange SDM protocol. After the T2 mutation was confirmed, the 2.6 kb promoter fragment was ligated back into the parent Axin2 luciferase promoter construct. Removal of the HBS cluster from the 5' end of the Axin2 luciferase promoter was performed by digestion of the promoter fragment from the parent vector using *XbaI* and *HindIII* sites and then ligation of the truncated Axin2 promoter fragment (missing the HBS cluster) into pGL3-Basic using *NheI* and *HindIII* sites to generate Axin2 Δ HBS. All mutagenesis thereafter was performed using GeneArt PLUS Seamless Cloning and Assembly Kit (Life Technologies). Triple mutation of TCF/LEF elements T3, T4 and T5 was performed simultaneously in the truncated Axin2 promoter to generate Axin2 Δ HBS T2-5 SDM. Subsequent triple mutation of elements T6, T7, and T8 was performed simultaneously in the Axin2 Δ HBS T2-5 SDM to generate a construct with every TCF/LEF site mutated (Axin2 Δ HBS T2-8 SDM). This required transfer of a *Spel-HindIII* fragment into PCR Blunt for mutagenesis as previously described and then religation of this fragment back into the Axin2 Δ HBS T2-5 SDM vector. All transformations were performed in high efficiency DH10 β cells (NEB). The nomenclature of the mutated Axin2 promoter constructs was based on previous work [Jho et al. 2002].

The cyclinD1 promoter luciferase reporter construct was a kind gift from Dr. Johann Auwerx [Botrugno et al. 2004]. Removal of the HBS motifs from the 5' end of the

construct was performed by PCR amplification with an internal forward *KpnI* primer and a reverse *HindIII* primer. This fragment was then ligated back in to empty pGL3-Basic to generate cyclinD1 Δ HBS. Mutagenesis of the single TCF/LEF element was performed using the QuikChange SDM protocol.

Swapping of the homeodomain regions between Barx2 and Pax7 cDNAs was performed by amplifying both homeodomain regions by PCR using primers that introduced *NheI* sites at each end, and then inserting these fragments into Barx2 and Pax7 expression constructs from which the corresponding homeodomain regions had been removed [Zhuang et al. 2014].

6.2.2 Electrophoretic mobility shift assay

6.2.2.1 Preparation of nuclear extracts

Nuclear extracts of C2C12 and HEK293T cells for use in electrophoretic mobility gel shift assays (gel shifts) were prepared as follows. Cell monolayers grown in T75 flasks were washed once with cold 1 x PBS, and then scraped from the flasks in 10 ml cold PBS with PIC. Cells were pelleted at 2500 rpm for 5 minutes at 4°C, supernatant was removed and cells were resuspended in 400 μ l Hypotonic Lysis Buffer followed by a 15 minute incubation on ice. Nuclei were pelleted by centrifugation at 14,000 rpm for 1 minute at 4°C and resuspended in 40-50 μ l of Nuclear Extract Buffer. Lysis of nuclei was promoted by a 30 minute incubation at 4°C with agitation. Debris was removed by centrifugation at 14,000 rpm, 4°C for 10 minutes and the supernatant was snap-frozen on dry ice and stored at -80°C until required. Protein concentration of extracts was determined by spectrophotometry using the following equation: Concentration (μ g/ μ l) = (1.55*A₂₈₀) – (0.76*A₂₆₀) * dilution factor. Buffer details are

listed in Appendix 2.

6.2.2.2 Preparation of non-radioactive DNA probes

As an alternative to traditional radio-labelled oligonucleotide probes for electrophoretic mobility shift assays, oligonucleotide probes can be labelled with biotin or a fluorophore [Jullien & Herman 2011]. The method employed here is called LUEGO (labelled universal electrophoretic gel shift oligonucleotide) and involves a labelled universal oligonucleotide that could hybridize to the oligonucleotide duplex containing the protein binding sequence of interest forming a tripartite complex [Jullien & Herman 2011]. To achieve this complex, one of the probe oligonucleotides is extended at its 3' end with a sequence complementary to the LUEGO oligonucleotide. The advantage of this approach is that only one labelled oligonucleotide needs to be generated, and it can then be used to make multiple different probes, saving time, effort and cost. The sequence of LUEGO is 5'-GTGCCCTGGTCTGG-3' as described by Jullien and Herman and contains no binding sites for known transcription factors [Jullien & Herman 2011]. The LUEGO probe used for these studies was double-labelled with Cy5 fluorophores at the 5' and 3' ends.

The sequences of all oligonucleotides used in gel shift assays are listed in Table 6.1. All oligonucleotide probes were stored at 100 μ M stock concentration. Double-stranded oligonucleotide probes were made by annealing 2 μ l LUEGO 2xCy5 oligonucleotide, 2 μ l sense oligonucleotide (that includes a region complementary to the LUEGO sequence) and 1 μ l anti-sense oligonucleotide in a total 50 μ l of annealing buffer (10 mM Tris pH 8, 1 mM EDTA, 50 mM NaCl). Oligonucleotides were heated to 95°C for 2 minutes, rapidly cooled to 70°C for 2 minutes (5°C/sec), and then slowly

cooled to 18°C (ramp rate of 0.4%, corresponding to 1.2°C/minute) using a gradient cycler. Double-stranded probes were diluted 1:10 before use.

6.2.2.3 Gel shift

Gel shift reactions were carried out with 30 µg nuclear extract and 0.4 µg deoxyinosine-deoxycytidine polymer (dIdC) in a 15 µl reaction containing EMSA buffer (10 mM Tris pH 8, 100 mM NaCl, 1 mM MgCl₂, 20% glycerol). The labelled double-stranded oligonucleotide probe (2 µl) was added to the reaction mixture, and samples were incubated for 20 minutes at room temperature. To elucidate the identity of proteins in a DNA-protein complex, 2 µg of antibody was added directly after the addition of the labelled probe (supershift assay). DNA-protein complexes were resolved in 0.5x TBE (45 mM Tris-borate, 1 mM EDTA) on 5% non-denaturing polyacrylamide gels at 80V for 1 hour and 45 minutes at 4°C. Gels were then imaged on the Typhoon FLA9000 scanner (GE Healthcare) for Cy5 visualisation.

Table 6.1: List of all primers used during this chapter

<u>Name</u>	<u>Sequence</u>
<u>Mutagenesis/Deletions</u>	
Axin2 T2 SDM F	gcgctttcgc <u>ca</u> aggtcctggcaactca
Axin2 T2 SDM R	ggaccttgcgaaagcgcagccggctc
Axin2 T3 SDM F	cggccgcgcctttcgc <u>gt</u> gcacagttaaadc
Axin2 T3 SDM R	gatttaactgtgcacgc <u>g</u> aaaggcgcgagccg
Axin2 T4+5 SDM F	cggcgcgctttcgc <u>gt</u> gcggggcggcgctttcgcggttgca
Axin2 T4+5 SDM R	ggcctgccaacgcgaaagcgcgcccccgcacgcgaaagcgc
Axin2 F Pst	ctctctggccctttgctgcagcccggttctttc
Axin2 R Spe	ggatgggaggggggagactagtggggaagaag

Axin2 T6 SDM F	tttaaaagtttgaaggcgaaagcctctaagtta
Axin2 T6 SDM R	taacttagaggctttcgcttcaaactttttaa
Axin2 T7 SDM F	tcagatttcgctttcgcaaagctgctcgat
Axin2 T7 SDM R	atccgacgcagctttcgaaaggcgaaatctga
Axin2 T8 SDM F	ttactttcttgctttcggttgggtagatctgg
Axin2 T8 SDM R	ccagatctaccaacgcgaaagcaagaaagtaa
CyclinD1 F Kpn	gcggtaccggccaccatcttgagctgttg
CyclinD1 R HindIII	gcaagcttatgggtctccacttcgcagcac
CyclinD1 TCF SDM F	ccggctttcgctctgcttaacaacag
CyclinD1 TCF SDM R	aagcagaggcgaaagccgggcagagaaa
<u>Gel shift</u>	
LUEGO	gtgccctggtctgg
Axin2 T3 WT Top	ggctcgcgcctttgaagtgcacag
Axin2 T3 WT Bottom	ctgtgcacttcaaaggcgcgagccccagaccagggcac
Axin2 T3 mut Top	ggctcgcgcctttcgctgacacag
Axin2 T3 mut Bottom	ctgtgcacgcgaaaggcgcgagccccagaccagggcac
3xTCF cons Top	agatcaaaggagatcaaaggagatcaaaggag
3xTCF cons Bottom	ctcctttgatctcctttgatctcctttgatctccagaccag
HBS Top	ccaattatatttcaataattatctg
HBS Bottom	cagataattattgaaatataattggccagaccagggcac
<u>Chromatin Immunoprecipitation</u>	
TOPflash CHIP F	ccgagctcttacgcgagatc
TOPflash CHIP R	caagctggaattcgagcttcc
β 2-microglobulin CHIP F	cggagaatgggaagccgaacat
β 2-microglobulin CHIP R	gtgaggcgggtggaactgtgt
Axin2 T3 F	tacctcccttccaggacc

Axin2 T3 R	cctccgggcgcttccaac
Axin2 T4/5 F	ggagtgcgccagcggatc
Axin2 T4/5 R	agcgcgccccgaaatagc
Axin2 HBS F	ccagtttctaggcaaccatg
Axin2 HBS R	gcccggtctttaactcac
Axin2 T7/8 F	ccaacatcaaagcaagaaag
Axin2 T7/8 R	gcctttgaaaaagctgcgtcg
Axin2 T2 F	gcctctgtgattggcgcg
Axin2 T2 R	gggctgttactgagttgc
<u>siRNA</u>	
Pax7 sense	tgtctccaagattctgtgccgatat
Pax7 antisense	acacagaggttctaagacacggctata

6.3 Results

6.3.1 Barx2-mediated activation of Axin2 and cyclinD1 is regulated through TCF/LEF motifs

As discussed briefly in Chapter 5 (Section 5.3.5), co-transfection of full length Barx2 plasmid with a 1 kb cyclinD1 promoter construct or a 6 kb Axin2 promoter/intron construct identified Barx2 as an activator of both genes via these proximal regions within C2C12 cells. Here, the mechanism of the Barx2-mediated activation was further investigated through generation of extensive mutagenesis and deletion promoter constructs. The wildtype cyclinD1 promoter construct (referred to as just cyclinD1) contains a single TCF/LEF binding motif approximately 100 bp upstream of the transcription start site and four potential HBS motifs, all further upstream of the TCF/LEF element (Figure 6.1A). Although the level of cyclinD1 promoter activity

observed after Barx2 over-expression in C2C12 cells was not very high, the induction was consistent across multiple experiments and was similar to the level of activation observed after transfection of constitutively active (ca.) β -catenin. To determine the role of the HBS motifs in the cyclinD1 promoter, a promoter construct lacking the upstream HBS motifs (cyclinD1 Δ HBS) was generated. Unexpectedly, removal of the HBS motifs resulted in a greater activation by Barx2 (1.8-fold to 2.8-fold), but not by ca. β -catenin (Figure 6.1B), suggesting a repressive function for Barx2 via the HBS elements. Next, the role of the single TCF/LEF motif in Barx2-mediated activation was investigated. Site directed mutagenesis of the TCF/LEF motif in the context of both the WT (cyclinD1 TCF SDM) and the Δ HBS (cyclinD1 Δ HBS TCF SDM) promoters was performed in order to mutate the essential core of the binding site (CTTTGAG to CTTTCGC). In both cases, transfection of Barx2 or ca. β -catenin failed to activate the promoters containing a mutated TCF/LEF binding site (Figure 6.1B).

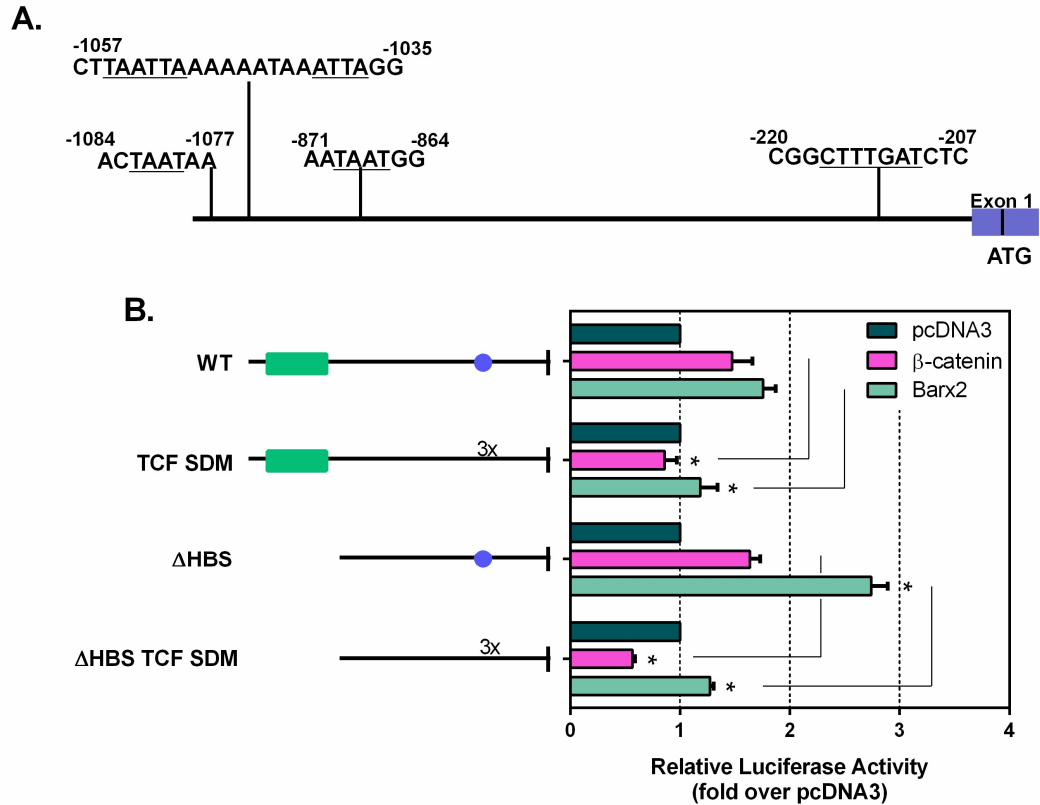


Figure 6.1: Barx2-mediated regulation of cyclinD1 is regulated through a TCF/LEF motif

(A): Schematic of the cyclinD1 proximal promoter luciferase construct. The single TCF/LEF binding site and four potential HBS are underlined. (B): Left: schematic of cyclinD1 promoter mutants. Green – HBS cluster; blue – TCF/LEF binding site; 3x – triple mutation in TCF/LEF motif. Right: cyclinD1 promoter constructs (0.5 μ g) were co-transfected with Barx2 or β -catenin (1 μ g) in to C2C12 myoblasts. Transfection of empty pcDNA3 vector served as a negative control. Luciferase activity was assayed 48 hours post transfection. All data are normalised to a Renilla luciferase internal control, expressed as the mean firefly/Renilla luciferase ratio. Data were then normalised to the promoterless pGL3-basic vector, and then to pcDNA3 empty vector transfection (set to a value of 1). The results shown are the average of at least three independent experiments performed in triplicate. Error bars represent SEM. * $p < 0.05$ relative to WT unless otherwise marked.

The Axin2 6 kb promoter/intronic region (designated Axin2-luc) contains 8 putative TCF/LEF binding sites (T1-T8), some of which are highly conserved between human and mouse [Jho et al. 2002]. Similar to the cyclinD1 promoter, there are also numerous HBS motifs, the majority of which are clustered at the 5' end of the Axin2-luc construct and hence upstream of the TCF/LEF motifs (Figure 6.2A). Truncation of

Axin2-luc removed all but one HBS motif as well as the T1 site. Similar to the result observed with the cyclinD1 promoter, removal of the HBS cluster did not diminish the ability of Barx2 to activate the Axin2-luc construct, and in fact modestly (but not significantly) increased activation (Figure 6.2B). To determine if Barx2 regulation of Axin2 was mediated through one or multiple of the TCF/LEF motifs, promoter constructs harbouring mutations within these elements were generated step-wise. Firstly, a triple nucleotide mutation was introduced within the T2 motif of the Axin2-luc construct. As shown in Figure 6.2B, this was not sufficient to alter the levels of β -catenin or Barx2-mediated activation. The same triple nucleotide mutations were then introduced into sites T3, T4 and T5 simultaneously within the previously T2-mutated construct (Axin2 Δ HBS T2-5 SDM). With all four TCF/LEF elements mutated, approximately 50% decrease in Barx2 and β -catenin mediated activation was seen (Figure 6.2B). Further mutation of the T6 and T7/T8 sites within the context of the T2-T5 SDM Axin2-luc construct abolished all activation by β -catenin, however there was still residual Barx2-mediated activation. It is possible that the residual activation seen with Barx2 is mediated through the one remaining proximal HBS motif, or other as yet undefined motifs.

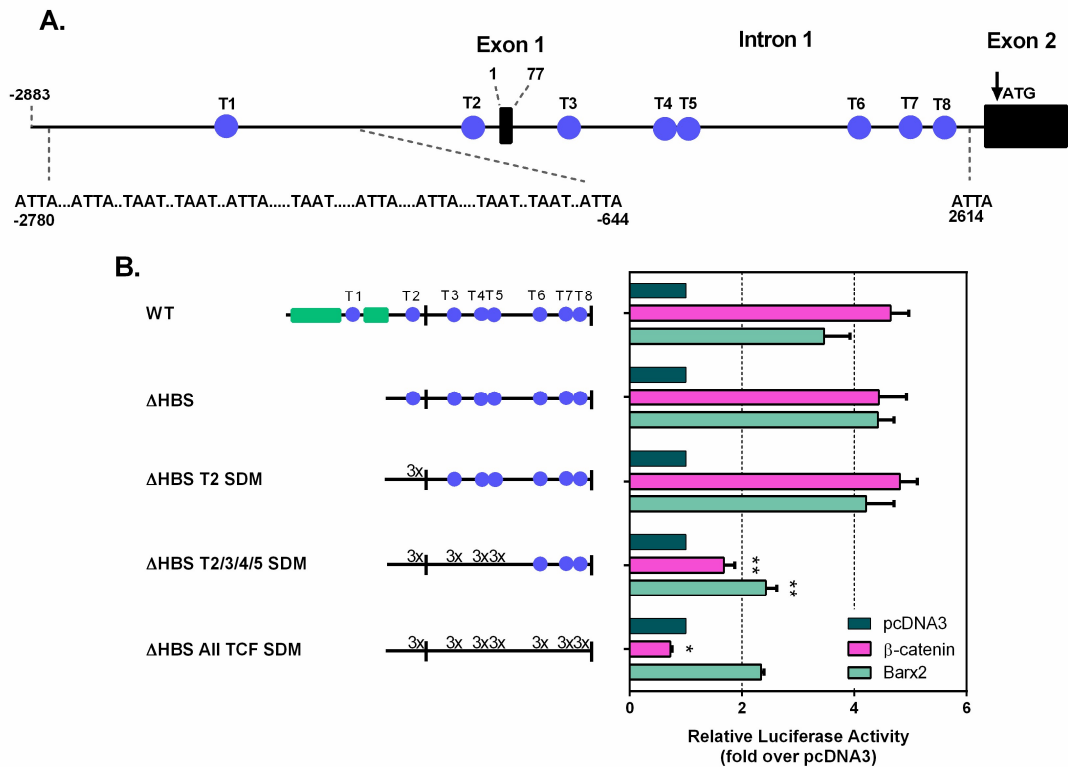


Figure 6.2: Barx2-mediated regulation of Axin2 is regulated through TCF/LEF motifs

(A): Schematic of the Axin2 promoter/intronic luciferase construct. Blue circles – TCF/LEF binding sites, designated T1 – T8. Adapted from Jho et al. (2002). (B): Left: schematic of Axin2 promoter mutants. Green – HBS cluster; blue – TCF/LEF binding site; 3x – triple mutation in TCF/LEF motif. Right: Axin2 promoter constructs (0.5 μg) were co-transfected with Barx2 or β-catenin (1 μg) in to C2C12 myoblasts. Transfection of empty pcDNA3 vector served as a negative control. Luciferase activity was assayed 48 hours post transfection. All data are normalised to a Renilla luciferase internal control, expressed as the mean firefly/Renilla luciferase ratio. Data were then normalised to the promoterless pGL3-basic vector, and then to pcDNA3 empty vector transfection (set to a value of 1). The results shown are the average of at least three independent experiments performed in triplicate. Error bars represent SEM. * $p < 0.05$ and ** $p < 0.001$ relative to WT unless otherwise marked.

6.3.2 The C-terminal activation domain and homeodomain of Barx2 are required for Axin2 and cyclinD1 promoter regulation

As previously discussed in Chapters 2 and 3, Barx2 contains a centrally located homeodomain (HD) and adjacent 17 amino acid Barx basic region (BBR) that together (HDBBR) mediate DNA-binding. This region is flanked by N- and C-terminal domains [Edelman et al. 2000]. To identify the domains of Barx2 responsible for the activation

of the cyclinD1 and Axin2 promoters, Barx2 expression constructs containing different protein domains were co-transfected with promoter-luciferase constructs in C2C12 cells. Studies performed using the WT cyclinD1 promoter showed that Barx2 HDBBRC was slightly more activating than FL Barx2 (1.9-fold compared to 1.6-fold) while Barx2 NHDBBR was not able to activate WT cyclinD1 (Figure 6.3A). In contrast the 5'-truncated cyclinD1 Δ HBS promoter was significantly activated by all three Barx2 constructs: 2.8-fold with FL Barx2, 2.5-fold with HDBBRC and 2-fold with NHDBBR. This is consistent with previous observations that the HBS elements located at the 5' end of the cyclinD1 promoter have a repressive function. Mutation of the single TCF/LEF motif in the cyclinD1 promoter (cyclinD1 Δ HBS TCF SDM) blocked the majority of activation observed with any of the aforementioned Barx2 expression constructs (Figure 6.3A).

The Axin2-luc construct was activated by both Barx2 HDBBRC and NHDBBR, although HDBBRC was much more potent (Figure 6.3B). When these Barx2 domains were co-transfected with the Axin2 Δ HBS T2-5 SDM promoter reporter construct, a 50% reduction in activation was observed for HDBBRC when compared to the WT Axin2-luc construct, but the level of activation produced by NHDBRR remained the same (Figure 6.3C). Progressive truncation of the Barx2 C-terminus led to decreasing activation of this Axin2-luc promoter, and the HDBBR region alone was not sufficient to activate the promoter. Similarly, a Barx2 construct lacking the homeodomain (Δ HD) was unable to activate the Axin2 promoter (Figure 6.3B). Overall these data showed that the different Barx2 protein domains functioned similarly in regulation of the Axin2, cyclinD1 and TOPflash (Chapter 5) promoters, consistent with functioning

via a similar mechanism that involves recruitment to TCF/LEF elements and likely interaction of coactivators with the C-terminal domain.

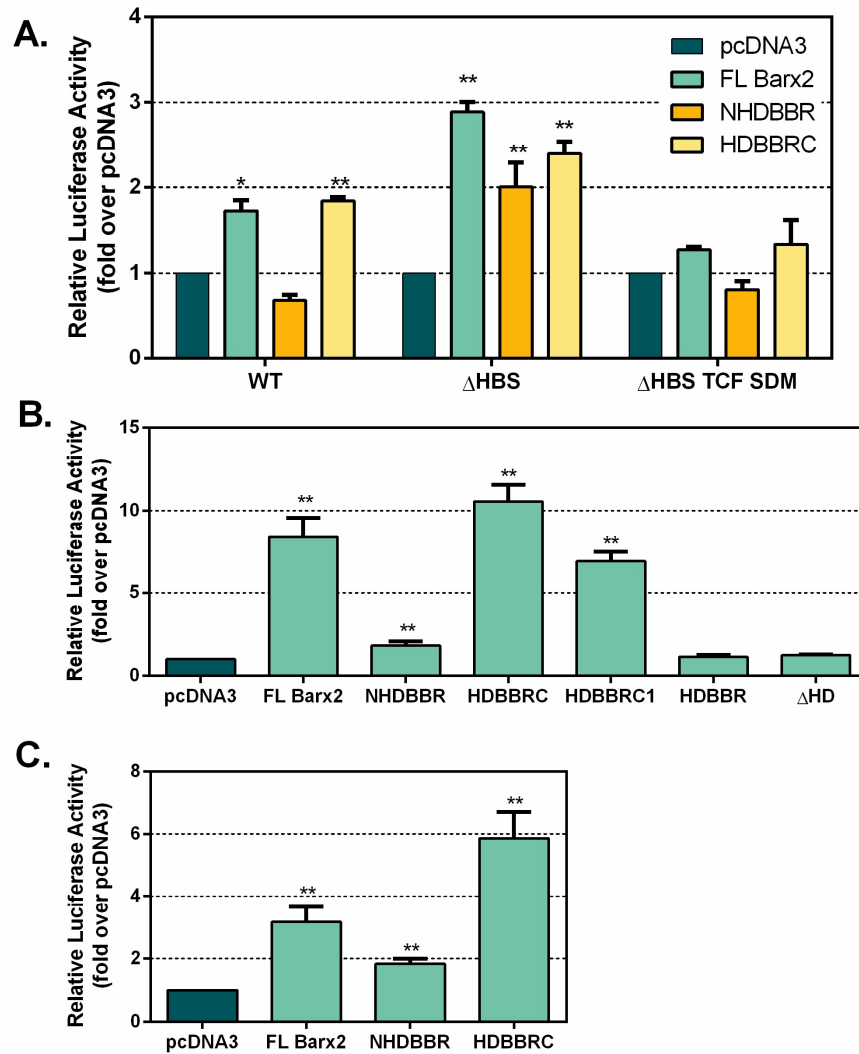


Figure 6.3: Activation of Axin2 and cyclinD1 promoter constructs by Barx2 domains

cyclinD1 (A), Axin2-luc (B) or Axin2 T2-5 SDM (C) promoter constructs (0.5 μ g) were co-transfected with Barx2 domain constructs (1 μ g) in to C2C12 myoblasts. Transfection of empty pcDNA3 vector served as a negative control. Luciferase activity was assayed 48 hours post transfection. All data are normalised to a Renilla luciferase internal control, expressed as the mean firefly/Renilla luciferase ratio. Data were then normalised to the promoterless pGL3-basic vector, and then to pcDNA3 empty vector transfection (set to a value of 1). The results shown are the average of two independent experiments. Error bars represent SEM. * $p < 0.05$ and ** $p < 0.001$ relative to pcDNA3. $n=6$.

6.3.3 Barx2 binds to the Axin2 T3-5 intronic region and promotes recruitment of β -catenin

To determine whether exogenously expressed Barx2 is recruited to the endogenous Axin2 promoter in C2C12 cells, CHIP assays were performed. The stable C2C12 cell line carrying an integrated TOPflash promoter/luciferase reporter (TOPPuro) was used so that recruitment of Barx2 to TOPflash (Chapter 3 [Zhuang et al. 2014]) could be used as an internal positive control. Following Barx2 transfection, a 2.3-fold enrichment of the Axin2 T3 promoter region was observed in samples immunoprecipitated with Barx2 antibodies, and an enrichment of 3-fold of the same region was observed in samples immunoprecipitated with β -catenin antibodies (Figure 6.4). Although the fold enrichment was not high, it was extremely consistent (data shown are the average of 3-9 experiments per condition). This indicated that exogenously expressed Barx2 could recruit endogenous β -catenin to the Axin2 promoter in the absence of β -catenin over-expression or stabilization by Wnt3a treatment. As a control, recruitment of exogenously expressed ca. β -catenin was demonstrated using the same β -catenin antibodies. The binding of Barx2 to the HBS elements located between 1.5-3 kb upstream of the T3 motif was assessed in the same CHIP samples, and Barx2 was not found to be recruited to this region (Figure 6.4). Overexpression of the Barx2 Δ HD construct followed by CHIP with Barx2 antibodies resulted in no enrichment of Axin2 T3 promoter DNA, thus indicating that the Barx2 homeodomain is necessary for the recruitment of Barx2 to the Axin2 TCF/LEF elements. As shown in Figure 6.4, no Axin2 promoter enrichment was observed with Barx2 or β -catenin antibodies when cells were transfected with empty pcDNA3 vector, indicating no occupancy by these factors under basal conditions.

Recruitment of these factors, under the same conditions, was also examined at the Axin2 T4/5 region. However, this genomic region showed consistent poor amplification in C2C12 cells and was thus unable to be assessed.

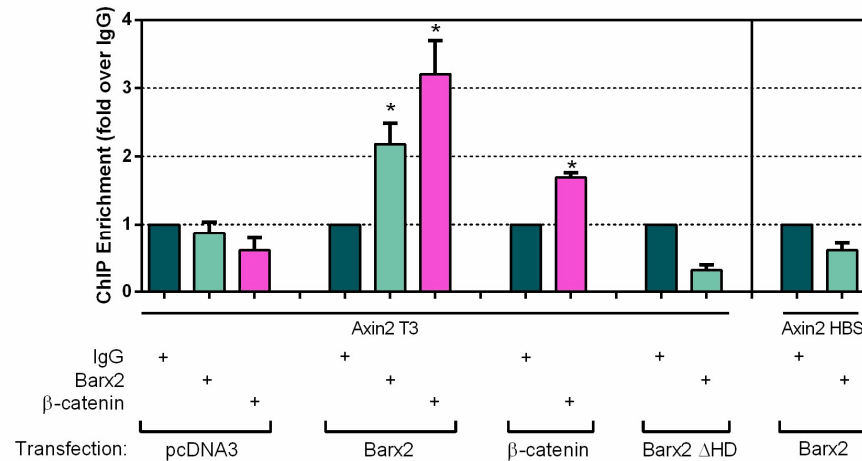


Figure 6.4: ChIP analysis of Barx2 recruitment to the Axin2 promoter after heterologous overexpression

ChIP was performed on chromatin from the C2C12 TOPPuro stable cell line following transfection of empty vector, Barx2, β-catenin or Barx2 ΔHD. ChIP was performed with 2 μg of the indicated antibodies. Data are PCR amplification values for the Axin2 T3 region or the Axin2 HBS region, normalised to amplification values for a control non-target locus (β2-microglobulin), with enrichment values for each antibody subsequently normalised to the mock ChIP with preimmune IgG, set to a value of 1. The results shown are the average of three to nine independent experiments. Error bars represent SEM. * p < 0.05 relative to IgG controls.

As detailed in Chapter 4, endogenous Barx2 expression is induced by Wnt3a treatment in primary myoblasts [Zhuang et al. 2014], suggesting that it may be involved in induction of the Axin2 promoter by Wnt/β-catenin. For an understanding of endogenous Barx2 recruitment to TCF/LEF motifs under these conditions, ChIP was performed in primary myoblasts which had been cultured in the presence of either L-cell CM or Wnt3a CM for 24 or 48 hours. As shown in Figure 6.5, ChIP with Barx2 antibodies at 48 hours post Wnt3a treatment produced approximately 2 to 4-fold

enrichment of DNA corresponding to the Axin2 promoter T3 and T4/5 regions, indicating that endogenous Barx2 is recruited to these elements after induction by Wnt3a. No significant enrichment of the same DNA regions by Barx2-ChIP was observed at 24 hours post Wnt3a treatment, consistent with the low level of Barx2 mRNA induction previously observed at this time point (Chapter 4, Section 4.3.8). Contrastingly, 24 hours of Wnt3a treatment was sufficient to observe recruitment of endogenous β -catenin to TCF/LEF sites (3-fold). The level of β -catenin recruitment was increased by longer Wnt3a stimulation (7-fold). ChIP with either Barx2 or β -catenin antibodies in the L-cell control condition resulted in no enrichment of DNA corresponding to the Axin2 T3/4/5 regions, indicating low or non-existent basal binding of these factors in the absence of Wnt3a stimulation.

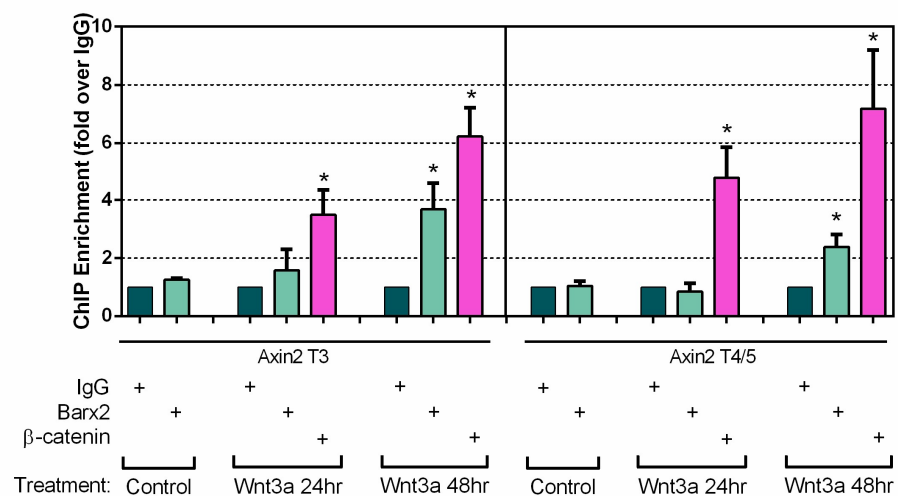


Figure 6.5: ChIP analysis of Barx2 and β -catenin recruitment after Wnt3a stimulation in primary myoblasts

ChIP was performed on chromatin from primary myoblasts following treatment with a 1:2 dilution of Wnt3a CM for 24 or 48 hours. ChIP was performed with 2 μ g of the indicated antibodies. Data are PCR amplification values for the Axin2 T3 region or the Axin2 T4/5 region, normalised to amplification values for a control non-target locus (β 2-microglobulin), with enrichment values for each antibody subsequently normalised to the mock ChIP with preimmune IgG, set to a value of 1. The results shown are the average of three to six independent experiments. Error bars represent SEM. * $p < 0.05$ relative to IgG controls.

Under the same transfection conditions in C2C12 cells described above, recruitment of both Barx2 and β -catenin to the remaining TCF/LEF motifs within the Axin2 proximal promoter/intronic region was assessed. Recruitment to these motifs (T2 and T7/8) was very poor and inconsistent between experiments (Figure 6.6). This result is consistent with luciferase assay data demonstrating that these motifs have no role in Barx2-mediated regulation of the Axin2 promoter.

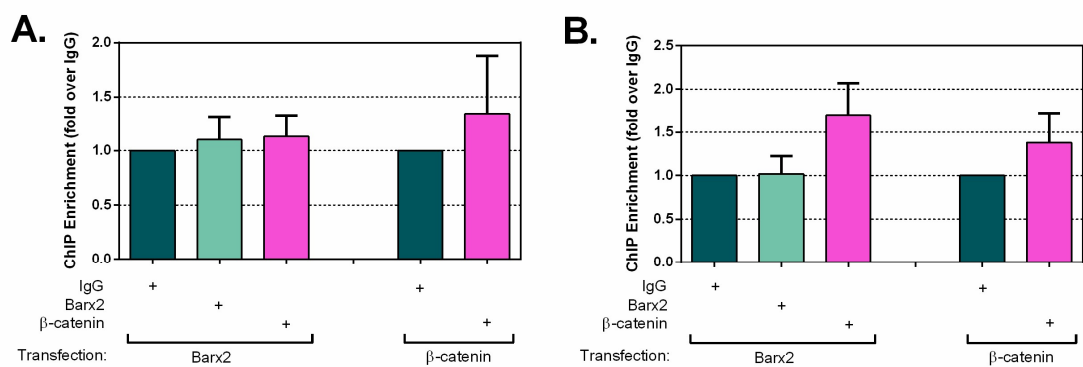


Figure 6.6: ChIP analysis of Barx2 and β -catenin recruitment to distal Axin2 TCF motifs

ChIP was performed on chromatin from the C2C12 TOPPuro stable cell line following transfection of Barx2 or β -catenin. ChIP was performed with 2 μ g of the indicated antibodies. Data are PCR amplification values for the (A) Axin2 T2 region or the (B) Axin2 T7/8 region, normalised to amplification values for a control non-target locus (β 2-microglobulin), with enrichment values for each antibody subsequently normalised to the mock ChIP with preimmune IgG, set to a value of 1. The results shown are the average of two independent experiments. Error bars represent SEM. n=6.

6.3.4 Barx2 cannot bind to oligonucleotide probes containing TCF/LEF motifs in vitro

To determine whether the recruitment of Barx2 to the Axin2 promoter/intronic region that is enriched in ChIP assays is mediated by a specific interaction of Barx2 with TCF/LEF elements, gel shift assays were performed. Three double-stranded oligonucleotide probes were prepared containing: 1) three copies of the consensus

TCF/LEF motif found in the TOPflash reporter (3xTCFcons), 2) the wildtype Axin2 'T3' TCF/LEF motif (Axin2 T3-wt) and 3) the mutated Axin2 T3 motif (Axin2 T3-mut). These probes were incubated with nuclear extracts as described in Methods (Section 6.2.3). Nuclear extracts were prepared from C2C12 cells transfected with either empty vector, TCF4, or β -catenin expression plasmids using the previously described high efficiency transfection method (Lipofectamine 2000)

The binding of nuclear extract proteins to a labelled oligonucleotide probe can be observed by the formation of one or more DNA-protein complexes with differing mobility to the free probe when separated on a native polyacrylamide gel. An intense DNA-protein complex was observed with TCF4 transfected nuclear extract and the Axin2 T3-wt probe, as shown in Figure 6.7A and B (Lane 3). This same DNA-protein complex was also weakly observed in control-transfected nuclear extracts, and presumably represents the interaction of the consensus probes with endogenous TCF proteins (Figure 6.7B (Lane 1)). A weaker DNA-protein complex, migrating slightly higher, was observed with β -catenin transfected nuclear extract and the same probes (Figure 6.7B (Lane 2)), and likely represents a complex including both TCF and β -catenin. Consistent with this, the formation of this complex was blocked by the addition of anti- β -catenin antibody but not by control IgG or a non-specific human anti-HNF4 α antibody (Figure 6.7C). As shown in Figure 6.7A and B, none of the aforementioned complexes were observed with the probes containing mutated TCF/LEF motifs. When nuclear extracts prepared from Barx2-transfected C2C12 cells were tested, no specific DNA-protein complexes were observed with the Axin2 T3-wt probe that were not also observed with the corresponding mutant probes. Similar

results were obtained following lentiviral transduction of C2C12 cells and primary myoblasts with Barx2 expression constructs (not shown).

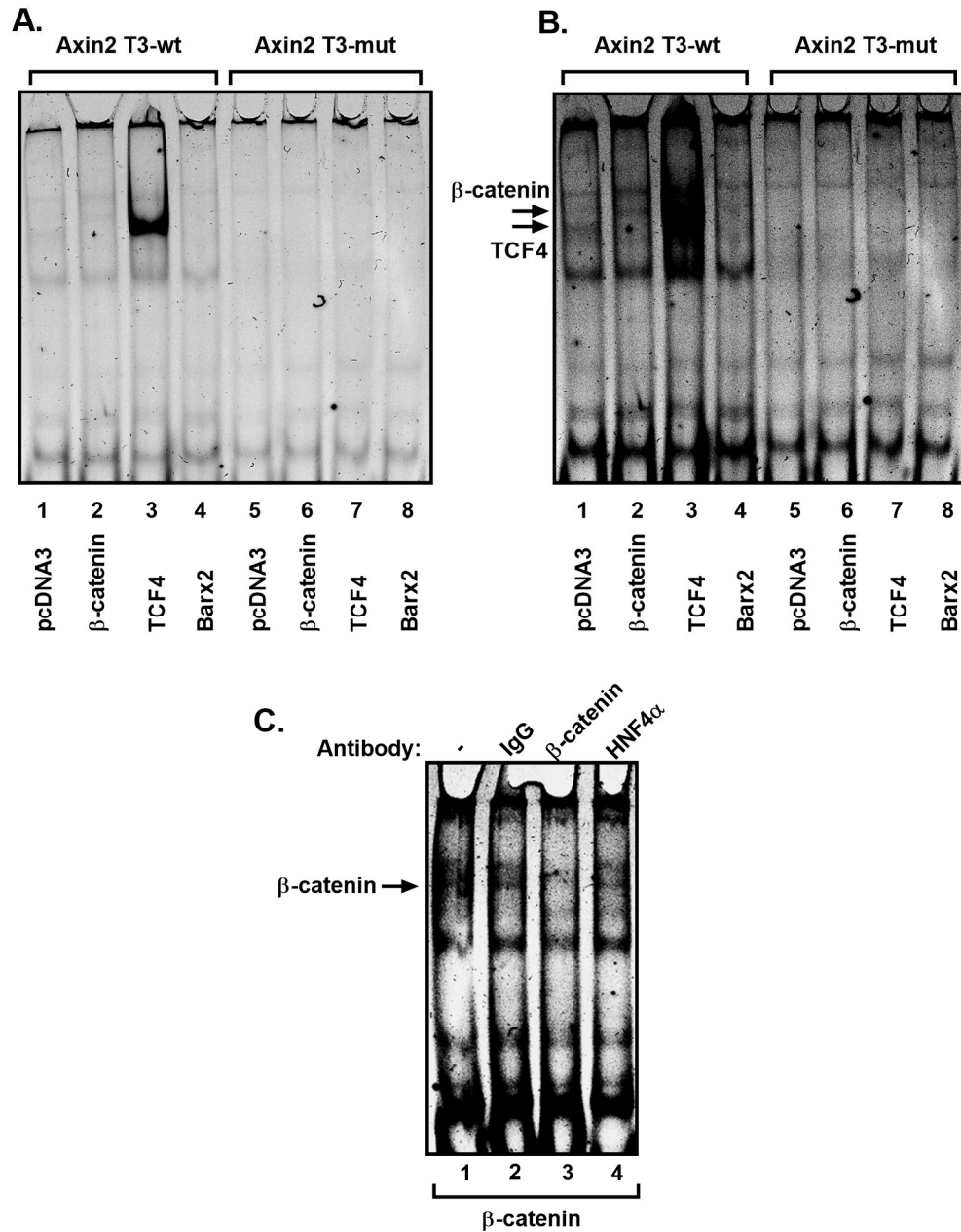


Figure 6.7: Gel shift assays with C2C12 nuclear extracts

Double-stranded oligonucleotide probes corresponding to the wildtype and mutant Axin2 T3 site were incubated with C2C12 nuclear extracts and resolved on a 5% non-denaturing polyacrylamide gel. (A) and (B) show the same image with a difference in image intensity to demonstrate the intensity of the TCF4-DNA complex compared to the β -catenin-DNA complex. (C): Double-stranded oligonucleotide probes corresponding to the wildtype Axin2 T3 site were incubated with β -catenin-transfected C2C12 nuclear extracts and the indicated antibodies (3 μ g).

Due to a concern about Barx2 protein stability in C2C12 cells, combined with the relative inefficiency of C2C12 cell transfection, gel shift assays were also performed using extracts from Barx2-transfected HEK293T cells. Furthermore, as a control for Barx2-DNA binding, a probe containing multiple optimal HBS consensus elements (HBScons) was also prepared. With HEK293T extracts, a DNA-protein complex was observed with the HBScons probe, confirming successful expression of Barx2 protein (Figure 6.8 (Lane 6)). However, there was still no specific complex formed with either the 3xTCFcons or Axin2 T3-wt probes (Figure 6.8 (Lanes 4 and 5)). These results suggest that the binding of Barx2 at TCF/LEF elements in DNA is not direct, and is likely mediated by its interactions with TCF/LEF proteins and likely also β -catenin. Such indirect interactions may not be stable enough to capture under *in vitro* binding conditions.

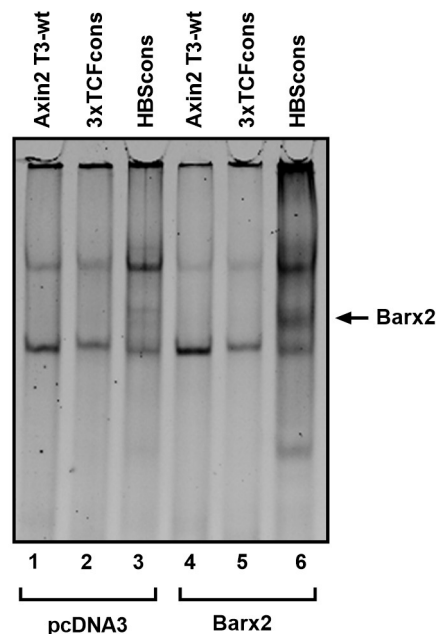


Figure 6.8: Gel shift assay with HEK293T nuclear extracts

Double-stranded oligonucleotide probes corresponding to the wildtype Axin2 T3 site, a 3x TCF consensus sequence or a HBS consensus sequence were incubated with HEK293T nuclear extracts and resolved on a 5% non-denaturing polyacrylamide gel.

6.3.5 Pax7 partially antagonizes Barx2- and β -catenin-mediated induction of Axin2 promoter activity

Chapter 3 highlighted the opposing roles for Barx2 and Pax7 in regulation of the canonical Wnt reporter, TOPflash, and the importance of the homeodomains of each protein in this regulation [Zhuang et al. 2014]. The data presented thus far indicate that the mechanism of Axin2 promoter regulation by Barx2 is very similar to that of TOPflash. Given that Pax7 strongly represses Barx2-mediated activation of TOPflash, the ability of Pax7 to modulate Barx2-mediated activation of the Axin2 promoter was assessed. The Axin2 Δ HBS promoter construct was used for this analysis because it showed greatest activation by Barx2. Furthermore, it had the same basal activity level as the Axin2 WT promoter (data not shown), indicating that endogenous Pax7 was not capable of regulating activity via the deleted HBS motif. In C2C12 cells, transfection of Pax7 alone had no impact on basal Axin2 promoter activity (Figure 6.9A). However, co-transfection of Pax7 with Barx2 or β -catenin reduced the ability of these factors to activate the Axin2 promoter by approximately 50% (Figure 6.9A). Conversely, knockdown of Pax7 by co-transfection of siRNA directed against Pax7 led to increased Barx2 and β -catenin-mediated activation of the Axin2 promoter (Figure 6.9C).

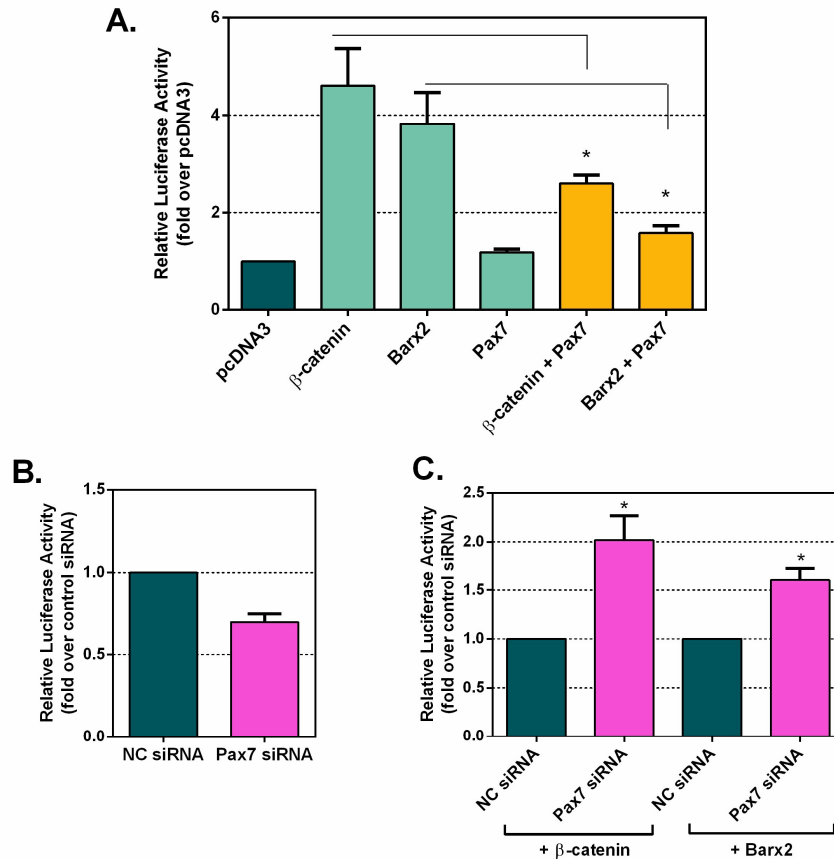


Figure 6.9: Pax7 antagonises the activating effect of Barx2 and β-catenin on the Axin2 promoter

(A): Axin2 ΔHBS (0.5 μg) was co-transfected with β-catenin, Barx2 and/or Pax7 (1 μg total) into C2C12 cells. (B, C): Axin2 ΔHBS (0.5 μg) was co-transfected with β-catenin or Barx2 with siRNA (total 1 μg) into C2C12 cells. Transfection of empty pcDNA3 vector served as a negative control. Luciferase activity was assayed 48 hours post transfection. All data are normalised to a Renilla luciferase internal control, expressed as the mean firefly/Renilla luciferase ratio. Data were then normalised to the promoterless pGL3-basic vector, and then to pcDNA3 empty vector transfection or NC siRNA (set to a value of 1). The results shown are the average of at least three independent experiments. Error bars represent SEM. * p < 0.05 relative to pcDNA3 or NC siRNA unless otherwise marked.

In Chapter 3, the importance of the homeodomains for both Barx2- and Pax7-mediated regulation of TOPflas was demonstrated. To further understand the roles that the homeodomains play in this differential regulation of Wnt target promoters, the homeodomain and the Barx basic region from Barx2 (Barx2HDBBR) was swapped with the homeodomain of Pax7 (Pax7HD), and vice versa, to generate two new

chimeric transcription factors: Barx2/Pax7HD and Pax7/Barx2HDBBR. The effects of these chimeric factors were examined on both the Axin2 Δ HBS reporter and the TOPflash reporter. Chimeric Barx2 containing the Pax7 homeodomain (Barx2/Pax7HD), was able to activate both promoters (Figure 6.10A and B), but was significantly less activating than wildtype (WT) Barx2. Chimeric Pax7 containing the Barx2 homeodomain and BBR (Pax7/Barx2HDBBR) was still repressive of basal TOPflash activity; however, it was significantly less so than WT Pax7 (Figure 6.10A). Unlike WT Pax7, Pax7/Barx2HDBBR had an activating effect on basal Axin2 Δ HBS activity (Figure 6.10B). When co-transfected with Barx2, Pax7/Barx2HDBBR reduced Barx2-mediated activation of TOPflash by approximately 12-fold but, unlike WT Pax7, did not completely abolish activation (Figure 6.10A). Pax7/Barx2HDBBR did not significantly reduce Barx2-mediated activation of Axin2 Δ HBS (Figure 6.10B). Thus, despite the important roles of the Barx2 and Pax7 homeodomains in mediating their respective activation and repression functions, the homeodomains are not autonomous and their function varies according to their context within the whole protein.

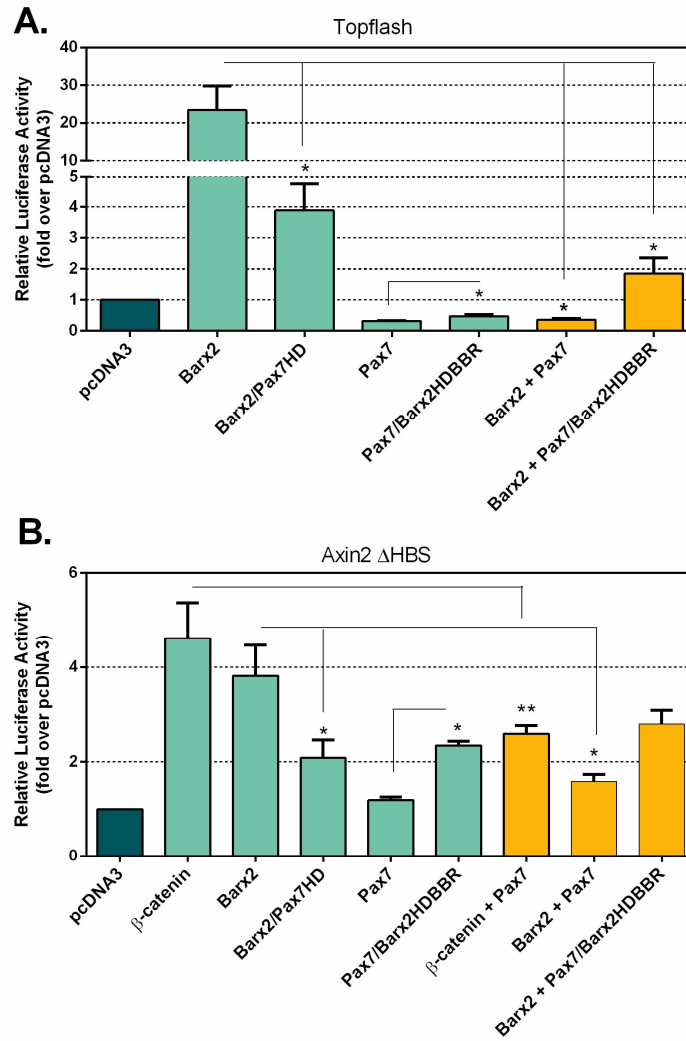


Figure 6.10: The effect of chimeric Barx2/Pax7 factors on Axin2 promoter activity

(A): TOPflash reporter or (B) Axin2 ΔHBS (0.5 μg) was co-transfected with combination of Barx2 and Pax7 expression plasmids (1 μg total) into C2C12 cells. Transfection of empty pcDNA3 vector served as a negative control. Luciferase activity was assayed 48 hours post transfection. All data are normalised to a Renilla luciferase internal control, expressed as the mean firefly/Renilla luciferase ratio. Data were then normalised to the promoterless pGL3-basic vector, and then to pcDNA3 empty vector transfection (set to a value of 1). The results shown are the average of at least three independent experiments. Error bars represent SEM. * $p < 0.05$ relative to pcDNA3 unless otherwise marked.

6.3.6 Pax7 is recruited to the Axin2 T3 region

Pax7-ChIP was performed following over-expression of Pax7 in C2C12 TOPPuro cells.

Consistent with Pax7 playing an inhibitory role in TOPflash and Axin2-luc luciferase

assays, Pax7-ChIP analysis showed that Pax7 was recruited to the Axin2 T3 region (Figure 6.11). The Axin2 T3 region of DNA was enriched on average 2.5-fold following Pax7 transfection (Pax7-ChIP compared to IgG control IPs). Pax7 also appeared to be recruited to TOPflash promoter DNA, however the result was not statistically significant because one experiment showed a much higher fold-enrichment than the other replicate experiments. The level of Pax7 present at these promoters under basal conditions was not assessed, nor was the presence of Pax7 at any other TCF/LEF site within the Axin2 promoter/intron.

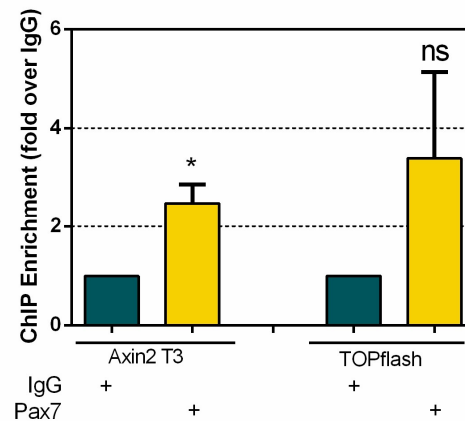


Figure 6.11: Pax7 is recruited to Axin2 and TOPflash promoter DNA

ChIP was performed on chromatin from the C2C12 TOPPuro stable cell line following transfection of Pax7. ChIP was performed with 2 µg of the indicated antibodies. Data are PCR amplification values for the Axin2 T3 region or the TOPflash promoter, normalised to amplification values for a control non-target locus (β2-microglobulin), with enrichment values for each antibody subsequently normalised to the mock ChIP with preimmune IgG, set to a value of 1. The results shown are the average of three independent experiments. Error bars represent SEM. * p < 0.05 relative to IgG. n=6.

6.3.7 Barx2 and Wnt signalling alter histone modifications of the Axin2 promoter region

ChIP studies thus far showed that Barx2, β-catenin and Pax7 all interact with the

endogenous Axin2 promoter. It was hypothesised that the changes in the level of Axin2 transcription observed following Wnt3a stimulation and Barx2/ β -catenin over-expression were epigenetically mediated. To this end, the distribution of activating and repressive histone modifications at the Axin2 promoter T3 region were examined using ChIP with antibodies specific for histone H3 Lysine acetylation (H3Kac), histone H3 Lysine 4 tri-methylation (H3K4me3) and histone H3 Lysine 27 tri-methylation (H3K27me3). These studies were performed in both primary myoblasts as well as the stable TOPPuro C2C12 cell line, with the latter allowing simultaneous assessment of histone modifications at both the TOPflash and Axin2 promoter regions. Interestingly, the histone modification signature at the Axin2 T3 region differed in these two cell types in basal growth conditions, as shown in Figure 6.12. Specifically, across the Axin2 T3 region in C2C12 cells the level of positive histone marks H3Kac and H3K4me3 were very low, whereas the repressive histone mark H3K27me3 was enriched (8-fold relative to IgG). Conversely, in primary myoblasts the T3 region was enriched for H3Kac and H3K4me3 and showed a low level of H3K27me3 (4-fold relative to IgG), suggesting that it is in a more accessible state in these cells. Consistent with this, RNA analysis of primary myoblasts versus the stable TOPPuro line revealed that basal Axin2 mRNA level was higher in primary myoblasts (not shown). As a comparison, the basal chromatin state of TOPflash in the stable TOPPuro cell line was examined. As shown in Figure 6.12, this locus was enriched for the active histone marks; this may relate to its random integration into an accessible locus.

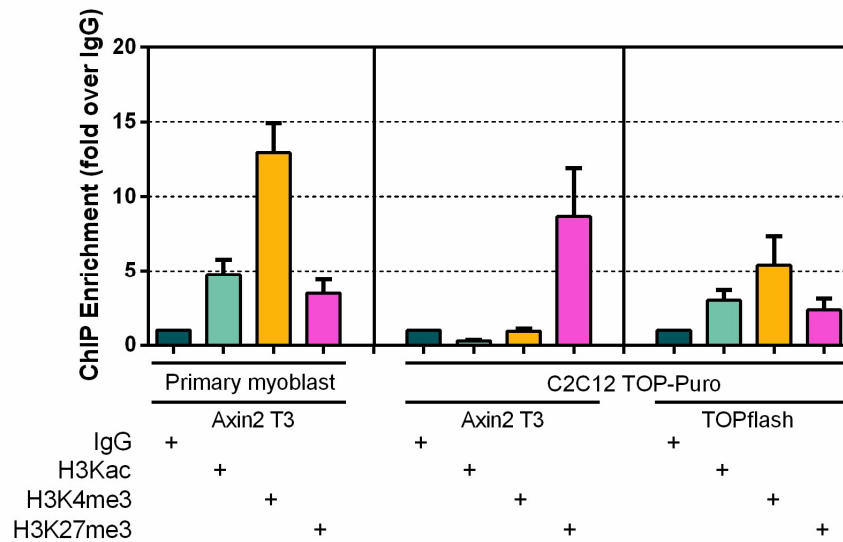


Figure 6.12: Basal chromatin signature of TOPflash and Axin2 T3

ChIP was performed on chromatin from primary myoblasts or the C2C12 TOP-Puro stable cell line with 2 μ g of the indicated antibodies. Data are PCR amplification values for the Axin2 T3 region or the TOPflash promoter, normalised to amplification values for a control non-target locus (β 2-microglobulin), with enrichment values for each antibody subsequently normalised to the mock ChIP with preimmune IgG, set to a value of 1. The results shown are the average of at least three independent experiments. Error bars represent SEM.

To assess changes in chromatin state at these Wnt-target loci following treatment with Wnt3a, the level of each histone modification was assessed by ChIP in both primary myoblasts and C2C12 cells after 48 hours of stimulation with Wnt3a CM. Consistent with active transcription, a dramatic increase in the level of activating histone modifications (H3Kac and H3K4me3) and a decrease in the level of a repressive histone modification (H3K27me3) was observed at the Axin2 T3 region relative to control L-cell treatment (Figure 6.13). The integrated TOPflash reporter exhibited similar changes, but to a lesser degree, and is not shown here.

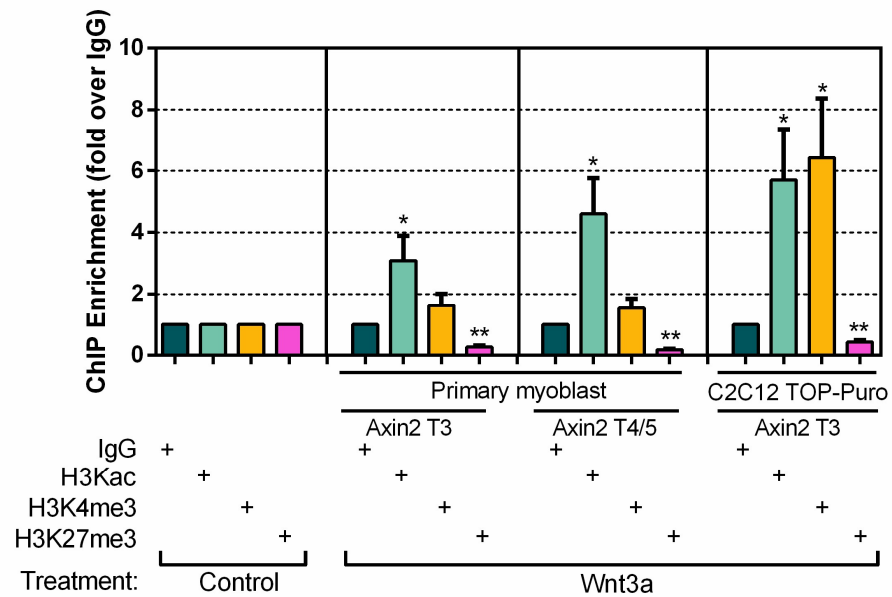


Figure 6.13: Chromatin signature of Axin2 following Wnt3a stimulation

ChIP was performed on chromatin from primary myoblasts or the C2C12 TOPPuro stable cell line with 2 μg of the indicated antibodies. Data are PCR amplification values for the Axin2 T3 region or T4/5 region, normalised to amplification values for a control non-target locus (β 2-microglobulin). Enrichment values for each antibody were subsequently normalised to control treatment and the mock ChIP with preimmune IgG, set to a value of 1. The results shown are the average of at least three independent experiments. Error bars represent SEM. * $p < 0.05$ and ** $p < 0.001$ relative to IgG.

Next, it was asked whether over-expression of β -catenin or Barx2 could induce similar histone modifications to those produced by Wnt3a-treatment; i.e. can these factors alone phenocopy the epigenetic response to a canonical Wnt signal. Due to difficulties in transfecting primary myoblasts efficiently, and at the scale required for ChIP experiments, these studies were only performed in C2C12 TOPPuro cells. As shown in Figure 6.14A and B, transfection of β -catenin and Barx2 in TOPPuro cells resulted in a more active epigenetic signature at both the Axin2 promoter (increased H3Kac and H3K4me3) and the integrated TOPflash promoter (increased H3Kac). Interestingly, TOPflash did not show an increase in the H3K4me3 modification, this is likely due to the high level of H3K4me3 already present in basal conditions, as

discussed above. As expected, transfection of the Barx2 Δ HD construct (that does not activate the Axin2 or TOPflash promoters in luciferase assays) had no effect on histone modifications (Figure 6.14A). Interestingly, the level of the repressive histone mark H3K27me3 at the Axin2 T3 region was also enriched following expression of either β -catenin or Barx2, relative to control empty vector transfection (Figure 6.14B). Thus, expression of these factors induced an increase in both active and repressive histone marks at the same region of the Axin2 promoter. The enrichment of all three histone marks was not an artefact of transfection alone, as all data are normalized to transfection of empty pcDNA3 vector. This result contrasted with the reduction in repressive histone marks at this locus observed after treatment with Wnt3a, and suggests that Wnt signals induce epigenetic change at target loci by multiple mechanisms, of which stabilization and recruitment of β -catenin and Barx2 are only a part.

To determine the effect of Pax7 on epigenetic signatures at Wnt target loci, Pax7 was transfected into the TOPPuro line and ChIP was performed again with antibodies to H3Kac. No enrichment of the Axin2 T3 region was observed following Pax7 transfection relative to empty vector transfection. Moreover, when Pax7 was co-transfected with Barx2, there was reduced enrichment of H3Kac relative to Barx2 transfection alone (Figure 6.14A). The same results were obtained when the TOPflash promoter was examined. These results suggest that Pax7 reduces promoter acetylation and are consistent with Pax7 having a repressive function on both TOPflash and Axin2 luciferase reporters, including its ability to repress Barx2-mediated promoter activation.

Overall, these data indicate that Barx2 can recruit factors that induce histone remodelling (particularly H3K acetylation) at the Axin2 and TOPflash promoters and that this is similar to the effect of β -catenin. Moreover, Pax7 may be antagonistic to the function of Barx2 in part by inhibiting the ability of Barx2 to remodel chromatin to a more accessible state by increasing histone acetylation.

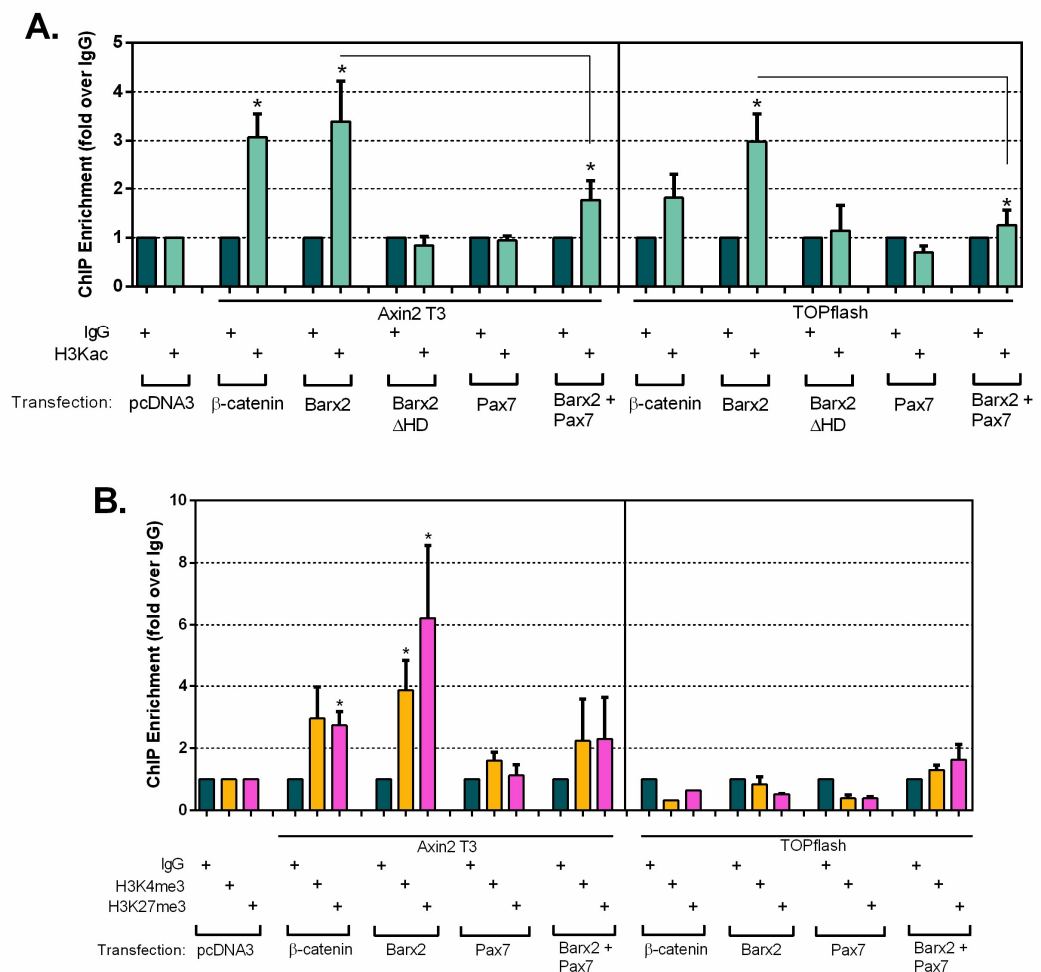


Figure 6.14: Chromatin signature of Axin2 and TOPflash following Barx2 or β -catenin transfection

ChIP was performed on chromatin from the C2C12 TOPPuro stable cell line with 2 μ g of the indicated antibodies. Data are PCR amplification values for the Axin2 T3 region, T4/5 region or TOPflash, normalised to amplification values for a control non-target locus (β -microglobulin). Enrichment values for each antibody were subsequently normalised to control treatment and the mock ChIP with preimmune IgG, set to a value of 1. The results shown are the average of at least three independent experiments. Error bars represent SEM. * $p < 0.05$ relative to IgG.

6.3.8 The histone acetyltransferase GRIP-1 synergizes with Barx2 in regulation of Axin2 promoter activity and is actively recruited to TCF/LEF elements

To further understand how Barx2 promotes histone modification at Wnt target promoters, possible co-activators of Barx2 were examined. A series of co-activators were selected based on their known HAT activity and/or previous association with either β -catenin or Wnt signalling. These co-activators were screened for their ability to synergize with Barx2 in activation of the Axin2 Δ HBS luciferase reporter construct (Figure 6.15) in C2C12 myoblasts. In each case, the amount of co-activator plasmid transfected (2.5 μ g) was five times that of Barx2 plasmid (0.5 μ g). The rationale for this ratio was that co-activators are recruited to numerous transcriptional complexes within the cell and not exclusively to Barx2-containing complexes. Due to a limit in the total amount of plasmid that can be transfected into cells without causing toxicity, the amount of Barx2 transfected under these conditions was necessarily less than previously used in these studies. Thus, the activation produced by Barx2 in these experiments is reduced accordingly. The role of these co-activators was not assessed on TOPflash.

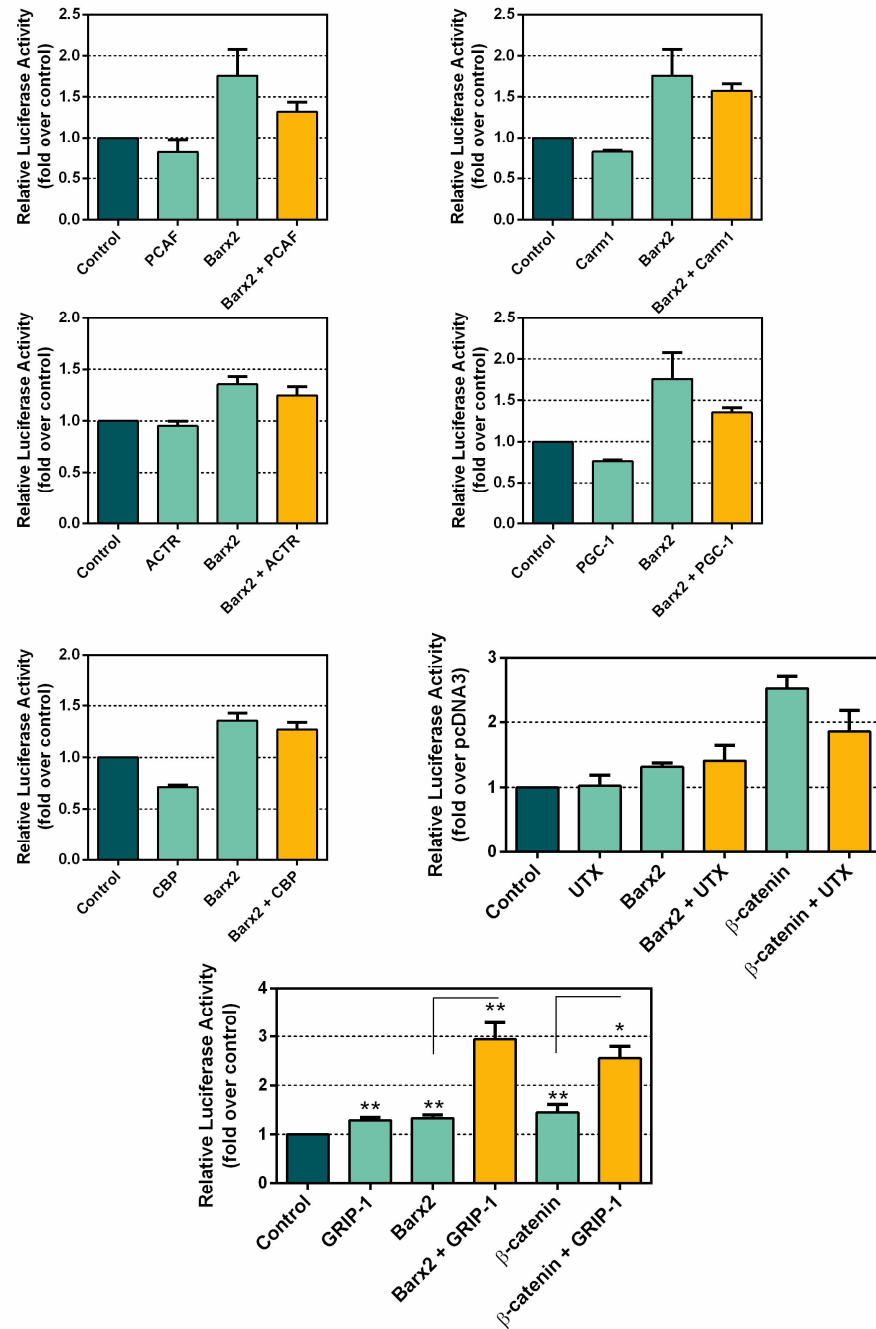


Figure 6.15: Screening of potential Barx2 co-activators in luciferase assays

Axin2 Δ HBS (0.25 μ g) was co-transfected with Barx2 or β -catenin and various co-activators expression plasmids (3 μ g total) into C2C12 cells. Luciferase activity was assayed 48 hours post transfection. All data are normalised to a Renilla luciferase internal control, expressed as the mean firefly/Renilla luciferase ratio. Data were then normalised to the promoterless pGL3-basic vector, and then to empty vector transfection (set to a value of 1). The results shown are representative experiments except for GRIP-1, which is the average of four independent experiments. Error bars represent SEM. * $p < 0.05$ and ** $p < 0.001$ relative to control unless otherwise marked.

Of those coactivators screened, only GRIP-1 was able to synergistically activate the Axin2 Δ HBS luciferase construct when co-transfected with either Barx2 or β -catenin, (Figure 6.15). GRIP-1 has previously been shown to directly interact with β -catenin [Li et al. 2004; Song & Gelmann 2005]. Importantly, transfection of GRIP-1 alone was not sufficient to induce reporter activity above basal levels.

The ability of GRIP-1 to co-activate the Axin2 Δ HBS luciferase construct with both β -catenin and Barx2 suggests that it is co-recruited with these factors to the promoter. To determine whether this co-recruitment also occurs on the endogenous Axin2 promoter, ChIP assays were performed using GRIP-1 antibodies in TOPPuro cells that had been treated with Wnt3a, or transfected with either Barx2 or ca. β -catenin plasmids. As in previous studies, promoter DNA enrichment with the GRIP-1 antibody was normalised to enrichment at a control locus and to enrichment by non-immune IgG. As shown in Figure 6.16B, ChIP using antibodies to GRIP-1 showed that GRIP-1 binding was greatly enriched at both the Axin2 T3 region and the TOPflash promoter following 48 hours of Wnt3a-treatment (5 to 10-fold). Over-expression of Barx2 and β -catenin also resulted in enrichment of endogenous GRIP-1 at both loci, but to a lesser extent (2 to 3-fold). Pax7 overexpression did not change the basal level of GRIP-1 binding at the Axin2 T3 region relative to empty vector transfection. However, Pax7 overexpression did reduce binding of GRIP-1 to the TOPflash promoter under basal conditions (Figure 6.16B). This result is consistent with observations that Pax7 is repressive to basal TOPflash promoter activity (Chapter 3, Section 3.3.4) and may suggest that Pax7 is able to displace co-activators and recruit co-repressors at some Wnt-target promoters.

To determine whether GRIP-1 can physically interact with Barx2, co-immunoprecipitation experiments were performed in HEK293T cells, which were selected because of their high transfection efficiency. GRIP-1 was expressed in excess to myc-tagged Barx2 (2:1 microgram ratio), cell lysates were immunoprecipitated with anti-GRIP-1 antibody, and immunoprecipitates were assessed by western blotting using an antibody to the myc-tag. These studies showed that GRIP-1 can interact with Barx2 (Figure 6.16A), lending support to the hypothesis that GRIP-1 is involved in Barx2 mediated induction of Wnt-responsive promoters. Collectively, these data suggest that GRIP-1 is involved in the increase in H3K acetylation at Wnt-responsive promoters following either Wnt3a stimulation or β -catenin/Barx2 over-expression.

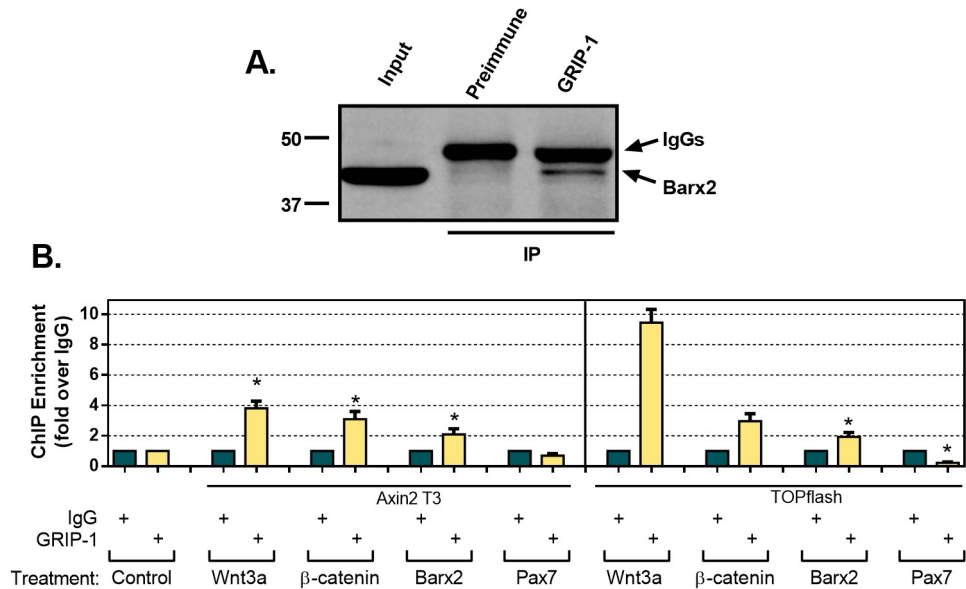


Figure 6.16: GRIP-1 is actively recruited to TCF/LEF elements

(A): GRIP-1 and Myc-epitope-tagged Barx2 were expressed in HEK293T cells and immunoprecipitated using polyclonal antibodies to GRIP-1. Proteins were resolved on a 10% SDS-PAGE gel, transferred to nitrocellulose membrane and probed with monoclonal antibodies to the myc-tag. (B): ChIP was performed on chromatin from the C2C12 TOPPuro stable cell line with 2 μ g of the indicated antibodies. Data are PCR amplification values for the Axin2 T3 region or TOPflash, normalised to amplification values for a control non-target locus (β 2-microglobulin). Enrichment values for each antibody were subsequently normalised to control treatment and the mock ChIP with preimmune IgG, set to a value of 1. The results shown are the average of at least three independent experiments. Error bars represent SEM. * $p < 0.05$ relative to IgG.

6.3.9 Pax7 associates with the histone deacetylase HDAC1

As previously discussed, Pax7 can at least partly inhibit the ability of both Barx2 and β -catenin to activate the Axin2 promoter; moreover, Pax7 may prevent the remodelling of chromatin to a more accessible state including inhibiting histone acetylation (Section 6.3.7). The question was then asked whether Pax7 recruits co-repressors to Wnt target promoters and whether this may prevent an association between Barx2/ β -catenin and co-activators. Due to known involvement of HDAC1 in TCF/LEF-mediated repression (i.e. in the absence of β -catenin) [Billin et al. 2000; Arce

et al. 2009], it was hypothesised that HDAC1 may also be one of the co-repressors associating with Pax7. To analyse the role of HDAC1 in regulation of Wnt target promoters, TOPflash and Axin2 reporter luciferase assays were performed. These reporter constructs were co-transfected with either the Barx2 or ca. β -catenin plasmids in combination with HDAC1 plasmid. Figure 6.17 shows that co-transfection of HDAC1 significantly inhibited both Barx2 and β -catenin-mediated activation of TOPflash and Axin2 Δ HBS constructs. Next the role of HDAC1 in Pax7 mediated repression of the Axin2 reporter construct was assessed. While neither Pax7 nor HDAC1 alone repressed basal Axin2 promoter activity when compared to transfection of empty pcDNA3 vector, co-expression of Pax7 with HDAC1 led to significant repression of the Axin2 promoter (Figure 6.17). The TOPflash promoter was not assessed in co-transfection assays as it already showed dramatic repression by Pax7 alone. These studies suggests that HDAC1 is involved in Pax7-mediated repression of Wnt target promoters.

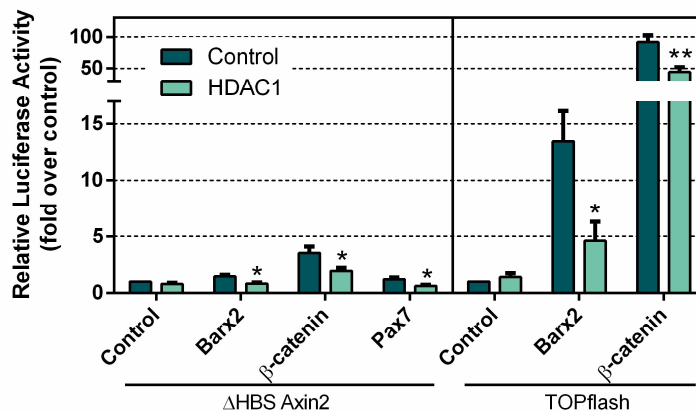


Figure 6.17: HDAC1 represses Barx2 and β-catenin-mediated activation of Axin2 and TOPflash

Axin2 ΔHBS or TOPflash (0.25 μg) was co-transfected with Barx2, β-catenin or Pax7 with HDAC1 (3 μg total) into C2C12 cells. Luciferase activity was assayed 48 hours post transfection. All data are normalised to a Renilla luciferase internal control, expressed as the mean firefly/Renilla luciferase ratio. Data were then normalised to the promoterless pGL3-basic vector, and then to empty vector transfection (set to a value of 1). The results shown are the average of at least three independent experiments. Error bars represent SEM. * $p < 0.05$ and ** $p < 0.001$ relative to control.

To assess recruitment of HDAC1 to either the endogenous Axin2 promoter or the integrated TOPflash promoter in C2C12 TOPPuro cells, ChIP was attempted with an antibody to HDAC1 following transient overexpression of Pax7. Multiple experimental replicates showed a trend towards increased recruitment of HDAC1 to both promoter regions, but the effect was small and did not reach statistical significance (Figure 6.18A). Similarly, there was a non-significant trend towards reduced HDAC1 binding at these loci following transfection of Barx2 or β-catenin. The low enrichment values seen in these experiments may suggest that the HDAC1 antibody is not optimal for ChIP analyses.

To determine whether HDAC1 could interact with Pax7, co-immunoprecipitation with these two proteins was performed after co-transfection in HEK293T cells. HDAC1 and

myc-tagged Barx2 (2:1 microgram ratio) were co-expressed, lysates were immunoprecipitated with anti-HDAC1 antibody, and immunoprecipitates were assessed by immunoblotting. These co-immunoprecipitations revealed that Pax7 and HDAC1 interact (Figure 6.18B), however, this interaction appeared very weak. This may suggest that the interaction between Pax7 and HDAC1 is indirect and is not easily captured by the antibody in immunoprecipitation reactions.

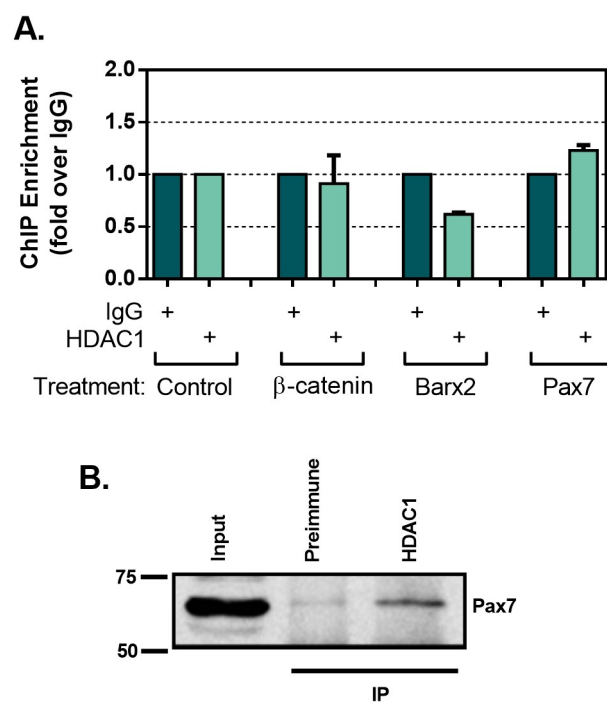


Figure 6.18: HDAC1 interacts with Pax7

(A): ChIP was performed on chromatin from the C2C12 TOPPuro stable cell line with 2 μ g of the indicated antibodies. Data are PCR amplification values for the Axin2 T3 region, normalised to amplification values for a control non-target locus (β 2-microglobulin). Enrichment values for each antibody were subsequently normalised to control treatment and the mock ChIP with preimmune IgG, set to a value of 1. The results shown are the average of two independent experiments. Error bars represent SEM. $n=4$. (B): HDAC1 and Myc-epitope-tagged Pax7 were expressed in HEK293T cells and immunoprecipitated using polyclonal antibodies to HDAC1. Proteins were resolved on a 10% SDS-PAGE gel, transferred to nitrocellulose membrane and probed with monoclonal antibodies to the myc-tag.

The net activity of HATs and HDACs determines promoter activity. To investigate the balance between HAT and HDAC activities at Wnt target promoters, C2C12 cells were

transfected with the TOPflash reporter and treated with HDAC inhibitors Trichostatin A (TSA, 60 nM) or sodium (Na) butyrate (2 mM) to relieve HDAC-associated repression. As expected, a large induction in basal reporter activity was observed compared to vehicle treated cells (approximately 300-fold, Figure 6.19A). To determine whether the repression of TOPflash by Pax7 required HDAC activity, cells were transfected with Pax7 plasmid and then treated with either vehicle or HDAC inhibitors. Intriguingly, the presence of HDAC inhibitors did not abolish Pax7-mediated repression of reporter activity (Figure 6.19B). Thus Pax7 may repress TOPflash by both HDAC-dependent and HDAC-independent mechanisms.

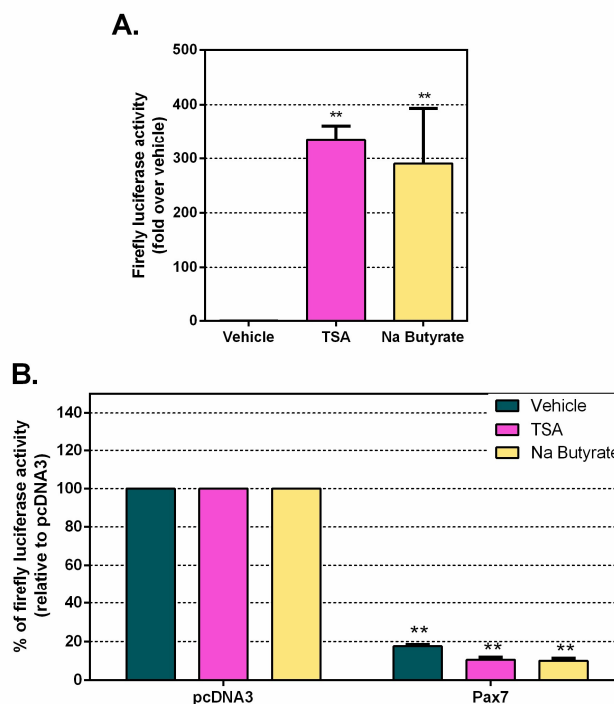


Figure 6.19: Pax7 inhibits TOPflash activity in the presence of HDAC inhibitors

C2C12 cells were transfected with TOPflash (0.5 μ g) and treated with vehicle, TSA or Na Butyrate alone (A) or following Pax7 transfection (B). Luciferase activity was assayed 48 hours post transfection. All data are normalised to a Renilla luciferase internal control, expressed as the mean firefly/Renilla luciferase ratio. Data were then normalised to the promoterless pGL3-basic vector, and then to empty vector transfection (set to a value of 1). The results shown are the average of three independent experiments. Error bars represent SEM. ** $p < 0.001$ relative to vehicle or pcDNA3 control. $n=9$.

6.4 Discussion

Whilst the role of Axin2 as a negative regulator of the Wnt signalling pathway via its involvement in the β -catenin destruction complex is well-known, only a handful of studies have examined the regulation of Axin2 downstream of a Wnt signal [Jho et al. 2002; Lustig et al. 2002; Wohrle et al. 2007]. A region of the Axin2 promoter and first intron capable of responding to Wnt signalling in reporter assays, and faithfully recapitulating the Axin2 expression pattern *in vivo*, was cloned by Jho and colleagues [Jho et al. 2002]. This region, identical to the Axin2-luc promoter construct used here, consists of the proximal promoter and the first intron, and contains eight predicted TCF/LEF binding motifs (designated T1 to T8). In contrast, the cyclinD1 proximal promoter construct used in these studies contains only a single predicted TCF/LEF site. Unlike the synthetic TOPflash promoter, these endogenous promoter regions also contain an array of predicted binding sites for other transcription factors, including potential HBS motifs clustered at the 5' end. The role of these HBS motifs in Barx2-mediated activation of the Axin2 and cyclinD1 promoter luciferase constructs was assessed by generating shorter constructs, thus deleting these motifs. Luciferase assays performed with the truncated reporters demonstrated no significant role for the HBS motifs in Barx2-mediated activation of Axin2, but did suggest a possible role in *repression* of cyclinD1 by Barx2. This result is consistent with previous published work on the dual role that Barx2 can play as both an activator and a repressor of target promoters [Edelman et al. 2000].

A previous study of Axin2 luciferase reporter constructs with mutated TCF/LEF motifs [Jho et al. 2002] suggested that activation by β -catenin involved multiple TCF/LEF

elements. In the studies presented in this chapter, mutation of elements T2-T5 resulted in a 50% reduction in β -catenin-mediated activation, and mutation of the remaining elements (T6-T8) abolished all activation by β -catenin. These data are consistent with previous reports. An important new finding of these studies was that mutation of the TCF/LEF elements within the Axin2 and cyclinD1 promoter constructs also inhibited their activation by Barx2, supporting our hypothesis that Barx2, like β -catenin, activates through TCF/LEF sites. Moreover, full length Barx2 may have a dual role at some Wnt-target promoters, repressing via HBS elements, and activating via TCF/LEF elements. The balance between other co-factors within the cell may determine whether Barx2 activates or suppresses these targets at any point in time.

The studies described in this chapter demonstrated striking similarities between the regulation of Axin2 and the synthetic reporter TOPflash. Luciferase assays using the Axin2 Δ HBS reporter construct and different domains of Barx2 revealed a potent activation domain within the Barx2 C-terminus, and a less potent activating function in the N-terminus, consistent with previous work [Edelman et al. 2000; Zhuang et al. 2014]. ChIP experiments confirmed recruitment of Barx2 to a region of genomic DNA spanning the Axin2 T3, T4 and T5 elements following over-expression in C2C12 cells, or induction by Wnt3a in primary myoblasts. The level of Barx2 recruitment to the Axin2 and TOPflash promoters were similar (Sections 3.3.8 and 6.3.3). Also consistent with previous observations at the TOPflash promoter, over-expression of Barx2 could increase the level of β -catenin bound at the Axin2 T3 site. The Barx2 homeodomain was necessary, but not sufficient, for both recruitment of Barx2 (and β -catenin) to the Axin2 T3 region and activation of the Axin2 promoter. A lack of β -catenin

recruitment to Axin2 promoter DNA following overexpression of the Barx2 Δ HHD construct further supports a role for the homeodomain in either stabilising β -catenin or facilitating an interaction between Barx2, β -catenin, TCF/LEF and other co-factors thus allowing it to occupy promoter DNA. This is consistent with previous work which demonstrated the requirement of the Barx2 homeodomain for physical interaction between Barx2 and β -catenin (Chapter 3) [Zhuang et al. 2014]. Attempts to use gel shift assays to capture the interaction between Barx2 and TCF/LEF elements were unsuccessful. There may be a number of explanations for this result. First, it is likely that Barx2, like β -catenin, does not directly bind TCF/LEF DNA elements, and, unlike ChIP assays, gel shift assays do not employ a crosslinking step to covalently link otherwise weakly-associated protein complexes to DNA. In support of this, a strong protein-probe complex was observed after over-expression of TCF4 (which binds DNA directly), but only a weak β -catenin/TCF complex was observed following β -catenin over-expression. This weaker interaction is consistent with previous reports in the literature [Zhurinsky et al. 2000; Sampson et al. 2001; Jho et al. 2002; Zhang et al. 2009]. The Barx2/ β -catenin/TCF complex may also be less stable on a short, synthetic probe than in the native genome. This could be due to conformational constraints or lack of other binding sites for co-factors required for complex formation.

Treatment of primary myoblasts and C2C12 cells with Wnt3a CM changed the histone modification signature at both the Axin2 promoter and the TOPflash promoter. As expected, under basal conditions the Axin2 promoter was marked by high levels of H3K27 tri-methylation and low levels of H3K4 tri-methylation and H3K acetylation, a signature that is generally characteristic of a repressive chromatin state [Tse et al.

1998; Marks et al. 2000; Litt et al. 2001; Bernstein 2006; Boyer et al. 2006; Squazzo 2006; Bender et al. 2013; Voigt et al. 2013]. Consistent with the dramatic upregulation of Axin2 mRNA expression observed in these studies (Chapter 4), Wnt3a stimulation switched the promoter to a permissive or active state, characterised by lower H3K27 tri-methylation and increased levels of H3K4 tri-methylation and H3K acetylation. Curiously, a previous study by Wohrle and colleagues reported no significant change in H3K acetylation or H3K4 tri-methylation across the same region of the Axin2 promoter in C2C12 cells after Wnt signalling activation [Wohrle et al. 2007]. However, there were several differences between their study and the one presented here. In particular, they used a GSK inhibitor, SB-216763, rather than a natural Wnt ligand, and in addition they reported a high basal level of H3K acetylation in their cell line. Changes in histone modifications post Wnt-stimulation have also been observed at other Wnt-responsive promoters, such as increased H3K4 methylation *in vivo* at the c-Myc promoter [Sierra et al. 2006]. In the work presented here, over-expression of either constitutively active β -catenin or Barx2 was sufficient to induce a more active chromatin state indicated by increased H3K acetylation and H3K4 tri-methylation at both TOPflash and Axin2 promoter regions. However, these experiments also revealed a small increase in the repressive histone mark H3K27 tri-methylation, which was in contrast to the effect of Wnt3a CM. This suggests that Wnt ligand-receptor mediated signalling leads to more transcriptional/epigenetic effects than simply stabilising β -catenin and inducing Barx2 expression. In particular, expression of β -catenin and Barx2 may not be sufficient to recruit H3K27 demethylases. Consistent with this idea, the H3K27 demethylase UTX did not synergize with Barx2 or β -catenin in promoter luciferase assays. Bivalent chromatin

domains that simultaneously display both activating (H3K4me3) and repressing (H3K27me3) marks have previously been reported in embryonic stem cells [Bernstein 2006]; this combination of modifications marks key developmental genes that are expressed at low levels but are poised for rapid transcription upon differentiation into a specific lineage. It is possible that β -catenin (and Barx2) alone 'prime' target promoters for activity, whereas ligand-mediated Wnt signalling drives the target promoters to a more defined active state that includes loss of H3K27 tri-methylation.

Multiple histone-modifying and chromatin-remodelling proteins that are able to alter chromatin structure and facilitate recruitment of essential transcription factors have been identified among the co-factors of β -catenin and TCF/LEF proteins. Like other HMG box-containing proteins, TCF/LEF proteins possess minimal transcriptional activity on their own and must therefore affect transcription by recruiting various binding co-factors, which in turn recruit chromatin modifiers to suppress or activate target genes [Lien & Fuchs 2014]. Examples of activating co-factors include Brg-1 (Brahma-related gene-1), the central catalytic subunit of numerous chromatin-modifying enzymatic complexes [Trotter & Archer 2008] which interacts with β -catenin [Barker et al. 2001], p300/CBP co-activator family members which contain histone acetyltransferase domains and synergise and interact with β -catenin [Ogryzko et al. 1996; Hecht et al. 2000; Takemaru & Moon 2000], and GRIP-1, a member of the steroid receptor coactivator (SRC) class of co-factors, which also has intrinsic histone acetyltransferase activity and interacts directly with β -catenin [Li et al. 2004; Song & Gelmann 2005].

In an effort to understand how Barx2 may modify the epigenetic signature at Wnt

target genes, a number of coactivators with histone modifying activity were screened in luciferase assays for their ability to enhance Barx2-mediated activation of the Axin2 Δ HBS reporter construct. These coactivators included the aforementioned HATs CBP and GRIP-1, as well as PGC-1 (Peroxisome proliferator-activated receptor gamma coactivator 1-alpha) which forms part of a HAT complex by interacting with other HATs CBP and SRC-1 [Puigserver et al. 1999], PCAF (p300/CBP-associated factor) which can associate with p300/CBP, has intrinsic HAT activity and is essential for activation of the myogenic program [Yang et al. 1996; Puri et al. 1997], and ACTR which also possesses HAT activity and the ability to recruit other HATs [Chen et al. 1997]. In addition, two coactivators that do not have any HAT activity were tested due to previously identified roles within the Wnt pathway. These were Carm1 (Coactivator-associated arginine methyltransferase 1), a protein arginine methyltransferase that functions as a secondary coactivator through its association with the p160 family of coactivators [Bedford & Clarke 2009] and plays a critical role in β -catenin-dependent signaling in colorectal cancers [Ou et al. 2011], and UTX (KDM6A; lysine(K)-specific demethylase 6A), a H3K27 demethylase [Agger et al. 2007; Hong et al. 2007] that is required for Wnt/ β -catenin mediated induction of Brachyury in ES cells [Wang et al. 2012]. Of all the coactivators that were screened, only GRIP-1 synergized with Barx2 in activation of the Axin2 reporter. This synergy was observed when GRIP-1 was transfected as a 5-fold excess of Barx2; this is consistent with the idea that cofactors are present in “limiting” concentrations and that there is competition for cofactor recruitment to multiple DNA-binding complexes. An example of this is in Rubinstein-Taybi syndrome, in which haplosufficiency for CBP results in severe development and regulatory abnormalities [Miller & Rubinstein

1995; Petrij et al. 1995; Yao et al. 1998]. The same synergy was observed when GRIP-1 was co-expressed with β -catenin and is consistent with previous reports that β -catenin and GRIP-1 cooperate [Li et al. 2004; Song & Gelmann 2005]. Interestingly, like Barx2, GRIP-1 has been reported to be expressed in satellite cells and myoblasts with its expression increasing during differentiation [Chen et al. 2000], suggesting that it may cooperate with Barx2 in regulation of differentiation. Further analysis by CHIP revealed that GRIP-1 was actively recruited to the Axin2 T3 region and to TOPflash following treatment of C2C12 cells with Wnt3a or transfection of β -catenin or Barx2, which is consistent with the increased H3K acetylation under the same conditions. Moreover, co-immunoprecipitation experiments showed that Barx2 and GRIP-1 physically interact. All of these observations support the idea that GRIP1 may mediate induction of muscle specific Wnt target gene expression by Barx2.

Consistent with the previous findings that Pax7 is inhibitory to both β -catenin and Barx2 mediated activation of TOPflash [Zhuang et al. 2014] (Chapter 3), the work presented within this chapter also showed that Pax7 could antagonise the activation of Axin2 by Barx2 or β -catenin, and the Pax7 homeodomain was required for this repressive function. Moreover, knockdown of endogenous Pax7 led to enhanced activation of the Axin2 luciferase reporter by both Barx2 and β -catenin, suggesting that Pax7 may limit the response of these genes to these two factors. Although forced expression of Pax7 resulted in its recruitment to both TOPflash and the Axin2 T3 promoter region, the repression of the Axin2 promoter by Pax7 was not as dramatic as the repression of TOPflash, and in particular, basal Axin2 activity was not suppressed. It is possible that Pax7 cooperates with multiple TCF/LEF-corepressor

complexes at the multimerized TCF/LEF elements in TOPflash to nucleate a strongly repressive chromatin structure. This may not occur at distributed TCF/LEF sites (as in Axin2) or single TCF/LEF sites (as in cyclinD1).

The epigenetic effects of Pax7 at Wnt target genes were explored by CHIP analysis of histone modifications. While Pax7 alone had no impact on the basal level of H3K acetylation at either the TOPflash or Axin2 T3 promoter regions, Pax7 inhibited the ability of Barx2 to induce H3K acetylation. Conceptually, Pax7 could inhibit H3K acetylation by blocking the recruitment of Barx2 and/or β -catenin and therefore GRIP-1. Unfortunately, several attempts to determine whether Pax7 affected Barx2 or β -catenin recruitment gave inconclusive results. This was due to difficulties in co-transfecting multiple factors and subsequently performing CHIP with an antibody directed to one of those factors. In particular, expression levels of individual factors tended to be higher when transfected alone, relative to when two or more factors were co-transfected.

TCF/LEF proteins associate with co-repressors in the absence of nuclear β -catenin to mediate repression of target genes, resulting in transcriptionally silent chromatin. Of these co-repressors, the Groucho family are probably the most well-known and have critical roles in many developmental processes [Cavallo et al. 1998; Levanon et al. 1998; Roose et al. 1998; Brantjes et al. 2001; Sekiya & Zaret 2007]. Several models for Groucho-mediated repression have been proposed, but the exact mode of regulation of Groucho proteins remains unclear. However, *Drosophila* Groucho has been shown to interact with the HDAC1 equivalent Rpd3 [Chen et al. 1999] and thus Groucho potentially mediates repression, at least in part, by direct recruitment of

HDACs. HDAC1 itself has been implicated as a binding partner for Lef1 *in vivo*, and repression mediated by Lef1 in the absence of β -catenin requires this HDAC activity [Billin et al. 2000]. APC-mediated repression of c-Myc in colorectal cancer cells involves stable recruitment of both TLE-1 and HDAC1 [Sierra et al. 2006]. NCoR (Nuclear receptor corepressor) and the closely related SMRT (silencing mediator for retinoid and thyroid hormone receptor) have also been identified as negative regulators of β -catenin/TCF4-induced transcription, directly interacting with both β -catenin and TCF4 [Song & Gelmann 2008]. Both NCoR and SMRT also interact directly with multiple HDACs [Guenther et al. 2000; Kao et al. 2000] and may associate with HDAC1 via the Sin3 protein [Heinzel et al. 1997; Nagy et al. 1997]. Finally, HDAC1 expression has been shown to be down-regulated by Wnt3a in the P19CL6 cardiomyocyte model [Liu et al. 2009]. With many studies indicating a role for HDAC1 in repression of Wnt/ β -catenin signalling, a role for HDAC1 in regulating the repressive action of Pax7 within this system in myoblasts was hypothesised. Over-expression of HDAC1 demonstrated that HDAC1 had no effect on basal activity of Axin2 Δ HBS and TOPflash luciferase reporters, but it reduced activation by both Barx2 and β -catenin. Similarly, co-transfection of HDAC1 with Pax7 enhanced the ability of Pax7 to repress the Axin2 promoter. ChIP assays to assess the recruitment of endogenous HDAC1 to genomic DNA showed a trend of increased HDAC1 binding following Pax7 transfection, and decreased HDAC1 binding following Barx2 or β -catenin transfection, however the data did not reach statistical significance. It is possible that the HDAC1 antibody used was not ideal for ChIP however time constraints precluded additional studies with another antibody. Furthermore, endogenous HDAC1 in C2C12 myoblasts may be too low for successful ChIP assays.

The latter idea is somewhat supported by results from co-immunoprecipitation experiments in which Pax7 and HDAC1 were found to interact, however the amount of Pax7 co-precipitated with HDAC1 was very low. This could be due to low levels of HDAC1, or poor recognition of native HDAC1 by the antibody. As further support for the dominant role of Pax7 at Wnt target promoters, Pax7 remained repressive to basal TOPflash promoter activity even in the presence of the HDAC inhibitors TSA and Na butyrate, thus suggesting that Pax7 is able to maintain the balance of positive and negative co-factors in favour of a repressive state, possibly by recruiting not only HDACs, but also other corepressors including H3K methyltransferases.

Taken together, the studies in this chapter have provided mechanistic insights into Barx2 and Pax7 mediated regulation of the canonical Wnt target gene Axin2 in myoblasts and generalized these mechanisms by showing that they are similar in the TOPflash model. Barx2 activates an Axin2 luciferase construct by recruiting β -catenin and GRIP-1 to TCF/LEF elements upstream of the Axin2 translation start site. In turn, H3K acetylation is increased at the same genomic region, resulting in a more permissive and active chromatin state for transcription. Pax7 is inhibitory to both Barx2 and β -catenin-mediated activation, and when co-expressed with Barx2 blocks recruitment of GRIP-1, thus reducing levels of H3K acetylation. This is likely through its interaction with HDAC1.

Overall, these studies defined promoter-based mechanisms for differential gene regulation by Barx2 and Pax7. It remains to be determined whether the opposing *molecular functions* of Barx2 and Pax7 in regulation of Wnt target genes underlies their opposing *cellular functions* in myoblast lineage progression; i.e. that Pax7

inhibits differentiation [Zammit et al. 2006; Olguin et al. 2007] whilst Barx2 promotes differentiation [Brack et al. 2008; Makarenkova et al. 2009; Tanaka et al. 2011]. Whilst this is a tempting model, further studies are required to determine whether Wnt signals in fact drive a differentiation-associated transcriptional program through the activation of β -catenin and Barx2 in myoblasts.

Chapter 7

General discussion and conclusions

The process of skeletal muscle regeneration is under tight transcriptional control by MRFs and is responsive to many of the same signalling molecules that mediate embryonic myogenesis, such as Wnt and Notch. In particular, Wnts play central roles in myogenesis and muscle repair. The majority of literature focused on the role of Wnts in myogenesis suggests that the canonical Wnt signalling pathway is transiently activated during adult muscle regeneration *in vivo* [Otto et al. 2009] and canonical Wnt ligands (such as Wnt3a and Wnt1) promote myoblast differentiation *in vitro* [Bernardi et al. 2011; Pansters et al. 2011; Tanaka et al. 2011; Jones et al. 2015].

Several homeobox proteins functionally interact with the Wnt and Notch signalling pathways and with MRFs during regenerative myogenesis. The most well-studied homeobox factor in muscle, Pax7, is critical for satellite cell survival [Seale et al. 2000] and is indispensable for adult skeletal muscle regeneration [Sambasivan et al. 2011; von Maltzahn et al. 2013]. In recent years, the homeobox transcription factor Barx2 has emerged as a novel regulator of both skeletal muscle development and myofibre regeneration following injury. The important role that Barx2 plays in muscle regeneration has been highlighted by use of a *Barx2* null mouse model [Olson et al. 2005; Meech et al. 2012] and further studies have shown that Barx2 is co-expressed with Pax7 in satellite cells, is regulated by MRFs, interacts directly with MyoD and promotes myoblast differentiation [Makarenkova et al. 2009; Meech et al. 2010; Meech et al. 2012].

At the commencement of this thesis, preliminary data generated in the Meech laboratory had identified Barx2 as a novel downstream effector of the canonical Wnt signalling pathway: luciferase assays had demonstrated the ability of Barx2 to

activate the synthetic Wnt reporter TOPflash in C2C12 cells, both on its own and in potent synergy with MyoD [Zhuang et al. 2014]. A hypothesis was thus established that Barx2 is a regulator of canonical Wnt signalling in myoblasts, and that disruption of this network in satellite cells is a primary mechanism underlying defective growth, maintenance and repair in *Barx2* null mice. In an effort to address this hypothesis and to advance our understanding of the roles of Barx2 and MyoD in Wnt target gene regulation in muscle, the study described here had several overarching aims. Briefly, these were to define the mechanisms by which Barx2 activates the synthetic reporter, in part through characterisation of functional interactions between Barx2 and other Wnt effectors/cofactors (Chapter 3), and to then identify and extend this knowledge to regulation of endogenous target genes in myoblasts (Chapter 5 and 6). In addition, this study examined the role of Pax7 in Wnt signalling and the functional relationship between Barx2 and Pax7 (Chapter 3 and 6), as well as characterising the relationships between Barx2 and Wnt and Notch signalling in *Barx2* null mice (Chapter 4).

The work presented and discussed in this thesis has demonstrated a novel pathway for translation of canonical Wnt signals into gene expression changes in myoblasts. This pathway involves homeobox proteins (Barx2 and Pax7) and MRFs which act in concert with the core Wnt effector proteins TCF/LEF and β -catenin. TCF/LEF proteins and β -catenin are ubiquitously expressed, and thus the role of Barx2, Pax7 and MRFs in this system is likely to transduce the activities of these proteins into tissue-specific effects.

Data initially obtained during this project was restricted to regulation of the synthetic

TOPflash reporter gene. Characterisation of Barx2-mediated activation of TOPflash revealed that Barx2 associates with TOPflash promoter DNA, likely through functional interactions with TCF/LEF proteins and β -catenin, and that Barx2 could actively recruit β -catenin to TOPflash promoter DNA. Analysis of β -catenin expression with fluorescence immunostaining showed that over-expression of Barx2 induced a higher nuclear:cytoplasmic ratio of β -catenin, suggesting Barx2 plays a role in sequestering β -catenin in the nucleus and providing a mechanism for Barx2-mediated activation of Wnt target genes even in the absence of a Wnt ligand. Delineation of Barx2 protein domains identified that the homeodomain was critical for interactions with β -catenin and therefore also the binding of Barx2/ β -catenin to promoter DNA and activation of TOPflash. In addition, Barx2 could synergise with all members of the MRF family to activate TOPflash, which on their own exhibit no effect on promoter activity. Whilst MyoD had previously been shown to interact with Barx2 [Makarenkova et al. 2009] and β -catenin [Kim et al. 2008], this was the first evidence that MRFs can assist in promoting transcription from TCF/LEF sites. Significantly, the fact that Barx2 could also activate TOPflash in a non-myogenic cell line and thus in the absence of MRF expression suggests that Barx2 may mediate Wnt signalling in other tissues, such as skin or gut [Sander & Powell 2004; Olson et al. 2005], with relevant tissue-specific co-factors.

In contrast to Barx2, Pax7 was antagonistic to TOPflash activity in C2C12 cells. Pax7 was not only highly inhibitory to basal TOPflash activity, but also significantly repressed Barx2-mediated activation, β -catenin-mediated activation and activation mediated by Wnt3a ligand signalling. Although the Pax7 homeodomain was not

critical for the repressive function of Pax7, it was at least partly required. Co-immunoprecipitation experiments showed that both Barx2 and Pax7 could interact with β -catenin through their respective homeodomains, and this may indicate a direct competition for formation of an activating Barx2/ β -catenin/TCF complex versus a repressive Pax7/ β -catenin/TCF complex. Although Barx2 and Pax7 are both expressed in quiescent satellite cells, Barx2 expression increases as myoblasts progress through differentiation, whilst Pax7 expression is downregulated. Furthermore, forced expression of Pax7 actually blocks differentiation [Olguin & Olwin 2004]. As such, the functional antagonism observed between Barx2 and Pax7, with respect to Wnt signalling, may be involved in the transition from myoblast proliferation to differentiation. This prompts a model in which a Barx2^{low}/Pax7^{high} expression ratio in quiescent and proliferating cells blocks the pro-differentiation effects of Wnt signals. The subsequent downregulation of Pax7 and upregulation of Barx2 in myoblasts committed to differentiation (Barx2^{high}/Pax7^{low} ratio) may allow Barx2 to activate pro-differentiation target genes in co-operation with β -catenin and MRFs. An intriguing question raised by this model is how the inhibition of Wnt targets by Pax7 is relieved in order to allow differentiation to proceed. Ongoing work in the laboratory has suggested that microRNAs previously shown to block Pax7 translation [Chen et al. 2010] are induced by Wnt3a, thus providing a mechanism for Wnt signals to inhibit Pax7 function.

Consistent with the model presented above, a switch from Notch signalling to Wnt signalling has been proposed to mediate the switch from myoblast proliferation to differentiation [Brack et al. 2008]. RNA-Seq data presented within this thesis

identified misregulation of Wnt as well as Notch pathway components and target genes in myoblasts isolated from *Barx2*^{-/-} mice compared to *Barx2*^{+/+} mice. In general, there was a trend for Wnt target/pathway genes to be downregulated in *Barx2*^{-/-} mice, whilst Notch target/pathway genes were mostly upregulated. Whether the latter effect is direct or due to feedback between Wnt and Notch pathways is yet to be determined. Overall, this differential pattern of Wnt and Notch pathway regulation is consistent with a reduction in differentiation of *Barx2*^{-/-} myoblasts in culture and a reduced capacity of *Barx2*^{-/-} mice to grow and repair muscle [Meech et al. 2012]. Although outside the scope of this study and not investigated further here, the possibility exists that *Barx2* functions directly with components of the Notch signalling pathway such as RBP-Jk and/or Hes/Hey bHLH transcription factors to positively regulate expression of Notch target genes. In addition to this, *Pax7* has been identified as a direct downstream target of Notch signalling in myoblasts [Wen et al. 2012]. Taken together, the functional antagonism between *Barx2* and *Pax7* may be an intermediate control in this Notch to Wnt signalling switch.

Whilst TOPflash was a valuable tool for the initial identification of *Barx2*, *Pax7* and MRFs as modulators of Wnt signalling in myoblasts, it possesses no biological significance. Hence a major aim of this thesis was to identify 'natural' endogenous Wnt target genes in muscle that are also direct targets of *Barx2* activation. The RNA-Seq analysis, and Wnt target and pathway PCR array (Qiagen) analysis produced highly concordant results. A cohort of Wnt target genes including *Axin2*, *Follistatin*, *Wif1*, *Dlk1* and *cyclinD1* were significantly and consistently downregulated in *Barx2*^{-/-} myoblasts. However, due to the germline deletion of *Barx2* in the *Barx2*-LacZ knockin

mouse model, there is a possibility that the near-normal development and growth of *Barx2*^{-/-} mice involves compensatory effects such as upregulation of other gene pathways involved in myoblast function. Furthermore, the Wnt signalling pathway is complex, consisting of multiple levels of regulation by both positive and negative feedback loops. Absence of Barx2 expression may indirectly alter expression of many components and targets of the pathway.

To begin to elucidate *direct* Barx2 target genes a C2C12 Barx2 Tet-ON cell line was generated. This allowed for over-expression of Barx2 and analysis of expression of potential downstream targets. Although no specific differentiation-associated target genes were identified via this method, the expression of downstream Wnt targets Axin2 and cyclinD1 was significantly increased by Barx2. Importantly, the regulation of these two target genes was consistent with the aforementioned RNA-Seq and PCR array analysis of *Barx2*^{+/+} and *Barx2*^{-/-} myoblasts. Further analysis of cyclinD1 and Axin2 as downstream targets of Barx2 strongly suggested that promoter TCF/LEF binding sites were involved in this response. The ability of both Barx2 and β -catenin to activate cyclinD1 and Axin2 promoter constructs was blocked by the addition of dnTCF4 and was significantly decreased upon mutation of the core sequence of the TCF/LEF motifs. A more in-depth analysis of Barx2-mediated activation of Axin2 was undertaken and this revealed many parallels between Axin2 and TOPflash regulation. These studies revealed that multiple TCF/LEF motifs were required for activation of the Axin2 promoter by Barx2, with ChIP assays demonstrating recruitment of Barx2 and endogenous β -catenin to these motifs following Barx2 over-expression. An assessment of histone modifications showed that stimulation by Wnt3a ligand or

over-expression of β -catenin or Barx2 induced changes in histone acetylation across the Axin2 TCF/LEF motifs, which is consistent with a more permissive, active state. This is likely to be mediated in part by the histone acetyltransferase GRIP-1, which was demonstrated to interact with Barx2 within this study, and has previously been identified to interact with β -catenin [Li et al. 2004; Song & Gelmann 2005].

The model of opposing functions for Barx2 and Pax7 in regulation of Wnt-responsive genes that was first suggested by studies of TOPflash also applied to the regulation of Axin2. Although Pax7 did not completely abolish β -catenin and Barx2-mediated activation of the Axin2 luciferase construct, it was significantly inhibitory. The study of Pax7-mediated repression of Axin2, in conjunction with TOPflash, showed that Pax7 was recruited to the same TCF/LEF sites as Barx2 and β -catenin and inhibited Barx2-mediated histone acetylation when over-expressed. The data presented in this thesis suggest that Pax7 mediates repression through a physical interaction with HDAC1. This interaction might maintain HDAC1 (and other co-repressors) at TCF/LEF sites in a manner that is dominant over β -catenin-mediated co-repressor dismissal, although due to technical constraints ChIP experiments could not confirm Pax7 mediated recruitment of HDAC1 at Axin2 or TOPflash promoters. Overall, these data suggested an involvement of HDAC1 and GRIP-1 in the Pax7/ β -catenin/TCF repressing complex and the Barx2/ β -catenin/TCF activating complex, respectively (Figure 7.1). A more detailed analysis of protein-protein interactions and complex formation involving Barx2 and Pax7 in proliferating versus differentiating myoblasts by means of affinity purification-mass spectrometry analysis may generate meaningful data in regards to these interaction networks. This may further reveal mechanisms and

enhance our understanding of the opposing functions of Barx2 and Pax7 in Wnt target gene regulation.

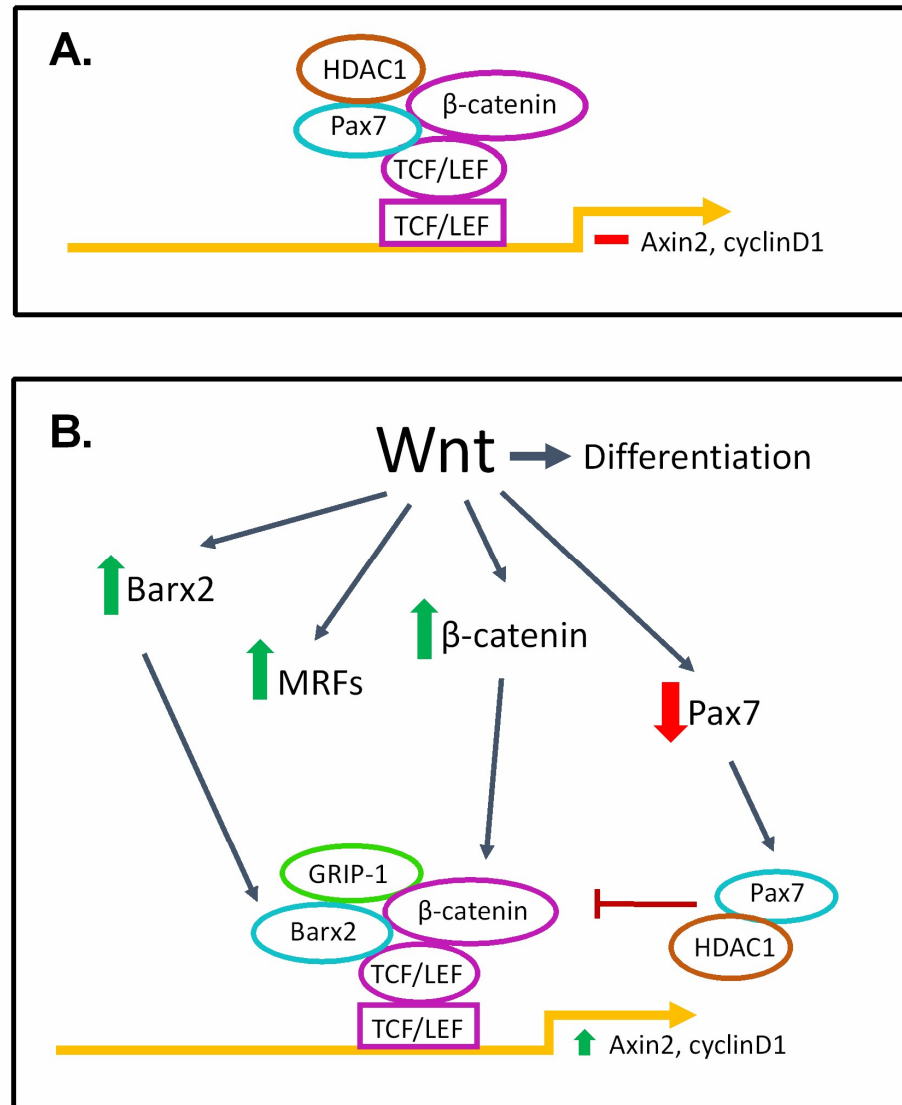


Figure 7.1: Model for the function of Barx2 and Pax7 downstream of Wnt signalling

(A): Under normal growth conditions, in the absence of a Wnt ligand, the Barx2^{low}/Pax7^{high} expression ratio in myoblasts maintains the cells in a proliferating state. Pax7 interacts with β -catenin and the co-repressor HDAC1 at target gene promoters and may function to block dismissal of such co-repressors from the TCF/LEF complex. (B): Barx2 protein is induced by Wnt3a whilst Pax7 is reduced, resulting in a Barx2^{high}/Pax7^{low} expression ratio. With the Pax7/HDAC1 repression removed, Barx2 associates with β -catenin-TCF/LEF complexes and the co-activator GRIP-1 to activate Wnt-responsive target genes such as Axin2 via TCF/LEF binding motifs. Whilst this represents a model for the feedback and termination of Wnt signalling via regulation of Axin2, and possibly other Wnt/TCF-responsive target genes, it does not describe a model for regulation of myogenesis. For a more detailed discussion on these two models, please refer to Hulin et al. 2016.

The role that Axin2 plays as a component of the Wnt signalling pathway is well established. Axin2 is a key player in the termination of the transient Wnt response via its involvement in the destruction complex with GSK-3 β and APC to phosphorylate and destabilise β -catenin [Behrens et al. 1998; Yamamoto et al. 1998; Stamos & Weis 2013]. As we and others have demonstrated, Axin2 is a direct downstream target of Wnt signalling [Jho et al. 2002; Leung et al. 2002]. Axin2 therefore works in a feedback loop to regulate its own expression and to attenuate Wnt signalling. Given very recent evidence suggesting that β -catenin is redundant in adult muscle, but that excessive signalling through β -catenin is deleterious to muscle differentiation and repair [Murphy et al. 2014], an understanding of how β -catenin activity is controlled or terminated is important for understanding the overall role of canonical Wnts in adult muscle. It is therefore possible that Barx2, which promotes Axin2 induction, is an important factor in this feedback loop. Consistent with this idea, the phenotype resulting from uncontrolled expression of constitutively active β -catenin in myoblasts *in vivo* is similar to that of loss of Barx2 *in vivo*: after muscle injury there is delayed expression of genes controlling differentiation, decreased ability to differentiate, continued presence of myocytes, and unresolved fibrosis [Meech et al. 2012; Murphy et al. 2014].

Work presented within this thesis has also demonstrated a role for canonical Wnt signalling upstream of Barx2 in primary myoblasts. A significant increase in Barx2 mRNA was observed following treatment with Wnt3a, however this translated to only a small increase in Barx2 protein. The evidence to date suggests that regulation of Barx2 by Wnt3a is via an indirect mechanism, but that it at least partially involves

stabilisation of Barx2 protein. Taken together, the studies presented here suggest a novel explanation for the muscle phenotype of *Barx2* null mice: specifically, a lack of Barx2 protein induction in null muscle by Wnt signals associated with growth and repair may impair Axin2 induction and thus the timely attenuation of the Wnt signal. In this model, Barx2 is important for preventing the deleterious effects of uncontrolled Wnt signalling through limitation of either signal duration or intensity.

In contrast to the effect of Wnt3a, no increase in Barx2 mRNA or protein was observed following β -catenin lentiviral transduction, and thus the role of Wnt3a in mediating Barx2 expression is likely independent of β -catenin. Recent work indicates that β -catenin is redundant for muscle regeneration [Murphy et al. 2014], however it is unclear if this redundancy extends to the Wnt ligand/receptor signalling complex itself. It is formally possible that 'canonical' Wnt signals are in fact required for myogenesis (eg. myoblast differentiation), but that the function of β -catenin downstream of this signalling event is not. The possible β -catenin-independent effects of canonical Wnt ligands in myoblasts are an important topic for further investigation. Ongoing work in the laboratory using CRISPR/Cas9 genome editing techniques to ablate β -catenin expression in primary myoblasts will allow for the functions of 'canonical' Wnt ligands such as Wnt3a (including inducing Barx2 and differentiation) to be explored in the absence of the canonical effector β -catenin. Importantly, this model will also help to establish the precise role that β -catenin plays in Barx2-mediated activation and Pax7-mediated repression of canonical Wnt target genes.

In addition to the role of Axin2 in controlling β -catenin levels, negative feedback to

Wnt signalling also occurs at the ligand-receptor complex by factors such as Wif1, Sfrps, and Dkk1. Wif1 was identified as a potential target of Barx2 in both RNA-Seq and PCR array analysis, yet was not tested in the C2C12 Barx2 Tet-ON stable lines; the roles of Sfrps and Dkk1 downstream of Barx2 have not yet been assessed. It would be interesting to test the ability of Barx2 to regulate these target genes, particularly Dkk1, which contains TCF/LEF consensus binding sites within the promoter region and is a direct target of Wnt signalling [Niida et al. 2004].

A major question raised by the studies presented here is the extent to which Barx2 and β -catenin target genes are directly involved in controlling myogenesis (eg. myoblast differentiation), versus regulation of the Wnt signalling feedback network. In particular, to date our studies have not clearly identified a network of differentiation-associated genes that are regulated by Barx2 and β -catenin through TCF/LEF motifs. A ChIP-Seq experiment to identify promoter regions that may be co-bound by Barx2 and β -catenin was undertaken as part of this project. However, due to time constraints this data could not be fully analysed and was thus not presented here. A thorough analysis of this data combined with additional ChIP-Seq experiments and the aforementioned affinity purification-mass spectrometry could potentially identify cohorts of genes that are regulated by different complexes involving Barx2 and β -catenin. Presently it is hypothesised that these genes may fall into two categories: those with a role in differentiation of myoblasts, and those which are involved in feedback and termination of a canonical Wnt signal.

Degenerative diseases of skeletal muscle such as DMD represent a significant cause of morbidity and mortality for which there are few effective therapies currently

available. It is clear, however, that a recapitulation of signals to and from the satellite cell niche are critical for effective regeneration. As such, a more detailed understanding of the biological pathways and regulatory networks which govern skeletal muscle development and regeneration following injury could potentially lead to development of novel therapeutics. Specifically, soluble factors such as Wnts which signal to the satellite cell niche and are able to activate satellite cells or promote myoblast proliferation and differentiation represent potential targets for therapeutic manipulation. Characterisation of the downstream pathways that mediate Wnt signalling could facilitate development of Wnt-based approaches to improve such muscle stem cell therapies, perhaps through stimulation of satellite cells to more effectively compensate for damage, thus reducing symptoms and extending life. The study presented in this thesis has revealed new molecular interaction networks controlling muscle differentiation and thus regeneration and repair. These molecular networks which involve Barx2, Pax7, β -catenin and TCF/LEF factors provide critical new information on muscle-specific mechanisms of Wnt signalling that may provide new avenues for intervening in muscle disease by enhancing endogenous regenerative myogenesis.

Appendices

Appendix 1

Reagent	Supplier
Buffer Chemicals	
Acetic acid	Ajax Finechem, New South Wales, Australia
Boric acid	Sigma-Aldrich, New South Wales, Australia
Bovine serum albumin (BSA) solution	New England Biolabs (NEB), Massachusetts, USA
Bromophenol blue	Sigma-Aldrich
CaCl ₂ .2H ₂ O	Ajax Finechem (Thermo Fisher Scientific), Victoria, Australia
Dimethyl sulfoxide (DMSO)	Merck, New Jersey, USA
Ethylenediaminetetra-acetic acid, disodium salt (EDTA)	Astral Scientific, New South Wales, Australia
Glycerol	Amresco, Ohio, USA
Glycine	Amresco
HCl	VWR, Pennsylvania, USA
Isopropanol	Chem-Supply, South Australia, Australia
KCl	Amresco
KH ₂ PO ₄	Amresco
Methanol	Chem-Supply
Na ₂ HPO ₄	Ajax Finechem
NaCl	Astral Scientific
Nondiet P-40	Sigma-Aldrich
Proteinase K	NEB
Sucrose	Astral Scientific
Sodium dodecyl sulphate (SDS)	AG Scientific, California, USA
Tris[hydroxymethyl]aminomethane (Tris)	Astral Scientific
Xylene cyanol FF	Sigma-Aldrich
Mammalian Tissue Culture	
Actinomycin D	Sigma-Aldrich
Cycloheximide	Sigma-Aldrich
Doxycycline	Sigma-Aldrich
Dulbecco's modified Eagle's medium (DMEM)	Invitrogen (Thermo Fisher Scientific)
Foetal calf serum	Bovogen Biologicals, Victoria, Australia
Geneticin (G418)	AG Scientific
Ham's F-10 Nutrient Mix	Life Technologies (Thermo Fisher Scientific)

MEM non-essential amino acids	Invitrogen (Thermo Fisher Scientific)
MEM sodium pyruvate	Invitrogen (Thermo Fisher Scientific)
Penicillin Streptomycin (Pen Strep)	Life Technologies (Thermo Fisher Scientific)
Puromycin	Astral Scientific
Tissue culture flasks and plates	Nunc, Roskilde, Denmark
Trypsin-EDTA	Invitrogen (Thermo Fisher Scientific)
Trypan blue	Sigma-Aldrich
Transfection and Reporter Gene Assays	
Dual-luciferase Reporter Assay System	Promega, Wisconsin, USA
Lipofectamine 2000	Invitrogen (Thermo Fisher Scientific)
Bacterial Culture	
Agar	Amresco
Ampicillin	Aspen Pharmacare, New South Wales, Australia
Kanamycin	Sigma-Aldrich
Luria Broth (LB) EZMix	Amresco
DNA Detection, Purification and Modification	
30% Acrylamide/Bis solution 19:1	BioRad, California, USA
Agarose	Astral Scientific
Ethidium bromide	Amresco
Restriction enzymes	NEB
QIAGEN Plasmid Midiprep kit	Qiagen, Victoria, Australia
QIAprep Spin Miniprep kit	Qiagen
QIAquick Gel Extraction kit	Qiagen
QIAquick PCR Purification kit	Qiagen
Quick Ligation kit	NEB
RNA Purification and cDNA Synthesis	
Amplification grade DNaseI	Life Technologies (Thermo Fisher Scientific)
Chloroform	VWR
TRIzol	Life Technologies (Thermo Fisher Scientific)
NxGen M-MuLV Reverse Transcriptase	Lucigen, Wisconsin, USA
NxGen RNase Inhibitor	Lucigen
Polymerase Chain Reaction (PCR)	
Deoxynucleotide-triphosphate mix (dNTP)	NEB
Oligonucleotides	Geneworks or Integrated DNA Technologies

Phire HotStart DNA Polymerase	Thermo Fisher Scientific
Phusion High-Fidelity DNA Polymerase	Thermo Fisher Scientific
GoTaq qPCR master mix	Promega
Western Blot	
30% Acrylamide/Bis solution (29:1)	BioRad
Ammonium persulphate	Amresco
BioRad Protein Assay Reagent	BioRad
Complete Proteinase Inhibitor tablets	Roche Diagnostics, South Australia, Australia
N,N,N',N'-Tetramethyl-1-,2-diaminomethane (Temed)	Sigma-Aldrich
Skim milk powder	Fonterra Brands, New Zealand
SuperSignal West Pico chemiluminescent (ECL) HRP substrate	Thermo Fisher Scientific
Trans-blot nitrocellulose membrane	BioRad
Tween-20	Astral Scientific
Chromatin Immunoprecipitation (ChIP)	
ChIP grade Protein G magnetic beads	Cell Signaling Technology, Massachusetts, USA
Formaldehyde	Sigma-Aldrich
Protein A sepharose beads	GE Healthcare, New South Wales, Australia
Primary Myoblast Isolation	
Basic fibroblast growth factor (murine)	Cell Signaling Technology
Collagen	Gibco (Thermo Fisher Scientific)
Collagenase	Gibco (Thermo Fisher Scientific)
Dispase	Gibco (Thermo Fisher Scientific)
Primary Antibodies	
c-Myc	Santa Cruz (sc-40), Texas, USA
Barx2	Santa Cruz (sc-9128)
Pax7	Santa Cruz (sc-7748)
GRIP-1	Santa Cruz (sc-8996)
HDAC1	Santa Cruz (sc-7872 X)
β -catenin	Cell Signaling Technology (9562L)
Active (non-phospho) β -catenin	Merck Millipore (05-665), Victoria, Australia
MyoD	Santa Cruz (sc-32758)
DAPI (4',6-diamidino-2-phenylindole)	Sigma-Aldrich
Normal rabbit IgG	Cell Signaling Technology (2779S)
Histone H3K acetylation	Merck Millipore (06-599)
Histone H3K4 tri-methylation	Merck Millipore (07-473)
Histone H3K27 tri-methylation	Merck Millipore (07-449)

CD34 PE rat-anti-mouse	BD Biosciences (551387), New Jersey, USA
CD45 APC rat-anti-mouse	BD Biosciences (559864)
Scal FITC rat-anti-mouse	BD Biosciences (557405)
Secondary Antibodies	
Donkey anti-Rabbit IgG-Horseradish Peroxidase conjugate	Jackson ImmunoResearch, Pennsylvania, USA
Donkey anti-mouse IgG-Horseradish Peroxidase conjugate	Jackson ImmunoResearch
Rabbit anti-goat IgG-Horseradish Peroxidase conjugate	Jackson ImmunoResearch
DyLight 488 Horse-anti-mouse	Vector Laboratories (DI-2488), California, USA
DyLight 594 Goat-anti-rabbit	Vector Laboratories (DI-1594)
Donkey-anti-mouse Cy5	Jackson ImmunoResearch (26558)
Donkey-anti-goat Alexa 546	Jackson ImmunoResearch (7191)

Appendix 2

<p><u>Chromatin Immunoprecipitation</u></p> <p>Lysis Buffer 1 (Cell Lysis) 1 % Nonidet P40 15 mM Tris pH 8.0 0.5 mM EGTA 15 mM NaCl 60 mM KCl 300 mM Sucrose 0.5 mM B-mercaptoethanol</p> <p>Lysis Buffer 2 (Nuclear Lysis) 1 % SDS 10 mM EDTA 50 mM Tris pH 8.0</p> <p>Dilution Buffer % SDS 1% Triton X-100 1.2 mM EDTA 16.7 mM Tris pH 8.0 150 mM NaCl</p> <p>High Salt Wash Buffer 0.1% SDS 1% Triton X-100 1 mM EDTA 20 mM TrisCl pH 8.0 500 mM NaCl</p> <p>LiCl Buffer 1% NP-40 1% deoxycholic acid sodium salt 1 mM EDTA 10 mM Tris pH 8.0 250 mM LiCl</p> <p>TE Buffer 1 mM EDTA 10 mM Tris pH 8.0</p> <p>Elution Buffer 20 mM Tris pH 8.0 5 mM EDTA 50 mM NaCl 1% SDS</p>	<p><u>Co-immunoprecipitation</u></p> <p>Hypotonic Lysis Buffer 20 mM Tris pH 7.4 10 mM MgCl₂ 10 mM KCl 1 mM EDTA 10% glycerol 1% Triton X-100 1 mM DTT 2.5 mM glycerol-2-phosphate</p> <p><u>Electrophoretic Mobility Shift Assay</u></p> <p>Hypotonic Lysis Buffer 20 mM Tris pH 7.4 10 mM MgCl₂ 10 mM KCl 1 mM EDTA 10% glycerol 1% Triton X-100 1 mM DTT 10 mM glycerol-2-phosphate</p> <p>Nuclear Extract Buffer 20 mM HEPES 420 mM NaCl 5 mM EDTA 10% glycerol 10 mM glycerol-2-phosphate</p> <p>EMSA Buffer 10 mM Tris pH 8 100 mM NaCl 1 mM MgCl₂ 20% glycerol</p>
--	--

Appendix 3

Original email to Dr Kudo and Dr Kii in regards to TOPEGFP transgenic mouse

Dear Dr. Kudo and Dr. Kii,

Thank you very much for your help in identifying the precise sequence of the TOP-EGFP transgenic mouse promoter region. Unfortunately we were not able to amplify the promoter from the mouse genomic DNA using primers corresponding to the sequence that you sent. However, we were able to amplify the promoter region using a forward primer in the HS4 insulator and a reverse primer in the EGFP gene. We sequenced this PCR product and regret to inform you that the mice do not appear to contain the promoter region from the TOP-flash vector as you described.

Instead the region between the HS4 insulator and the EGFP gene contains 6 copies of a 44bp sequence from the Epstein Barr Virus LMP2B gene promoter. This 44bp sequence contains two copies of the RBP-Jk consensus element (C/T)GTGGGAA. Thus the promoter contains in total 12 RBP-Jk binding elements and no TCF/LEF sites. I have attached the sequence and our analysis to this email as a word file.

Basically, the mice contain a Notch reporter gene not a Wnt reporter gene. Curiously, in our experiments primary myoblasts from the mice did respond to Wnt3a with about a 4-fold increase in EGFP mRNA. This could be due to Wnt signals secondarily inducing Notch signaling.

The mice were obtained from the RIKEN BRC under the Resource number/name RBRC02229/TOP-EGFP. Our shipping records confirm that these were the mice sent and we have no other EGFP-containing mice in our animal facility that they could have been mixed up with. Therefore I think that the mice distributed as your TOP-EGFP mice by the RIKEN BRC are not correct.

While it is possible that the BRC just sent me a wrong breeder pair, I cannot find any Notch reporter strain in their catalog that they could have sent me by mistake. Thus I wonder if their entire colony is in fact wrong and I think that they should check the colony identity by PCR and sequencing. You may also want to check your laboratory records regarding the mice that were deposited.

I am sorry to send you this news.

Kind regards,
Robyn

Robyn Meech, Ph.D.
ARC Future Fellow
Department of Clinical Pharmacology
Flinders University
Bedford Park, 5042, S.A.
Australia
Ph. 8204 4795 (ext 6-4795)
Fax. 8204 5114

Reply email from Dr Kudo

From: Akira Kudo
Sent: Tuesday, 9 July 2013 11:54 AM
To: Robyn Meech
Cc: KII Isao
Subject: Re: TOP-EGFP mice - promoter error

Dear Dr. Meech

Thank you for sending this information. I am very surprised to see your data because we have never touched the Notch reporter construct and mice.

I have transferred this E-mail to my collaborator Dr. Saga who contributed this mouse to Riken BRC.

Alternatively, I recommend you to use another TOP-EGFP mouse or TOP-GAL mouse (RBRC02228).

Sincerely,
Akira Kudo

Tokyo Institute of Technology

Notice from RIKEN BioResource Center identifying strain mixup

July 18, 2013

[Urgent Notice for users of **TOP-EGFP (02229)** mouse strain]

Dear Dr. Robyn Meech,

robyn.meech@flinders.edu.au

We, the RIKEN BioResource Center, regret to inform you that the TOP-EGFP (02229) which was sent to you on March 28, 2011 was a wrong strain. We sent you TP1-Venus, instead. The depositor sent us a wrong strain by mistake and we did not recognize this mistake until the depositor informed us on July 9, 2013. We understand that mistake of the mouse strain might cause serious scientific damage. But, it is our hope that the damage is the minimum.

Please do not use this mouse strain 'TOP-EGFP (02229)' any more unless you have a compelling reason to keep using the mouse strain. The TP1 contains twelve Rbpj binding sites and a minimum promoter [1, 2], while the TOP contains six Tcf/Lef consensus binding sites and a minimum promoter [De Souza et al. 2004], thus, visualizing different signals such as activation of Notch and canonical Wnt signals, respectively.

Unfortunately, neither the depositor nor we have the authentic TOP-EGFP strain. However, we have TOP-GAL which can be used as a replacement of TOP-EGFP and expresses b-galactosidase instead of EGFP under the control of the TOP promoter. If you would like to use TOP-GAL mice, we will provide you the mice as a replacement. Regarding refund of the distribution fee and shipping cost, we will write you as soon as the paper work is finished.

If you have published a scientific paper using the TOP-EGFP (02229) mice, please let us know. If you need, we will send a letter to an editor of a journal and explain the details of this accident.

The mouse was deposited as TOP-EGFP at RIKEN BRC on May 15, 2007. Since then, we have genotyped by using PCR, maintained and distributed the mice to scientists in Japan and abroad. The primer design for the genotyping to amplify only a part of EGFP gene was instructed by the depositor. Immediately after report of the mistake of this mouse strain from the depositor on July 9, 2013, we analyzed DNA samples of deposited mice and detected a part of the TP1 sequence and Venus as reported by the depositor.

We have been operating mouse resource center in Japan since 2001 and distributing nearly 3,000 mice annually around the world. Quality control of mouse strains is the most important task for us. Through this unfortunate lesson, we will continue every effort to establish an accurate method for rigorous quality control to serve better to the scientific community. We appreciate you for your support and understanding for our activities.

If you have any question and concern on this matter, please feel free to contact me.

Sincerely yours,

Atsushi Yoshiki, Ph. D.

Head

Experimental Animal Division

RIKEN BioResource Center

References:

- [1] Kohyama J, Tokunaga A, Fujita Y, Miyoshi H, Nagai T, Miyawaki A, Nakao K, Matsuzaki Y, Okano H. Visualization of spatiotemporal activation of Notch signaling: live monitoring and significance in neural development. *Dev Biol.* 286(1):311-25 (2005). <http://www.sciencedirect.com/science/article/pii/S0012160605005221>
- [De Souza et al. 2004] Sasaki N, Kiso M, Kitagawa M, Saga Y. The repression of Notch signaling occurs via the destabilization of mastermind-like 1 by Mesp2 and is essential for somitogenesis. *Development* 138:55-64 (2011). <http://dev.biologists.org/content/138/1/55.long>
- [De Souza et al. 2004] Moriyama A, Kii I, Sunabori T, Kurihara S, Takayama I, Shimazaki M, Tanabe H, Oginuma M, Fukayama M, Matsuzaki Y, Saga Y, Kudo A. GFP transgenic mice reveal active canonical Wnt signal in neonatal brain and in adult liver and spleen. *Genesis* 45(2):90-100 (2007). <http://onlinelibrary.wiley.com/doi/10.1002/dvg.20268/abstract>

Appendix 4

Exon 1

#2clone	-----DELISFKDEGEQEEKNSENSSAERDLADVKSSSLVNESETNQNSS
#7clone	-----DELXSFXDEGEQEEKNSENSSAERDLADVKSSSLVNESETNQNSS
#8clone	-----DELISFXDEGEQEEKNSENSSAERDLADVKSSSLVNESETNQNSS
#1clone	-----DELISFXDEGEQEEKNSENSSAERDLADVKSSSLVNESETNQNSS
Variant4	MPQLNGGGGDDLGADELISFKDEGEQEEKNSENSSAERDLADVKSSSLVNESETNQNSS
Variant2	MPQLNGGGGDDLGADELISFKDEGEQEEKNSENSSAERDLADVKSSSLVNESETNQNSS
Variant1	MPQLNGGGGDDLGADELISFKDEGEQEEKNSENSSAERDLADVKSSSLVNESETNQNSS
Variant6	MPQLNGGGGDDLGADELISFKDEGEQEEKNSENSSAERDLADVKSSSLVNESETNQNSS
#6clone	-----DELISFXDEGEQEEKNSENSSAERDLADVKSSSLVNESETNQNSS
Variant5	MPQLNGGGGDDLGADELISFKDEGEQEEKNSENSSAERDLADVKSSSLVNESETNQNSS
Variant3	MPQLNGGGGDDLGADELISFKDEGEQEEKNSENSSAERDLADVKSSSLVNESETNQNSS
Variant7	MPQLNGGGGDDLGADELISFKDEGEQEEKNSENSSAERDLADVKSSSLVNESETNQNSS
#5clone	-----ELISFXDEGEQEEKNSENSSAERDLADVKSSSLVNESETNQNSS

#2clone	DSEAEERRPPRSESFRDKSRESLEEAAKRQDGGGLFKGPPYPGYFFIMI	PDLTSPYLPNGS
#7clone	DSEAEERRPPRSESFRDKSRESLEEAAKRQDGGGLFKGPPYPGYFFIMI	PDLTSPYLPNGS
#8clone	DSEAEERRPPRSESFRDKSRESLEEAAKRQDGGGLFKGPPYPGYFFIMI	PDLTSPYLPNGS
#1clone	DSEAEERRPPRSESFRDKSRESLEEAAKRQDGGGLFKGPPYPGYFFIMI	PDLTSPYLPNGS
Variant4	DSEAEERRPPRSESFRDKSRESLEEAAKRQDGGGLFKGPPYPGYFFIMI	PDLTSPYLPNGS
Variant2	DSEAEERRPPRSESFRDKSRESLEEAAKRQDGGGLFKGPPYPGYFFIMI	PDLTSPYLPNGS
Variant1	DSEAEERRPPRSESFRDKSRESLEEAAKRQDGGGLFKGPPYPGYFFIMI	PDLTSPYLPNGS
Variant6	DSEAEERRPPRSESFRDKSRESLEEAAKRQDGGGLFKGPPYPGYFFIMI	PDLTSPYLPNGS
#6clone	DSEAEERRPPRSESFRDKSRESLEEAAKRQDGGGLFKGPPYPGYFFIMI	PDLTSPYLPNGS
Variant5	DSEAEERRPPRSESFRDKSRESLEEAAKRQDGGGLFKGPPYPGYFFIMI	PDLTSPYLPNGS
Variant3	DSEAEERRPPRSESFRDKSRESLEEAAKRQDGGGLFKGPPYPGYFFIMI	PDLTSPYLPNGS
Variant7	DSEAEERRPPRSESFRDKSRESLEEAAKRQDGGGLFKGPPYPGYFFIMI	PDLTSPYLPNGS
#5clone	DSEAEERRPPRSESFRDKSRESLEEAAKRQDGGGLFKGPPYPGYFFIMI	PDLTSPYLPNGS

#2clone	LSPTARTLHFQSGSTHYSAYKTIHQIAIQYLQMKWPLLDVQAGSLQSRQTLKDARS	PSP
#7clone	LSPTARTLHFQSGSTHYSAYKTIHQIAIQYLQMKWPLLDVQAGSLQSRQTLKDARS	PSP
#8clone	LSPTARTLHFQSGSTHYSAYKTIHQIAIQYLQMKWPLLDVQAGSLQSRQTLKDARS	PSP
#1clone	LSPTARTLHFQSGSTHYSAYKTIHQIAIQYLQMKWPLLDVQAGSLQSRQTLKDARS	PSP
Variant4	LSPTARTLHFQSGSTHYSAYKTIHQIAIQYLQMKWPLLDVQAGSLQSRQTLKDARS	PSP
Variant2	LSPTART-----YLQMKWPLLDVQAGSLQSRQTLKDARS	PSP
Variant1	LSPTART-----YLQMKWPLLDVQAGSLQSRQTLKDARS	PSP
Variant6	LSPTART-----YLQMKWPLLDVQAGSLQSRQTLKDARS	PSP
#6clone	LSPTART-----YLQMKWPLLDVQAGSLQSRQTLKDARS	PSP
Variant5	LSPTART-----YLQMKWPLLDVQAGSLQSRQTLKDARS	PSP
Variant3	LSPTART-----YLQMKWPLLDVQAGSLQSRQTLKDARS	PSP
Variant7	LSPTART-----YLQMKWPLLDVQAGSLQSRQTLKDARS	PSP
#5clone	LSPTART-----YLQMKWPLLDVQAGSLQSRQTLKDARS	PSP

#2clone	AHIVSNKVPVVQHPHHVHPLTPLITYSNEHFTPGNPPPHLPADVDPK	-----
#7clone	AHIVSNKVPVVQHPHHVHPLTPLITYSNEHFTPGNPPPHLPADVDPK	GIPRPPHPPDIS
#8clone	AHIVSNKVPVVQHPHHVHPLTPLITYSNEHFTPGNPPPHLPADVDPK	GIPRPPHPPDIS
#1clone	-----	-----
Variant4	AHIVSNKVPVVQHPHHVHPLTPLITYSNEHFTPGNPPPHLPADVDPK	GIPRPPHPPDIS
Variant2	AHIVSNKVPVVQHPHHVHPLTPLITYSNEHFTPGNPPPHLPADVDPK	GIPRPPHPPDIS
Variant1	AHIVSNKVPVVQHPHHVHPLTPLITYSNEHFTPGNPPPHLPADVDPK	GIPRPPHPPDIS
Variant6	AHIVSNKVPVVQHPHHVHPLTPLITYSNEHFTPGNPPPHLPADVDPK	GIPRPPHPPDIS
#6clone	AHIVSNKVPVVQHPHHVHPLTPLITYSNEHFTPGNPPPHLPADVDPK	GIPRPPHPPDIS
Variant5	AHIVSNKVPVVQHPHHVHPLTPLITYSNEHFTPGNPPPHLPADVDPK	GIPRPPHPPDIS
Variant3	AHIVSNKVPVVQHPHHVHPLTPLITYSNEHFTPGNPPPHLPADVDPK	GIPRPPHPPDIS
Variant7	AHIVSNKVPVVQHPHHVHPLTPLITYSNEHFTPGNPPPHLPADVDPK	GIPRPPHPPDIS
#5clone	AHIVSNKVPVVQHPHHVHPLTPLITYSNEHFTPGNPPPHLPADVDPK	GIPRPPHPPDIS

	Exon 7	Exon 8
#2clone	-----	
#7clone	PYYPLSPGTVGQIPHPLGW	-----FPP
#8clone	PYYPLSPGTVGQIPHPLGW	-----FPP
#1clone	-----PHPLGW	---QGQPVYPITTTGGFRHPYPTALTVNASMS---RFPP
Variant4	PYYPLSPGTVGQIPHPLGW	---QGQPVYPITTTGGFRHPYPTALTVNASMS---SFLSSRFPP
Variant2	PYYPLSPGTVGQIPHPLGW	LVPQGGQPVYPITTTGGFRHPYPTALTVNASMS---RFPP
Variant1	PYYPLSPGTVGQIPHPLGW	LVPQGGQPVYPITTTGGFRHPYPTALTVNASMS---RFPP
Variant6	PYYPLSPGTVGQIPHPLGW	LVPQGGQPVYPITTTGGFRHPYPTALTVNASMS---RFPP
#6clone	PYYPLSPGTVGQIPHPLGW	---QGQPVYPITTTGGFRHPYPTALTVNASMS---RFPP
Variant5	PYYPLSPGTVGQIPHPLGW	LVPQGGQPVYPITTTGGFRHPYPTALTVNASMS---SFLSSRFPP
Variant3	PYYPLSPGTVGQIPHPLGW	LVPQGGQPVYPITTTGGFRHPYPTALTVNASMS---RFPP
Variant7	PYYPLSPGTVGQIPHPLGW	LVPQGGQPVYPITTTGGFRHPYPTALTVNASMS---RFPP
#5clone	PYYPLSPGTVGQIPHPLGW	LVPQGGQPVYPITTTGGFRHPYPTALTVNASMS---RFPP

	Exon 9	Exon 10
#2clone	-----	
#7clone	HMVPPHHTLHTTGIHPHAIPTVKQESSQSDVGLHSSKHQDSKKEEKKKPHIKKPLN	
#8clone	HMVPPHHTLHTTGIHPHAIPTVKQESSQSDVGLHSSKHQDSKKEEKKKPHIKKPLN	
#1clone	HMVPPHHTLHTTGIHPHAIPTVKQESSQSDVGLHSSKHQDSKKEEKKKPHIKKPLN	
Variant4	HMVPPHHTLHTTGIHPHAIPTVKQESSQSDVGLHSSKHQDSKKEEKKKPHIKKPLN	
Variant2	HMVPPHHTLHTTGIHPHAIPTVKQESSQSDVGLHSSKHQDSKKEEKKKPHIKKPLN	
Variant1	HMVPPHHTLHTTGIHPHAIPTVKQESSQSDVGLHSSKHQDSKKEEKKKPHIKKPLN	
Variant6	HMVPPHHTLHTTGIHPHAIPTVKQESSQSDVGLHSSKHQDSKKEEKKKPHIKKPLN	
#6clone	HMVPPHHTLHTTGIHPHAIPTVKQESSQSDVGLHSSKHQDSKKEEKKKPHIKKPLN	
Variant5	HMVPPHHTLHTTGIHPHAIPTVKQESSQSDVGLHSSKHQDSKKEEKKKPHIKKPLN	
Variant3	HMVPPHHTLHTTGIHPHAIPTVKQESSQSDVGLHSSKHQDSKKEEKKKPHIKKPLN	
Variant7	HMVPPHHTLHTTGIHPHAIPTVKQESSQSDVGLHSSKHQDSKKEEKKKPHIKKPLN	
#5clone	HMVPPHHTLHTTGIHPHAIPTVKQESSQSDVGLHSSKHQDSKKEEKKKPHIKKPLN	

	Exon 11
#2clone	-----
#7clone	AFMLYMKEMRAKVVAECTLKE SAAINQIXGRRWHALSREEQAKYYELARKERQLHMQLYP
#8clone	AFMLYMKEMRAKVVAECTLKE SAAINQIXGRRWHALSREEQAKYYELARKERQLHMQLYP
#1clone	AFMLYMKEMRAKVVAECTLKE SAAINQILGRRWHALSREEQAKYYELARKERQLHMQLYP
Variant4	AFMLYMKEMRAKVVAECTLKE SAAINQILGRRWHALSREEQAKYYELARKERQLHMQLYP
Variant2	AFMLYMKEMRAKVVAECTLKE SAAINQILGRRWHALSREEQAKYYELARKERQLHMQLYP
Variant1	AFMLYMKEMRAKVVAECTLKE SAAINQILGRRWHALSREEQAKYYELARKERQLHMQLYP
Variant6	AFMLYMKEMRAKVVAECTLKE SAAINQILGRRWHALSREEQAKYYELARKERQLHMQLYP
#6clone	AFMLYMKEMRAKVVAECTLKE SAAINQILGRRWHALSREEQAKYYELARKERQLHMQLYP
Variant5	AFMLYMKEMRAKVVAECTLKE SAAINQILGRRWHALSREEQAKYYELARKERQLHMQLYP
Variant3	AFMLYMKEMRAKVVAECTLKE SAAINQILGRRWHALSREEQAKYYELARKERQLHMQLYP
Variant7	AFMLYMKEMRAKVVAECTLKE SAAINQILGRRWHALSREEQAKYYELARKERQLHMQLYP
#5clone	AFMLYMKEMRAKVVAECTLKE SAAINQILGRRWHALSREEQAKYYELARKERQLHMQLYP

	Exon 12	Exon 13	Exon 17	Exon 14
#2clone	-----			
#7clone	GWSARDNYGKKKKRKRDKQPGETNEHSECFLNPCLSLPPIITGKKKSAFATYKVKAAASAH			
#8clone	GWSARDNYGKKKKRKRDKQPGETNEHSECFLNPCLSLPPIITGKKKSAFATYKVKAAASAH			
#1clone	GWSARDNYGKKKKRKRDKQPGETN-----GEKKSATYKVKAAASAH			
Variant4	GWSARDNYEKKKVRSLHTR-----			
Variant2	GWSARDNYGKKKKRKRDKQPGETN-----DLSAPKKCRARFGLDQNN			
Variant1	GWSARDNYGKKKKRKRDKQPGETNEHSECFLNPCLSLPPIITDLSAPKKCRARFGLDQNN			
Variant6	GWSARDNYGKKKKRKRDKQPGETNEHSECFLNPCLSLPPIITDLSAPKKCRARFGLDQNN			
#6clone	GWSARDNYGKKKKRKRDKQPGETN-----GEKKSATYKVKAAASAH			
Variant5	GWSARDNYGKKKKRKRDKQPGETN-----GEKKSATYKVKAAASAH			
Variant3	GWSARDNYGKKKKRKRDKQPGETNEHSECFLNPCLSLPPIITGKKKSAFATYKVKAAASAH			
Variant7	GWSARDNYGKKKKRKRDKQPGETN-----GEKKSATYKVKAAASAH			
#5clone	GWSARDNYGKKKKRKRDKQPGETN-----GEKKSATYKVKAAASAH			

References

- Aberle, H., Bauer, A., Stappert, J., Kispert, A. and Kemler, R. (1997). "beta-catenin is a target for the ubiquitin-proteasome pathway." Embo j **16**(13): 3797-3804.
- Abu-Elmagd, M., Robson, L., Sweetman, D., Hadley, J., Francis-West, P. and Munsterberg, A. (2010). "Wnt/Lef1 signaling acts via Pitx2 to regulate somite myogenesis." Dev Biol **337**(2): 211-219.
- Agger, K., Cloos, P. A., Christensen, J., Pasini, D., Rose, S., Rappsilber, J., Issaeva, I., Canaani, E., Salcini, A. E. and Helin, K. (2007). "UTX and JMJD3 are histone H3K27 demethylases involved in HOX gene regulation and development." Nature **449**: 731-734.
- Alexakis, C., Partridge, T. and Bou-Gharios, G. (2007). "Implication of the satellite cell in dystrophic muscle fibrosis: a self-perpetuating mechanism of collagen overproduction." Am J Physiol Cell Physiol **293**(2): C661-669.
- Allen, R. E. and Boxhorn, L. K. (1989). "Regulation of skeletal muscle satellite cell proliferation and differentiation by transforming growth factor-beta, insulin-like growth factor I, and fibroblast growth factor." J Cell Physiol **138**(2): 311-315.
- Amen, M., Liu, X., Vadlamudi, U., Elizondo, G., Diamond, E., Engelhardt, J. F. and Amendt, B. A. (2007). "PITX2 and {beta}-Catenin Interactions Regulate Lef-1 Isoform Expression." Mol. Cell. Biol. **27**(21): 7560-7573.
- Amit, S., Hatzubai, A., Birman, Y., Andersen, J. S., Ben-Shushan, E., Mann, M., Ben-Neriah, Y. and Alkalay, I. (2002). "Axin-mediated CKI phosphorylation of beta-catenin at Ser 45: a molecular switch for the Wnt pathway." Genes Dev **16**(9): 1066-1076.
- Amthor, H., Nicholas, G., McKinnell, I., Kemp, C. F., Sharma, M., Kambadur, R. and Patel, K. (2004). "Follistatin complexes Myostatin and antagonises Myostatin-mediated inhibition of myogenesis." Developmental Biology **270**(1): 19-30.
- Andres, V., Cervera, M. and Mahdavi, V. (1995). "Determination of the consensus binding site for MEF2 expressed in muscle and brain reveals tissue-specific sequence constraints." J Biol Chem **270**(40): 23246-23249.
- Arce, L., Pate, K. T. and Waterman, M. L. (2009). "Groucho binds two conserved regions of LEF-1 for HDAC-dependent repression." BMC Cancer **9**: 159.
- Arce, L., Yokoyama, N. N. and Waterman, M. L. (2006). "Diversity of LEF/TCF action in development and disease." Oncogene **25**(57): 7492-7504.
- Atcha, F. A., Munguia, J. E., Li, T. W., Hovanes, K. and Waterman, M. L. (2003). "A new beta-catenin-dependent activation domain in T cell factor." J Biol Chem **278**(18): 16169-16175.
- Atcha, F. A., Syed, A., Wu, B., Hoverter, N. P., Yokoyama, N. N., Ting, J. H., Munguia, J. E., Mangalam, H. J., Marsh, J. L. and Waterman, M. L. (2007). "A unique DNA binding domain converts T-cell factors into strong Wnt effectors." Mol Cell Biol **27**(23): 8352-

8363.

Bajard, L., Relaix, F., Lagha, M., Rocancourt, D., Daubas, P. and Buckingham, M. E. (2006). "A novel genetic hierarchy functions during hypaxial myogenesis: Pax3 directly activates Myf5 in muscle progenitor cells in the limb." Genes Dev **20**(17): 2450-2464.

Baladron, V., Ruiz-Hidalgo, M. J., Nueda, M. L., Diaz-Guerra, M. J., Garcia-Ramirez, J. J., Bonvini, E., Gubina, E. and Laborda, J. (2005). "dlk acts as a negative regulator of Notch1 activation through interactions with specific EGF-like repeats." Exp Cell Res **303**(2): 343-359.

Balczarek, K. A., Lai, Z. C. and Kumar, S. (1997). "Evolution of functional diversification of the paired box (Pax) DNA-binding domains." Mol Biol Evol **14**(8): 829-842.

Bannister, A. J. and Kouzarides, T. (2011). "Regulation of chromatin by histone modifications." Cell Res **21**(3): 381-395.

Bao, X. L., Song, H., Chen, Z. and Tang, X. (2012). "Wnt3a promotes epithelial-mesenchymal transition, migration, and proliferation of lens epithelial cells." Mol Vis **18**: 1983-1990.

Bareja, A. and Billin, A. N. (2013). "Satellite cell therapy - from mice to men." Skelet Muscle **3**(1): 2.

Barker, N., Hurlstone, A., Musisi, H., Miles, A., Bienz, M. and Clevers, H. (2001). "The chromatin remodelling factor Brg-1 interacts with beta-catenin to promote target gene activation." EMBO J **20**: 4935-4943.

Bedford, M. T. and Clarke, S. G. (2009). "Protein arginine methylation in mammals: who, what, and why." Mol Cell **33**(1): 1-13.

Behrens, J., Jerchow, B. A., Wurtele, M., Grimm, J., Asbrand, C., Wirtz, R., Kuhl, M., Wedlich, D. and Birchmeier, W. (1998). "Functional interaction of an axin homolog, conductin, with beta-catenin, APC, and GSK3beta." Science **280**(5363): 596-599.

Behrens, J., von Kries, J. P., Kuhl, M., Bruhn, L., Wedlich, D., Grosschedl, R. and Birchmeier, W. (1996). "Functional interaction of [beta]-catenin with the transcription factor LEF-1." Nature **382**(6592): 638-642.

Benabdallah, B. F., Bouchentouf, M., Rousseau, J., Bigey, P., Michaud, A., Chapdelaine, P., Scherman, D. and Tremblay, J. P. (2008). "Inhibiting Myostatin With Follistatin Improves the Success of Myoblast Transplantation in Dystrophic Mice." Cell Transplantation **17**(3): 337-350.

Bendall, A. J., Ding, J., Hu, G., Shen, M. M. and Abate-Shen, C. (1999). "Msx1 antagonizes the myogenic activity of Pax3 in migrating limb muscle precursors." Development **126**(22): 4965-4976.

Bender, S., Tang, Y., Lindroth, A. M., Hovestadt, V., Jones, D. T., Kool, M., Zapatka, M., Northcott, P. A., Sturm, D., Wang, W., Radlwimmer, B., Hojfeldt, J. W., Truffaux, N., Castel, D., Schubert, S., Ryzhova, M., Seker-Cin, H., Gronych, J., Johann, P. D., Stark, S., Meyer, J., Milde, T., Schuhmann, M., Ebinger, M., Monoranu, C. M., Ponnuswami,

A., Chen, S., Jones, C., Witt, O., Collins, V. P., von Deimling, A., Jabado, N., Puget, S., Grill, J., Helin, K., Korshunov, A., Lichter, P., Monje, M., Plass, C., Cho, Y. J. and Pfister, S. M. (2013). "Reduced H3K27me3 and DNA hypomethylation are major drivers of gene expression in K27M mutant pediatric high-grade gliomas." Cancer Cell **24**(5): 660-672.

Bennicelli, J. L., Advani, S., Schafer, B. W. and Barr, F. G. (1999). "PAX3 and PAX7 exhibit conserved cis-acting transcription repression domains and utilize a common gain of function mechanism in alveolar rhabdomyosarcoma." Oncogene **18**(30): 4348-4356.

Bentzinger, C. F., von Maltzahn, J., Dumont, N. A., Stark, D. A., Wang, Y. X., Nhan, K., Frenette, J., Cornelison, D. D. and Rudnicki, M. A. (2014). "Wnt7a stimulates myogenic stem cell motility and engraftment resulting in improved muscle strength." J Cell Biol **205**(1): 97-111.

Berkes, C. A., Bergstrom, D. A., Penn, B. H., Seaver, K. J., Knoepfler, P. S. and Tapscott, S. J. (2004). "Pbx Marks Genes for Activation by MyoD Indicating a Role for a Homeodomain Protein in Establishing Myogenic Potential." Molecular Cell **14**(4): 465-477.

Bernardi, H., Gay, S., Fedon, Y., Vernus, B., Bonnieu, A. and Bacou, F. (2011). "Wnt4 activates the canonical β -catenin pathway and regulates negatively myostatin: functional implication in myogenesis." American Journal of Physiology - Cell Physiology **300**(5): C1122-C1138.

Bernstein, B. E. (2006). "A bivalent chromatin structure marks key developmental genes in embryonic stem cells." Cell **125**: 315-326.

Bhanot, P., Brink, M., Samos, C. H., Hsieh, J. C., Wang, Y., Macke, J. P., Andrew, D., Nathans, J. and Nusse, R. (1996). "A new member of the frizzled family from Drosophila functions as a Wingless receptor." Nature **382**(6588): 225-230.

Billin, A. N., Thirlwell, H. and Ayer, D. E. (2000). "Beta-catenin-histone deacetylase interactions regulate the transition of LEF1 from a transcriptional repressor to an activator." Mol Cell Biol **20**(18): 6882-6890.

Birbrair, A., Zhang, T., Wang, Z. M., Messi, M. L., Enikolopov, G. N., Mintz, A. and Delbono, O. (2013). "Role of pericytes in skeletal muscle regeneration and fat accumulation." Stem Cells Dev **22**(16): 2298-2314.

Bischoff, R. (1975). "Regeneration of single skeletal muscle fibers in vitro." Anat Rec **182**(2): 215-235.

Bittner, R. E., Schofer, C., Weipoltshammer, K., Ivanova, S., Streubel, B., Hauser, E., Freilinger, M., Hoger, H., Elbe-Burger, A. and Wachtler, F. (1999). "Recruitment of bone-marrow-derived cells by skeletal and cardiac muscle in adult dystrophic mdx mice." Anat Embryol (Berl) **199**(5): 391-396.

Bjornson, C. R. R., Cheung, T. H., Liu, L., Tripathi, P. V., Steeper, K. M. and Rando, T. A. (2012). "Notch Signaling Is Necessary to Maintain Quiescence in Adult Muscle Stem Cells." Stem Cells **30**(2): 232-242.

- Black, B. L., Martin, J. F. and Olson, E. N. (1995). "The mouse MRF4 promoter is trans-activated directly and indirectly by muscle-specific transcription factors." J Biol Chem **270**(7): 2889-2892.
- Black, B. L., Molkenkin, J. D. and Olson, E. N. (1998). "Multiple roles for the MyoD basic region in transmission of transcriptional activation signals and interaction with MEF2." Mol Cell Biol **18**(1): 69-77.
- Blau, H. M., Webster, C. and Pavlath, G. K. (1983). "Defective myoblasts identified in Duchenne muscular dystrophy." Proc Natl Acad Sci U S A **80**(15): 4856-4860.
- Bober, E., Franz, T., Arnold, H. H., Gruss, P. and Tremblay, P. (1994). "Pax-3 is required for the development of limb muscles: a possible role for the migration of dermomyotomal muscle progenitor cells." Development **120**(3): 603-612.
- Bober, E., Lyons, G. E., Braun, T., Cossu, G., Buckingham, M. and Arnold, H. H. (1991). "The muscle regulatory gene, Myf-6, has a biphasic pattern of expression during early mouse development." J Cell Biol **113**(6): 1255-1265.
- Boldrin, L., Zammit, P. S. and Morgan, J. E. (2015). "Satellite cells from dystrophic muscle retain regenerative capacity." Stem Cell Res **14**(1): 20-29.
- Borello, U., Berarducci, B., Murphy, P., Bajard, L., Buffa, V., Piccolo, S., Buckingham, M. and Cossu, G. (2006). "The Wnt/beta-catenin pathway regulates Gli-mediated Myf5 expression during somitogenesis." Development **133**(18): 3723-3732.
- Borello, U., Coletta, M., Tajbakhsh, S., Leyns, L., De Robertis, E. M., Buckingham, M. and Cossu, G. (1999). "Transplacental delivery of the Wnt antagonist Frzb1 inhibits development of caudal paraxial mesoderm and skeletal myogenesis in mouse embryos." Development **126**(19): 4247-4255.
- Botrugno, O. A., Fayard, E., Annicotte, J.-S., Haby, C., Brennan, T., Wendling, O., Tanaka, T., Kodama, T., Thomas, W., Auwerx, J. and Schoonjans, K. (2004). "Synergy between LRH-1 and β -Catenin Induces G1 Cyclin-Mediated Cell Proliferation." Molecular Cell **15**(4): 499-509.
- Boyer, L., Plath, K., Zeitlinger, J., Brambrink, T., Medeiros, L., Lee, T., Levine, S., Wernig, M., Tajonar, A., Ray, M., Bell, G., Otte, A., Vidal, M., Gifford, D., Young, R. and Jaenisch, R. (2006). "Polycomb complexes repress developmental regulators in murine embryonic stem cells." Nature **441**: 349 - 353.
- Brack, A. S., Conboy, I. M., Conboy, M. J., Shen, J. and Rando, T. A. (2008). "A Temporal Switch from Notch to Wnt Signaling in Muscle Stem Cells Is Necessary for Normal Adult Myogenesis." Cell Stem Cell **2**(1): 50-59.
- Brack, A. S., Conboy, M. J., Roy, S., Lee, M., Kuo, C. J. and Keller, C. (2007). "Increased Wnt signaling during aging alters muscle stem cell fate and increases fibrosis." Science **317**: 807-810.
- Brack, A. S., Murphy-Seiler, F., Hanifi, J., Deka, J., Eyckerman, S. and Keller, C. (2009). "BCL9 is an essential component of canonical Wnt signaling that mediates the differentiation of myogenic progenitors during muscle regeneration." Dev Biol **335**: 93-105.

- Brannon, M., Gomperts, M., Sumoy, L., Moon, R. T. and Kimelman, D. (1997). "A beta-catenin/XTcf-3 complex binds to the siamois promoter to regulate dorsal axis specification in *Xenopus*." Genes Dev **11**(18): 2359-2370.
- Brantjes, H., Roose, J., van De Wetering, M. and Clevers, H. (2001). "All Tcf HMG box transcription factors interact with Groucho-related co-repressors." Nucleic Acids Res **29**(7): 1410-1419.
- Braun, T. and Arnold, H. H. (1991). "The four human muscle regulatory helix-loop-helix proteins Myf3-Myf6 exhibit similar hetero-dimerization and DNA binding properties." Nucleic Acids Res **19**(20): 5645-5651.
- Braun, T. and Arnold, H. H. (1995). "Inactivation of Myf-6 and Myf-5 genes in mice leads to alterations in skeletal muscle development." Embo j **14**(6): 1176-1186.
- Braun, T., Bober, E., Winter, B., Rosenthal, N. and Arnold, H. H. (1990). "Myf-6, a new member of the human gene family of myogenic determination factors: evidence for a gene cluster on chromosome 12." Embo j **9**(3): 821-831.
- Braun, T., Buschhausen-Denker, G., Bober, E., Tannich, E. and Arnold, H. H. (1989). "A novel human muscle factor related to but distinct from MyoD1 induces myogenic conversion in 10T1/2 fibroblasts." Embo j **8**(3): 701-709.
- Braun, T., Rudnicki, M. A., Arnold, H. H. and Jaenisch, R. (1992). "Targeted inactivation of the muscle regulatory gene Myf-5 results in abnormal rib development and perinatal death." Cell **71**(3): 369-382.
- Bray, S. J. (2006). "Notch signalling: a simple pathway becomes complex." Nat Rev Mol Cell Biol **7**(9): 678-689.
- Buas, M. F., Kabak, S. and Kadesch, T. (2010). "The Notch Effector Hey1 Associates with Myogenic Target Genes to Repress Myogenesis." Journal of Biological Chemistry **285**(2): 1249-1258.
- Buchberger, A., Ragge, K. and Arnold, H. H. (1994). "The myogenin gene is activated during myocyte differentiation by pre-existing, not newly synthesized transcription factor MEF-2." J Biol Chem **269**(25): 17289-17296.
- Buckingham, M., Bajard, L., Chang, T., Daubas, P., Hadchouel, J., Meilhac, S., Montarras, D., Rocancourt, D. and Relaix, F. (2003). "The formation of skeletal muscle: from somite to limb." Journal of Anatomy **202**(1): 59-68.
- Buckingham, M. and Relaix, F. (2007). "The role of Pax genes in the development of tissues and organs: Pax3 and Pax7 regulate muscle progenitor cell functions." Annu Rev Cell Dev Biol **23**: 645-673.
- Bulfield, G., Siller, W. G., Wight, P. A. and Moore, K. J. (1984). "X chromosome-linked muscular dystrophy (mdx) in the mouse." Proc Natl Acad Sci U S A **81**(4): 1189-1192.
- Burgess-Beusse, B., Farrell, C., Gaszner, M., Litt, M., Mutskov, V., Recillas-Targa, F., Simpson, M., West, A. and Felsenfeld, G. (2002). "The insulation of genes from external enhancers and silencing chromatin." Proc Natl Acad Sci U S A **99** **Suppl 4**: 16433-16437.

- Bushby, K., Finkel, R., Birnkrant, D. J., Case, L. E., Clemens, P. R., Cripe, L., Kaul, A., Kinnett, K., McDonald, C., Pandya, S., Poysky, J., Shapiro, F., Tomezsko, J. and Constantin, C. (2010). "Diagnosis and management of Duchenne muscular dystrophy, part 2: implementation of multidisciplinary care." Lancet Neurol **9**(2): 177-189.
- Castrop, J., van Norren, K. and Clevers, H. (1992). "A gene family of HMG-box transcription factors with homology to TCF-1." Nucleic Acids Res **20**(3): 611.
- Cavallo, R. A., Cox, R. T., Moline, M. M., Roose, J., Polevoy, G. A., Clevers, H., Reifer, M. and Bejsovec, A. (1998). "Drosophila Tcf and Groucho interact to repress wingless signalling activity." Nature **395**(6702): 604-608.
- Chalepakis, G. and Gruss, P. (1995). "Identification of DNA recognition sequences for the Pax3 paired domain." Gene **162**(2): 267-270.
- Chalepakis, G., Jones, F. S., Edelman, G. M. and Gruss, P. (1994). "Pax-3 contains domains for transcription activation and transcription inhibition." Proc Natl Acad Sci U S A **91**(26): 12745-12749.
- Chamberlain, J. S., Metzger, J., Reyes, M., Townsend, D. and Faulkner, J. A. (2007). "Dystrophin-deficient mdx mice display a reduced life span and are susceptible to spontaneous rhabdomyosarcoma." FASEB J. **21**(9): +.
- Chen, G. and Courey, A. J. (2000). "Groucho/TLE family proteins and transcriptional repression." Gene **249**(1-2): 1-16.
- Chen, G., Fernandez, J., Mische, S. and Courey, A. J. (1999). "A functional interaction between the histone deacetylase Rpd3 and the corepressor groucho in Drosophila development." Genes Dev **13**(17): 2218-2230.
- Chen, H., Lin, R. J., Schiltz, R. L., Chakravarti, D., Nash, A., Nagy, L., Privalsky, M. L., Nakatani, Y. and Evans, R. M. (1997). "Nuclear receptor coactivator ACTR is a novel histone acetyltransferase and forms a multimeric activation complex with P/CAF and CBP/p300." Cell **90**(3): 569-580.
- Chen, J. F., Tao, Y., Li, J., Deng, Z., Yan, Z., Xiao, X. and Wang, D. Z. (2010). "microRNA-1 and microRNA-206 regulate skeletal muscle satellite cell proliferation and differentiation by repressing Pax7." J Cell Biol **190**(5): 867-879.
- Chen, S. L., Dowhan, D. H., Hosking, B. M. and Muscat, G. E. (2000). "The steroid receptor coactivator, GRIP-1, is necessary for MEF-2C-dependent gene expression and skeletal muscle differentiation." Genes Dev **14**(10): 1209-1228.
- Cheng, T. C., Wallace, M. C., Merlie, J. P. and Olson, E. N. (1993). "Separable regulatory elements governing myogenin transcription in mouse embryogenesis." Science **261**(5118): 215-218.
- Chesire, D. R., Ewing, C. M., Gage, W. R. and Isaacs, W. B. (2002). "In vitro evidence for complex modes of nuclear beta-catenin signaling during prostate growth and tumorigenesis." Oncogene. **21**(17): 2679-2694.
- Chevallier, A., Kieny, M. and Mauger, A. (1977). "Limb-somite relationship: origin of the limb musculature." J Embryol Exp Morphol **41**: 245-258.

- Choi, J., Costa, M. L., Mermelstein, C. S., Chagas, C., Holtzer, S. and Holtzer, H. (1990). "MyoD converts primary dermal fibroblasts, chondroblasts, smooth muscle, and retinal pigmented epithelial cells into striated mononucleated myoblasts and multinucleated myotubes." Proc Natl Acad Sci U S A **87**(20): 7988-7992.
- Christ, B., Jacob, H. J. and Jacob, M. (1977). "Experimental analysis of the origin of the wing musculature in avian embryos." Anat Embryol (Berl) **150**(2): 171-186.
- Christ, B. and Ordahl, C. P. (1995). "Early stages of chick somite development." Anat Embryol (Berl) **191**(5): 381-396.
- Chung, J. H., Bell, A. C. and Felsenfeld, G. (1997). "Characterization of the chicken beta-globin insulator." Proc Natl Acad Sci U S A **94**(2): 575-580.
- Clevers, H. (2006). "Wnt/beta-catenin signaling in development and disease." Cell **127**(3): 469-480.
- Clevers, H. and Nusse, R. (2012). "Wnt/beta-catenin signaling and disease." Cell **149**(6): 1192-1205.
- Clevers, H. and van de Wetering, M. (1997). "TCF/LEF factor earn their wings." Trends Genet **13**(12): 485-489.
- Cliffe, A., Hamada, F. and Bienz, M. (2003). "A role of Dishevelled in relocating Axin to the plasma membrane during wingless signaling." Curr Biol **13**(11): 960-966.
- Collins, C. A., Olsen, I., Zammit, P. S., Heslop, L., Petrie, A., Partridge, T. A. and Morgan, J. E. (2005). "Stem cell function, self-renewal, and behavioral heterogeneity of cells from the adult muscle satellite cell niche." Cell **122**(2): 289-301.
- Conboy, I. M., Conboy, M. J., Smythe, G. M. and Rando, T. A. (2003). "Notch-mediated restoration of regenerative potential to aged muscle." Science **302**: 1575-1577.
- Conboy, I. M. and Rando, T. A. (2002). "The Regulation of Notch Signaling Controls Satellite Cell Activation and Cell Fate Determination in Postnatal Myogenesis." Developmental Cell **3**(3): 397-409.
- Conway, K., Pin, C., Kiernan, J. A. and Merrifield, P. (2004). "The E protein HEB is preferentially expressed in developing muscle." Differentiation **72**(7): 327-340.
- Cooper, W. G. and Konigsberg, I. R. (1961). "Dynamics of myogenesis in vitro." Anat Rec **140**: 195-205.
- Copley, R. R. (2005). "The EH1 motif in metazoan transcription factors." BMC Genomics **6**: 169.
- Cornelison, D. D. W. and Wold, B. J. (1997). "Single-Cell Analysis of Regulatory Gene Expression in Quiescent and Activated Mouse Skeletal Muscle Satellite Cells." Developmental Biology **191**(2): 270-283.
- Cros, D., Harnden, P., Pellissier, J. F. and Serratrice, G. (1989). "Muscle hypertrophy in Duchenne muscular dystrophy. A pathological and morphometric study." J Neurol **236**(1): 43-47.
- Cserjesi, P. and Olson, E. N. (1991). "Myogenin induces the myocyte-specific enhancer

binding factor MEF-2 independently of other muscle-specific gene products." Mol Cell Biol **11**(10): 4854-4862.

Cullen, M. J. and Jaros, E. (1988). "Ultrastructure of the skeletal muscle in the X chromosome-linked dystrophic (mdx) mouse. Comparison with Duchenne muscular dystrophy." Acta Neuropathol **77**(1): 69-81.

Currier, N., Chea, K., Hlavacova, M., Sussman, D. J., Seldin, D. C. and Dominguez, I. (2010). "Dynamic expression of a LEF-EGFP Wnt reporter in mouse development and cancer." Genesis **48**(3): 183-194.

Dahl, J. A. and Collas, P. (2008). "A rapid micro chromatin immunoprecipitation assay (ChIP)." Nat. Protocols **3**(6): 1032-1045.

Dahlqvist, C., Blokzijl, A., Chapman, G., Falk, A., Dannaes, K., Ibanez, C. F. and Lendahl, U. (2003). "Functional Notch signaling is required for BMP4-induced inhibition of myogenic differentiation." Development **130**(24): 6089-6099.

Daniels, D. L. and Weis, W. I. (2005). "Beta-catenin directly displaces Groucho/TLE repressors from Tcf/Lef in Wnt-mediated transcription activation." Nat Struct Mol Biol **12**(4): 364-371.

DasGupta, R. and Fuchs, E. (1999). "Multiple roles for activated LEF/TCF transcription complexes during hair follicle development and differentiation." Development **126**(20): 4557-4568.

Daston, G., Lamar, E., Olivier, M. and Goulding, M. (1996). "Pax-3 is necessary for migration but not differentiation of limb muscle precursors in the mouse." Development **122**(3): 1017-1027.

Davis, R. L., Cheng, P. F., Lassar, A. B. and Weintraub, H. (1990). "The MyoD DNA binding domain contains a recognition code for muscle-specific gene activation." Cell **60**(5): 733-746.

Davis, R. L. and Weintraub, H. (1992). "Acquisition of myogenic specificity by replacement of three amino acid residues from MyoD into E12." Science **256**(5059): 1027-1030.

Day, K., Shefer, G., Shearer, A. and Yablonka-Reuveni, Z. (2010). "The depletion of skeletal muscle satellite cells with age is concomitant with reduced capacity of single progenitors to produce reserve progeny." Developmental Biology **340**(2): 330-343.

De Souza, M. V., #237 and R., c. N. (2004). "(+)-Discodermolide: A Marine Natural Product Against Cancer." TheScientificWorldJOURNAL **4**: 415-436.

Denetclaw, W. F. and Ordahl, C. P. (2000). "The growth of the dermomyotome and formation of early myotome lineages in thoracolumbar somites of chicken embryos." Development **127**(4): 893-905.

Dick, S. A., Chang, N. C., Dumont, N. A., Bell, R. A., Putinski, C., Kawabe, Y., Litchfield, D. W., Rudnicki, M. A. and Megeney, L. A. (2015). "Caspase 3 cleavage of Pax7 inhibits self-renewal of satellite cells." Proc Natl Acad Sci U S A **112**(38): E5246-5252.

Dietz, K. N., Miller, P. J. and Hollenbach, A. D. (2009). "Phosphorylation of serine 205

by the protein kinase CK2 persists on Pax3-FOXO1, but not Pax3, throughout early myogenic differentiation." Biochemistry **48**(49): 11786-11795.

Dodou, E., Xu, S. M. and Black, B. L. (2003). "mef2c is activated directly by myogenic basic helix-loop-helix proteins during skeletal muscle development in vivo." Mech Dev **120**(9): 1021-1032.

Dong, F., Sun, X., Liu, W., Ai, D., Klysik, E., Lu, M. F., Hadley, J., Antoni, L., Chen, L., Baldini, A., Francis-West, P. and Martin, J. F. (2006). "Pitx2 promotes development of splanchnic mesoderm-derived branchiomeric muscle." Development **133**(24): 4891-4899.

Duval, A., Rolland, S., Tubacher, E., Bui, H., Thomas, G. and Hamelin, R. (2000). "The human T-cell transcription factor-4 gene: structure, extensive characterization of alternative splicings, and mutational analysis in colorectal cancer cell lines." Cancer Res **60**(14): 3872-3879.

Edelman, D. B., Meech, R. and Jones, F. S. (2000). "The homeodomain protein Barx2 contains activator and repressor domains and interacts with members of the CREB family." J Biol Chem **275**(28): 21737-21745.

Edmondson, D. G., Cheng, T. C., Cserjesi, P., Chakraborty, T. and Olson, E. N. (1992). "Analysis of the myogenin promoter reveals an indirect pathway for positive autoregulation mediated by the muscle-specific enhancer factor MEF-2." Mol Cell Biol **12**(9): 3665-3677.

Edmondson, D. G. and Olson, E. N. (1989). "A gene with homology to the myc similarity region of MyoD1 is expressed during myogenesis and is sufficient to activate the muscle differentiation program." Genes Dev **3**(5): 628-640.

Ehebauer, M., Hayward, P. and Arias, A. M. (2006). "Notch, a universal arbiter of cell fate decisions." Science **314**(5804): 1414-1415.

Emery, A. E. (1991). "Population frequencies of inherited neuromuscular diseases--a world survey." Neuromuscul Disord. **1**(1): 19-29.

Emiliani, S., Fischle, W., Van Lint, C., Al-Abed, Y. and Verdin, E. (1998). "Characterization of a human RPD3 ortholog, HDAC3." Proc Natl Acad Sci U S A **95**(6): 2795-2800.

Ephrussi, A., Church, G. M., Tonegawa, S. and Gilbert, W. (1985). "B lineage--specific interactions of an immunoglobulin enhancer with cellular factors in vivo." Science **227**(4683): 134-140.

Fleming-Waddell, J. N., Olbricht, G. R., Taxis, T. M., White, J. D., Vuocolo, T., Craig, B. A., Tellam, R. L., Neary, M. K., Cockett, N. E. and Bidwell, C. A. (2009). "Effect of DLK1 and RTL1 but not MEG3 or MEG8 on muscle gene expression in Callipyge lambs." PLoS One **4**(10): e7399.

Fujimaki, S., Hidaka, R., Asashima, M., Takemasa, T. and Kuwabara, T. (2014). "Wnt protein-mediated satellite cell conversion in adult and aged mice following voluntary wheel running." J Biol Chem **289**(11): 7399-7412.

- Fukada, S., Yamaguchi, M., Kokubo, H., Ogawa, R., Uezumi, A., Yoneda, T., Matev, M. M., Motohashi, N., Ito, T., Zolkiewska, A., Johnson, R. L., Saga, Y., Miyagoe-Suzuki, Y., Tsujikawa, K., Takeda, S. and Yamamoto, H. (2011). "Hesr1 and Hesr3 are essential to generate undifferentiated quiescent satellite cells and to maintain satellite cell numbers." Development **138**(21): 4609-4619.
- Galceran, J., Farinas, I., Depew, M. J., Clevers, H. and Grosschedl, R. (1999). "Wnt3a/--like phenotype and limb deficiency in Lef1(-/-)Tcf1(-/-) mice." Genes Dev **13**(6): 709-717.
- Gat, U., DasGupta, R., Degenstein, L. and Fuchs, E. (1998). "De Novo hair follicle morphogenesis and hair tumors in mice expressing a truncated beta-catenin in skin." Cell **95**(5): 605-614.
- Gehring, W. J., Qian, Y. Q., Billeter, M., Furukubo-Tokunaga, K., Schier, A. F., Resendez-Perez, D., Affolter, M., Otting, G. and Wuthrich, K. (1994). "Homeodomain-DNA recognition." Cell **78**(2): 211-223.
- Gibson, M. C. and Schultz, E. (1983). "Age-related differences in absolute numbers of skeletal muscle satellite cells." Muscle Nerve **6**: 574-580.
- Gilson, H., Schakman, O., Kalista, S., Lause, P., Tsuchida, K. and Thissen, J.-P. (2009). "Follistatin induces muscle hypertrophy through satellite cell proliferation and inhibition of both myostatin and activin." American Journal of Physiology - Endocrinology And Metabolism **297**(1): E157-E164.
- Goldberg, A. L., Etlinger, J. D., Goldspink, D. F. and Jablecki, C. (1975). "Mechanism of work-induced hypertrophy of skeletal muscle." Med Sci Sports **7**(3): 185-198.
- Goldstein, R. E., Cook, O., Dinur, T., Pisante, A., Karandikar, U. C., Bidwai, A. and Paroush, Z. (2005). "An eh1-like motif in odd-skipped mediates recruitment of Groucho and repression in vivo." Mol Cell Biol **25**(24): 10711-10720.
- Gomez-Merino, E. and Bach, J. R. (2002). "Duchenne muscular dystrophy: prolongation of life by noninvasive ventilation and mechanically assisted coughing." Am J Phys Med Rehabil **81**(6): 411-415.
- Gonzalez, N., Moresco, J. J., Cabezas, F., de la Vega, E., Bustos, F., Yates, J. R., 3rd and Olguin, H. C. (2016). "Ck2-Dependent Phosphorylation Is Required to Maintain Pax7 Protein Levels in Proliferating Muscle Progenitors." PLoS One **11**(5): e0154919.
- Gorisch, S. M., Wachsmuth, M., Toth, K. F., Lichter, P. and Rippe, K. (2005). "Histone acetylation increases chromatin accessibility." J Cell Sci **118**(Pt 24): 5825-5834.
- Gossen, M. and Bujard, H. (1992). "Tight control of gene expression in mammalian cells by tetracycline-responsive promoters." Proc Natl Acad Sci U S A **89**(12): 5547-5551.
- Gossen, M., Freundlieb, S., Bender, G., Muller, G., Hillen, W. and Bujard, H. (1995). "Transcriptional activation by tetracyclines in mammalian cells." Science **268**(5218): 1766-1769.
- Goulding, M. D., Chalepakis, G., Deutsch, U., Erselius, J. R. and Gruss, P. (1991). "Pax-

3, a novel murine DNA binding protein expressed during early neurogenesis." Embo j **10**(5): 1135-1147.

Goupille, O., Saint Cloment, C., Lopes, M., Montarras, D. and Robert, B. (2008). "Msx1 and Msx2 are expressed in sub-populations of vascular smooth muscle cells." Dev Dyn **237**(8): 2187-2194.

Grewal, S. I. and Moazed, D. (2003). "Heterochromatin and epigenetic control of gene expression." Science **301**(5634): 798-802.

Gross, M. K., Moran-Rivard, L., Velasquez, T., Nakatsu, M. N., Jagla, K. and Goulding, M. (2000). "Lbx1 is required for muscle precursor migration along a lateral pathway into the limb." Development **127**(2): 413-424.

Guenther, M. G., Lane, W. S., Fischle, W., Verdin, E., Lazar, M. A. and Shiekhatar, R. (2000). "A core SMRT corepressor complex containing HDAC3 and TBL1, a WD40-repeat protein linked to deafness." Genes Dev **14**(9): 1048-1057.

Guha, S., Cullen, J. P., Morrow, D., Colombo, A., Lally, C., Walls, D., Redmond, E. M. and Cahill, P. A. (2011). "Glycogen synthase kinase 3 beta positively regulates Notch signaling in vascular smooth muscle cells: role in cell proliferation and survival." Basic Res Cardiol **106**(5): 773-785.

Gussoni, E., Blau, H. M. and Kunkel, L. M. (1997). "The fate of individual myoblasts after transplantation into muscles of DMD patients." Nature Med. **3**: 970-977.

Han, X. H., Jin, Y. R., Seto, M. and Yoon, J. K. (2011). "A WNT/beta-catenin signaling activator, R-spondin, plays positive regulatory roles during skeletal myogenesis." J Biol Chem **286**(12): 10649-10659.

Harridge, S. D. (2007). "Plasticity of human skeletal muscle: gene expression to in vivo function." Exp Physiol **92**(5): 783-797.

Hart, M. J., de los Santos, R., Albert, I. N., Rubinfeld, B. and Polakis, P. (1998). "Downregulation of beta-catenin by human Axin and its association with the APC tumor suppressor, beta-catenin and GSK3 beta." Curr Biol **8**(10): 573-581.

Hasty, P., Bradley, A., Morris, J. H., Edmondson, D. G., Venuti, J. M., Olson, E. N. and Klein, W. H. (1993). "Muscle deficiency and neonatal death in mice with a targeted mutation in the myogenin gene." Nature **364**(6437): 501-506.

Hawley, J. A. and Holloszy, J. O. (2009). "Exercise: it's the real thing!" Nutr Rev **67**(3): 172-178.

He, T. C., Sparks, A. B., Rago, C., Hermeking, H., Zawel, L., da Costa, L. T., Morin, P. J., Vogelstein, B. and Kinzler, K. W. (1998). "Identification of c-MYC as a target of the APC pathway." Science **281**(5382): 1509-1512.

Hecht, A. and Kemler, R. (2000). "Curbing the nuclear activities of beta-catenin. Control over Wnt target gene expression." EMBO Rep **1**(1): 24-28.

Hecht, A. and Stemmler, M. P. (2003). "Identification of a promoter-specific transcriptional activation domain at the C terminus of the Wnt effector protein T-cell factor 4." J Biol Chem **278**(6): 3776-3785.

- Hecht, A., Vleminckx, K., Stemmler, M. P., van Roy, F. and Kemler, R. (2000). "The p300/CBP acetyltransferases function as transcriptional coactivators of [beta]-catenin in vertebrates." EMBO J **19**(8): 1839-1850.
- Heidt, A. B., Rojas, A., Harris, I. S. and Black, B. L. (2007). "Determinants of myogenic specificity within MyoD are required for noncanonical E box binding." Mol Cell Biol **27**(16): 5910-5920.
- Heinzel, T., Lavinsky, R. M., Mullen, T. M., Soderstrom, M., Laherty, C. D., Torchia, J., Yang, W. M., Brard, G., Ngo, S. D., Davie, J. R., Seto, E., Eisenman, R. N., Rose, D. W., Glass, C. K. and Rosenfeld, M. G. (1997). "A complex containing N-CoR, mSin3 and histone deacetylase mediates transcriptional repression." Nature **387**(6628): 43-48.
- Hikida, R. S. (2011). "Aging changes in satellite cells and their functions." Curr Aging Sci **4**(3): 279-297.
- Hillen, W. and Berens, C. (1994). "Mechanisms underlying expression of Tn10 encoded tetracycline resistance." Annu Rev Microbiol **48**: 345-369.
- Hinterberger, T. J., Sassoon, D. A., Rhodes, S. J. and Konieczny, S. F. (1991). "Expression of the muscle regulatory factor MRF4 during somite and skeletal myofiber development." Developmental Biology **147**(1): 144-156.
- Hiroki, E., Abe, S., Iwanuma, O., Sakiyama, K., Yanagisawa, N., Shiozaki, K. and Ide, Y. (2011). "A comparative study of myostatin, follistatin and decorin expression in muscle of different origin." Anatomical Science International **86**(3): 151-159.
- Hoffman, E. P., Brown, R. H., Jr. and Kunkel, L. M. (1987). "Dystrophin: the protein product of the Duchenne muscular dystrophy locus." Cell **51**(6): 919-928.
- Hong, S., Cho, Y. W., Yu, L. R., Yu, H., Veenstra, T. D. and Ge, K. (2007). "Identification of JmjC domain-containing UTX and JMJD3 as histone H3 lysine 27 demethylases." Proc Natl Acad Sci USA **104**: 18439-18444.
- Hoppler, S. and Kavanagh, C. L. (2007). "Wnt signalling: variety at the core." J Cell Sci **120**(Pt 3): 385-393.
- Howng, S. L., Huang, F. H., Hwang, S. L., Lieu, A. S., Sy, W. D., Wang, C. and Hong, Y. R. (2004). "Differential expression and splicing isoform analysis of human Tcf-4 transcription factor in brain tumors." Int J Oncol **25**(6): 1685-1692.
- Hsiao, Y. C., Chang, H. H., Tsai, C. Y., Jong, Y. J., Horng, L. S., Lin, S. F. and Tsai, T. F. (2004). "Coat color-tagged green mouse with EGFP expressed from the RNA polymerase II promoter." Genesis **39**(2): 122-129.
- Hsieh, J. C., Rattner, A., Smallwood, P. M. and Nathans, J. (1999). "Biochemical characterization of Wnt-frizzled interactions using a soluble, biologically active vertebrate Wnt protein." Proc. Natl Acad. Sci. USA **96**: 3546-3551.
- Hsu, W., Zeng, L. and Costantini, F. (1999). "Identification of a domain of Axin that binds to the serine/threonine protein phosphatase 2A and a self-binding domain." J Biol Chem **274**(6): 3439-3445.
- Hu, J. S., Olson, E. N. and Kingston, R. E. (1992). "HEB, a helix-loop-helix protein

related to E2A and ITF2 that can modulate the DNA-binding ability of myogenic regulatory factors." Mol Cell Biol **12**(3): 1031-1042.

Hu, P., Geles, K. G., Paik, J. H., DePinho, R. A. and Tjian, R. (2008). "Codependent activators direct myoblast-specific MyoD transcription." Dev Cell **15**(4): 534-546.

Huard, J., Bouchard, J. P., Roy, R., Labrecque, C., Dansereau, G., Lemieux, B. and Tremblay, J. P. (1991). "Myoblast transplantation produced dystrophin-positive muscle fibres in a 16-year-old patient with Duchenne muscular dystrophy." Clin Sci (Lond) **81**(2): 287-288.

Huelsken, J., Vogel, R., Erdmann, B., Cotsarelis, G. and Birchmeier, W. (2001). "beta-Catenin controls hair follicle morphogenesis and stem cell differentiation in the skin." Cell **105**(4): 533-545.

Hughes, T. A. and Brady, H. J. M. (2005). "Expression of axin2 Is Regulated by the Alternative 5'-Untranslated Regions of Its mRNA." Journal of Biological Chemistry **280**(9): 8581-8588.

Hulin, J. A., Nguyen, T. D., Cui, S., Marri, S., Yu, R. T., Downes, M., Evans, R. M., Makarenkova, H. and Meech, R. (2016). "Barx2 and Pax7 Regulate Axin2 Expression in Myoblasts by Interaction with beta-Catenin and Chromatin Remodelling." Stem Cells **34**(8): 2169-2182.

Husmann, I., Soulet, L., Gautron, J., Martelly, I. and Barritault, D. (1996). "Growth factors in skeletal muscle regeneration." Cytokine Growth Factor Rev **7**(3): 249-258.

Hutcheson, D. A., Zhao, J., Merrell, A., Haldar, M. and Kardon, G. (2009). "Embryonic and fetal limb myogenic cells are derived from developmentally distinct progenitors and have different requirements for β -catenin." Genes & Development **23**(8): 997-1013.

Huxley, A. F. and Niedergerke, R. (1954). "Structural changes in muscle during contraction; interference microscopy of living muscle fibres." Nature **173**(4412): 971-973.

Huxley, H. and Hanson, J. (1954). "Changes in the cross-striations of muscle during contraction and stretch and their structural interpretation." Nature **173**(4412): 973-976.

Ichida, M., Nemoto, S. and Finkel, T. (2002). "Identification of a specific molecular repressor of the peroxisome proliferator-activated receptor gamma Coactivator-1 alpha (PGC-1alpha)." J Biol Chem **277**(52): 50991-50995.

Ikeda, S., Kishida, S., Yamamoto, H., Murai, H., Koyama, S. and Kikuchi, A. (1998). "Axin, a negative regulator of the Wnt signaling pathway, forms a complex with GSK-3beta and beta-catenin and promotes GSK-3beta-dependent phosphorylation of beta-catenin." Embo j **17**(5): 1371-1384.

Ikeya, M. and Takada, S. (1998). "Wnt signaling from the dorsal neural tube is required for the formation of the medial dermomyotome." Development **125**(24): 4969-4976.

- Jacob, M., Christ, B. and Jacob, H. J. (1978). "On the migration of myogenic stem cells into the prospective wing region of chick embryos. A scanning and transmission electron microscope study." Anat Embryol (Berl) **153**(2): 179-193.
- Jarriault, S., Brou, C., Logeat, F., Schroeter, E. H., Kopan, R. and Israel, A. (1995). "Signalling downstream of activated mammalian Notch." Nature **377**(6547): 355-358.
- Jensen, P. B., Pedersen, L., Krishna, S. and Jensen, M. H. (2010). "A Wnt Oscillator Model for Somitogenesis." Biophysical journal **98**(6): 943-950.
- Jho, E.-h., Zhang, T., Domon, C., Joo, C.-K., Freund, J.-N. and Costantini, F. (2002). "Wnt/ β -Catenin/Tcf Signaling Induces the Transcription of Axin2, a Negative Regulator of the Signaling Pathway." Molecular and Cellular Biology **22**(4): 1172-1183.
- Johanson, M., Meents, H., Ragge, K., Buchberger, A., Arnold, H. H. and Sandmoller, A. (1999). "Transcriptional activation of the myogenin gene by MEF2-mediated recruitment of myf5 is inhibited by adenovirus E1A protein." Biochem Biophys Res Commun **265**(1): 222-232.
- Johnson, S. E., Wang, X., Hardy, S., Taparowsky, E. J. and Konieczny, S. F. (1996). "Casein kinase II increases the transcriptional activities of MRF4 and MyoD independently of their direct phosphorylation." Mol Cell Biol **16**(4): 1604-1613.
- Jones, A. E., Price, F. D., Le Grand, F., Soleimani, V. D., Dick, S. A., Megeney, L. A. and Rudnicki, M. A. (2015). "Wnt/beta-catenin controls follistatin signalling to regulate satellite cell myogenic potential." Skelet Muscle **5**: 14.
- Jones, F. S., Kiuoussi, C., Copertino, D. W., Kallunki, P., Holst, B. D. and Edelman, G. M. (1997). "Barx2 , a new homeobox gene of the Bar class, is expressed in neural and craniofacial structures during development." Proceedings of the National Academy of Sciences of the United States of America **94**(6): 2632-2637.
- Jones, S. (2004). "An overview of the basic helix-loop-helix proteins." Genome Biol **5**(6): 226.
- Jostes, B., Walther, C. and Gruss, P. (1990). "The murine paired box gene, Pax7, is expressed specifically during the development of the nervous and muscular system." Mech Dev **33**(1): 27-37.
- Jullien, N. and Herman, J. P. (2011). "LUEGO: a cost and time saving gel shift procedure." Biotechniques **51**(4): 267-269.
- Kablar, B., Krastel, K., Tajbakhsh, S. and Rudnicki, M. A. (2003). "Myf5 and MyoD activation define independent myogenic compartments during embryonic development." Dev Biol **258**(2): 307-318.
- Kablar, B., Krastel, K., Ying, C., Tapscott, S. J., Goldhamer, D. J. and Rudnicki, M. A. (1999). "Myogenic determination occurs independently in somites and limb buds." Dev Biol **206**(2): 219-231.
- Kablar, B. and Rudnicki, M. A. (2000). "Skeletal muscle development in the mouse embryo." Histol Histopathol **15**(2): 649-656.

Kao, H. Y., Downes, M., Ordentlich, P. and Evans, R. M. (2000). "Isolation of a novel histone deacetylase reveals that class I and class II deacetylases promote SMRT-mediated repression." Genes Dev **14**(1): 55-66.

Kassar-Duchossoy, L., Gayraud-Morel, B., Gomes, D., Rocancourt, D., Buckingham, M., Shinin, V. and Tajbakhsh, S. (2004). "Mrf4 determines skeletal muscle identity in Myf5:Myod double-mutant mice." Nature **431**(7007): 466-471.

Kassar-Duchossoy, L., Giacone, E., Gayraud-Morel, B., Jory, A., Gomes, D. and Tajbakhsh, S. (2005). "Pax3/Pax7 mark a novel population of primitive myogenic cells during development." Genes Dev. **19**(12): 1426-1431.

Kim, C.-H., Neiswender, H., Baik, E. J., Xiong, W. C. and Mei, L. (2008). "{beta}-Catenin Interacts with MyoD and Regulates Its Transcription Activity." Mol. Cell. Biol. **28**(9): 2941-2951.

Kim, H., Kim, S., Song, Y., Kim, W., Ying, Q. L. and Jho, E. H. (2015). "Dual Function of Wnt Signaling during Neuronal Differentiation of Mouse Embryonic Stem Cells." Stem Cells Int **2015**: 459301.

Kishida, S., Yamamoto, H., Ikeda, S., Kishida, M., Sakamoto, I., Koyama, S. and Kikuchi, A. (1998). "Axin, a negative regulator of the wnt signaling pathway, directly interacts with adenomatous polyposis coli and regulates the stabilization of beta-catenin." J Biol Chem **273**(18): 10823-10826.

Kitamoto, T. and Hanaoka, K. (2010). "Notch3 Null Mutation in Mice Causes Muscle Hyperplasia by Repetitive Muscle Regeneration." Stem Cells **28**(12): 2205-2216.

Klenova, E., Chernukhin, I., Inoue, T., Shamsuddin, S. and Norton, J. (2002). "Immunoprecipitation techniques for the analysis of transcription factor complexes." Methods **26**(3): 254-259.

Ko, K. H., Holmes, T., Palladinetti, P., Song, E., Nordon, R., O'Brien, T. A. and Dolnikov, A. (2011). "GSK-3beta inhibition promotes engraftment of ex vivo-expanded hematopoietic stem cells and modulates gene expression." Stem Cells **29**(1): 108-118.

Kobayashi, M., Goldstein, R. E., Fujioka, M., Paroush, Z. and Jaynes, J. B. (2001). "Groucho augments the repression of multiple Even skipped target genes in establishing parasegment boundaries." Development **128**(10): 1805-1815.

Konigsberg, U. R., Lipton, B. H. and Konigsberg, I. R. (1975). "The regenerative response of single mature muscle fibers isolated in vitro." Dev Biol **45**(2): 260-275.

Korinek, V., Barker, N., Moerer, P., van Donselaar, E., Huls, G., Peters, P. J. and Clevers, H. (1998). "Depletion of epithelial stem-cell compartments in the small intestine of mice lacking Tcf-4." Nat Genet **19**(4): 379-383.

Korinek, V., Barker, N., Willert, K., Molenaar, M., Roose, J., Wagenaar, G., Markman, M., Lamers, W., Destree, O. and Clevers, H. (1998). "Two members of the Tcf family implicated in Wnt/beta-catenin signaling during embryogenesis in the mouse." Mol Cell Biol **18**(3): 1248-1256.

Kouzarides, T. and Ziff, E. (1988). "The role of the leucine zipper in the fos-jun

interaction." Nature **336**(6200): 646-651.

Kuang, S. (2007). "Asymmetric self-renewal and commitment of satellite stem cells in muscle." Cell **129**: 999-1010.

Kuang, S., Charge, S. B., Seale, P., Huh, M. and Rudnicki, M. A. (2006). "Distinct roles for Pax7 and Pax3 in adult regenerative myogenesis." J Cell Biol **172**(1): 103-113.

Kuang, S., Kuroda, K., Le Grand, F. and Rudnicki, M. A. (2007). "Asymmetric self-renewal and commitment of satellite stem cells in muscle." Cell **129**(5): 999-1010.

Kurdistani, S. K., Tavazoie, S. and Grunstein, M. (2004). "Mapping global histone acetylation patterns to gene expression." Cell **117**(6): 721-733.

Kuroda, K., Han, H., Tani, S., Tanigaki, K., Tun, T., Furukawa, T., Taniguchi, Y., Kurooka, H., Hamada, Y., Toyokuni, S. and Honjo, T. (2003). "Regulation of marginal zone B cell development by MINT, a suppressor of Notch/RBP-J signaling pathway." Immunity **18**(2): 301-312.

Lai, J. S. and Herr, W. (1992). "Ethidium bromide provides a simple tool for identifying genuine DNA-independent protein associations." Proc Natl Acad Sci U S A **89**(15): 6958-6962.

Lamey, T. M., Koenders, A. and Ziman, M. (2004). "Pax genes in myogenesis: alternate transcripts add complexity." Histol Histopathol **19**(4): 1289-1300.

Lassar, A. B., Davis, R. L., Wright, W. E., Kadesch, T., Murre, C., Voronova, A., Baltimore, D. and Weintraub, H. (1991). "Functional activity of myogenic HLH proteins requires hetero-oligomerization with E12/E47-like proteins in vivo." Cell **66**(2): 305-315.

Le Grand, F., Auda-Boucher, G., Levitsky, D., Rouaud, T., Fontaine-Perus, J. and Gardahaut, M. F. (2004). "Endothelial cells within embryonic skeletal muscles: a potential source of myogenic progenitors." Exp Cell Res **301**(2): 232-241.

Le Grand, F., Jones, A. E., Seale, V., Scimè, A. and Rudnicki, M. A. (2009). "Wnt7a Activates the Planar Cell Polarity Pathway to Drive the Symmetric Expansion of Satellite Stem Cells." Cell Stem Cell **4**(6): 535-547.

Lefaucheur JP, P. C., Sebille A (1995). "Phenotype of dystrophinopathy in old mdx mice." Anat Rec. **242**(1): 70-76.

Lepper, C., Conway, S. J. and Fan, C.-M. (2009). "Adult satellite cells and embryonic muscle progenitors have distinct genetic requirements." Nature **460**(7255): 627-631.

Leung, J. Y., Kolligs, F. T., Wu, R., Zhai, Y., Kuick, R., Hanash, S., Cho, K. R. and Fearon, E. R. (2002). "Activation of AXIN2 expression by beta-catenin-T cell factor. A feedback repressor pathway regulating Wnt signaling." J Biol Chem **277**(24): 21657-21665.

Levanon, D., Goldstein, R. E., Bernstein, Y., Tang, H., Goldenberg, D., Stifani, S., Paroush, Z. e. and Groner, Y. (1998). "Transcriptional repression by AML1 and LEF-1 is mediated by the TLE/Groucho corepressors." Proceedings of the National Academy of Sciences of the United States of America **95**(20): 11590-11595.

- Li, H. and Capetanaki, Y. (1993). "Regulation of the mouse desmin gene: transactivated by MyoD, myogenin, MRF4 and Myf5." Nucleic Acids Res **21**(2): 335-343.
- Li, H. and Capetanaki, Y. (1994). "An E box in the desmin promoter cooperates with the E box and MEF-2 sites of a distal enhancer to direct muscle-specific transcription." Embo j **13**(15): 3580-3589.
- Li, H., Kim, J. H., Koh, S. S. and Stallcup, M. R. (2004). "Synergistic effects of coactivators GRIP1 and beta-catenin on gene activation: cross-talk between androgen receptor and Wnt signaling pathways." J Biol Chem **279**(6): 4212-4220.
- Li, J., Sutter, C., Parker, D. S., Blauwkamp, T., Fang, M. and Cadigan, K. M. (2007). "CBP/p300 are bimodal regulators of Wnt signaling." Embo j **26**(9): 2284-2294.
- Li, J. and Wang, C. Y. (2008). "TBL1-TBLR1 and beta-catenin recruit each other to Wnt target-gene promoter for transcription activation and oncogenesis." Nat Cell Biol **10**(2): 160-169.
- Li, V. S. W., Ng, S. S., Boersema, P. J., Low, T. Y., Karthaus, W. R., Gerlach, J. P., Mohammed, S., Heck, A. J. R., Maurice, M. M., Mahmoudi, T. and Clevers, H. (2012). "Wnt Signaling through Inhibition of beta-Catenin Degradation in an Intact Axin1 Complex." Cell **149**(6): 1245-1256.
- Lien, W. H. and Fuchs, E. (2014). "Wnt some lose some: transcriptional governance of stem cells by Wnt/beta-catenin signaling." Genes Dev **28**(14): 1517-1532.
- Lin, Y.-S. and Green, M. R. (1991). "Mechanism of action of an acidic transcriptional activator in vitro." Cell **64**(5): 971-981.
- Litt, M. D., Simpson, M., Recillas-Targa, F., Prioleau, M. N. and Felsenfeld, G. (2001). "Transitions in histone acetylation reveal boundaries of three separately regulated neighboring loci." Embo j **20**(9): 2224-2235.
- Liu, C., Li, Y., Semenov, M., Han, C., Baeg, G. H., Tan, Y., Zhang, Z., Lin, X. and He, X. (2002). "Control of beta-catenin phosphorylation/degradation by a dual-kinase mechanism." Cell **108**(6): 837-847.
- Liu, X. X., Rubin, J. S. and Kimmel, A. R. (2005). "Rapid, Wnt-induced changes in GSK3 beta associations that regulate beta-catenin stabilization are mediated by G alpha proteins." Current Biology **15**(22): 1989-1997.
- Liu, Z., Li, T., Liu, Y., Jia, Z., Li, Y., Zhang, C., Chen, P., Ma, K., Affara, N. and Zhou, C. (2009). "WNT signaling promotes Nkx2.5 expression and early cardiomyogenesis via downregulation of Hdac1." Biochim Biophys Acta **1793**(2): 300-311.
- Logan, C., Hanks, M. C., Noble-Topham, S., Nallainathan, D., Provart, N. J. and Joyner, A. L. (1992). "Cloning and sequence comparison of the mouse, human, and chicken engrailed genes reveal potential functional domains and regulatory regions." Dev Genet **13**(5): 345-358.
- Logan, C. Y. and Nusse, R. (2004). "THE WNT SIGNALING PATHWAY IN DEVELOPMENT AND DISEASE." Annual Review of Cell and Developmental Biology **20**(1): 781-810.

- Londhe, P. and Davie, J. K. (2011). "Sequential association of myogenic regulatory factors and E proteins at muscle-specific genes." Skelet Muscle **1**(1): 14.
- Lustig, B., Jerchow, B., Sachs, M., Weiler, S., Pietsch, T., Karsten, U., van de Wetering, M., Clevers, H., Schlag, P. M., Birchmeier, W. and Behrens, J. (2002). "Negative feedback loop of Wnt signaling through upregulation of conductin/axin2 in colorectal and liver tumors." Mol Cell Biol **22**(4): 1184-1193.
- Ma, P. C., Rould, M. A., Weintraub, H. and Pabo, C. O. (1994). "Crystal structure of MyoD bHLH domain-DNA complex: perspectives on DNA recognition and implications for transcriptional activation." Cell **77**(3): 451-459.
- Mackenzie, S., Walsh, F. S. and Graham, A. (1998). "Migration of hypoglossal myoblast precursors." Dev Dyn **213**(4): 349-358.
- Maduro, M. F., Kasmir, J. J., Zhu, J. and Rothman, J. H. (2005). "The Wnt effector POP-1 and the PAL-1/Caudal homeoprotein collaborate with SKN-1 to activate C. elegans endoderm development." Dev Biol **285**(2): 510-523.
- Maffioletti, S. M., Noviello, M. and English, K. (2014). "Stem cell transplantation for muscular dystrophy: the challenge of immune response." **2014**: 964010.
- Makarenkova, H. P., Gonzalez, K. N., Kiosses, W. B. and Meech, R. (2009). "Barx2 Controls Myoblast Fusion and Promotes MyoD-mediated Activation of the Smooth Muscle-Actin Gene." Journal of Biological Chemistry **284**(22): 14866-14874.
- Makarenkova, H. P. and Meech, R. (2012). "Barx homeobox family in muscle development and regeneration." Int Rev Cell Mol Biol **297**: 117-173.
- Mansouri, A., Stoykova, A., Torres, M. and Gruss, P. (1996). "Dysgenesis of cephalic neural crest derivatives in Pax7^{-/-} mutant mice." Development **122**(3): 831-838.
- Maretto, S., Cordenonsi, M., Dupont, S., Braghetta, P., Broccoli, V., Hassan, A. B., Volpin, D., Bressan, G. M. and Piccolo, S. (2003). "Mapping Wnt/beta-catenin signaling during mouse development and in colorectal tumors." Proc Natl Acad Sci U S A **100**(6): 3299-3304.
- Marks, P. A., Richon, V. M. and Rifkind, R. A. (2000). "Histone deacetylase inhibitors: inducers of differentiation or apoptosis of transformed cells." J Natl Cancer Inst **92**(15): 1210-1216.
- Maroto, M., Reshef, R., Munsterberg, A. E., Koester, S., Goulding, M. and Lassar, A. B. (1997). "Ectopic Pax-3 activates MyoD and Myf-5 expression in embryonic mesoderm and neural tissue." Cell **89**(1): 139-148.
- Martin, J. F., Schwarz, J. J. and Olson, E. N. (1993). "Myocyte enhancer factor (MEF) 2C: a tissue-restricted member of the MEF-2 family of transcription factors." Proc Natl Acad Sci U S A **90**(11): 5282-5286.
- Massari, M. E. and Murre, C. (2000). "Helix-loop-helix proteins: regulators of transcription in eucaryotic organisms." Mol Cell Biol **20**(2): 429-440.
- Maulbecker, C. C. and Gruss, P. (1993). "The oncogenic potential of Pax genes." Embo j **12**(6): 2361-2367.

- Mauro, A. (1961). "Satellite cell of skeletal muscle fibers." J. Cell Biol. **9**(2): 493-495.
- Meech, R., Edelman, D. B., Jones, F. S. and Makarenkova, H. P. (2005). "The homeobox transcription factor Barx2 regulates chondrogenesis during limb development." Development **132**(9): 2135-2146.
- Meech, R., Gomez, M., Woolley, C., Barro, M., Hulin, J.-A., Walcott, E. C., Delgado, J. and Makarenkova, H. P. (2010). "The Homeobox Transcription Factor Barx2 Regulates Plasticity of Young Primary Myofibers." PLoS ONE **5**(7): e11612.
- Meech, R., Gonzalez, K. N., Barro, M., Gromova, A., Zhuang, L., Hulin, J.-A. and Makarenkova, H. P. (2012). "Barx2 Is Expressed in Satellite Cells and Is Required for Normal Muscle Growth and Regeneration." Stem Cells **30**(2): 253-265.
- Meech, R., Makarenkova, H., Edelman, D. B. and Jones, F. S. (2003). "The homeodomain protein Barx2 promotes myogenic differentiation and is regulated by myogenic regulatory factors." J Biol Chem **278**(10): 8269-8278.
- Meng, J., Muntoni, F. and Morgan, J. E. (2011). "Stem cells to treat muscular dystrophies - where are we?" Neuromuscul Disord **21**(1): 4-12.
- Mercuri, E. and Muntoni, F. (2013). "Muscular dystrophy: new challenges and review of the current clinical trials." Curr Opin Pediatr **25**(6): 701-707.
- Merrill, B. J., Pasolli, H. A., Polak, L., Rendl, M., Garcia-Garcia, M. J., Anderson, K. V. and Fuchs, E. (2004). "Tcf3: a transcriptional regulator of axis induction in the early embryo." Development **131**(2): 263-274.
- Miller, R. W. and Rubinstein, J. H. (1995). "Tumors in Rubinstein-Taybi syndrome." Am J Med Genet **56**(1): 112-115.
- Minasi, M. G., Riminucci, M., De Angelis, L., Borello, U., Berarducci, B., Innocenzi, A., Caprioli, A., Sirabella, D., Baiocchi, M., De Maria, R., Boratto, R., Jaffredo, T., Broccoli, V., Bianco, P. and Cossu, G. (2002). "The meso-angioblast: a multipotent, self-renewing cell that originates from the dorsal aorta and differentiates into most mesodermal tissues." Development **129**(11): 2773-2783.
- Mohamed, O. A., Clarke, H. J. and Dufort, D. (2004). "Beta-catenin signaling marks the prospective site of primitive streak formation in the mouse embryo." Dev Dyn **231**(2): 416-424.
- Molkentin, J. D., Black, B. L., Martin, J. F. and Olson, E. N. (1995). "Cooperative activation of muscle gene expression by MEF2 and myogenic bHLH proteins." Cell **83**(7): 1125-1136.
- Molkentin, J. D. and Olson, E. N. (1996). "Combinatorial control of muscle development by basic helix-loop-helix and MADS-box transcription factors." Proceedings of the National Academy of Sciences of the United States of America **93**(18): 9366-9373.
- Montarras, D., Chelly, J., Bober, E., Arnold, H., Ott, M. O., Gros, F. and Pinset, C. (1991). "Developmental patterns in the expression of Myf5, MyoD, myogenin, and MRF4 during myogenesis." New Biol **3**(6): 592-600.

- Montarras, D., Morgan, J., Collins, C., Relaix, F., Zaffran, S., Cumano, A., Partridge, T. and Buckingham, M. (2005). "Direct Isolation of Satellite Cells for Skeletal Muscle Regeneration." Science **309**(5743): 2064-2067.
- Moriyama, A., Kii, I., Sunabori, T., Kurihara, S., Takayama, I., Shimazaki, M., Tanabe, H., Oginuma, M., Fukayama, M., Matsuzaki, Y., Saga, Y. and Kudo, A. (2007). "GFP transgenic mice reveal active canonical Wnt signal in neonatal brain and in adult liver and spleen." genesis **45**(2): 90-100.
- Mourikis, P., Sambasivan, R., Castel, D., Rocheteau, P., Bizzarro, V. and Tajbakhsh, S. (2012). "A critical requirement for notch signaling in maintenance of the quiescent skeletal muscle stem cell state." Stem Cells **30**(2): 243-252.
- Muhr, J., Andersson, E., Persson, M., Jessell, T. M. and Ericson, J. (2001). "Groucho-Mediated Transcriptional Repression Establishes Progenitor Cell Pattern and Neuronal Fate in the Ventral Neural Tube." **104**(6): 861-873.
- Murphy, M. M., Keefe, A. C., Lawson, J. A., Flygare, S. D., Yandell, M. and Kardon, G. (2014). "Transiently active Wnt/beta-catenin signaling is not required but must be silenced for stem cell function during muscle regeneration." Stem Cell Reports **3**(3): 475-488.
- Musaro, A., Fulle, S. and Fano, G. (2010). "Oxidative stress and muscle homeostasis." Curr Opin Clin Nutr Metab Care **13**(3): 236-242.
- Nabeshima, Y., Hanaoka, K., Hayasaka, M., Esumi, E., Li, S., Nonaka, I. and Nabeshima, Y. (1993). "Myogenin gene disruption results in perinatal lethality because of severe muscle defect." Nature **364**(6437): 532-535.
- Nagy, L., Kao, H. Y., Chakravarti, D., Lin, R. J., Hassig, C. A., Ayer, D. E., Schreiber, S. L. and Evans, R. M. (1997). "Nuclear receptor repression mediated by a complex containing SMRT, mSin3A, and histone deacetylase." Cell **89**(3): 373-380.
- Naidu, P. S., Ludolph, D. C., To, R. Q., Hinterberger, T. J. and Konieczny, S. F. (1995). "Myogenin and MEF2 function synergistically to activate the MRF4 promoter during myogenesis." Mol Cell Biol **15**(5): 2707-2718.
- Narici, M. V. and de Boer, M. D. (2011). "Disuse of the musculo-skeletal system in space and on earth." Eur J Appl Physiol **111**(3): 403-420.
- Naya, F. J., Wu, C., Richardson, J. A., Overbeek, P. and Olson, E. N. (1999). "Transcriptional activity of MEF2 during mouse embryogenesis monitored with a MEF2-dependent transgene." Development **126**(10): 2045-2052.
- Nicks, D. K., Beneke, W. M., Key, R. M. and Timson, B. F. (1989). "Muscle fibre size and number following immobilisation atrophy." J Anat **163**: 1-5.
- Niida, A., Hiroko, T., Kasai, M., Furukawa, Y., Nakamura, Y., Suzuki, Y., Sugano, S. and Akiyama, T. (2004). "DKK1, a negative regulator of Wnt signaling, is a target of the beta-catenin/TCF pathway." Oncogene **23**(52): 8520-8526.
- Nowak, K. J. and Davies, K. E. (2004). "Duchenne muscular dystrophy and dystrophin: pathogenesis and opportunities for treatment." EMBO Rep **5**(9): 872-876.

- Nusse, R. (1999). "WNT targets. Repression and activation." Trends Genet **15**(1): 1-3.
- Nusse, R. (2008). "Wnt signaling and stem cell control." Cell Res **18**(5): 523-527.
- Odenwald, W. F., Garbern, J., Arnheiter, H., Tournier-Lasserre, E. and Lazzarini, R. A. (1989). "The Hox-1.3 homeo box protein is a sequence-specific DNA-binding phosphoprotein." Genes Dev **3**(2): 158-172.
- Ogryzko, V. V., Schiltz, R. L., Russanova, V., Howard, B. H. and Nakatani, Y. (1996). "The transcriptional coactivators p300 and CBP are histone acetyltransferases." Cell **87**: 953-959.
- Olguin, H. C. and Olwin, B. B. (2004). "Pax-7 up-regulation inhibits myogenesis and cell cycle progression in satellite cells: a potential mechanism for self-renewal." Dev Biol **275**(2): 375-388.
- Olguin, H. C., Yang, Z., Tapscott, S. J. and Olwin, B. B. (2007). "Reciprocal inhibition between Pax7 and muscle regulatory factors modulates myogenic cell fate determination." J. Cell Biol. **177**(5): 769-779.
- Olson, L. E., Tollkuhn, J., Scafoglio, C., Krones, A., Zhang, J., Ohgi, K. A., Wu, W., Taketo, M. M., Kemler, R., Grosschedl, R., Rose, D., Li, X. and Rosenfeld, M. G. (2006). "Homeodomain-Mediated ²-Catenin-Dependent Switching Events Dictate Cell-Lineage Determination." **125**(3): 593-605.
- Olson, L. E., Zhang, J., Taylor, H., Rose, D. W. and Rosenfeld, M. G. (2005). "Barx2 functions through distinct corepressor classes to regulate hair follicle remodeling." Proceedings of the National Academy of Sciences of the United States of America **102**(10): 3708-3713.
- Omer, C. A., Miller, P. J., Diehl, R. E. and Kral, A. M. (1999). "Identification of Tcf4 residues involved in high-affinity beta-catenin binding." Biochem Biophys Res Commun **256**(3): 584-590.
- Oosterwegel, M., van de Wetering, M., Dooijes, D., Klomp, L., Winoto, A., Georgopoulos, K., Meijlink, F. and Clevers, H. (1991). "Cloning of murine TCF-1, a T cell-specific transcription factor interacting with functional motifs in the CD3-epsilon and T cell receptor alpha enhancers." J Exp Med **173**(5): 1133-1142.
- Oosterwegel, M., van de Wetering, M., Timmerman, J., Kruisbeek, A., Destree, O., Meijlink, F. and Clevers, H. (1993). "Differential expression of the HMG box factors TCF-1 and LEF-1 during murine embryogenesis." Development **118**(2): 439-448.
- Ott, M. O., Bober, E., Lyons, G., Arnold, H. and Buckingham, M. (1991). "Early expression of the myogenic regulatory gene, myf-5, in precursor cells of skeletal muscle in the mouse embryo." Development **111**(4): 1097-1107.
- Otto, A., Collins-Hooper, H. and Patel, K. (2009). "The origin, molecular regulation and therapeutic potential of myogenic stem cell populations." Journal of Anatomy **9999**(9999).
- Otto, A., Schmidt, C., Luke, G., Allen, S., Valasek, P., Muntoni, F., Lawrence-Watt, D. and Patel, K. (2008). "Canonical Wnt signalling induces satellite-cell proliferation

- during adult skeletal muscle regeneration." *J Cell Sci* **121**(17): 2939-2950.
- Otto, A., Schmidt, C. and Patel, K. (2006). "Pax3 and Pax7 expression and regulation in the avian embryo." *Anatomy and Embryology* **211**(4): 293-310.
- Ou, C. Y., LaBonte, M. J., Manegold, P. C., So, A. Y., Ianculescu, I., Gerke, D. S., Yamamoto, K. R., Ladner, R. D., Kahn, M., Kim, J. H. and Stallcup, M. R. (2011). "A coactivator role of CARM1 in the dysregulation of beta-catenin activity in colorectal cancer cell growth and gene expression." *Mol Cancer Res* **9**(5): 660-670.
- Oustanina, S., Hause, G. and Braun, T. (2004). "Pax7 directs postnatal renewal and propagation of myogenic satellite cells but not their specification." *EMBO J* **23**(16): 3430-3439.
- Pansters, N., van der Velden, J., Kelders, M., Laeremans, H., Schols, A. and Langen, R. (2011). "Segregation of myoblast fusion and muscle-specific gene expression by distinct ligand-dependent inactivation of GSK-3 β ." *Cellular and Molecular Life Sciences* **68**(3): 523-535.
- Park, J.-S., Ma, W., O'Brien, Lori L., Chung, E., Guo, J.-J., Cheng, J.-G., Valerius, M. T., McMahon, Jill A., Wong, Wing H. and McMahon, Andrew P. (2012). "Six2 and Wnt Regulate Self-Renewal and Commitment of Nephron Progenitors through Shared Gene Regulatory Networks." *Developmental Cell* **23**(3): 637-651.
- Parker, D. S., Ni, Y. Y., Chang, J. L., Li, J. and Cadigan, K. M. (2008). "Wingless signaling induces widespread chromatin remodeling of target loci." *Mol Cell Biol* **28**(5): 1815-1828.
- Parker, M. H., Perry, R. L., Fauteux, M. C., Berkes, C. A. and Rudnicki, M. A. (2006). "MyoD synergizes with the E-protein HEB beta to induce myogenic differentiation." *Mol Cell Biol* **26**(15): 5771-5783.
- Parmacek, M. S., Ip, H. S., Jung, F., Shen, T., Martin, J. F., Vora, A. J., Olson, E. N. and Leiden, J. M. (1994). "A novel myogenic regulatory circuit controls slow/cardiac troponin C gene transcription in skeletal muscle." *Mol Cell Biol* **14**(3): 1870-1885.
- Passamano, L., Taglia, A., Palladino, A., Viggiano, E., D'Ambrosio, P., Scutifero, M., Rosaria Cecio, M., Torre, V., F. D. E. L., Picillo, E., Paciello, O., Piluso, G., Nigro, G. and Politano, L. (2012). "Improvement of survival in Duchenne Muscular Dystrophy: retrospective analysis of 835 patients." *Acta Myol* **31**(2): 121-125.
- Pellettieri, J. and Sanchez Alvarado, A. (2007). "Cell turnover and adult tissue homeostasis: from humans to planarians." *Annu Rev Genet* **41**: 83-105.
- Perissi, V. and Rosenfeld, M. G. (2005). "Controlling nuclear receptors: the circular logic of cofactor cycles." *Nat Rev Mol Cell Biol* **6**(7): 542-554.
- Petrij, F., Giles, R. H., Dauwerse, H. G., Saris, J. J., Hennekam, R. C., Masuno, M., Tommerup, N., van Ommen, G. J., Goodman, R. H., Peters, D. J. and et al. (1995). "Rubinstein-Taybi syndrome caused by mutations in the transcriptional co-activator CBP." *Nature* **376**(6538): 348-351.
- Polesskaya, A., Seale, P. and Rudnicki, M. A. (2003). "Wnt Signaling Induces the

Myogenic Specification of Resident CD45+ Adult Stem Cells during Muscle Regeneration." Cell **113**(7): 841-852.

Potts, W., Tucker, D., Wood, H. and Martin, C. (2000). "Chicken beta-globin 5'HS4 insulators function to reduce variability in transgenic founder mice." Biochem Biophys Res Commun **273**(3): 1015-1018.

Puigserver, P., Adelmant, G., Wu, Z., Fan, M., Xu, J., O'Malley, B. and Spiegelman, B. M. (1999). "Activation of PPARgamma coactivator-1 through transcription factor docking." Science **286**(5443): 1368-1371.

Puri, P. L., Avantaggiati, M. L., Balsano, C., Sang, N., Graessmann, A., Giordano, A. and Levrero, M. (1997). "p300 is required for MyoD-dependent cell cycle arrest and muscle-specific gene transcription." Embo j **16**(2): 369-383.

Rawls, A., Morris, J. H., Rudnicki, M., Braun, T., Arnold, H. H., Klein, W. H. and Olson, E. N. (1995). "Myogenin's functions do not overlap with those of MyoD or Myf-5 during mouse embryogenesis." Dev Biol **172**(1): 37-50.

Rawls, A., Valdez, M. R., Zhang, W., Richardson, J., Klein, W. H. and Olson, E. N. (1998). "Overlapping functions of the myogenic bHLH genes MRF4 and MyoD revealed in double mutant mice." Development **125**(13): 2349-2358.

Recillas-Targa, F., Pikaart, M. J., Burgess-Beusse, B., Bell, A. C., Litt, M. D., West, A. G., Gaszner, M. and Felsenfeld, G. (2002). "Position-effect protection and enhancer blocking by the chicken beta-globin insulator are separable activities." Proc Natl Acad Sci U S A **99**(10): 6883-6888.

Reimann, J., Irintchev, A. and Wernig, A. (2000). "Regenerative capacity and the number of satellite cells in soleus muscles of normal and mdx mice." Neuromuscul Disord **10**(4-5): 276-282.

Relaix, F., Montarras, D., Zaffran, S., Gayraud-Morel, B., Rocancourt, D., Tajbakhsh, S., Mansouri, A., Cumano, A. and Buckingham, M. (2006). "Pax3 and Pax7 have distinct and overlapping functions in adult muscle progenitor cells." J. Cell Biol. **172**(1): 91-102.

Relaix, F., Rocancourt, D., Mansouri, A. and Buckingham, M. (2004). "Divergent functions of murine Pax3 and Pax7 in limb muscle development." Genes Dev. **18**(9): 1088-1105.

Relaix, F., Rocancourt, D., Mansouri, A. and Buckingham, M. (2005). "A Pax3/Pax7-dependent population of skeletal muscle progenitor cells." Nature **435**(7044): 948-953.

Relaix, F. and Zammit, P. S. (2012). "Satellite cells are essential for skeletal muscle regeneration: the cell on the edge returns centre stage." Development **139**(16): 2845-2856.

Renault, V., Piron-Hamelin, G., Forestier, C., DiDonna, S., Decary, S., Hentati, F., Saillant, G., Butler-Browne, G. S. and Mouly, V. (2000). "Skeletal muscle regeneration and the mitotic clock." Exp Gerontol **35**(6-7): 711-719.

- Renault, V., Thorne, L.-E., Eriksson, P.-O., Butler-Browne, G. and Mouly, V. (2002). "Regenerative potential of human skeletal muscle during aging." *Aging Cell* **1**(2): 132-139.
- Rennie, M. J. (2007). "Exercise- and nutrient-controlled mechanisms involved in maintenance of the musculoskeletal mass." *Biochem Soc Trans* **35**(Pt 5): 1302-1305.
- Rhodes, S. J. and Konieczny, S. F. (1989). "Identification of MRF4: a new member of the muscle regulatory factor gene family." *Genes Dev* **3**(12b): 2050-2061.
- Rockman, S. P., Currie, S. A., Ciavarella, M., Vincan, E., Dow, C., Thomas, R. J. and Phillips, W. A. (2001). "Id2 is a target of the beta-catenin/T cell factor pathway in colon carcinoma." *J Biol Chem* **276**(48): 45113-45119.
- Roose, J., Molenaar, M., Peterson, J., Hurenkamp, J., Brantjes, H., Moerer, P., Van De Wetering, M., Destrée, O. and Clevers, H. (1998). "The Xenopus Wnt effector XTcf-3 interacts with Groucho-related transcriptional repressors." *Nature* **395**(6702): 608-612.
- Rosenfeld, M. G., Lunyak, V. V. and Glass, C. K. (2006). "Sensors and signals: a coactivator/corepressor/epigenetic code for integrating signal-dependent programs of transcriptional response." *Genes Dev* **20**(11): 1405-1428.
- Rubinfeld, B., Albert, I., Porfiri, E., Fiol, C., Munemitsu, S. and Polakis, P. (1996). "Binding of GSK3beta to the APC-beta-catenin complex and regulation of complex assembly." *Science* **272**(5264): 1023-1026.
- Rudnicki, M. A., Braun, T., Hinuma, S. and Jaenisch, R. (1992). "Inactivation of MyoD in mice leads to up-regulation of the myogenic HLH gene Myf-5 and results in apparently normal muscle development." *Cell* **71**(3): 383-390.
- Rudnicki, M. A., Schnegelsberg, P. N. J., Stead, R. H., Braun, T., Arnold, H.-H. and Jaenisch, R. (1993). "MyoD or Myf-5 is required for the formation of skeletal muscle." *Cell* **75**(7): 1351-1359.
- Ruegg, M. A. and Glass, D. J. (2011). "Molecular mechanisms and treatment options for muscle wasting diseases." *Annu Rev Pharmacol Toxicol* **51**: 373-395.
- Russo, S., Tomatis, D., Collo, G., Tarone, G. and Tato, F. (1998). "Myogenic conversion of NIH3T3 cells by exogenous MyoD family members: dissociation of terminal differentiation from myotube formation." *J Cell Sci* **111** (Pt 6): 691-700.
- Sabourin, L. A. and Rudnicki, M. A. (2000). "The molecular regulation of myogenesis." *Clin Genet* **57**(1): 16-25.
- Sacco, A., Doyonnas, R., Kraft, P., Vitorovic, S. and Blau, H. M. (2008). "Self-renewal and expansion of single transplanted muscle stem cells." *Nature* **456**: 502-506.
- Sacco, A., Mourkioti, F., Tran, R., Choi, J., Llewellyn, M., Kraft, P., Shkreli, M., Delp, S., Pomerantz, J. H., Artandi, S. E. and Blau, H. M. (2010). "Short telomeres and stem cell exhaustion model Duchenne muscular dystrophy in mdx/mTR mice." *Cell* **143**(7): 1059-1071.
- Sambasivan, R., Yao, R., Kissenpfennig, A., Van Wittenberghe, L., Paldi, A., Gayraud-

- Morel, B., Guenou, H., Malissen, B., Tajbakhsh, S. and Galy, A. (2011). "Pax7-expressing satellite cells are indispensable for adult skeletal muscle regeneration." Development **138**(17): 3647-3656.
- Sampson, E. M., Haque, Z. K., Ku, M. C., Tevosian, S. G., Albanese, C., Pestell, R. G., Paulson, K. E. and Yee, A. S. (2001). "Negative regulation of the Wnt-beta-catenin pathway by the transcriptional repressor HBP1." Embo j **20**(16): 4500-4511.
- Sanchez-Tillo, E., de Barrios, O., Siles, L., Cuatrecasas, M., Castells, A. and Postigo, A. (2011). "beta-catenin/TCF4 complex induces the epithelial-to-mesenchymal transition (EMT)-activator ZEB1 to regulate tumor invasiveness." Proc Natl Acad Sci U S A **108**(48): 19204-19209.
- Sander, G. R. and Powell, B. C. (2004). "Expression of the homeobox gene barx2 in the gut." J Histochem Cytochem **52**(4): 541-544.
- Santoso, B. and Kadonaga, J. T. (2006). "Reconstitution of chromatin transcription with purified components reveals a chromatin-specific repressive activity of p300." Nat Struct Mol Biol **13**(2): 131-139.
- Sasai, Y., Kageyama, R., Tagawa, Y., Shigemoto, R. and Nakanishi, S. (1992). "Two mammalian helix-loop-helix factors structurally related to Drosophila hairy and Enhancer of split." Genes Dev **6**(12b): 2620-2634.
- Sassoon, D., Lyons, G., Wright, W. E., Lin, V., Lassar, A., Weintraub, H. and Buckingham, M. (1989). "Expression of two myogenic regulatory factors myogenin and MyoD1 during mouse embryogenesis." Nature **341**(6240): 303-307.
- Schafer, B. W., Czerny, T., Bernasconi, M., Genini, M. and Busslinger, M. (1994). "Molecular cloning and characterization of a human PAX-7 cDNA expressed in normal and neoplastic myocytes." Nucleic Acids Res **22**(22): 4574-4582.
- Schevzov, G., Lloyd, C. and Gunning, P. (1992). "High level expression of transfected beta- and gamma-actin genes differentially impacts on myoblast cytoarchitecture." J. Cell Biol. **117**(4): 775-785.
- Schiaffino, S., Dyar, K. A., Ciciliot, S., Blaauw, B. and Sandri, M. (2013). "Mechanisms regulating skeletal muscle growth and atrophy." FEBS Journal **280**(17): 4294-4314.
- Schmidt-Ott, K. M., Masckauchan, T. N., Chen, X., Hirsh, B. J., Sarkar, A., Yang, J., Paragas, N., Wallace, V. A., Dufort, D., Pavlidis, P., Jagla, B., Kitajewski, J. and Barasch, J. (2007). "beta-catenin/TCF/Lef controls a differentiation-associated transcriptional program in renal epithelial progenitors." Development **134**(17): 3177-3190.
- Schrem, H., Klempnauer, J. and Borlak, J. (2002). "Liver-enriched transcription factors in liver function and development. Part I: the hepatocyte nuclear factor network and liver-specific gene expression." Pharmacol Rev **54**(1): 129-158.
- Schubert, F. R., Tremblay, P., Mansouri, A., Faisst, A. M., Kammandel, B., Lumsden, A., Gruss, P. and Dietrich, S. (2001). "Early mesodermal phenotypes in splotch suggest a role for Pax3 in the formation of epithelial somites." Dev Dyn **222**(3): 506-521.
- Schultz, E. and Jarzyzak, D. L. (1985). "Effects of skeletal muscle regeneration on the

- proliferation potential of satellite cells." Mech Ageing Dev **30**(1): 63-72.
- Seale, P., Polesskaya, A. and Rudnicki, M. A. (2003). "Adult stem cell specification by Wnt signaling in muscle regeneration." Cell Cycle **2**(5): 418-419.
- Seale, P., Sabourin, L. A., Girgis-Gabardo, A., Mansouri, A., Gruss, P. and Rudnicki, M. A. (2000). "Pax7 is required for the specification of myogenic satellite cells." Cell **102**(6): 777-786.
- Sekiya, T. and Zaret, K. S. (2007). "Repression by Groucho/TLE/Grg Proteins: Genomic Site Recruitment Generates Compacted Chromatin In Vitro and Impairs Activator Binding In Vivo." Molecular Cell **28**(2): 291-303.
- Shanmugam, V., Dion, P., Rochefort, D., Laganier, J., Brais, B. and Rouleau, G. A. (2000). "PABP2 polyalanine tract expansion causes intranuclear inclusions in oculopharyngeal muscular dystrophy." Ann Neurol **48**(5): 798-802.
- Shao, J.-S., Cheng, S.-L., Pingsterhaus, J. M., Charlton-Kachigian, N., Loewy, A. P. and Towler, D. A. (2005). "Msx2 promotes cardiovascular calcification by activating paracrine Wnt signals." The Journal of Clinical Investigation **115**(5): 1210-1220.
- Shefer, G., Rauner, G., Yablonka-Reuveni, Z. and Benayahu, D. (2010). "Reduced Satellite Cell Numbers and Myogenic Capacity in Aging Can Be Alleviated by Endurance Exercise." PLoS ONE **5**(10): e13307.
- Shih, H. P., Gross, M. K. and Kioussi, C. (2007). "Expression pattern of the homeodomain transcription factor Pitx2 during muscle development." Gene Expr Patterns **7**(4): 441-451.
- Shiina, H., Igawa, M., Breault, J., Ribeiro-Filho, L., Pookot, D., Urakami, S., Terashima, M., Deguchi, M., Yamanaka, M., Shirai, M., Kaneuchi, M., Kane, C. J. and Dahiya, R. (2003). "The human T-cell factor-4 gene splicing isoforms, Wnt signal pathway, and apoptosis in renal cell carcinoma." Clin Cancer Res **9**(6): 2121-2132.
- Shtutman, M., Zhurinsky, J., Simcha, I., Albanese, C., D'Amico, M., Pestell, R. and Ben-Ze'ev, A. (1999). "The cyclin D1 gene is a target of the beta-catenin/LEF-1 pathway." Proc Natl Acad Sci U S A **96**(10): 5522-5527.
- Sierra, J., Yoshida, T., Joazeiro, C. A. and Jones, K. A. (2006). "The APC tumor suppressor counteracts beta-catenin activation and H3K4 methylation at Wnt target genes." Genes Dev **20**(5): 586-600.
- Smith, C. K., Janney M.J., Allen R.E. (1994). "Temporal expression of myogenic regulatory genes during activation, proliferation, and differentiation of rat skeletal muscle satellite cells." Journal of Cellular Physiology **159**(2): 379-385.
- Smith, D. M. and Tabin, C. J. (1999). "Chick Barx2b, a marker for myogenic cells also expressed in branchial arches and neural structures." Mech Dev **80**(2): 203-206.
- Smith, S. T. and Jaynes, J. B. (1996). "A conserved region of engrailed, shared among all en-, gsc-, Nk1-, Nk2- and msh-class homeoproteins, mediates active transcriptional repression in vivo." Development **122**(10): 3141-3150.
- Snow, M. H. (1977). "The effects of aging on satellite cells in skeletal muscles of mice

and rats." Cell Tissue Res **185**(3): 399-408.

Soleimani, V. D., Yin, H., Jahani-Asl, A., Ming, H., Kockx, C. E., van Ijcken, W. F., Grosveld, F. and Rudnicki, M. A. (2012). "Snail regulates MyoD binding-site occupancy to direct enhancer switching and differentiation-specific transcription in myogenesis." Mol Cell **47**(3): 457-468.

Song, L. N. and Gelmann, E. P. (2005). "Interaction of beta-catenin and TIF2/GRIP1 in transcriptional activation by the androgen receptor." J Biol Chem **280**(45): 37853-37867.

Song, L. N. and Gelmann, E. P. (2008). "Silencing mediator for retinoid and thyroid hormone receptor and nuclear receptor corepressor attenuate transcriptional activation by the beta-catenin-TCF4 complex." J Biol Chem **283**(38): 25988-25999.

Springer, M. L., Ozawa, C. R. and Blau, H. M. (2002). "Transient production of alpha-smooth muscle actin by skeletal myoblasts during differentiation in culture and following intramuscular implantation." Cell Motil Cytoskeleton **51**(4): 177-186.

Squazzo, S. L. (2006). "Suz12 binds to silenced regions of the genome in a cell-type-specific manner." Genome Res. **16**: 890-900.

Staal, F. J., Noort Mv, M., Strous, G. J. and Clevers, H. C. (2002). "Wnt signals are transmitted through N-terminally dephosphorylated beta-catenin." EMBO Rep **3**(1): 63-68.

Stacey, D. W. (2003). "Cyclin D1 serves as a cell cycle regulatory switch in actively proliferating cells." Curr Opin Cell Biol **15**(2): 158-163.

Stamos, J. L. and Weis, W. I. (2013). "The beta-catenin destruction complex." Cold Spring Harb Perspect Biol **5**(1): a007898.

Stevens, T. A. and Meech, R. (2006). "BARX2 and estrogen receptor-[alpha] (ESR1) coordinately regulate the production of alternatively spliced ESR1 isoforms and control breast cancer cell growth and invasion." Oncogene **25**(39): 5426-5435.

Strigini, M. and Cohen, S. M. (2000). "Wingless gradient formation in the Drosophila wing." Curr Biol **10**(6): 293-300.

Struhl, G. and Greenwald, I. (2001). "Presenilin-mediated transmembrane cleavage is required for Notch signal transduction in Drosophila." Proc Natl Acad Sci U S A **98**(1): 229-234.

Sun, J., Kamei, C. N., Layne, M. D., Jain, M. K., Liao, J. K., Lee, M. E. and Chin, M. T. (2001). "Regulation of myogenic terminal differentiation by the hairy-related transcription factor CHF2." J Biol Chem **276**(21): 18591-18596.

Suzuki, A., Scruggs, A. and Iwata, J. (2015). "The temporal specific role of WNT/beta-catenin signaling during myogenesis." J Nat Sci **1**(8): e143.

Tajbakhsh, S. (2009). "Skeletal muscle stem cells in developmental versus regenerative myogenesis." J Intern Med **266**(4): 372-389.

Tajbakhsh, S., Bober, E., Babinet, C., Pournin, S., Arnold, H. and Buckingham, M.

(1996). "Gene targeting the myf-5 locus with nlacZ reveals expression of this myogenic factor in mature skeletal muscle fibres as well as early embryonic muscle." Dev Dyn **206**(3): 291-300.

Tajbakhsh, S., Borello, U., Vivarelli, E., Kelly, R., Papkoff, J., Duprez, D., Buckingham, M. and Cossu, G. (1998). "Differential activation of Myf5 and MyoD by different Wnts in explants of mouse paraxial mesoderm and the later activation of myogenesis in the absence of Myf5." Development **125**(21): 4155-4162.

Tajbakhsh, S. and Buckingham, M. E. (1994). "Mouse limb muscle is determined in the absence of the earliest myogenic factor myf-5." Proc Natl Acad Sci U S A **91**(2): 747-751.

Tajbakhsh, S., Rocancourt, D., Cossu, G. and Buckingham, M. (1997). "Redefining the Genetic Hierarchies Controlling Skeletal Myogenesis: Pax-3 and Myf-5 Act Upstream of MyoD." Cell **89**(1): 127-138.

Takemaru, K. I. and Moon, R. T. (2000). "The transcriptional coactivator CBP interacts with beta-catenin to activate gene expression." J Cell Biol **149**(2): 249-254.

Tanaka, S., Terada, K. and Nohno, T. (2011). "Canonical Wnt signaling is involved in switching from cell proliferation to myogenic differentiation of mouse myoblast cells." Journal of Molecular Signaling **6**(1): 12.

Tanigaki, K. and Honjo, T. (2010). "Two opposing roles of RBP-J in Notch signaling." Curr Top Dev Biol **92**: 231-252.

Tapscott, S. J., Davis, R. L., Thayer, M. J., Cheng, P. F., Weintraub, H. and Lassar, A. B. (1988). "MyoD1: a nuclear phosphoprotein requiring a Myc homology region to convert fibroblasts to myoblasts." Science **242**(4877): 405-411.

Tapscott, S. J. and Weintraub, H. (1991). "MyoD and the regulation of myogenesis by helix-loop-helix proteins." J Clin Invest **87**(4): 1133-1138.

Tetsu, O. and McCormick, F. (1999). "Beta-catenin regulates expression of cyclin D1 in colon carcinoma cells." Nature **398**(6726): 422-426.

Thayer, M. J., Tapscott, S. J., Davis, R. L., Wright, W. E., Lassar, A. B. and Weintraub, H. (1989). "Positive autoregulation of the myogenic determination gene MyoD1." Cell **58**(2): 241-248.

Thompson, W. R., Nadal-Ginard, B. and Mahdavi, V. (1991). "A MyoD1-independent muscle-specific enhancer controls the expression of the beta-myosin heavy chain gene in skeletal and cardiac muscle cells." J Biol Chem **266**(33): 22678-22688.

Tolkunova, E. N., Fujioka, M., Kobayashi, M., Deka, D. and Jaynes, J. B. (1998). "Two distinct types of repression domain in engrailed: one interacts with the groucho corepressor and is preferentially active on integrated target genes." Mol Cell Biol **18**(5): 2804-2814.

Trapnell, C., Roberts, A., Goff, L., Pertea, G., Kim, D., Kelley, D. R., Pimentel, H., Salzberg, S. L., Rinn, J. L. and Pachter, L. (2012). "Differential gene and transcript expression analysis of RNA-seq experiments with TopHat and Cufflinks." Nat Protoc

7(3): 562-578.

Travis, A., Amsterdam, A., Belanger, C. and Grosschedl, R. (1991). "LEF-1, a gene encoding a lymphoid-specific protein with an HMG domain, regulates T-cell receptor alpha enhancer function [corrected]." Genes Dev **5**(5): 880-894.

Tremblay, J. P., Bouchard, J. P., Malouin, F., Theau, D., Cottrell, F., Collin, H., Rouche, A., Gilgenkrantz, S., Abbadì, N., Tremblay, M. and et al. (1993). "Myoblast transplantation between monozygotic twin girl carriers of Duchenne muscular dystrophy." Neuromuscul Disord **3**(5-6): 583-592.

Trotter, K. W. and Archer, T. K. (2008). "The BRG1 transcriptional coregulator." Nucl Recept Signal **6**: e004.

Tsau, C., Ito, M., Gromova, A., Hoffman, M. P., Meech, R. and Makarenkova, H. P. (2011). "Barx2 and Fgf10 regulate ocular glands branching morphogenesis by controlling extracellular matrix remodeling." Development **138**(15): 3307-3317.

Tse, C., Sera, T., Wolffe, A. P. and Hansen, J. C. (1998). "Disruption of higher-order folding by core histone acetylation dramatically enhances transcription of nucleosomal arrays by RNA polymerase III." Mol Cell Biol **18**(8): 4629-4638.

Tsukada, Y., Fang, J., Erdjument-Bromage, H., Warren, M. E., Borchers, C. H., Tempst, P. and Zhang, Y. (2006). "Histone demethylation by a family of JmjC domain-containing proteins." Nature **439**(7078): 811-816.

Utsch, B., Becker, K., Brock, D., Lentze, M. J., Bidlingmaier, F. and Ludwig, M. (2002). "A novel stable polyalanine [poly(A)] expansion in the HOXA13 gene associated with hand-foot-genital syndrome: proper function of poly(A)-harbouring transcription factors depends on a critical repeat length?" Hum Genet **110**(5): 488-494.

Vadlamudi, U., Espinoza, H. M., Ganga, M., Martin, D. M., Liu, X., Engelhardt, J. F. and Amendt, B. A. (2005). "PITX2, β -catenin and LEF-1 interact to synergistically regulate the LEF-1 promoter." Journal of Cell Science **118**(6): 1129-1137.

Valenta, T., Lukas, J. and Korinek, V. (2003). "HMG box transcription factor TCF-4's interaction with CtBP1 controls the expression of the Wnt target Axin2/Conductin in human embryonic kidney cells." Nucleic Acids Res **31**(9): 2369-2380.

van Amerongen, R. e. and Nusse, R. (2009). "Towards an integrated view of Wnt signaling in development." Development **136**(19): 3205-3214.

van Beest, M., Dooijes, D., van De Wetering, M., Kjaerulff, S., Bonvin, A., Nielsen, O. and Clevers, H. (2000). "Sequence-specific high mobility group box factors recognize 10-12-base pair minor groove motifs." J Biol Chem **275**(35): 27266-27273.

van de Wetering, M. (2002). "The beta-catenin/TCF-4 complex imposes a crypt progenitor phenotype on colorectal cancer cells." Cell **111**: 241-250.

van de Wetering, M., Oosterwegel, M., Dooijes, D. and Clevers, H. (1991). "Identification and cloning of TCF-1, a T lymphocyte-specific transcription factor containing a sequence-specific HMG box." Embo j **10**(1): 123-132.

Veeman, M. T., Slusarski, D. C., Kaykas, A., Louie, S. H. and Moon, R. T. (2003).

"Zebrafish Prickle, a Modulator of Noncanonical Wnt/Fz Signaling, Regulates Gastrulation Movements." Current Biology **13**(8): 680-685.

Venuti, J. M., Morris, J. H., Vivian, J. L., Olson, E. N. and Klein, W. H. (1995). "Myogenin is required for late but not early aspects of myogenesis during mouse development." J Cell Biol **128**(4): 563-576.

Verbeek, S., Izon, D., Hofhuis, F., Robanus-Maandag, E., te Riele, H., van de Wetering, M., Oosterwegel, M., Wilson, A., MacDonald, H. R. and Clevers, H. (1995). "An HMG-box-containing T-cell factor required for thymocyte differentiation." Nature **374**(6517): 70-74.

Voigt, P., Tee, W. W. and Reinberg, D. (2013). "A double take on bivalent promoters." Genes Dev **27**(12): 1318-1338.

von Maltzahn, J., Jones, A. E., Parks, R. J. and Rudnicki, M. A. (2013). "Pax7 is critical for the normal function of satellite cells in adult skeletal muscle." Proc Natl Acad Sci U S A **110**(41): 16474-16479.

von Maltzahn, J., Renaud, J. M., Parise, G. and Rudnicki, M. A. (2012). "Wnt7a treatment ameliorates muscular dystrophy." Proc Natl Acad Sci U S A **109**(50): 20614-20619.

Waddell, J. N., Zhang, P., Wen, Y., Gupta, S. K., Yevtodiyanenko, A., Schmidt, J. V., Bidwell, C. A., Kumar, A. and Kuang, S. (2010). "Dlk1 Is Necessary for Proper Skeletal Muscle Development and Regeneration." PLoS ONE **5**(11): e15055.

Wagner, K. R., Lechtzin, N. and Judge, D. P. (2007). "Current treatment of adult Duchenne muscular dystrophy." Biochim Biophys Acta **1772**(2): 229-237.

Wallmen, B., Schrempp, M. and Hecht, A. (2012). "Intrinsic properties of Tcf1 and Tcf4 splice variants determine cell-type-specific Wnt/beta-catenin target gene expression." Nucleic Acids Res **40**(19): 9455-9469.

Walther, C., Guenet, J. L., Simon, D., Deutsch, U., Jostes, B., Goulding, M. D., Plachov, D., Balling, R. and Gruss, P. (1991). "Pax: a murine multigene family of paired box-containing genes." Genomics **11**(2): 424-434.

Wang, C., Lee, J. E., Cho, Y. W., Xiao, Y., Jin, Q., Liu, C. and Ge, K. (2012). "UTX regulates mesoderm differentiation of embryonic stem cells independent of H3K27 demethylase activity." Proc Natl Acad Sci U S A **109**(38): 15324-15329.

Watanabe, S., Kondo, S., Hayasaka, M. and Hanaoka, K. (2007). "Functional analysis of homeodomain-containing transcription factor Lbx1 in satellite cells of mouse skeletal muscle." J Cell Sci **120**(23): 4178-4187.

Waterman, M. L., Fischer, W. H. and Jones, K. A. (1991). "A thymus-specific member of the HMG protein family regulates the human T cell receptor C alpha enhancer." Genes Dev **5**(4): 656-669.

Webster, C. and Blau, H. M. (1990). "Accelerated age-related decline in replicative life-span of Duchenne muscular dystrophy myoblasts: implications for cell and gene therapy." Somat Cell Mol Genet **16**(6): 557-565.

- Weintraub, H., Dwarki, V. J., Verma, I., Davis, R., Hollenberg, S., Snider, L., Lassar, A. and Tapscott, S. J. (1991). "Muscle-specific transcriptional activation by MyoD." Genes Dev **5**(8): 1377-1386.
- Weintraub, H., Genetta, T. and Kadesch, T. (1994). "Tissue-specific gene activation by MyoD: determination of specificity by cis-acting repression elements." Genes Dev **8**(18): 2203-2211.
- Weise, A., Bruser, K., Elfert, S., Wallmen, B., Wittel, Y., Wohrle, S. and Hecht, A. (2010). "Alternative splicing of Tcf7l2 transcripts generates protein variants with differential promoter-binding and transcriptional activation properties at Wnt/beta-catenin targets." Nucleic Acids Res **38**(6): 1964-1981.
- Weiske, J. and Huber, O. (2005). "The histidine triad protein Hint1 interacts with Pontin and Reptin and inhibits TCF-beta-catenin-mediated transcription." J Cell Sci **118**(Pt 14): 3117-3129.
- Wen, Y., Bi, P., Liu, W., Asakura, A., Keller, C. and Kuang, S. (2012). "Constitutive Notch Activation Upregulates Pax7 and Promotes the Self-Renewal of Skeletal Muscle Satellite Cells." Molecular and Cellular Biology **32**(12): 2300-2311.
- West, A. G., Gaszner, M. and Felsenfeld, G. (2002). "Insulators: many functions, many mechanisms." Genes Dev **16**(3): 271-288.
- Widrick, J. J., Stelzer, J. E., Shoenberger, T. C. and Garner, D. P. (2002). "Functional properties of human muscle fibers after short-term resistance exercise training." Am J Physiol Regul Integr Comp Physiol **283**(2): R408-416.
- Willert, J., Epping, M., Pollack, J., Brown, P. and Nusse, R. (2002). "A transcriptional response to Wnt protein in human embryonic carcinoma cells." BMC Developmental Biology **2**(1): 8.
- Willert, K., Brown, J. D., Danenberg, E., Duncan, A. W., Weissman, I. L., Reya, T., Yates, J. R. and Nusse, R. (2003). "Wnt proteins are lipid-modified and can act as stem cell growth factors." Nature **423**(6938): 448-452.
- Wilson, J. J. and Kovall, R. A. (2006). "Crystal structure of the CSL-Notch-Mastermind ternary complex bound to DNA." Cell **124**(5): 985-996.
- Wodarz, A. and Nusse, R. (1998). "Mechanisms of Wnt signaling in development." Annu Rev Cell Dev Biol **14**: 59-88.
- Wohrle, S., Wallmen, B. and Hecht, A. (2007). "Differential control of Wnt target genes involves epigenetic mechanisms and selective promoter occupancy by T-cell factors." Mol Cell Biol **27**(23): 8164-8177.
- Wright, W. E., Sassoon, D. A. and Lin, V. K. (1989). "Myogenin, a factor regulating myogenesis, has a domain homologous to MyoD." Cell **56**(4): 607-617.
- Wu, B., Crampton, S. P. and Hughes, C. C. (2007). "Wnt signaling induces matrix metalloproteinase expression and regulates T cell transmigration." Immunity **26**(2): 227-239.
- Xu, B., Chen, C., Chen, H., Zheng, S. G., Bringas, P., Jr., Xu, M., Zhou, X., Chen, D.,

- Umans, L., Zwijsen, A. and Shi, W. (2011). "Smad1 and its target gene Wif1 coordinate BMP and Wnt signaling activities to regulate fetal lung development." Development **138**(5): 925-935.
- Yamamoto, H., Ihara, M., Matsuura, Y. and Kikuchi, A. (2003). "Sumoylation is involved in [beta]-catenin-dependent activation of Tcf-4." EMBO J **22**(9): 2047-2059.
- Yamamoto, H., Kishida, S., Uochi, T., Ikeda, S., Koyama, S., Asashima, M. and Kikuchi, A. (1998). "Axil, a member of the Axin family, interacts with both glycogen synthase kinase 3beta and beta-catenin and inhibits axis formation of Xenopus embryos." Mol Cell Biol **18**(5): 2867-2875.
- Yan, D., Wiesmann, M., Rohan, M., Chan, V., Jefferson, A. B., Guo, L., Sakamoto, D., Caothien, R. H., Fuller, J. H., Reinhard, C., Garcia, P. D., Randazzo, F. M., Escobedo, J., Fantl, W. J. and Williams, L. T. (2001). "Elevated expression of axin2 and hnkd mRNA provides evidence that Wnt/beta -catenin signaling is activated in human colon tumors." Proc Natl Acad Sci U S A **98**(26): 14973-14978.
- Yanagawa, S., Matsuda, Y., Lee, J. S., Matsubayashi, H., Sese, S., Kadowaki, T. and Ishimoto, A. (2002). "Casein kinase I phosphorylates the Armadillo protein and induces its degradation in Drosophila." Embo j **21**(7): 1733-1742.
- Yang, X. J., Ogryzko, V. V., Nishikawa, J., Howard, B. H. and Nakatani, Y. (1996). "A p300/CBP-associated factor that competes with the adenoviral oncoprotein E1A." Nature **382**(6589): 319-324.
- Yao, T. P., Oh, S. P., Fuchs, M., Zhou, N. D., Ch'ng, L. E., Newsome, D., Bronson, R. T., Li, E., Livingston, D. M. and Eckner, R. (1998). "Gene dosage-dependent embryonic development and proliferation defects in mice lacking the transcriptional integrator p300." Cell **93**(3): 361-372.
- Yin, H., Price, F. and Rudnicki, M. A. (2013). "Satellite Cells and the Muscle Stem Cell Niche." Physiological Reviews **93**(1): 23-67.
- Yoon, H. G., Chan, D. W., Huang, Z. Q., Li, J., Fondell, J. D., Qin, J. and Wong, J. (2003). "Purification and functional characterization of the human N-CoR complex: the roles of HDAC3, TBL1 and TBLR1." Embo j **22**(6): 1336-1346.
- Yost, C., Torres, M., Miller, J. R., Huang, E., Kimelman, D. and Moon, R. T. (1996). "The axis-inducing activity, stability, and subcellular distribution of beta-catenin is regulated in Xenopus embryos by glycogen synthase kinase 3." Genes Dev **10**(12): 1443-1454.
- Young, R. M., Reyes, A. E. and Allende, M. L. (2002). "Expression and splice variant analysis of the zebrafish tcf4 transcription factor." Mech Dev **117**(1-2): 269-273.
- Yu, Y. T., Breitbart, R. E., Smoot, L. B., Lee, Y., Mahdavi, V. and Nadal-Ginard, B. (1992). "Human myocyte-specific enhancer factor 2 comprises a group of tissue-restricted MADS box transcription factors." Genes Dev **6**(9): 1783-1798.
- Zammit, P. and Beauchamp, J. (2001). "The skeletal muscle satellite cell: stem cell or son of stem cell?" Differentiation **68**(4-5): 193-204.

- Zammit, P. S. (2004). "Muscle satellite cells adopt divergent fates: a mechanism for self-renewal?" J. Cell Biol. **166**: 347-357.
- Zammit, P. S., Golding, J. P., Nagata, Y., Hudon, V., Partridge, T. A. and Beauchamp, J. R. (2004). "Muscle satellite cells adopt divergent fates: a mechanism for self-renewal?" J. Cell Biol. **166**(3): 347-357.
- Zammit, P. S., Heslop, L., Hudon, V., Rosenblatt, J. D., Tajbakhsh, S. and Buckingham, M. E. (2002). "Kinetics of myoblast proliferation show that resident satellite cells are competent to fully regenerate skeletal muscle fibers." Exp Cell Res **281**: 39-49.
- Zammit, P. S., Relaix, F., Nagata, Y., Ruiz, A. P., Collins, C. A., Partridge, T. A. and Beauchamp, J. R. (2006). "Pax7 and myogenic progression in skeletal muscle satellite cells." J Cell Sci **119**(9): 1824-1832.
- Zhang, C. G., Jia, Z. Q., Li, B. H., Zhang, H., Liu, Y. N., Chen, P., Ma, K. T. and Zhou, C. Y. (2009). "beta-Catenin/TCF/LEF1 can directly regulate phenylephrine-induced cell hypertrophy and Anf transcription in cardiomyocytes." Biochem Biophys Res Commun **390**(2): 258-262.
- Zhang, L., Shi, S., Zhang, J., Zhou, F. and ten Dijke, P. (2012). "Wnt/beta-catenin signaling changes C2C12 myoblast proliferation and differentiation by inducing Id3 expression." Biochem Biophys Res Commun **419**(1): 83-88.
- Zhang, Q., Shi, X. E., Song, C., Sun, S., Yang, G. and Li, X. (2015). "BAMBI Promotes C2C12 Myogenic Differentiation by Enhancing Wnt/beta-Catenin Signaling." Int J Mol Sci **16**(8): 17734-17745.
- Zhang, S., Li, Y., Wu, Y., Shi, K., Bing, L. and Hao, J. (2012). "Wnt/beta-catenin signaling pathway upregulates c-Myc expression to promote cell proliferation of P19 teratocarcinoma cells." Anat Rec (Hoboken) **295**(12): 2104-2113.
- Zhang, W., Behringer, R. R. and Olson, E. N. (1995). "Inactivation of the myogenic bHLH gene MRF4 results in up-regulation of myogenin and rib anomalies." Genes Dev **9**(11): 1388-1399.
- Zhu, J., Li, Y., Lu, A., Gharaibeh, B., Ma, J., Kobayashi, T., Quintero, A. J. and Huard, J. (2011). "Follistatin Improves Skeletal Muscle Healing after Injury and Disease through an Interaction with Muscle Regeneration, Angiogenesis, and Fibrosis." The American Journal of Pathology **179**(2): 915-930.
- Zhuang, L., Hulin, J. A., Gromova, A., Tran Nguyen, T. D., Yu, R. T., Liddle, C., Downes, M., Evans, R. M., Makarenkova, H. P. and Meech, R. (2014). "Barx2 and Pax7 have antagonistic functions in regulation of wnt signaling and satellite cell differentiation." Stem Cells **32**(6): 1661-1673.
- Zhurinsky, J., Shtutman, M. and Ben-Ze'ev, A. (2000). "Differential mechanisms of LEF/TCF family-dependent transcriptional activation by beta-catenin and plakoglobin." Mol Cell Biol **20**(12): 4238-4252.